Sequential action of Rab proteins along the endocytic-recycling pathway

Thesis

Sequential Action of Rab Proteins Along the Endocytic-Recycling Pathway

Stefano De Renzis M.D.

A thesis submitted in partial fulfilment of the requirements of the Open University for the degree of Doctor of Philosophy

April 2002

Sponsoring establishment

National Institute for Medical Research, London

Table of Contents

		Page
TITLE		**a**
TABLE OF CONTENTS		**b**
ABBREVATIONS		**h**
LIST OF FIGURES and TABLES		**k**
ABSTRACT		**o**
1	**INTRODUCTION**	**1**
1.1	General introduction to the endocytic pathway	1
1.2	Endosomes: classification and function	5
1.3	Vesicles formation	13
1.3.1	Adaptors	14
1.3.2	Invagination and detachment of clathrin coated vesicles	20
1.4	Endocytic transport: role of the cytoskeleton	23
1.5	Vesicle and organelle docking and fusion	28
1. 6	Ypt1/Sec4/Rab family of small G-proteins	33
1.6.1	The Rab cycle(s): The dual life of a Rab protein	35
1.6.2	Post-translational modification of Rab proteins	38
1.7	Function of Rab proteins	39
1.7.1	Membrane tethering	40
1.7.2	Functional link between Rabs and SNAREs	43
1.7.3	Function of Rab proteins in vesicular budding and organelle-vesicle motility	44

1.7.4 Localisation of Rab proteins along the endocytic pathway 47

1.7.5 Multiplicity of Rab5 effectors and

their function in the biogenesis of a Rab domain 48

1.8 Membrane domain: general considerations 53

1.8.1 Membrane domains in endocytic organelles 56

1.9 Molecular regulation of endocytic sorting and recycling 60

1.10 Aim of the thesis 69

1.10.1 Topic 69

1.10.2 Question 69

1.10.3 Hypothesis 70

1.11 Experimental strategy 71

1.11.1 The marker followed to study

the endocytic-recycling pathway 72

1.11.2 The cell line 73

2 RESULTS **75**

2.1 Introduction to results (part-1) 75

2.2 In vitro reconstitution of the transferrin

recycling pathway in SLO-permeabilised cells 76

2.3 Rab GDI inhibits transferrin recycling

in SLO-permeabilised cells 84

2.4 Rab 4 and Rab11 are required for

transferrin recycling in SLO permeabilised cells 87

2.5 Studies on the function of Rabaptin-5 using

the in vitro reconstituted transferrin recycling assay 91

2.6 Introduction to results (part-2) 97

2.6.1 Why the GFP tag ? 98

2.6.2 Why fluorescence microscopy ? 99

2.7 The GFP-Rab4 A431 cell line 100

2.8 Transferrin moves sequentially through Rab5-Rab4 and Rab11 positive endosomes 105

2.9 The Rab5 effector EEA1 is specifically localised to Rab5 domains 114

2.10 Introduction to results (part-3) 118

2.10 Identification of proteins interacting with both active Rab5 and Rab4 120

2.12 Biochemical characterisation of the interaction between Rabenosyn-5 and Rab4 125

2.13 Rabenosyn-5 labels the endosomes where Rab5 and Rab4 colocalise 128

2.14 Rabenosyn-5 interacts simultaneously with both active Rab5 and Rab4 132

2.15 Overexpression of Rabenosyn-5 increases the overlap between Rab5 and Rab4, but not between Rab5 and Rab11 endosomal domains 135

2.16 Over-expression of Rabenosyn-5 stimulates transferrin

recycling and diverts it from peri-nuclear recycling endosomes 144

3 DISCUSSION 152

3.1 Visualisation of Rab4, Rab5 and Rab11 domains

on early endosomes 154

3.2 Molecular regulation of transport through Rab domains 162

3.3 Open questions and future directions 170

4 MTERIAL and METHODS 175

4.1 Cell culture 175

4.2 Transient expression systems in eukaryotic cells 176

4.2.1 Infection of HeLa cells with vaccinia virus T7 176

4.2.2 Microinjection of plasmid DNAs

into A431 and CHO cell nucleus 177

4.3 Generation of A431 cells stably expressing GFP-Rab4 178

4.4 Permeabilisation of A431 cells with Streptolysin O 179

4.5 In vitro recycling assay in SLO-permeabilised A431 cells 180

4.6 Cytosol Preparation of Spinner Hela cells 181

4.7 Kinetic Analysis of Transferrin recycling and EGF degradation 182

4.7.1 Detection systems – Electrochemiluminescence (ECL)

Detection System 183

4.7.2 Ruthenium labelling of secondary antibodies 186

4.8 Confocal Microscopy, Image Processing

and Quantitation of Signal Overlap on Fixed Cells 187

4.9 Electron Microscopy 189

4.10 Sequential Affinity Chromatography 190

4.11 In Vitro Binding Assay and affinity measurement 191

4.12 Expression and purification of recombinant proteins 193

4.12.1 Production of GST fusion proteins in bacteria 193

4.12.2 Production of Histidine-tagged proteins in bacteria 194

4.12.3 Expression and purification of Rab4 and Rab11

using the Baculovirus expression System 195

4.12.4 Purification of Rab4 and Rab11- RabGDI complex

by Gel –filtration column chromatography 197

4.12.5 Expression of Rabenosyn-5/hvps45 ExpresSf+

using the baculovirus expression system 197

4.13 Rabenosyn-5/hvps45 ExpresSf+ Cytosol Preparation 198

4.14 Western Blot analysis 198

4.15 Silver staining of proteins 199

4.16 Protein sequencing 199

4.17 Antibodies and Plasmids 200

4.18 Preparation of competent *E. coli* for electroporation 202

4.19 Plasmid preparation in large scale (Maxi-prep)

and small scale Mini-prep 203

4.20 Electroporation of *E. coli* 203

4.21 Restriction enzyme digestion of DNA 204

4.22 Ligation of DNA 204

ACKNOWLEDGMENTS **205**

5 REFERENCES **206**

PhD PUBLICATIONS **233**

ABBREVIATIONS

ADP	adenosine diphosphate
AEE	apical early endosome
AP	adaptor protein
ARE	apical recycling endosome
ARF	ADP-ribosylation factor
ATP	adenosine triphosphate
BSA	bovine serum albumin
CCV	clathrin-coated vesicle
cDNA	complementary DNA
CGN	cis Golgi network
CMV	Cytomegalovirus
D-MEM	Dulbecco's MEM
DMSO	dimethyl sulfoxide
DOTAP	N-[1-(2.3 Dioleoyloxy)propyl]- N,N,N-trimethylammoniumsulfate
ECL	electrochemiluminescence
EDTA	ethylenediaminetetraacetate
EGTA	ethyleneglycol-bis (β-aminoethylether)- N, N, N', N'-tetraacetate

ER	endoplasmic reticulum
FCS	fetal calf serum
FITC	fluorescein-β-isothiocyanate
GAP	GTPase activating protein
GDI	GDP dissociation inhibitor
GDP	guanosine disphosphate
GDF	GDP displacement factor
GEF	guanine nucleotide exchange factor
GGTase	geranylgeranyl transferase
GTP	guanosine triphosphate
HRP	horse radish peroxidase
kB	kilobases
Da	Dalton
IFN	interferon
ivu	infectious vector unit
LDL	low density lipoprotein
MTOC	microtubule organizing centre
NSF	N-ethylmaleimide sensitive fusion protein
PBS	phosphate-buffered saline
PCR	polymerase chain reaction

pfu	plaque forming units
PI(3)P	phosphatidylinositol 3-phosphate
PLD	Phospholipase D
PtdOH	phosphatidic acid
ras	rat sarcoma
REP	rab escort protein
SDS	sodium dodecyl sulfate
SLO	Streptolysin-O
SNAP	soluble NSF attachment protein
SNARE	SNAP receptor
Tf	transferrin
TGN	trans Golgi network
TPA	tripropilamine
TR	transferrin receptor

LIST OF FIGURES and TABLES

	Page
Figure 1: The endocytic pathway	3
Figure 2: The Early endosome	9
Figure 3: Organization of the actin and microtubule cytoskeletal elements	26
Figure 4: Working model for SNARE proteins function in homotypic vacuole fusion	32
Figure 5: GTPase molecular switch	36
Figure 6: Model proposing the role of Rab5 and its effectors in the organization of a membrane domain	51
Figure 7: Release of cytosolic LDH with increasing concentration of SL-O and immuno-fluorescence microscopy analysis of cell treated with SL-O	77
Figure 8: Schematic representation of the *in vitro* reconstituted transferrin recycling assay	78
Figure 9: Fluorescent transferrin recycling assay in SL-O-permeabilized cells	79
Figure 10: EGF is retained intracellularly in SL-O-permeabilized cells	80
Figure 11: Biochemical quantification of transferrin recycling in SL-O-permeabilized cells	81
Figure 12: Reconstituted transferrin recycling is dependent on the concentration of exogenously added cytosol	82
Figure 13: transferrin recycling in SL-O permeabilized cells is not due to vesicle leakage	83
Figure 14: Recombinant RabGDI inhibits transferrin recycling in SL-O-permeabilized cells	85

Figure 15: Recombinant RabGDI extracts Rab5 and Rab11
from the membranes in SL-O-permeabilized cells 86
Figure 16: Histidine-tagged purified Rab4 and Rab11 expressed
using the baculovirus expression system 88
Figure 17: Purification of Rab4- and Rab11-RabGDI
complexes by gel filtration chromatography 90
Figure 18: Purified Rab4- and Rab11-RabGDI complexes partially rescue
the RabGDI inhibitory effect on transferrin recycling in SL-O-permeabilized cells 91
Figure 19: Rabaptin-5 immuno-depleted cytosol does not inhibit transferrin
recycling in SL-O- permeabilized cells 92
Figure 20: Rab GDI treatment of SLO-permeabilized cells increases
the extraction of Rabaptin-5 from the membranes 94
Figure 21: A431 cells expressing GFP-Rab4 102
Figure 22: GFP-Rab4 is correctly localized to early endosomes 103
Figure 23: Fluorescence microscopy analysis of GFP-Rab4 expressing
cell line treated with RabGDI 104
Figure 24: Biochemical measurement of transferrin recycling in
A431 cells expressing GFP-Rab4 105
Figure 25: Morphological quantification of rhodamine transferrin
trafficking in GFP-Rab4-, Rab5- and Rab11- cell lines 108
Figure 26: Schematic representation of the methods used to
quantify the endosomal distribution of Rab4, Rab5 and Rab11 109
Figure 27: Confocal analysis of YFP-Rab4 and CFP-Rab5
on transferrin-filled endosomes 110
Figure 28: Confocal analysis of YFP-Rab4 and CFP-Rab11
on transferrin-filled endosomes 112
Figure 29: Confocal analysis of Rab4, Rab5 and Rab11 endosomes 113

Figure 30: Localization of EEA1 in the GFP-Rab4 and GFP-Rab5 stable cell lines 115

Figure 31: Differential response of Rab5 and Rab4-positive endosomes to BFA 117

Figure 32: Differential response of Rab4 and Rab11 positive endosomes to BFA 117

Figure 33: Schematic representation of sequential affinity chromatography strategy 121

Figure 34: Purification and identification of Rab5 and Rab4 common effectors using sequential affinity chromatography 124

Figure 35: Cytosolic Rabenosyn-5 interacts with Rab4 125

Figure 36: Rabenosyn-5 interacts directly with Rab4 and recruits hVPS45 to Rab4 127

Figure 37: Rabenosyn-5 does not interact with Rab11 127

Figure 38: Confocal immunofluorescence analysis of Rab5, Rab4 and Rabenosyn-5 labelled endosomes 130

Figure 39: Rabenosyn-5 interacts with similar affinity with Rab5 and Rab4 131

Figure 40: Western blot analysis of Rabenosyn-5 over-expression in insect cells 132

Figure 41: Rabenosyn-5 can bind simultaneously to Rab5 and Rab4 134

Figure 42: Over-expression of Rabenosyn-5 and Rabaptin-5, but not of EEA1, increases the co-localization between Rab5 and Rab4 137

Figure 43: Electron microscopy analysis of cells over-expressing Rabenosyn-5 139

Figure 44: Summary of the in vitro binding assay results to determine Rab4 and Rab5 binding sites of Rabenosyn-5 140

Figure 45: Rabenosyn-5/Rab4 interaction is necessary to redistribute Rab4 endosomes 141

Figure 46: Rabenosyn-5 over-expression does not change the peri-nuclear localization of Rab11-postive membranes 143

Figure 47: Morphological analysis of transferrin trafficking 146

Figure 48: Effects of Rabenosyn-5 over-expression on transferrin recycling 148

Figure 49: Effects of Rabenosyn-5 over-expression on transferrin recycling 149

Figure 50: Effects of Rabenosyn-5 over-expression on transferrin recycling 150

Figure 51: Effects of Rabenosyn-5 over-expression on EGF degradation 151

Figure 52: Model proposing the sub-compartment organization of the early endosomal system in different Rab domains 158

Figure 53: Model proposing the function of Rabenosyn-5 in coupling Rab5 and Rab4 domains 166

Figure 54: Model proposing the function of divalent Rab effectors in regulating the communication between Rab domains along the endocytic pathway 173

Figure 55: The electrochemiluminescence reaction 184

Table 1: Quantification of Rab5, Rab4 and Rab11 on transferrin-labelled endosomes 111

Table 2: Quantification of Rab5, Rab4 and Rab11 overlap on the same endosomes 143

ABSTRACT

The endocytic pathway in eukaryotic cells is organized into distinct compartments. Early endosomes are heterogeneous and dynamic organelles, which are found both spread through the cortical cytoplasm (sorting-early endosomes) and in the perinuclear region (recycling endosomes). Endocytosed molecules that enter sorting endosomes can be directed to the degradative pathway or recycled back to the plasma membrane, either directly or by passing through perinuclear-recycling endosomes. Very little is known about the molecular mechanisms that regulate transport between these different compartments and the functional properties of endocytic organelles. In this thesis, I have investigated the molecular regulation of the endocytic-recycling pathway and, in particular, how endocytosis and recycling are co-ordinated at the level of early endosomes. To this end, I have addressed the function of Rab5, Rab4, and Rab11, three small GTPases that control trafficking from the plasma membrane to the early endosomes, sorting of cargo within early endosomes and recycling to the plasma membrane, respectively. Rab proteins function in their GTP-bound active state through the recruitment of effector proteins to the membrane compartment where they are localized. The identification of a large number of Rab5 effectors, together with the realization that these proteins act co-operatively, led to the proposal that this GTPase organizes the endosomal membrane into a biochemically and

functionally distinct membrane domain. If generalized to other family members, this model would predict that other Rab proteins present on endosomes such as Rab4 and Rab11 should be localized to discrete, non-overlapping membrane domains distinct from the one occupied by Rab5. Moreover, the finding that one Rab5 effector, Rabaptin-5, interacts also with Rab4 raises the possibility that the activity of these two GTPases is molecularly co-ordinated. Given the complementary role of Rab5 and Rab4 in regulating entry in, and exit out, of early endosomes the coupling of their activity through a common effector may ensure co-ordination of the endocytic and recycling functions of early endosomes. I have experimentally tested the working hypothesis predicting that divalent Rab effectors may regulate the association between contiguous Rab domains to allow the sequential transport of cargo along the endocytic-recycling pathway. To provide evidence for this model, two complementary approaches have been undertaken. First, I have developed an *in vitro* recycling assay to identify and characterize molecules involved in this process. Second, I have conducted a high-resolution morphological analysis of the endocytic-recycling pathway in stable cell lines expressing GFP-tagged versions of Rab proteins. The results obtained support the idea that endosomes are indeed organized into distinct domains, harbouring Rab5, Rab4 and Rab11. The association between these domains follows a non-random distribution giving rise to three major

populations of endosomes: one containing Rab5, a second with Rab4 and Rab5, and a third containing Rab4 and Rab11. Upon endocytosis, recycling cargo first enters Rab5 domains, and then progresses through Rab5/Rab4 and Rab4/Rab11 endosomes before returning to the plasma membrane. Based on these observations, I then addressed the question of how the communication between neighbouring domains is regulated by specifically searching for Rab5 and Rab4 common effectors using an affinity chromatography approach. The results of these experiments led me to identify Rabenosyn-5 as a novel Rab5 and Rab4 common effector. Subsequently, I demonstrated that Rabenosyn-5, as well as Rabaptin-5 over-expression specifically increased the association between Rab5 and Rab4 endosomal domains and stimulated transferrin recycling. Concomitantly, the fraction of Rab4+Rab11 positive structures was reduced and transport to peri-nuclear recycling endosomes decreased. Thus, divalent Rab5 and Rab4 effectors regulate endocytosis and recycling by connecting Rab5 and Rab4 domains on early endosomes. These results provide support for the hypothesis that Rab proteins and their effectors regulate the compartmental organization and trafficking function of early endosomes.

1. INTRODUCTION

1.1 General overview of the endocytic pathway

Eukaryotic cells continuously remodel their plasma membrane composition by a process known as endocytosis. This process involves the internalization of extra-cellular components through the regulated formation of vesicles at the plasma membrane (for review see (Mellman, 1996; Riezman et al., 1997; Robinson et al., 1996)). According to the size of the internalized particles, endocytosis can be subdivided into phagocytosis (cell eating) and pinocytosis (cell drinking) (Silverstein et al., 1977). Phagocytosis is responsible for the uptake of large particles (> 0.5 μm diameter) which bind to specific cell surface receptors capable of transducing a phagocytic stimulus to the cytoplasm. This stimulus causes the formation of F-actin-driven pseudopods that engulf the bound particles into a cytoplasmic phagosome (Greenberg et al., 1990; Greenberg et al., 1991). This form of endocytosis is associated with specific cell types such as leukocytes of the mammalian immune system or phagocytic protozoa like *Dictostelium.* In contrast to phagocytosis, all eukaryotic cells exhibit one or more forms of pinocytosis. According to the different size of internalized vesicles, pinocytosis can be further subdivided into micropinocytosis and macropinocytosis. Micropinocytosis refers to the constitutive formation of small vesicles (50-150 nm

diameter) carrying extracellular fluid and macromolecules specifically or non-specifically bound to cell surface receptors. These vesicles are usually initiated at clathrin-coated pits and depend on clathrin function although alternatives have been described (see below). Possible alternatives to clathrin-mediated endocytosis involve caveolae and/or actin based-mechanisms. To different extents, two or more of these mechanisms co-exist in a single cell type. Macropinocytosis is characterized by the formation of relatively large vacuoles (0.5-2 μm diameter) and preferentially occurs in certain cell types (dendritic cells, macrophages and fibroblast) (Steinman and Swanson, 1995) in response to specific stimuli (growth factors) (Haigler et al., 1979). Although, the function of this form of endocytosis has not yet been elucidated, it has been suggested that the high ratio of volume to surface area of macropinosomes may reflect a function in sampling the fluid in the extracellular environment (Sallusto et al., 1995).

Following internalization, cell surface receptors, along with their ligands, solutes and other plasma membrane constituents, first appear in early endosomes. Here, components destined for degradation are transported to late endosomes and lysosomes, while recycling receptors and bulk membranes are returned back to the plasma membrane for a next round of internalization (Dunn et al., 1989; Hopkins, 1983; Mayor et al., 1993) (see Figure 1 for a schematic representation of the endocytic pathway).

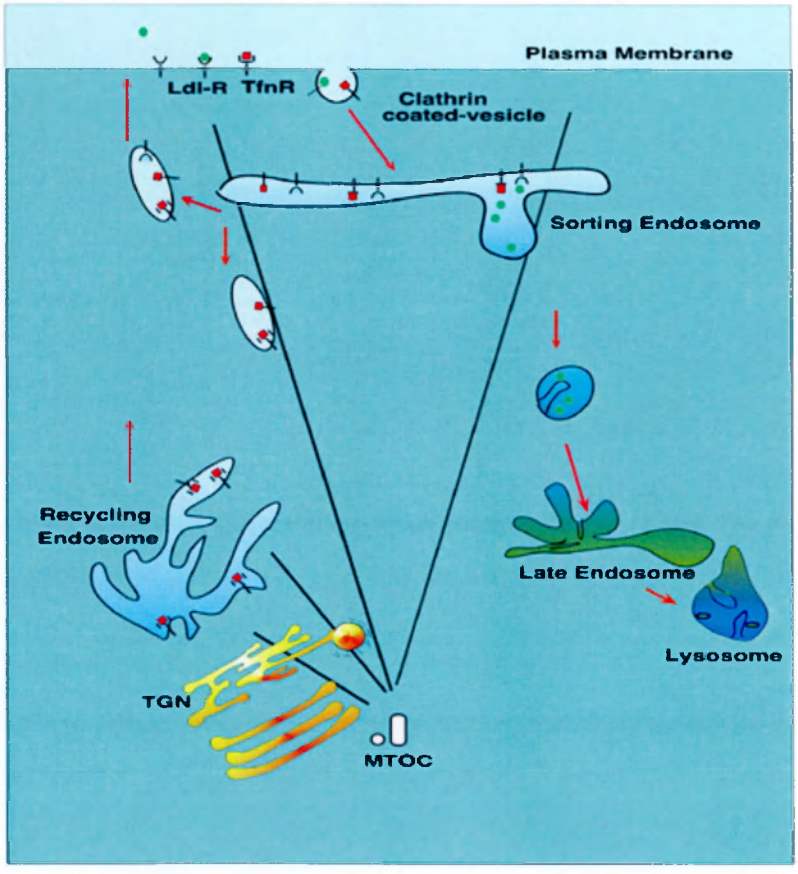

Figure 1: The endocytic pathway
This figure indicates the major routes of endosomal membrane transport along the degradative and recycling pathways. As an example, the trafficking of transferrin receptor (TR) is shown. MTOC: microtubule organizing centre; PM: plasma membrane. See text for details.

Early endosomes also act as central node in connecting membrane traffic between the biosynthetic and the endocytic pathway (Rohn et al., 2000; Wilcke et al., 2000). Downregulation of growth factor receptors plays an essential role in controlling growth and differentiation, while endocytic-recycling balances the internalization of membrane components and avoids consumption of certain receptors. Beside these basic functions, common to all nucleated cells, early

endosomes also play more specialized functions in certain cell types. Endocytic-recycling guarantees re-utilization of synaptic vesicle components in neurons (Mundigl and De Camilli, 1994), and allows antigen-presenting cells to expose MHC-peptide complex to the cell surface to elicit an appropriate immuno-response (Tulp et al., 1994). Other examples include fat and muscle cells, where a fine tuning of the rate of endocytosis and recycling in response to insulin, regulates the plasma membrane localization of GLUT4, a glucose transporter (Herman et al., 1994). Finally, the endosomal system of polarized cells controls transport of trans-cytotic molecules across epithelial tissues and is important for the establishment of morphogenetic gradients during pattern formation and organogenesis (Entchev et al., 2000).

The sorting and recycling activity of early endosomes is, therefore, fundamental for intra and inter-cellular communication, and hence for the assembly of multi-cellular organisms. The endocytic pathway can be hijacked by parasites leading to diseases. Pathogens have indeed evolved, and are continuously evolving mechanisms to survive inside, and spread between host cells, by modulating the function of the endosomal compartment.

Like the secretory pathway, the endocytic pathway can be thought to be organized in functionally and physically distinct compartments, each fulfilling a specific function in sorting, recycling and degradation (Kornfeld and Mellman,

1989). However, different from the secretory pathway, the boundaries between these compartments are less clear. The reasons for this difference are several-fold. Firstly, the functions of endocytic organelles do not involve the predictable and easily determined enzymatic activities associated with the synthesis and processing of glycoproteins and lipids. Secondly, endosomes are extremely plastic and pleiomorphic organelles and their morphology can vary between different cell types or even within the same cell type under different conditions. Therefore, they cannot be identified on the basis of morphological criteria alone, which is often the case for organelles along the secretory pathway. Thirdly, the movement of internalized markers is not synchronous enough to follow their progression through individual membrane compartments. Nevertheless, a combination of different experimental approaches based on morphology, position in the cytoplasm, presence of biochemical markers and functional criteria, has led to the operational definition of distinct organelles in the endocytic pathway. In the next paragraph, I will describe in more detail the compartment organization of the endocytic pathway. Given the topic of this thesis, particular emphasis will be given to the organization of the early endosomal system.

1.2 Endosomes: classification and function

Endosomes are highly dynamic and heterogeneous membrane-bound organelles spread throughout the cytoplasm of eukaryotic cells. Functionally distinct, early and late endosomes have been described according to different kinetics of labelling upon internalization of endocytic tracers. Early and late endosomes differ also in their biochemical composition, morphological appearance and topology.

Early endosomes, also referred to as sorting endosomes (Gruenberg and Maxfield, 1995), are operationally defined as the first intracellular organelle where incoming endocytic vesicles deliver their contents (Dunn et al., 1989; Geuze et al., 1983). Due to their slightly acidic internal pH (~6.2), early endosomes facilitate the dissociation of many internalized receptor-ligand complexes and, therefore, functionally correspond to the previously described compartment of uncoupling of receptors and ligands (CURL) (Mayor et al., 1993). Early endosomes next engage in the physical separation, or sorting, of recycling components from those undergoing degradation. While the latter are delivered to late endosomes and lysosomes, recycling receptors are sorted into membrane containers destined for the plasma membrane. Although some of these containers may fuse directly with the plasma membrane, others accumulate in a population of membranes, generally named recycling endosomes, which in many cell types are

tightly clustered in the peri-nuclear region (Hopkins, 1983; Yamashiro et al., 1984). Recycling endosomes are devoid of material destined for degradation suggesting that they do not play a role in receptor-ligand sorting. Moreover, their pH is slightly higher than that of early endosomes (Yamashiro et al., 1984) and certain regulatory molecules (such as Rab and SNARE proteins) differentially localize to these two membrane pools (Daro et al., 1996; Ullrich et al., 1996). Altogether these observations lead to a proposal that early and recycling endosomes are physically distinct compartments. Further support of this hypothesis is given by the recent establishment of protocols allowing purification of two separate populations of early and recycling endosomes (Sheff et al., 1999). However, the biogenesis, the boundaries and the communication routes connecting early and recycling endosomes remain difficult to trace. For example, morphological analysis using confocal and video-microscopy techniques has described the early endosomal compartment of an epidermoid carcinoma cell line (Hep-2) as a ''continuous network of tubular membranes and varicosity structures through which endocytic tracers move'' (Hopkins et al., 1990). Whether this is a peculiarity of the specific cell line analyzed in this study or a more general rule, is still unclear. Tubular elements are indeed very sensitive and tend to break down at low temperature incubation (below 37^0 C) or after exposure to common fixative

compounds. These reasons might explain why, in most cases, early endosomes appear as individual structures scattered throughout the cytoplasm.

Also controversial is the exact function of recycling endosomes. Trafficking through this compartment is apparently not mandatory, as recycling can occur directly from early endosomes with high efficiency (Sheff et al., 1999). A better understanding of its function might come from studies in polarized epithelial cells where, assuming that this compartment corresponds to the apical recycling endosomal compartment, it participates in directing membrane recycling to distinct apical and basolateral plasma membrane surfaces (Apodaca et al., 1994; Barroso and Sztul, 1994). Recycling endosomes might also perform a polarized function during cell locomotion. Re-directing membrane recycling to the leading edge (a transient polarized plasma membrane region of a migrating cell) indeed involves passage through this organelle (Hopkins et al., 1994).

From the ultra-structural point of view, early and recycling endosomes also differ. Early endosomes can be similar to the shape of an octopus. They are composed of a large cisternal region (0.3-0.5 nm in diameter) from which several narrow (60 nm in diameter) tubulo-vesicular elements emanate (Figure 2) (Griffiths et al., 1989; Marsh et al., 1986).

Recycling endosomes are composed mainly of tubular elements having the same diameter and shape as the one emanating from sorting endosomes (Hopkins,

1983). This similarity led to a proposal that recycling endosomes originate from early endosomes upon budding of tubular elements (Gruenberg and Maxfield, 1995). This model is also consistent with the sequential movement of recycling receptors from early to recycling endosomes and with the different sorting functions these elements play along the endocytic pathway.

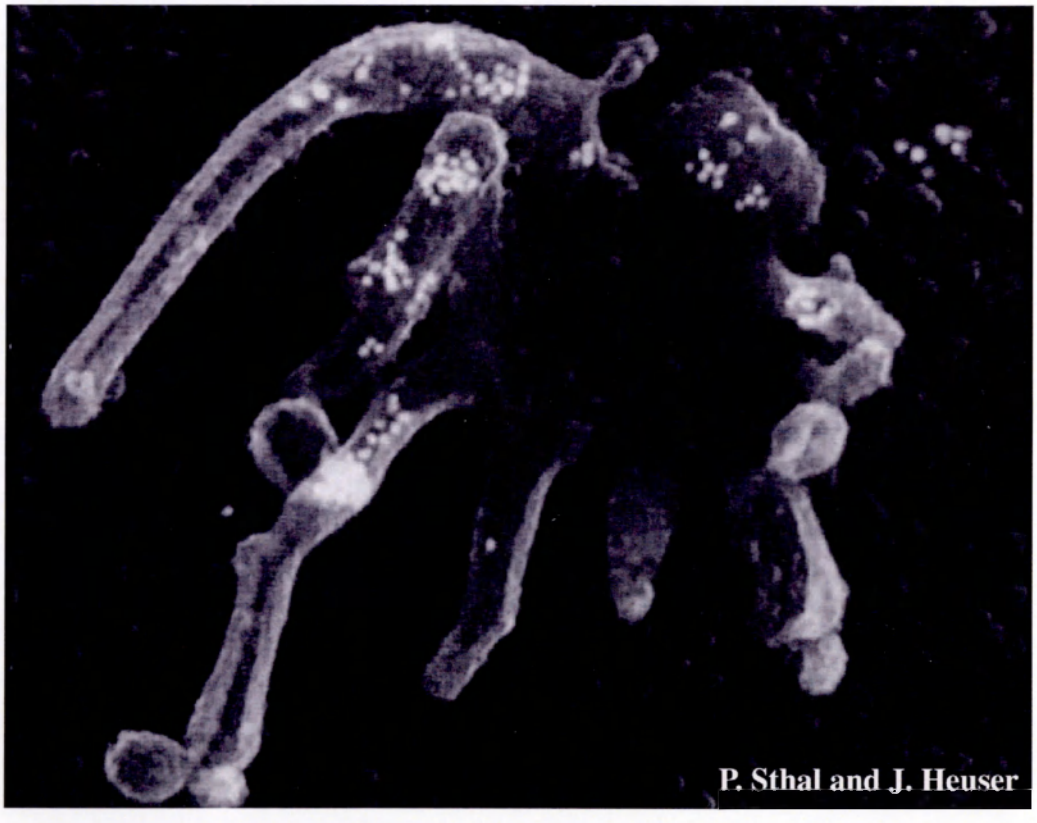

Figure 2: The Early endosome
Taken from Gruenberg J., 2001. Freeze-etch electron microscopy analysis of early endosomes containing low-density lipoprotein-gold particles (white spots).

As already mentioned above, in some cell types early and recycling endosomes are also geographically segregated. Recycling endosomes are indeed

often localized in the peri-nuclear region close to the microtubule organizing centre, while early endosomes are more peripherally distributed (Hopkins, 1983). This segregation is dependent on intact microtubules, as treatment of cells with microtubules depolymerising drugs redistribute recycling endosomes to the cell periphery and mix them with early endosomes (Daro et al., 1996).

Late endosomes can be functionally defined as organelles that receive endocytic particles destined for lysosomes after their passage through early endosomes. Transport between early and late endosomes involves large (300-400 nm in diameter) vesicular containers named endosomal carrier vesicles (ECV) or, according to their structural composition, multivesicular bodies (MVB) (Aniento et al., 1993; Clague et al., 1994; Felder et al., 1990; Gruenberg et al., 1989). These containers indeed contain internal vesicles, which are derived from invaginations of the limiting endosomal membrane (Cohn, 1966; McKanna et al., 1979).

An additional communication route connects late endosomes with the trans-Golgi network (TGN). Clathrin-coated vesicles derived from the TGN deliver newly synthesized lysosomal enzymes into late endosomes via the mannose-6-phosphate receptors (M6PR) (Kornfeld and Mellman, 1989). Owing to the acquisition of these enzymes and their acidic pH (5.5), late endosomes initiate breakdown of internalized cargo (Geuze et al., 1988; Griffiths et al., 1988). These

lysosome-like features lead in some cases to late endosomes being referred to also as pre-lysosomes.

Morphologically, late endosomes appear as tubular-vesicular elements located in the peri-nuclear region of the cell, but differ from early endosomes because of typical high content of internal membranes and lack of recycling molecules (Griffiths et al., 1988). According to the different organization of these internal membranes, late endosomes can have an onion (multilamellar) or pomegranate (multivesicular) type appearance. Very little is known about the biogenesis, the biochemical composition and the functional significance of these different types of membranes. Also unclear is to what extent the formation of these inner membranes is regulated by the same mechanisms as those controlling MVBs inner vesicles budding. The observation that down-regulated receptors accumulate in these inner membranes has led to the idea that these membranes are destined to be degraded in lysosomes. However, the finding that also molecules trafficking between late endosomes and TGN such as M6PRs are contained within these membranes (Griffiths et al., 1988) question this hypothesis.

Lysosomes are involved in the final degradation of internalized cargo and can also function as a storage place for indigestible materials (Kornfeld and Mellman, 1989). However, it has been very difficult to trace the boundary between late endosomes and lysosomes, as the communication between these two

organelles is very dynamic. Indeed, late endosomes and lysosomes can efficiently exchange contents and membrane proteins and they probably interact dynamically to form a hybrid intermediate. Both compartments contain lysosomal enzymes, their pH is similar (~5.5) and their limiting membrane is composed of the same glycoproteins. Lysosomes can only be distinguished from late endosomes by their higher density on Percoll gradients, by their electron-dense appearance (Kornfeld and Mellman, 1989) and by the lack of some proteins found in late endosomes including M6PRs, Rab7 and Rab9 (Gruenberg and Maxfield, 1995).

This elaborate array of membrane-bounded organelles allows a continual exchange of components among them. According to the pioneering work of Palade, an established mode of communication between organelles is the transport of vesicular carriers (Palade, 1975). According to this model, cargo molecules are incorporated into nascent vesicles based on the presence of specific sorting signals (Pryer et al., 1992). Adaptor proteins recognize these sorting signals and regulate the assembly of coat proteins. Coat proteins were originally believed to bring the necessary mechanical force required for membrane curvature and vesicle formation. However, recent data have shown that this process requires the activity of lipid modifying enzymes which catalyze the lipid imbalance required for membrane bending to occur (Schmidt et al., 1999). Coat proteins might allow bending and vesicles budding to be controlled and localized (Sprong et al., 2001).

Upon budding from a donor compartment, vesicles are transported to their target compartment within an architectural framework. Cytoskeletal components, particularly microtubules and their associated motor proteins, regulate vesicular transport between geographically segregated organelles, and determine the steady-state localization of the organelles themselves (Cole and Lippincott-Schwartz, 1995). The final event is the docking and fusion of carrier vesicles with the proper acceptor compartment and the release of their cargo (Cole and Lippincott-Schwartz, 1995).

The molecular mechanisms controlling membrane transport have been extensively characterized using different approaches such as yeast genetics, cell-free assays and morphological analysis. The regulatory components so far identified have revealed that the fundamental mechanisms of vesicular traffic are extremely conserved from yeast to mammals (Ferro-Novick and Jahn, 1994; Rothman and Warren, 1994). The following sections give an overview of how vesicles are a) formed at the donor compartment, b) transported along cytoskeletal elements, c) targeted and fuse with the appropriate acceptor compartment.

1.3 Vesicles formation

The process of vesicle formation requires the recruitment of cytosolic proteins to a specific site on a donor organelle where they assemble into a coat.

Coat components ensure incorporation of cargo molecules into nascent vesicles by interacting with sorting signals present in their cytoplasmic tails (Rothman and Wieland, 1996). Two major classes of coated vesicles have been identified: those containing clathrin and those containing coatamer coat proteins (COPs). In the endocytic pathway, clathrin-coated vesicles play a major role connecting trafficking between the plasma membrane, the endosomal compartment and the TGN (Mellman, 1996). Clathrin consists of three copies each of clathrin heavy chain and clathrin light chain, arranged into a three-legged structure called triskelion (Robinson, 1994). Under certain experimental conditions, purified clathrin is able to self-assemble *in vitro* into a lattice of hexagons and pentagons to form a cage-like structure, virtually identical to the coat on coated vesicles present *in vivo* (Kirchhausen, 2000). In this paragraph, I will describe the different steps and molecules involved in the formation of clathrin-coated vesicles. Given, that much of our understanding of this process comes from the molecular characterization of clathrin-mediated endocytosis, I will describe in detail the molecules involved in this process.

1.3.1 Adaptors

The assembly of clathrin coat is initiated by the binding of adaptor molecules to a docking site or receptor present on the membrane. To date, four

adaptors have been identified: AP-1, AP-3 and AP-4 have been localized to TGN and endosome-like structures, while AP-2 is localized to the plasma membrane and endocytic clathrin-coated vesicles. Each adaptor complex is composed of four sub-units: two large (γ,β1 in AP-1; α,β2 in AP-2; δ,β3 in AP-3; ε,β4 in AP-4), one medium (μ1 in AP-1, μ2 in AP-2, μ3 in AP-3 and μ4 in AP-4) and one small (σ1 in AP-1, σ2 in AP-2, σ3 in AP-3 and σ4 in AP-4), each performing distinct functions. The structure of an adaptor complex resembles the figure of Mickey Mouse head. The amino-terminal region of the two large sub-units together with the small and medium sub-units define the head, while the two ears are composed of the carboxyl-terminal of the two large sub-units and are connected to the head by flexible hinges (Robinson and Bonifacino, 2001).

AP-2 is involved in the assembly of endocytic clathrin-coated vesicles at the plasma membrane. The large β2 sub-unit is involved in clathrin binding through its hinge region and in cargo selection by interacting with di-leucine sorting sequences. The medium sub-unit μ2 recognizes tyrosine-based internalization signals such as NPXY or YXX0 (0 is a bulky hydrophobic residue). The ear domain of the α sub-unit interacts with accessory proteins (Epsin, Eps15, AP180, amphiphysin) necessary for clathrin-coated pit function (Owen and Luzio, 2000). The mechanisms, whereby the AP-2 complex is recruited specifically to the plasma membrane, have not yet been elucidated.

Sorting signals present in receptor tails cannot alone account for the specificity of adaptors recruitment, since receptors are widely distributed. A membrane-bound docking apparatus has therefore been postulated to account for the specific organelle distribution of these molecules. The identity of the putative AP-2 docking apparatus remains unknown at the present. Recently, $PI(4,5)P_2$ has been proposed to act as a target signal for clathrin-coated vesicle assembly on the plasma membrane, as both AP-2 complexes and several of the AP-2 and clathrin-interacting proteins contain $PI(4,5)P_2$ binding domains. The upstream regulators of $PI(4,5)P_2$ production at the plasma membrane have not yet been identified. Once the coat is assembled, the nascent vesicle is released by membrane fission within the bud neck. In the case of plasma membrane-coated vesicles, this step requires the GTPase Dynamin (see below) (Damke, 1996; Hinshaw and Schmid, 1995).

In contrast to AP-2, the trafficking step regulated by the AP-1 complex is still controversial. The original proposal for the function of AP-1 was to regulate M6PR transport from the TGN to late endosomes. Consistently, AP-1 was localized to TGN (Robinson and Pearse, 1986), co-purified with clathrin-coated vesicles and interacted with M6PR tails, although not with the di-leucine motive involved in sorting at the TGN (Le Borgne et al., 1993). AP-1 recruitment to the TGN is regulated by the small GTPase ARF1 (Robinson and Kreis, 1992; Stamnes

and Rothman, 1993). This small GTPase was first shown to regulate the membrane association of coatomer, the coat components of the COP-I-coated vesicles involved in vesicular traffic in the secretory pathway (Orci et al., 1993). ARF proteins exist in the cytosol in the inactive GDP-bound form. An enzyme localized to the donor compartment catalyses the exchange of GDP for GTP (Barlowe and Schekman, 1993), and the resulting ARF-GTP molecules can bind the membrane (Barlowe and Schekman, 1993) and recruit coat sub-units (Waters et al., 1991). After budding, the GTP must be hydrolyzed by ARF in order for the coat to dissociate (Barlowe et al., 1994; Tanigawa et al., 1993). The mechanism by which ARF promotes recruitment of coat components onto the membrane is still not clear. One possibility is that ARF acts stoichiometrically by interacting directly with coat proteins/adaptors (Zhao et al., 1997). A second possibility is that ARF interacts with the hypothesized 'docking site', inducing conformational changes that would allow the docking site to bind the adaptor complex with high affinity (Le Borgne et al., 1996; Traub et al., 1993). A third possibility is that ARF may exert its effect catalytically. ARF has been reported to activate phospholipase D (PLD) (Brown et al., 1993), phosphatidylinositol-4 kinase (PI(4)P-kinase) and phosphatidylinositol,4 phosphate,5-kinase (PI(4)P-5 kinase) (Jones et al., 2000). PLD catalyses the hydrolysis of phosphatidylcholine (PC) into choline and the negatively-charged lipid-phosphatidic acid (PtdOH). PtdOH can in turn activate

PI(4)P-5 kinase, which phosphorylates PI(4)P, the product of the PI4-kinase, to PI(4,5)P2. Local increase in PI(4,5)P2 was shown to increase coatomer recruitment to TGN membranes (Ktistakis et al., 1996). However, given that PI(4,5)P2 is present also on the plasma membrane, additional docking factors must be envisaged to account for the specific localization of AP-1.

The function of AP-1 in regulating TGN to endosome transport has recently been questioned since the identification of the GGA proteins. GGAs (Golgi-localized, γ ear-containing, ARF-binding proteins) were independently identified by several groups as ARF-binding proteins and as protein-containing homology to the ear domain of γ–adaptin (Boman et al., 2000; Dell'Angelica et al., 2000; Hirst et al., 2000). GGA proteins are multi-modular molecules having all the features necessary to create a clathrin coat on Golgi membranes (Black and Pelham, 2001). They consist of four domains: the VHS domain, a domain of unknown function present in various proteins involved in vesicular traffic (Vps27, Hrs, STAM), which bind to the di-leucine-sorting signal of the M6PR and sortilin. The adjacent GAT (GGA and TOM1) domain binds ARF-1:GTP while the hinge like domain binds clathrin and the ear domain interacts with accessory proteins. GGA proteins have been shown unambiguously to regulate MPR traffic from TGN to late endosomes (Black and Pelham, 2000; Puertollano et al., 2001; Zhu et al., 2001). The obvious question raised by these findings, therefore concerns, the function of

AP-1. Are AP-1 and GGAs localized in the same vesicles? Several scenarios might be envisaged: AP-1 might function in TGN to early endosome transport or vice versa in retrograde traffic from early endosome to TGN. In agreement with this last possibility are the observations that in μ1A knockout cells M6PRs accumulate in endosomal membranes (Meyer et al., 2000), and that in addition to TGN, γ-adaptin is also found on endosomes (Futter et al., 1998). Alternatively, AP-1 and GGAs might regulate sorting of different receptors or budding from different sub-domains of the TGN (Black and Pelham, 2001).

AP-3 has recently been identified and shown to localize to TGN and to peripheral structures partially co-localizing with endosomal markers (Simpson et al., 1996). The functional characterization of this adaptor complex has been greatly facilitated by the identification of naturally occurring mutants in *Drosophila*, mouse, and human, and by creating mutations in the yeast homologue. All together these studies led to the conclusion that AP-3 is involved in regulating trafficking from the TGN-endosome to lysosome and lysosome-related organelles such as melanosomes and platelet dense granules (Simpson et al., 1996). A still open issue is whether AP-3 binds to clathrin. *In vitro* binding experiments would suggest so (Dell'Angelica et al., 1998), but it has not been possible so far to demonstrate AP-3 immuno-reactivity on purified clathrin coated vesicles, nor has co-localization between AP-3 sub-units and clathrin *in vivo* been

detected (Simpson et al., 1996). AP-4 has been just recently discovered and its function is currently unknown. It is localized mainly to TGN membranes in area not labelled with clathrin, indicating that also this adaptor may function independently from clathrin (Dell'Angelica et al., 1999).

The molecular characterization of clathrin-mediated endocytosis has revealed that the AP-2 sub-units are involved in an extensive network of protein-protein interactions. Many proteins that are engaged in these interactions are large multi-modular proteins containing one or more protein-protein interaction domains such as EH domain (Eps15 homology domains), NPF (single amino acid code) repeats, SH3 domains (Src homology), proline rich domains (PRD) and coil-coiled domains. The picture emerging from the functional characterization of these molecules is that the process of cargo recognition and coat assembly is tightly coupled to the actin cytoskeleton (see below) as well as to the machinery, which is required for vesicles budding, targeting and fusion with early endosomes (Owen and Luzio, 2000).

1.3.2 Invagination and detachment of clathrin-coated vesicles

Using GFP-tagged clathrin light chain it has been shown that invagination of clathrin-coated pits at the plasma membrane displays limited mobility within the membrane (Gaidarov et al., 1999). Moreover, despite their apparent random

distributions, coated pits form preferentially at a defined site. Treatment of cells with latrunculin B, a drug which interferes with actin assembly, increased the area of movement of coated pits suggesting that an actin-based framework is involved in the structural organization of clathrin-coated pits at the cell surface (Owen and Luzio, 2000) (see also next paragraph).

The mechanism by which an invaginated coated pit is converted into a vesicle is still poorly understood. One key regulator of this process is dynamin (Kelly, 1999). The involvement of dynamin in endocytosis was initially described in *Drosophila*. The shibire gene encoding for the fly homologue of dynamin (Chen et al., 1991; van der Bliek and Meyerowitz, 1991) bearing a temperature-sensitive mutation, presented defects in endocytosis of synaptic vesicles: the number of constricted vesicle profiles at the presynaptic membrane was increased and fewer synaptic vesicles were detected (Poodry and Edgar, 1979). In mammalian cells, dynamin has been localized to the clathrin lattice surface and is then redistributed to the neck of the invaginated coated pits. It was initially proposed that dynamin function was to constrict the neck of invaginated coated pits and that the energy was provided by the GTPase activity of dynamin (Damke et al., 1994; Sweitzer and Hinshaw, 1998; van der Bliek et al., 1993). More recently, dynamin was shown to contain a GTPase-activating domain promoting dynamin self-assembly. Over-expression of dynamin mutant in the GTPases-

activating domain resulted in the unexpected increase of endocytosis (Sever et al., 1999). These data are difficult to reconcile with the idea that dynamin is the mechanical driving force to sever coated pits and rather suggests that dynamin functions, like most GTP binding proteins, via recruiting effector proteins. Besides dynamin, other important molecules involved in clathrin-coated vesicle formation are endophilin and synaptojanin. Endophilin is localized to presynaptic terminals and interacts via its SH3 domains with dynamin and with synaptojanin (Micheva et al., 1997; Simpson et al., 1999). Both endophilin and synaptojanin are lipid-modifying enzymes. Endophilin exhibits lysophosphatidic acid acyl transferase activity (Schmidt et al., 1999). This activity results in the conversion of lysophosphatidic acid (LPA) to phosphatidic acid by transfer of arachidonate. On the basis of these results it has been proposed that membrane curvature at the neck of a clathrin-coated pit may be induced by the conversion of an inverted cone-shape lipid (LPA) into a cone-shaped lipid (phosphatidic acid) in the cytoplasmic leaflet (Schmidt et al., 1999; Sprong et al., 2001). Synaptojanin is a major presynaptic protein associated with endocytic-coated intermediates, which exhibits polyphosphoinositide phosphatase activity. Synaptojanin -/- mice have elevated levels of phosphatidylinositol 4,5-bisphosphate (PtdInsP2) and show an accumulation of clathrin-coated vesicles, indicative of a role for synaptojanin in uncoating (the uncoating process is characterized by the disassembly of clathrin

and adaptors in the cytoplasm). Vesicles uncoating may be a pre-requisite for membrane fusion to occur and may allow recycling of clathrin and adaptors for a next round of internalization (Cremona et al., 1999). PI(4,5)P2 is required for clathrin-coated vesicle formation (Jost et al., 1998) and many proteins involved in the formation of clathrin-coated vesicles bind to PI(4,5)P2, including dynamin and AP-2 (Corvera et al., 1999). Therefore the polyphosphoinositide phosphatase activity of synaptojanin may favour uncoating by reducing the level of PI(4,5)P2 in the vesicle, which in turn would cause the dissociation of AP2 and clathrin (Hill et al., 2001). Another protein involved in uncoating is auxillin. Auxillin was first identified as a coat protein enriched in brain (Ahle and Ungewickell, 1990). Auxillin binds to clathrin lattices and in the presence of ATP recruits the cofactor hsp70 and mediates coat disassembly (Ungewickell et al., 1995).

1.4 Endocytic transport: role of the cytoskeleton

Intracellular organelles are highly dynamic entities continuously changing their shape and position during time. Organelle motility facilitates transport of cargo molecules from one destination to the other and might significantly reduce the distance vesicles need to travel before docking and fusing with target compartments. The term "organelle dynamics'' refers here also to the complex series of events determining membrane remodelling and changes in organelle

shape. These changes might favour vesicular budding and fusion, or, as in the case of early endosomes, might function as sorting mechanisms. Other examples of membrane remodelling include plasma membrane changes during cell migration and phagocytosis. All these processes are tightly regulated and require interaction of organelles with cytoskeletal filaments.

Actin filaments lying beneath the plasma membrane are cross-linked into a network by actin-binding proteins and form the so-called cell cortex (Figure 3).

Almost all components of the endocytic machinery interact directly or indirectly with actin or with one of the actin binding proteins (Qualmann et al., 2000). Several lines of evidence suggest a role for the cortical actin in early steps of endocytosis. A functional actin cytoskeleton is essential for the receptor-mediated uptake of the α-Factor in yeast *Saccharomyces cerevisiae* (Kubler and Riezman, 1993; Mulholland et al., 1994). Depolymerisation of actin filaments by the fungal metabolite cytochalasin D completely abolishes phagocytosis by macrophages, a process which requires a major reorganization of the plasma membrane to engulf large particles (Axline and Reaven, 1974). Morphological and kinetic evidence for the involvement of actin in facilitating the uptake of ligands via coated pits, as well as the sorting of recycled ligands concentrated in the perinuclear area of the cells, have also been provided (Durrbach et al., 1996). Moreover, in polarized epithelial cells actin has been shown to be required for

apical endocytosis of membrane-bound and fluid-phase markers (Jackman et al., 1994).

The precise molecular mechanism underlying actin functions in endocytosis remains unclear. One possibility is that the rigid cortical actin lying beneath the plasma membrane constitutes a physical barrier and that local actin de-polymerization is required for endocytosis to occur. Indeed the immediate vicinity of clathrin-coated pits is almost devoid of actin fibres (Fujimoto et al., 2000). A second possibility might be that the actin cytoskeleton participates in late scission events of clathrin vesicles formation providing the driving force leading to vesicular budding (Simpson et al., 1999). This function would involve an actin-binding motor molecule such as unconventional myosin motors. A type I myosin molecule represents a good candidate to act as a molecular motor, since this molecule was shown to be able to move actin filaments on a phospholipid substrate (Adams and Pollard, 1989; Zot, 1995). Recently, Myosin VI has been shown to associate with clathrin-coated vesicles and to modulate clathrin-mediated endocytosis (Buss et al., 2001). Alternatively, actin may help to organize the endocytic machinery at the plasma membrane by defining specific sites of endocytosis (Owen and Luzio, 2000; Roos and Kelly, 1999). Finally actin might regulate vesicle movement. Clathrin-coated vesicles and endosomes have been

described to be associated with actin comet tails both *in vivo* (Frischknecht et al., 1999; Rozelle et al., 2000) and *in vitro* (Taunton et al., 2000).

Microtubules are involved in maintaining the steady-state distribution of organelles in the cytoplasm and in regulating their long-range bi-directional movement (Kelly, 1990). Microtubules radiate outward from the perinuclear microtubule-organising centre (MTOC), with their plus-ends facing the cell periphery (Cole and Lippincott-Schwartz, 1995). They have been compared to highways along which endocytosed material move from peripheral sorting endosome to perinuclear late and recycling endosomes (see Figure 3) (Bomsel et al., 1990; Gruenberg et al., 1989).

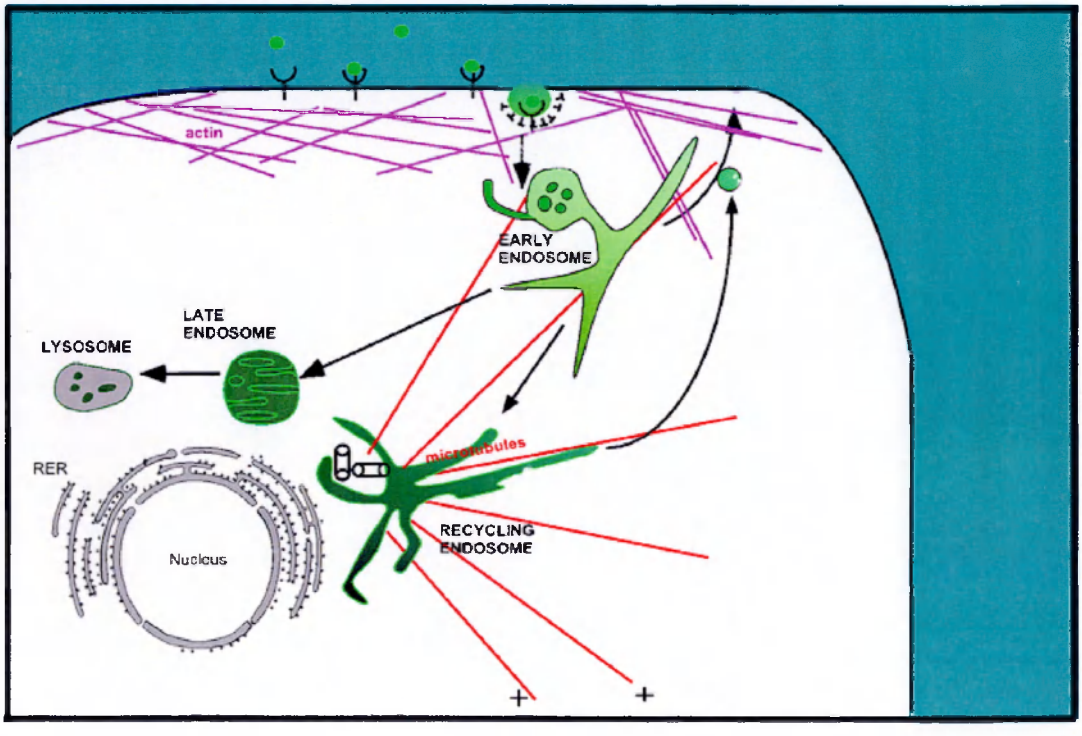

Figure 3: Organization of the actin and microtubule cytoskeletal elements. Actin filaments are organized into a variety of linear bundles and three-dimensional networks most highly concentrated beneath the plasma membrane. Microtubules are nucleated from the MTOC and radiate out towards the cell periphery.

Movement of organelles along microtubules requires 'motor proteins' that use the energy derived from the hydrolysis of ATP to promote organelle motility. Two families of microtubule-stimulated ATPases, kinesin and dynein, have been shown to function as motors for microtubule-based transport (Allan, 1995; Bloom, 1992). Kinesin motors primarily move toward the plus end of microtubules, although some kinesins have been shown to be minus ended-directed motors (Schroer et al., 1988; Vale et al., 1985). Dynein moves only toward the minus end (Schroer et al., 1989) and is required for fusion of endosomal carrier vesicles with late endosomes *in vitro* (Aniento et al., 1993). The motors regulating early endosome motility have not yet been identified. Interestingly, two recent reports have implicated members of the Rab family of small GTPases as regulators of organelle motility providing an explanation of how motor proteins might be recruited and activated in an organelle-specific manner (see next section). Microtubules are not only required for endosome motility and positioning but determine also the extent to which processes such as endosome tubulation occur (Wood and Brown, 1992). The mechanisms and functional implications controlling endosome tubulation will be treated in more detail in the chapter describing the molecular regulation of endocytic-sorting and membrane recycling (see chapter 1.9).

1.5 Vesicle and organelle docking and fusion

Upon budding from a donor compartment a vesicle has to find its target compartment, fuse and release its content. The specificity of this membrane transport reaction is fundamental in preserving organelle identity and to ensure proper flow of cargo. The SNARE (soluble NSF attachment protein receptor, where NSF stands for N-ethylmaleimide-sensitive factor) hypothesis was proposed to explain in molecular terms the mechanism of vesicular docking and fusion. It postulates that each vesicle carries a specific integral membrane protein, a v-SNARE, that pairs with a corresponding t-SNARE on the target membrane. Subsequently, NSF binds to the SNARE complex, via the soluble NSF attachment protein (α-SNAP), and its ATPase activity leads to SNARE complex dissociation and membrane fusion (Sollner et al., 1993). In detergent extract, v- and t-SNAREs can indeed assemble with NSF and α-SNAP into a 20S particle, which is dissociated upon ATP hydrolysis by NSF (Paek et al., 1997; Sogaard et al., 1994; Sollner et al., 1993). According to this model, therefore, NSF and SNAPs are universal components of a conserved docking-fusion apparatus, while SNARE proteins are thought to provide specificity to each single docking and fusion event.

The best-characterized members of the SNARE proteins family are the neuronal SNAREs involved in synaptic vesicle exocytosis. Their function has

provided a paradigm for SNAREs function in membrane fusion. The SNAREs hypothesis indeed originated from the molecular dissection of proteins involved in synaptic vesicle exocytosis (reviewed by: (Sudhof, 1995). Synaptic transmission requires a v-SNARE, known as VAMP (vesicle-associated membrane protein) or synaptobrevin (Trimble et al., 1988) and two t-SNAREs, syntaxin-1 and SNAP25. Upon pairing, these SNAREs form an extremely stable ternary complex ('SNARE core complex'). Many SNAREs have now been identified and localized to distinct organelles along both the secretory and the endocytic pathway in cells as evolutionary distant as yeast and neurons (Aalto et al., 1993; Becherer et al., 1996; Bennett and Scheller, 1994; Dascher et al., 1994; Hardwick and Pelham, 1992; Nagahama et al., 1996). The hallmark of all SNARE proteins is that they contain conserved heptad repeat sequences that form coiled-coiled structures. Recently, the crystal structure of the neuronal SNARE 'core complex' has been solved. In the complex, one coil of syntaxin-1 and VAMP, and two coils of SNAP-25 intertwine to form a four-stranded coiled-coil structure. These data are in agreement with several other studies that predicted a parallel arrangement of the core complex (Hanson et al., 1997; Lin and Scheller, 1997; Poirier et al., 1998). This topological configuration strongly supports the hypothesis that formation of the SNARE complex fuses two membranes by bringing them into close apposition rather than simply docking them. According to this view, the SNARE complex

'zips' from the membrane distal amino termini to the membrane-proximal carboxyl termini overcoming the energy barrier to drive fusion of the lipid bilayers. It is therefore the assembly and not the disassembly, as originally postulated, of the core complex that would drive membrane fusion. Moreover, although the function of NSF and α-SNAP in dissociating the SNARE complex has not been disproved, studies of homotypic vacuole fusion in *Saccharomyces cerevisiae* have been challenging their role in the final step of membrane fusion (Wickner and Haas, 2000). A current working model considers the homotypic vacuole fusion reaction as divided into three sequential steps: priming, docking and fusion (Figure 4). Priming is characterized by the set of reactions that activate vacuoles for subsequent docking and does not require vacuole-to- vacuole contact. Docking is characterized by the association of vacuoles and can be divided into a reversible tethering step, when vacuoles at a distance of up to 100 nm are captured and tethered to each other by extended coil-coiled molecules, and a subsequent step of close association caused by *trans*-SNARE pairing. After docking, the paired vacuoles undergo fusion, which is assayed by the mixing of vacuoles contents. These studies have established that the function of NSF (Sec18p)/α-SNAP (Sec17p) is more consistent with a role in priming SNAREs for interaction, possibly by dissociating pre-existing v-t-SNARE complexes on the vacuole membranes (Conradt et al., 1994; Mayer and Wickner, 1997; Mayer et al., 1996;

Ungermann et al., 1998). The ATPase activity of NSF would provide the energy required to disassemble v- and t-SNARE complexes on the same membrane so that they become available for a new round of membrane docking and fusion. In this way NSF/SNAP would be responsible for an early 'priming' reaction preceding docking and fusion (ATP-dependent priming and ATP-independent fusion). Tethering is mediated by Rab proteins and their effectors (see below and next section), while trans-SNAREs pairing renders docking irreversible. SNARE pairing does not seems to be required for the final step of vacuolar membrane fusion as SNARE complexes could be dissociated and prevented from reassembly without affecting content mixing of the vacuoles (Ungermann et al., 1998).

The relatively restricted intracellular localization of SNARE proteins, coupled with the observation of a stable SNARE complex *in vitro* led to the hypothesis that formation of SNARE complexes *in vivo* mediates the specificity of vesicle docking and fusion. When yeast SNAREs were reconstituted into liposomes in all possible combinations and content mixing was used as read-out of fusion, a remarkable specificity of interactions was observed. This result implies that, at least *in vitro*, SNAREs are the minimal requirement for specific vesicular docking and fusion (McNew et al., 2000). However, although SNAREs are enriched in certain organelles, they inevitably spread throughout cellular compartments as a consequence of vesicular traffic. SNAREs must therefore be

kept inactive until they return to their specific site of function. For instance, accessory proteins are required to protect SNAREs from promiscuous binding and to impede their rebinding *in cis* after fusion and disassembly of the core complex. Such function seems to be the task of the yeast sec1 related proteins (Jahn, 2000).

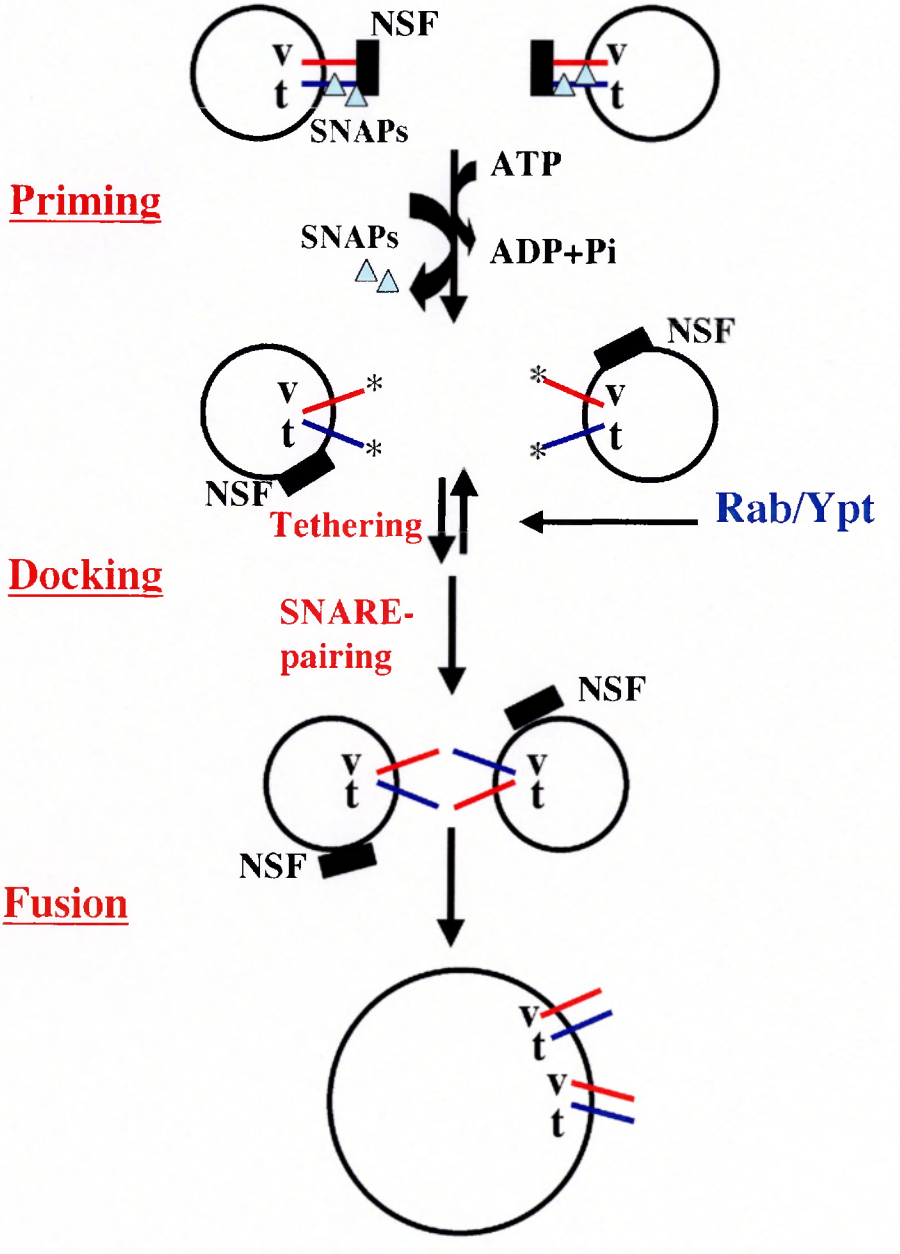

Figure 4: Working model for SNARE proteins function in homotypic vacuole fusion (according to Ungermann et *al.*, 1998)
NSF is thought to activate v- and t-SNARE marked (with an "*") allowing them to interact. V= v-SNARE, t=t-SNARE. See text for details.

Munc-18, a mammalian homologue of the yeast Sec1p, has been shown to bind directly to the t-SNARE syntaxin-1 (Garcia et al., 1994; Hata et al., 1993; Pevsner et al., 1994), and to be excluded from the SNARE complex, consistent with the t-SNARE protection model (Garcia et al., 1995; Sollner et al., 1993).

The role of SNAREs in docking has also been challenged by the findings of several laboratories. SNARE-cleaving neurotoxins do not reduce vesicle docking at the synapse (Hunt et al., 1994), and SNARE-deficient flies have an increased rather than a decreased number of docked vesicles (Schulze et al., 1995). It seems therefore, that SNARE molecules alone cannot account for the high fidelity and specificity of vesicle docking and fusion. Such specificity is more likely provided at the stage of vesicular targeting and tethering by long, extended proteins localized to the target membrane that recognize, capture and tether the appropriate vesicles (Zerial and McBride, 2001). The formation of productive SNARE complexes may also depend on such molecules. Small GTPases of the Rab family have all the propriety required to provide regulation to SNARE complex assembly and to ensure specificity of membrane tethering.

1. 6 Ypt1/Sec4/Rab family of small G-proteins

Ypt1/Sec4/Rab proteins are small Ras-related GTPases involved in regulation of intracellular transport. The first identified members of this class were two yeast proteins: Ypt1p (Gallwitz et al., 1983) and Sec4p (Salminen and Novick, 1987). Further proteins belonging to this family have been discovered in both budding and fission yeast and other eukaryotes (reviewed by (Novick and Zerial, 1997)). There are more than 40 mammalian homologues of Ypt1/Sec4 identified to date and named Rab proteins (because they were originally isolated as Ras-like genes from rat brain). In human there are as many as 63 family members as estimated from the now available genome sequence and from expressed-sequence tags (ESTs) (Zerial and McBride, 2001).

A characteristic feature of Rab/Ypt proteins is their specific intracellular distribution (Simons and Zerial, 1993). Each member of the class is localized to membranes of certain organelles and regulates, therefore, a particular step in transport pathways. For example, Ypt1p in *Saccharomyces cerevisiae* mediates ER to Golgi transport and is found in association with these organelles (Jedd et al., 1995). In temperature-sensitive Ypt1p mutants, transport from the endoplasmic reticulum to the Golgi complex was impaired, leading to an accumulation of carrier vesicles unable to deliver their cargo (Segev et al., 1988). The same phenotype was demonstrated for Sec4p mutant cells and in this case the traffic block was localized between the Golgi and the cell surface (Goud et al., 1988;

Salminen and Novick, 1987). The Sec4p localization to secretory vesicles and to the plasma membrane is consistent with the trafficking impairment present in Sec4p mutants.

The crystal structure of p21/Ras, in both its active and inactive conformation, has been solved and has been used as a paradigm for the function of individual domains of the Ras-like GTPases (de Vos et al., 1988; Krengel et al., 1990). Based on the high degree of similarity between Rab proteins and Ras, four highly conserved sequence motifs have been identified and shown to be necessary to form the nucleotide/Mg^{2+}binding domain (GNB), containing the key residues for binding and hydrolysis of GTP. Point mutations within these motifs can change the nucleotide affinity of p21/Ras stabilizing this GTPase either in the GTP-bound or in the GDP-bound conformation. Those mutations, leading to a protein that is constitutively active, cause neoplastic growth because they constitutively transduce mitogenic signals, by-passing the normal regulation by growth factor receptors.

By analogy to Ras, similarly Rab mutants have been engineered and successfully used to investigate the function of these proteins in membrane traffic.

1.6.1 The Rab cycle(s): The dual life of a Rab protein

Like other GTPases, Rab proteins have the ability to bind guanine nucleotides and to hydrolyze GTP. However, their intrinsic rates of nucleotide exchange and GTP hydrolysis are very low and therefore Rab/Ypt proteins can exist in three different conformational states: inactive GDP-bound, nucleotide free and active GTP-bound (Novick and Brennwald, 1993). Due to alternating between active and inactive forms, Rab/Ypt proteins can act as "molecular switches". In the GTP-bound active form Rab proteins are able to recognize specific downstream effectors of the transport machinery, while the GTPase activity ensures that the protein remains in the active conformation only for a limited length of time. As the spontaneous rate of nucleotide hydrolysis and exchange occurs at low rates, this cycle, *in vivo*, is regulated by the interaction with accessory proteins. Guanine nucleotide exchange factors (GEF), convert GDP-bound Rab proteins into the GTP-bound, and GTPase-activating proteins (GAP) convert GTP-bound Rab protein into a GDP form (Figure 5) (Boguski and McCormick, 1993).

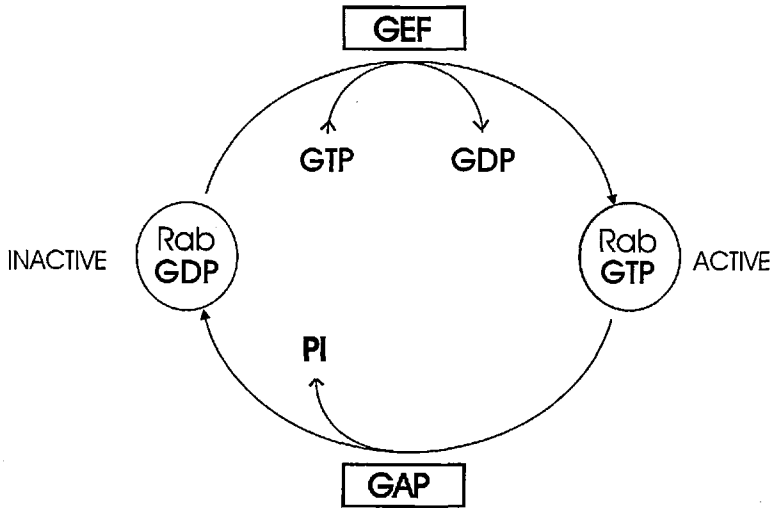

Figure 5: GTPase molecular switch
See text for details.

In a nucleotide-dependent manner Rab proteins also undergo cycles of membrane association and dissociation. In cytosol, Rab proteins are bound to Rab GDP dissociation inhibitor (GDI), an important co-factor in the Rab cycle that inhibits GDP dissociation and maintains Rab proteins in their GDP-bound conformation (Pfeffer et al., 1995; Soldati et al., 1993). RabGDI maintains Rab proteins in a dynamic equilibrium by delivering them to their appropriate compartment (Soldati et al., 1994; Ullrich et al., 1994) and, upon GTP hydrolysis, by extracting them from the membrane. The mechanisms regulating the membrane association of Rab proteins are not completely understood. A GDI-displacement factor (GDF) is subject to the Rab:RabGDI protein complex. This factor would cause release of GDI into the cytosol and would allow binding of Rab:GDP to the membrane. A specific GDP-GTP exchange factor/activity would then convert the Rab protein into the GTP-bound, active conformation (Pfeffer, 1994). In

agreement with this model, a protein functioning as GDI-displacement factor for endosomal Rab proteins which is lacking nucleotide exchange activity (Dirac-Svejstrup et al., 1997) as well as exchange factors lacking GDI-displacement factor activity, have been identified (Horiuchi et al., 1997). However, it is still unknown whether recognition of RabGDI complex and release of GDI are events mediated by the same factor.

1.6.2 Post-translational modification of Rab proteins

After being synthesized as soluble proteins, Rab proteins are isoprenylated on cysteine residues at their C-terminus as a requisite for membrane binding. This reaction is catalyzed by the Rab geranylgeranyl-transferase (RabGGTase) (Seabra et al., 1992; Seabra et al., 1992), a multisubunit enzyme, comprising a catalytic heterodimer of tightly associated α and β subunits, and an accessory factor, the Rab Escort Protein (REP) (Armstrong et al., 1993). According to the current model based on the mammalian system (Alexandrov et al., 1994), a newly synthesized Rab protein is bound by REP and the complex is recognized by Rab GGTase, which then allows the subsequent digeranylgeranylation of the bound Rab protein. The mechanism of this reaction has been described in detail and comprises the formation of a stable complex between monogeranylgeranylated Rab and REP. This complex enables the subsequent addition of an isoprenoid moiety to the second C-terminal cysteine residue to produce digeranylgeranylated Rab (Shen and Seabra, 1996). Moreover, geranylgeranylation requires Rab protein in its GDP-bound form (Seabra, 1996). After completing the prenylation reaction, REP stays associated with the modified Rab and, like GDI, acts as a chaperone to deliver it to its specific target membrane. Upon membrane association of Rab, REP is released into the cytosol for another round of prenylation.

REP-1 protein shares structural homology and many functional features with Rab GDI, such as the ability to inhibit GDP dissociation from Rabs and to deliver and to extract Rabs from membranes (Alexandrov et al., 1994). Despite these similarities it has been shown that, *in vivo*, REP is responsible for prenylation and initial membrane delivery of a Rab protein, while further recycling is performed by Rab GDI that is unable to assist in the prenylation reaction (Alexandrov et al., 1994).

1.7 Functions of Rab proteins

The first function assigned to Rab proteins was to control the specificity of membrane fusion by regulating the pairing between v- and t-SNAREs. Experiments conducted in the yeast *S. cerevisiae* revealed a genetic link between Rab and SNARE proteins, although no biochemical proof for a direct link could be provided. Recent data have revealed additional functions of Rab proteins in vesicle and organelle motility along cytoskeleton elements as well as in vesicular budding events. These findings might indicate that sequential steps of vesicular transport are co-ordinated by the same GTPase (Pfeffer, 2001; Segev, 2001; Zerial and McBride, 2001).

As for all the other GTPases, Rab proteins function in their GTP active state by recruiting downstream effector proteins to the membrane compartment

where they are localized. The identification of the molecular machinery controlled by these GTPases has been, and will be, therefore fundamental to understanding the basic principles of membrane transport. In the following paragraph, I will summarize the functions so far attributed to Rab proteins and their effectors in i) membrane tethering and SNARE assembly regulation, ii) vesicular budding and iii) organelle-vesicle motility. In the last section, the molecular evidence supporting a role of Rab proteins in organelle biogenesis and maintenance will be described, using Rab5 as paradigm of function for the other family members.

1.7.1 Membrane tethering

As previously discussed, the specificity of membrane targeting was believed to depend upon the correct pairing between v- and t-SNAREs. Although there is evidence for this hypothesis from *in vitro* studies, it appears that the specificity of vesicle targeting is conferred by a pre-SNARE step, when vesicles at a distance of up to 100 nm from their target compartment are captured and tethered by extended coil-coiled molecules (Chen and Scheller, 2001; Pelham, 2001; Wickner and Haas, 2000). These molecules are therefore referred to as tethering molecules and several studies both in yeast and mammals have shown that Rab effectors are tethering factors (Zerial and McBride, 2001). According to this view, SNARE pairing would be required in a post-docking step, presumably

for membrane fusion. Very likely, the specificity of Rab-mediated membrane tethering is directly linked and superimposed onto the specificity of SNARE-mediated membrane fusion ensuring the highest reliability to intracellular transport (Chen and Scheller, 2001). Indeed, recently several reports have provided evidence for a direct interaction between SNAREs and tethering molecules. In the yeast secretory pathway, tethering of ER-derived vesicles to the Golgi complex depends on the membrane recruitment of USO1p by Ypt1p (Cao et al., 1998). Whereas in yeast Uso1p is recruited selectively to the Golgi complex, in mammalian cells p115, the functional and structural ortholog of USO1p, is recruited already by Rab1 to COPII vesicles as they bud from the ER (Allan et al., 2000). It should be noted, however, that Rab1 and p115 were shown to interact directly, whereas no direct interaction could be detected between USO1p and Ypt1p. A multi-protein complex called TRAPP (transport protein particle) also functions in tethering ER-derived vesicles to the Golgi complex and catalyses nucleotide exchange on Ypt1p (Sacher et al., 1998). The precise function of this complex is still unknown. Another complex, the exocyst, functions both in mammalian and yeast cells, in tethering Golgi-derived vesicles to the plasma membrane. In yeast, Sec15p, one of the eight proteins of the exocyst, binds to the Rab protein Sec4p, (Guo et al., 1999) while Sec3p, another component of the complex, is associated with the plasma membrane (Finger et al., 1998).

Very few tethering molecules have been identified in the endocytic pathway. The Rab5 effector EEA1 mediates tethering/docking of early endosomes and of CCVs to early endosomes (Christoforidis et al., 1999; Rubino et al., 2000). EEA1 is an extended coiled-coil molecule specifically localized to early endosomes and containing, at the two opposite N and C-terminal ends, a Rab5 binding site (Lawe et al., 2000). EEA1 has been proposed to confer directionality to vesicular transport from the plasma membrane to the early endosome by bringing together two membranes bearing Rab5 (Rubino et al., 2000; Simonsen et al., 1998). Consistent with this hypothesis Rab5 localizes to both CCVs and early endosomes and is required for heterotypic fusion between CCVs and early endosomes, as well as for homotypic fusion between early endosomes (Rubino et al., 2000). EEA1, interacts directly with syntaxin 13 and syntaxin 6 , two SNAREs involved in endosomal fusion events, providing a direct link between the tethering and fusion machinery (McBride et al., 1999; Simonsen et al., 1999). In yeast, the Rab protein Ypt7p binds to and regulates the localization of HOPS, a multi-protein complex involved in vacuolar membrane docking. The HOPS complex and Ypt7p are required on both vacuolar partners undergoing homotypic fusion indicating also in this case, a symmetrical requirement (Haas et al., 1995; Price et al., 2000).

On the basis of these results, the asymmetric requirement model originally proposed (Bourne, 1988) is no longer tenable. According to this view, a GEF localized to the donor compartment converts Rab:GDP to Rab:GTP. Rab:GTP is incorporated into a nascent vesicle, transported towards the acceptor compartment where it promotes fusion. Here, a GAP catalyses GTP hydrolysis and Rab:GDP is recycled for a next round of transport (Bourne, 1988). This model is, however, difficult to reconcile with the most recent results, especially those obtained on Rab5 and its sequential role in endocytosis. First, Rab5 is localized on CCVs (functioning as transport intermediate) (Horiuchi et al., 1995) as well as early endosomes (acceptor compartment) (Bucci et al., 1992) and is required on both CCVs and early endosomes for productive fusion to take place (Rubino et al., 2000). Second, membrane-bound Rab5 undergoes futile cycles of nucleotide binding and hydrolysis even in the absence of membrane fusion. (Rybin et al., 1996). Therefore, at least in the case of Rab5, the physical segregation model of active Rab proteins between acceptor and donor compartment cannot be applied.

1.7.2 Functional links between Rabs and SNAREs

Several Rab effectors have been shown to bind either directly or indirectly to SNARE molecules and thus regulate their assembly. Sec1-related proteins (like Vps33p and Vps45) regulate SNARE pairing by binding to syntaxin molecules

and preventing their binding to cognate v-SNAREs. Rab effectors, such as Vac1p and Rabenosyn-5, have been shown, both in yeast and mammalian cells, to bind Sec1 related proteins (Nielsen et al., 2000; Tall et al., 1999). The function of these interactions might be the removal of the inhibitors from the SNAREs and/or the stabilization of the trans-paired conformation (Pevsner et al., 1994; Yang et al., 2000). Other Rab effectors bind directly to SNAREs as in the case of the Rab5 effector EEA1 which, as discussed above, interacts with syntaxin13 and 6 (McBride et al., 1999; Simonsen et al., 1999), or the Ypt7p effector proteins and their interaction with the Vam3p complex (Sato and Wickner, 1998). Rab effectors and SNARE molecules can also form oligomeric complexes with α-SNAP and NSF, whose assembly is regulated by the ATPase activity of NSF (McBride et al., 1999). All these interactions provide convincing support to the hypothesis that membrane tethering and SNARE-dependent membrane fusion are directly linked processes co-ordinated by the same GTPase.

1.7.3 Function of Rab proteins in vesicular budding and organelle-vesicle motility

Rab proteins have also been implicated in vesicle budding, although the mechanisms of action in the regulation of this process are not clear and in some cases contradictory data have been obtained from *in vivo* versus *in vitro* studies.

Rab proteins might influence vesicle budding either by regulating the assembly of coat components or by controlling the sorting of cargo molecules into nascent vesicles.

Rab1 was suggested to act at the vesicle budding stage during *in vitro* ER-to-Golgi transport (Peter et al., 1994). However, more recently it has been shown not to be required for the formation of COPII vesicles (Allan et al., 2000). The yeast Rab proteins, Ypt31p and Ypt32p, seem to play a role in budding of secretory vesicles from the trans-Golgi network as mutations in these genes lead to accumulation of aberrant Golgi structures (Benli et al., 1996). These data are also compatible with a role for these proteins in intra-Golgi transport or in the formation of vesicles at the exit point of the Golgi complex (Jedd et al., 1997). Rab6 was found associated with a protein complex, and this complex was shown to be needed for TGN-derived vesicle budding *in vitro* (Jones et al., 1993). Moreover, RabGDI abolishes vesicle formation in various cell-free systems indicating a possible role for Rab proteins in this process (Deretic et al., 1996). Rab5 has been shown to be required during the process of clathrin-coated pit formation (McLauchlan et al., 1998) *in vitro* as well as in the regulation of the half-life of clathrin-coated pits *in vivo* (Bucci et al., 1992). The small GTPase Rab9 was shown to be required for retrograede transport of M6PR from late endosomes to TGN, presumably functioning in a budding step (Lombardi et al.,

1993). Recently, the Rab9 effector TIP47 has been shown to bind the cytoplasmic tail of the M6PR, thus providing an additional function for Rab effectors in cargo sorting (Carroll et al., 2001).

Collectively, these findings suggest that the mechanisms underlying the formation of transport vesicles are tightly coupled to the targeting and fusion machinery (i.e. Rab proteins and their effectors) necessary for later transport steps.

As already mentioned in the paragraph on vesicle and organelle motility (see paragraph 1.4), Rab proteins also regulate the attachment and movement of organelles along cytoskeletal elements. Rab6 was shown to interact with a kinesin motor named Rabkinesin6 and to regulate retrogade transport from the Golgi back to the ER (Echard et al., 1998). Rab5 was shown to regulate both the attachment to, as well as the movement of early endosomes along, microtubules and to stimulate minus-end directed motility (Nielsen et al., 1999). The involvement of Rab proteins and their effectors in regulating vesicle budding, organelle motility, membrane tethering and fusion reflects the need to co-ordinate all steps of a vesicle transport process, ensuring that they occur at the right time and in the right place.

Novel evidence links the function of Rab proteins also to actin-dependent vesicle motility. Genetic interactions between Sec4p and the myosin heavy chain Myo2p suggests that exocytic vesicles are propelled by motor proteins along actin

filaments towards their site of fusion with the plasma membrane (Pruyne et al., 1998; Schott et al., 1999). Another genetic link between Rab and myosin proteins is the one between Rab27 and myosin-Va (Menasche et al., 2000). Both these proteins are involved in melanosome transport in melanocytes and their corresponding genes have been found mutated in a human disease and in a mouse model of melanosomes dysfunction (Bahadoran et al., 2001). Rab11 and MyosinVb have been shown to interact directly, and to function in, the delivery of endocytic-recycling vesicles to the plasma membrane (Lapierre et al., 2001).

1.7.4 Localization of Rab proteins along the endocytic pathway

Many Rab proteins have been localized to endocytic organelles, reflecting the need for a sophisticated molecular machinery to control multiple membrane transport reactions in which these organelles are engaged. Rab5 and Rab4 are both localized to sorting endosomes and exert complementary functions in controlling entry and exit out of this compartment (Bucci et al., 1992; van der Sluijs et al., 1992). While Rab5 controls traffic from the plasma membrane to sorting endosomes, Rab4 has been implicated in the regulation of a recycling step not yet identified. Rab4 may regulate the fusion of early endosome-derived transport vesicles with recycling endosomes or, alternatively, it may function in the 'short circuit' of the recycling pathway, mediating the fusion of early endosome-derived

vesicles with the plasma membrane (Daro et al., 1996; van der Sluijs et al., 1992). Rab11 was localized to pericentriolar recycling endosomes and shown to regulate traffic through this compartment (Ullrich et al., 1996). Since recycling endosomes have thus far been distinguished only on the basis of itinerant cargo and their position in the cytosol, this finding has provided further support for the existence of biochemically distinct sorting (positive for Rab5 and Rab4) and recycling (positive for Rab11) endosomes. Other Rab proteins localized to early endosomes include Rab15 and Rab22 (Zuk and Elferink, 1999), Rab17, 18, 20 and 25, some being expressed only in polarized cells where they associate with apical endocytic structures (Lutcke et al., 1993; McMurtrie et al., 1997; Zacchi et al., 1998).

Rab7 and Rab9 are both localized to late endosomes (Chavrier et al., 1990; Lombardi et al., 1993), and control different transport steps. Rab7 seems to be involved in the delivery of material from early sorting endosomes to late endosomes (Feng et al., 1995), whereas Rab9 regulates transport from late endosomes to the TGN (Lombardi et al., 1993).

1.7.5 Multiplicity of Rab5 effectors and their function in the biogenesis of a Rab domain.

The finding that the same Rab protein can regulate multiple membrane transport processes such as vesicle budding, movement and tethering provides on

the one hand a mechanism of molecular co-ordination to sequential transport reactions. However, on the other hand, how can a single GTPase efficiently deal with such a variety of tasks? In this respect the multiple roles played by Rab5 in the early endocytic pathway provide a representative example. This GTPase is localized to the plasma membrane, CCVs and early endosomes and acts as a rate-limiting component in endocytosis (Bucci et al., 1992). It is involved in clathrin-coated vesicle formation at the plasma membrane (McLauchlan et al., 1998) and is required for their subsequent fusion with early endosomes as well as for homotypic fusion between early endosomes (Gorvel et al., 1991). Moreover, Rab5 regulates endosome motility and attachment to microtubules (Nielsen et al., 1999). The recent identification of a large number of Rab5 effectors has given important insights into the mechanism of action of this GTPase. Using an affinity chromatography approach more than twenty proteins were shown to interact specifically with active GTP-bound Rab5 (Christoforidis et al., 1999). It is likely therefore that Rab5 uses each of these effectors- or subgroups thereof-, to carry out different functions.

Even if to date only some of Rab5 effectors have been identified, an important principle has nevertheless emerged from their functional characterization which is unique among GTPases of the Ras superfamily: Rab5 effectors act co-operatively. The Rabaptin-5/Rabex-5 complex activates Rab5

(Horiuchi et al., 1997; Lippe et al., 2001) which can in turn bind to hVPS34, a phosphatidylinositol-3 kinase, that specifically generates phosphatidyinositol-3-phosphate (PI(3)P) (Christoforidis et al., 1999). The concomitant presence of PI(3)P in the environment of active Rab5 is essential for the localization of two other Rab5 effectors, EEA1 (Stenmark et al., 1996) and Rabenosyn-5 (Nielsen et al., 2000). Both proteins bind to PI(3)P through their FYVE finger domain, a protein modular element that specifically interacts with this phospholipid (Stenmark and Aasland, 1999) and, as described above, provide complementary regulatory functions on the SNARE machinery (McBride et al., 1999; Nielsen et al., 2000). In addition, EEA1, the Rabaptin-5/Rabex-5 complex and syntaxin13 form large molecular weight oligomers whose assembly is regulated by the ATPase activity of NSF (McBride et al., 1999). On the basis of protein-lipid interactions, cooperativity between effectors and protein oligomerization, it has been proposed that Rab5, through its effector proteins, organizes a membrane domain defining the site of entry into early endosomes (Figure 6) (McBride et al., 1999; Miaczynska and Zerial, 2002; Sonnichsen et al., 2000; Zerial and McBride, 2001). The biogenesis of this membrane domain depends on the localized production of PI(3)P and its functional properties are determined by the recruitment of specific molecules that bind both PI(3)P and Rab5 (Zerial and McBride, 2001). Rabenosyn-5 regulates SNARE pairing through VPS45 (Nielsen

et al., 2000) while EEA1 functions as a tethering molecule and interacts directly with syntaxin13, the t-SNARE regulating fusion between early endosome (McBride et al., 1999). The compartmentalization of Rab5 effectors within a restricted membrane domain may contribute to ensure specificity and efficiency to membrane fusion events by retaining and locally activating SNARE molecules at their site of action.

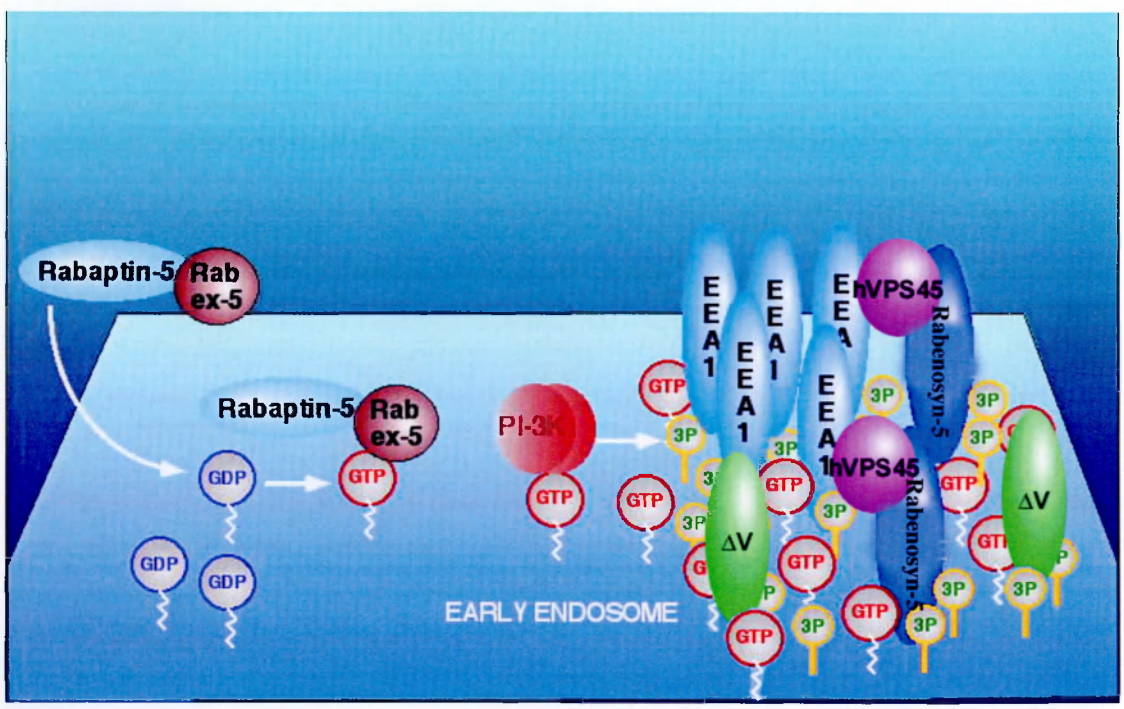

Figure 6: Model proposing the role of Rab5 and its effectors in the organization of a membrane domain.

Rab5GDP is indicated as a blue circle labelled GDP. Rab5GTP as a red circle labelled GTP. The Rabaptin-Rabex-5 complex catalyses nucleotide exchange on Rab5. Active GTP-bound Rab5 interacts with the PI-3 kinase VPS34 and stimulates PI(3)P production. The concomitant presence of active Rab5 and PI(3)P allows the membrane recruitment of EEA1 and Rabenosyn-5. ΔV indicates the putative Rab5 effectors controlling endosome motility. See text for details.

Interestingly, the Rab5-dependent movement of endosomes along microtubles also requires PI(3)P production (Nielsen et al., 1999). This observation suggests that a Rab5 effector, possibly a microtubular associated protein and/or a motor protein, is also a PI(3)P binding protein or recruited via interaction with PI(3)P-dependent mechanisms. It appears, therefore that the formation of a PI(3)P-Rab5 enriched membrane domain is presumably required for both endosome fusion and motility. Functional specificity to this membrane domain would instead be conferred by the nature of the effector molecule recruited (Miaczynska and Zerial, 2002).

The Rab5-dependent organization of a restricted membrane domain on early endosomes is spatially and temporarily regulated by its GTP cycle. The higher the levels of GTP-Rab5, the higher the recruitment of Rab5 effectors, the higher the fusion activity (Bucci et al., 1992) and motility of endosomes towards the minus end of microtubles (Nielsen et al., 1999). Consistent with this proposal, over-expression of a Rab5 mutant deficient in GTP hydrolysis has profound effects on endosome morphology, topology and function, leading to the accumulation of expanded vacuoles in the peri-nuclear region (Bucci et al., 1992).

The model of membrane domain compartmentalization of Rab5 effectors on the early endosomes is in agreement with the heterogeneous morphological appearance of these organelles (see Figure 2) as well as with the most recent

theories concerning the structural and functional organization of biological membranes. Since this model deals with the mechanisms of membrane compartmentalization, it seems appropriate now to review the current models of biological membrane organization and structures (see below).

1.8 Membrane domain: general considerations

The delimiting membrane of intracellular organelles is composed of proteins and lipids. While the latter confers mechanical stability and tendency to form closed structures, proteins ensure functional specificity and regulate the different biochemical reactions each organelle is performing. Several lines of evidence suggest that proteins and lipids do not randomly distribute within the plane of the membrane but rather aggregate and organize into compact regions or membrane domains (Simons and Ikonen, 1997; Sprong et al., 2001). In this context, the term domain bears no information about size, but just defines a membrane area of a given biochemical composition, which differs from its immediate neighbouring environment. With the term microdomain I refer to an area in the order of tens of nanometers in diameter.

It is now clear that the fluid mosaic model, proposing that lipids function as neutral solvents having little influence on protein function and distribution, is in contradiction with the most recent advances in membrane biology research.

Membrane lipids have indeed been shown to exist in different phases of fluidity ranging from gel, liquid-ordered and liquid-disordered states (Brown and London, 1998). Transition between these different phases might be achieved by different mechanisms. One such mechanisms is based on lateral interaction between lipids, such as cholesterol and sphingolipids, which can lead to phase separation in biological membranes. These lipid microdomains, also named rafts, form distinct liquid-ordered phases within the more fluid liquid-disordered surrounding matrix (Simons and van Meer, 1988). Lipid rafts are localized in the exoplasmic leaflet of several cellular membranes and play a key role in protein sorting and signal transduction (Simons and Toomre, 2000). While formation of rafts is mainly based on lateral interaction between lipids, protein-lipid and protein-protein interactions are the basis for the assembly of other membrane domains such as Rab-domains (see also previous section). Lipid modifying enzymes can be recruited to specific areas of the membrane and create homogenous lipid environments based on their specific enzymatic activity. These lipids act as targeting signals for the recruitment of effector proteins containing corresponding lipid-binding domains. A network of protein-protein interactions and oligomerization is then envisaged to stabilize the components of these membrane domains and impeding their diffusion in the bilayer (Gruenberg, 2001; Miaczynska and Zerial, 2002; Zerial and McBride, 2001).

Combinations of various domains with different biophysical properties will likely determine the shape and function of cellular organelles. According to this view, the multitude of functions each organelle is performing would therefore be topologically organized into distinct domains and regulated through the recruitment of cytosolic proteins. This model is in agreement with morphological studies showing organelles, along both the biosynthetic and endocytic pathway, to be composed of functionally and structurally distinct territories. Moreover, the subcompartmentalization of intracellular organelles also provides an explanation for how multiple reactions can occur at the same time and with high efficiency without compromising the integrity of the whole organelle. Indeed, intracellular organelles communicate via extensive tubulo-vesicular traffic, and still maintain their distinct membrane composition. This implies that proteins and lipids are laterally segregated and specifically incorporated in one set of transporters and excluded from others. Proteins may be sorted differentially via targeting motifs within the amino acid sequence or via their preference to associate with specific lipid domains. Lipids are sorted depending on their structure and capability for inserting into nascent vesicles or tubules as they bud off from an organelle (Sprong et al., 2001).

1.8.1 Membrane domains in endocytic organelles

Endosomes are a good system to study the organization of membrane domains. Different lipid domains are indeed differentially distributed between sorting, recycling and late endosomes (Gruenberg, 2001; Miaczynska and Zerial, 2002). The complex geometry of sorting endosomes is a clear example of how multiple and functionally distinct membrane regions associate into an organelle (Marsh et al., 1986). The cisterna-vacuolar portion acts as a fusion-competent region for clathrin-coated vesicles derived from the plasma membrane or TGN, while tubular extensions mainly function in receptor sorting and recycling (Gruenberg and Maxfield, 1995; Mayor et al., 1993). The lipid composition of these regions has also started to be characterized. At least one lipid, phosphatidylinositol-3-phosphate PI(3)P, is enriched in the cisterna vacuolar region, and depleted from recycling tubules (Gaullier et al., 2000). The function of this membrane domain and the role of Rab5 in its biogenesis has been described in the previous section. Another phosphoinsitide PI (4,5)P2 is instead localized to specific region of the plasma membrane and plays an essential role in the formation, budding and uncoating of CCVs (Jost et al., 1998). Whether this and other forms of phosphoinsitides PI(3,5)P2, PI(3,4)P2 and PI(3,4,5)P3 are also present on endosomes remains to be established.

Purification of recycling endosomes allowed analysis of its proteins and lipid contents. Local enrichment of cholesterol, sphingomyelin as well as phosphatidylserine suggests that these organelles are enriched in raft components (Gagescu et al., 2000). The first function attributed to these microdomains was to regulate protein sorting in the biosynthetic pathway. It is now clear that rafts regulate multiple aspects of vesicular trafficking in both the biosynthetic and endocytic pathway. As some signal transduction molecules also localize to plasma membrane rafts, it is likely that these microdomains play a key role also in signalling and differentiation (Simons and Toomre, 2000).

The exact function of lipid rafts in the endocytic-recycling pathway is however still elusive. Disassembly of raft microdomains through cholesterol depletion specifically interferes with the recycling rate of raft-associated proteins, such as GPI anchored proteins, but not of transferrin receptor (Chatterjee et al., 2001; Mayor et al., 1998). This observation suggests a role of raft microdomain in endocytic sorting and recycling of a subset of proteins. Recently an additional function of lipid rafts in actin-membrane interaction has been proposed. Sphingolipid-cholesterol membrane lipids were identified in vesicles of both the biosynthetic and endocytic pathway as preferential sites for actin recruitment and polymerisation, implying a role of lipid rafts also in actin-mediated vesicular movement (Rozelle et al., 2000).

In contrast to early endosomes, late endosomal membranes contain abundant internal membranes within their lumens, hence the name multivesicular endosomes or multilamellar bodies. Proteins and lipids differentially distribute within the multivesicular system of these organelles indicating the existence of separate membrane domains (Griffiths et al., 1988). Highly glycosylated membrane proteins such as lamp1 and lamp2 localize exclusively to the external membranes, whereas down-regulated EGF receptor, MHC class II or the IGF2/MPR receptor distribute preferentially within internal membranes (Felder et al., 1990). The reasons for this differential distribution is not yet clear but the fact that all these proteins are found on internal membranes, and have in common the capacity to traffic between TGN, plasma membrane and late endosomes, suggests a role in protein sorting.

The lipid composition of late endosomal membranes also differs from the one of early endosomes. Late endosomes are poor in free cholesterol, sphingomyelin and phosphatidylserine and enriched in neutral lipids such as triglycerides and cholesterol esters. An unusual poorly degradable phospholipid, Lysobisphosphatidic acid (LBPA) has been recently identified to be enriched in the internal membranes of late endosomes. Antibodies against this lipid block trafficking of IGF2/MPR, indicating LBPA enriched lipid domains are involved in protein sorting within the endosomal system (Kobayashi et al., 1998).

The localization of some members of the annexin protein family to endosomal membranes probably reflects the existence of other membrane domains. Indeed, annexins are lipid and Ca^{++} binding proteins involved in membrane structure and dynamics (Kobayashi et al., 1998). *In vitro* experiments using protein-free liposomes of proper lipid composition showed that upon membrane binding, annexins have the property to self assemble and to organize the liposomes surface into regular area or annexin domains. Consistent with this observation, Annexin II distributes in a non-random manner on early endosomes and is concentrated in morphologically distinct regions (Harder et al., 1997; Harder and Simons, 1997). The precise function of Annexin II is not known but this protein seems to be involved in early endosome membrane dynamics via interaction with proteins of the cortical actin cytoskeleton. An additional function in endosome fusion and formation of MVB has also been recently proposed (Gruenberg, 2001).

Although the association of annexin II with membranes is cholesterol-dependent, this protein is depleted from recycling endosomes, whereas cholesterol is enriched on these membranes. This suggests the requirement of additional targeting determinants for annexin II membrane binding (Kobayashi et al., 2001).

Further work will be required to better define the biogenesis and function of those as well as other not yet identified membrane domains. For example, by

analogy to Rab GTPases, also Arf GTPases might form distinct membrane domains through the recruitment of lipid modifying enzymes such as PI(4)P 5-kinase and phospholipase D. The products of these enzymes might indeed create a suitable lipid environment for recruitment of the many multi-protein complexes required for vesicular budding to occur.

Having described the structural and functional organization of endocytic organelles and, in the previous paragraphs, the general principles underlying membrane transport among intracellular compartments, in the next section, I will focus in more detail on the molecular mechanisms regulating the endocytic-recycling pathway.

1.9 Molecular regulation of endocytic sorting and recycling

Very little is known about the molecular regulation of the endocytic-recycling pathway and the principles underlying protein and lipid sorting within endocytic organelles are still under investigation. Endocytic sorting occurs primarily in tubulo-vesicular and cisternal elements, usually referred to as sorting endosomes, and it can be illustrated by transferrin, which recycles bound to its receptor and LDL, which dissociates from the LDLR and is delivered to lysosomes (Gruenberg and Maxfield, 1995; Mellman, 1996). It has been proposed that the physical structure of these organelles is the basis for a simple sorting

mechanism based on geometrical principles (Marsh et al., 1986; Dunn et al., 1989; Linderman and Lauffenburger, 1988). Membranes and solutes would stochastically partition between tubules (60 nm in diameter, 3-4 μm in length) and vacuoles (0.3-0.4 μm in diameter), because of the different surface-to-volume ratios of these two structures (Dunn et al., 1989). Acid-released ligands dissociate from their receptors because of the low pH (6.0-6.2) found in this compartment and accumulate in the large vacuolar part, which will presumably form a MVB. In addition, specific sorting signals would ensure retention of receptors destined for degradation into the vacuolar region (Felder et al., 1990; Johnson and Kornfeld, 1992; Johnson and Kornfeld, 1992), while recycling receptors would be passively incorporated into tubules. These tubules would then pinch off or serve as sites for budding of carrier vesicles involved in receptor recycling. Recycling components can return directly from sorting endosomes to the plasma membrane via a fast recycling route (Mayor et al., 1993; Schmid et al., 1988) or can take a slow recycling pathway via peri-nuclear recycling endosomes (Hopkins, 1983; Yamashiro et al., 1984).

Several lines of evidence support the hypothesis that recycling of membrane proteins can occur in the absence of any specific sorting signal. First, transferrin receptor mutants with complete deletion of their cytoplasmic tails recycle at equal rates as wild-type receptors or certain lipid analogues (Mayor et

al., 1993; Mukherjee et al., 1999). These results indicate that at least this receptor follows the bulk of membrane recycling. Recently, it has been shown that lipids can be differentially sorted to late or recycling endosomes solely on the basis of their different biochemical properties (Mukherjee et al., 1999). As recycling tubules are particularly enriched in lipid rafts they may represent a differentiated membrane domain capable of concentrating receptors in an adaptor–independent fashion.

However, tubules in the early endosome system have been found to contain clathrin coats that are devoid of α- adaptins, implying that these are different from plasma membrane-derived coated vesicles (Stoorvogel et al., 1996). These buds contain TR and are quite numerous on peripheral sorting endosomes indicating that they may function in recycling to the plasma membrane. The first, although indirect evidence, in support of a role of coat proteins in endosomal function came from experiments using the fungal metabolite Brefeldin A. This drug has been shown to inhibit transport from the ER to the Golgi compartment by interfering with the assembly of coatamer-containing coat complexes (Doms et al., 1989; Pelham, 1991). Treatment of cells with BFA causes extensive tubulation of the early endosomal compartment analogous to the effects on Golgi membranes (Lippincott-Schwartz et al., 1991). Although BFA did not block endocytosis or recycling per se, it did interfere with polarised recycling of transferrin receptor to

the basolateral surface of MDCK cells (Futter et al., 1998). The observation that in this cell line transferrin receptor is concentrated in endosomal clathrin-coated buds containing γ-adaptin, and that these buds disassemble upon BFA treatment, suggests that AP-1 clathrin-coated vesicles function in polarised recycling (Futter et al., 1998). BFA is known to inhibit GDP-GTP exchange factors for the ARF subfamily of small GTPases. As such, its effects might be directly or indirectly related to defects of Arf-dependent coat complex assembly. Arf6 has been localized to early endosomes and shown to regulate transferrin recycling. Over-expression of a GDP-bound inactive mutant causes accumulation of non clathrin-coated domains on tubular structures and inhibits transferrin recycling (D'Souza-Schorey et al., 1995). However, it seems that Arf6 is BFA-insensitive and therefore the possibility remains that other family members or other regulatory molecules are the target of BFA.

Rab proteins and SNARE molecules also function in the recycling pathway. The v-SNARE cellubrevin and t-SNARE syntaxin13 have been shown in an *in vitro* assay to be required for transferrin recycling, although their precise site of action remains to be established (Galli et al., 1994; Prekeris et al., 1998). Also, very little is known about the mechanisms of action of Rab4, Rab11 and Rab5 and which step along the endocytic-recycling pathway they regulate. Rab4 has been proposed to regulate an early sorting event as its over-expression inhibits

iron discharge from transferrin and causes redistribution of transferrin receptor from the endosomes to the plasma membrane. Rab4 over-expression also stimulates the recycling of internalized fluid phase marker, further pointing to defects in endosomal sorting (van der Sluijs et al., 1992). Interestingly, the Rab5 effector, Rabaptin5, was shown to interact also with Rab4 (Vitale et al., 1998). As these two GTPases exert complementary function in regulating entry in, and exit out, of sorting endosomes, it was proposed that Rabaptin5, by interacting with both Rab5 and Rab4, might contribute to maintaining organelle homeostasis.

Over-expression of dominant negative mutant of Rab11 selectively inhibited the slow recycling pathway, consistent with its localization to peri-nuclear recycling endosomes (Ullrich et al., 1996). The Rab11 effector, Rabphilin has been shown to interact with the mammalian homologue of the yeast Sec13, a component of COP II, suggesting a potential link between this GTPase and coated vesicle formation and/or targeting (Mammoto et al., 2000).

The phosphatidylinositol 3-kinases are a family of lipid kinases involved in several vital processes including signal transduction and membrane trafficking. These kinases phosphorylate the 3-position of the inositol ring on phosphoinositides (Stenmark and Aasland, 1999). PI-3 kinases have been found to regulate various steps in endocytic trafficking. These effects were initially discovered by using wortmannin, a fungal metabolite, which binds to and inhibits

the catalytic subunit of this enzyme. Wortmannin causes a significant down-regulation of cell-surface transferrin receptor resulting from increased internalization and decreased recycling rates (Spiro et al., 1996). In mammals there are three classes of PI-3 kinases displaying different substrate specificity and regulatory proprieties. The Class I, hVsp34 and p85-P110βcomplex has been shown to interact with Rab5 and to regulate endosome fusion (see previous section) (Christoforidis et al., 1999). The molecular mechanisms whereby transferrin recycling is inhibited upon wortmannin treatment are not known. Presumably, one of the PI phosphorylated derivatives regulates the recruitment of lipid binding proteins whose activity is required for recycling.

Wortmannin was also shown to block traffic between early and late endosomes (Fernandez-Borja et al., 1999). Transport between these compartments is mediated by relatively large vesicles (0.4-0.5 μm in diameter), which have a typical multivesicular appearance (endosomal carrier vesicles ECVs or multivesicular bodies MVB). Once formed on early endosomes, ECVs move along microtubules until they dock and fuse with late endosomes (Aniento et al., 1993; Gruenberg et al., 1989). PI(3)P has been specifically localized to discrete patches on the surface of sorting endosomes as well as on the internal membrane of MVB, but it is absent from late endosomes. This suggests that it is either modified or degraded (Gaullier et al., 2000). Recently, it has been proposed that

PI(3)P is necessary to promote inward budding of the limiting membrane of the endosomal vacuolar portion to generate the multivesicular regions (Fernandez-Borja et al., 1999). This model is supported by the observation that wortmannin blocks MVB formation and causes vacuolation of sorting endosomes.

As already mentioned, retention of transmembrane proteins in the vacuolar region and their subsequent incorporation into multivesicular bodies, is a signal-dependent process. *In vitro* and *in vivo* studies have shown that some components of the COP-I coat complex, known to regulate the early secretory pathway, play a role also in endocytosis. For example, down-regulation of Nef-CD4 complex is in part mediated via direct interaction of Nef with βCOP (Piguet et al., 1999). Recruitment of COP components to endosomes is pH-dependent and *in vitro* formation of ECV is both pH and COPI dependent. In the biosynthetic pathway, COPI recruitment requires Arf1 and PLD activity. Arf1 is also required for COPI recruitment to endosomes, whereas PLD activity is not (Gu and Gruenberg, 2000). Additional evidence for a role of COPI components in transport from early to late endosomes are also provided by studies in a temperature-sensitive ε-COP mutant cell line. At the non-permissive temperature transport from sorting endosomes to late endosomes was impeded and this defect could be rescued by over-expression of wild type ε-COP (Daro et al., 1997).

More recently, the ubiquitin system has been shown to act not only to target cytosolic proteins for degradation by the proteosomes, but also to target internalized receptors to late endosomes. Ubiquitin was first implicated in the regulation of endocytosis of a number of yeast plasma membrane proteins, including transporters and signalling receptors (for review see Bonifacino and Weissman, 1998; Wendland et al., 1998). Ubiquitination of these proteins was shown to be required for their inclusion into primary endocytic vesicles budding from the plasma membrane. Subsequently, studies performed in mammalian cells on activated growth factor receptors suggested an additional role for ubiquitin in controlling sorting into MVBs (Levkowitz et al., 1998). More recently, experiments performed in yeast have further strengthened this idea. Ubiquitination of the cytoplasmic tail of carboxypeptidease S (CPS), a vacuolar hydrolase, was shown to be required for the entry of this enzyme into MVBs. Moreover, addition of the CPS ubiquitination site to a vacuolar membrane protein, which is normally not sorted into MVBs, resulted in targeting of the chimera protein into MVBs (Katzmann et al., 2001). Also in agreement with these studies is the finding that in yeast mutant cells, which have reduced levels of free ubiquitin, sorting of two other membrane proteins (the polyphosphatase Phm5p and a presumptive haem oxygenase, Ylr205p/Hmx1p) into MVBs was also impeded (Reggiori and Pelham, 2001). However, the function of ubiquitin in membrane transport is not only

limited to regulate cargo sorting in the endocytic pathway. At least in yeast, ubiquitin was shown to regulate cargo sorting also in the secretory pathway at the level of the TGN (Beck et al., 1999; Helliwell et al., 2001). Therefore, ubiquitin regulates cargo sorting at the plasma membrane, late endosomes and at TGN. The mechanisms the cell uses to recognize and sort cargo-carrying ubiquitin signal are still poorly understood. The observation that, at least in some cases, adaptor complexes are not required for internalization of ubiquitinated receptors (D'Hondt et al., 2000), and that in yeast (where most proteins are endocytosed by ubiquitin signals) adaptors are not required for internalization, suggests an adaptor-like function for ubiquitin in linking cargo to the endocytic machinery. This hypothesis is supported by the finding that many members of the basic endocytic machinery (epsin, Eps 15) and proteins involved in the MVBs pathway (HRS, Vps27) contain a conserved peptide sequence, which can bind to ubiquitin (Hofmann and Falquet, 2001).

1.10 Aim of the thesis

1.10.1 Topic

The objective of the work described in this thesis was to study the molecular machinery responsible for controlling transport in the endocytic-recycling pathway. The molecular principles underlying the regulation of this pathway are largely uncharacterized, owing to the poor definition of compartment boundaries of the organelles constituting this pathway and lack of regulatory molecules. Defining the limits of this system and identifying its regulatory mechanisms are therefore of considerable interest, especially if considering the important functions in which this pathway is involved.

1.10.2 Question

Endocytosis and recycling can be viewed as two directionally opposite membrane transport reactions ending in, and starting from, early endosomes, respectively. Membrane flow in and out of these organelles must be co-ordinated to maintain the structural and functional homeostasis of these organelles and to ensure sequential transport of cargo along the endocytic-recycling pathway. How is import to, and export from, early endosomes co-ordinated? To answer this question it is necessary to identify and functionally characterize the molecules

involved in these processes. To this aim, I have been focusing on Rab5, Rab4 and Rab11. These three GTPases have been previously localized to early and recycling endosomes and have been implicated in the regulation of the endocytic-recycling pathway. Moreover, recent data suggest that Rab proteins play a key role in organelle biogenesis and in specifying organelle identity. Therefore, the study of their mechanisms of action is expected to give important insights towards the problem that I decided to address in this thesis.

1.10.3 Hypothesis

The finding that one of the Rab5 effectors, Rabaptin-5, interacts also with Rab4 suggests the presence of a molecular cross-talk between these two GTPases. Given the complementary role of Rab5 and Rab4 in regulating entry in, and exit from, early endosomes, this molecular cross-talk may be part of a mechanism which higher eukaryotes have evolved to co-ordinate endocytosis and recycling. According to the hypothesis (which I will refer to as the Rab domain hypothesis) proposed by Zerial and co-workers, Rab proteins and their effectors are not randomly distributed within the plane of the membrane, but rather self-organize into macromolecular complexes, so called Rab domains (see paragraph 1.7.5). In this view Rab5 recruits its effectors, several of which being key components of endosome tethering and fusion, into a defined region constituting the site of entry

into early endosomes. If generalized to other family members, this model would predict that Rab proteins regulating membrane recycling and their effectors should be localized to domains on early endosomes distinct from the one occupied by Rab5. The partitioning of these regulatory machineries into different membrane sub-compartments would allow multiple reactions to occur simultaneously and with high efficiency, whilst little or no intermixing between its regulatory elements would occur. In this context the function of divalent Rab effectors, such as Rabaptin-5, may be to regulate the association between different domains (in this specific case Rab5 and Rab4 domains) to allow the sequential flow and efficient distribution of cargo from one domain to another. To test this hypothesis three complementary approaches were undertaken.

1.11 Experimental strategy

(A) An *in vitro* assay was developed to reconstitute and measure the endocytic-recycling pathway in SL-O-permeabilized cells with the aim of gaining a molecular understanding of this process.

(B) An *in vivo* system based on a combination of cell transfection assays and light microscopy techniques was developed with the aim of studying the role of Rab proteins and their effectors in the membrane organization of the

endocytic-recycling pathway. This system also offers the opportunity to study *in vivo* the function of these molecules in the endocytic-recycling pathway.

(C) Having established these two assays, I went on to characterize the function of Rab GTPases by searching for their downstream effectors using an affinity chromatography approach. The role of these effectors in the endocytic-recycling pathway has been further characterized using both *in vivo* as well as *in vitro* assays.

1.11.1 The marker followed to study the endocytic-recycling pathway

To study the endocytic-recycling pathway I followed the intracellular trafficking of the iron binding protein Transferrin (Tf). Tf is a well-established marker for monitoring endocytic-recycling trafficking because it remains associated with its receptor until it returns to the plasma membrane. Upon internalization, Tf is delivered to early endosomes where the bound iron is released. From these organelles, Apo-Tf (iron-free) can return directly to the plasma membrane via a "fast" recycling route or can take a "slow" recycling pathway passing through peri-nuclear recycling endosomes. Given that Apo-Tf dissociates from its receptor at the neutral pH of the extracellular medium, the release of previously internalized Tf can be used to monitor the endocytic-recycling of transferrin receptor.

1.11.2 The cell line

The cell line selected for the vast majority of the experiments conducted in this thesis was the human epithelial cell line (A431) derived from a vulval carcinoma. The reasons for this choice are several-fold. First, the membrane compartments involved in the endocytic-recycling pathway have been extensively studied in these cells. A detailed morphological analysis and kinetic measurements of the endocytic-recycling transport of transferrin receptor which was conducted in these cells led to the first description of peripheral early endosomes and peri-nuclear recycling endosomes (Hopkins, 1983). Therefore, the conditions and the criteria to identify early endosomes and peri-nuclear recycling endosomes are well established in this cell line. Applying these very same criteria to identify these organelles in other cell types may generate several problems. The morphology, the topology and the kinetics of transport of recycling markers through these organelles are indeed cell type specific. Given that the molecular definition of early and recycling endosomes is still very preliminary and that part of the aim of this thesis was to molecularly characterize these organelles, I considered it opportune to use A431 cells as a cellular system. Second, experiments conducted in the laboratory have established that, compared to other cell lines such HeLa or CHO, A431 cells are more resistant to the toxic side effects of SL-O (which

causes detachment from the solid support on which adherent cells are grown). Third, A431 cells express high level of transferrin receptor and thus avoid the need for its over-expression to follow the endocytic-recycling trafficking of transferrin.

2 RESULTS

2.1 Introduction to results (part-1)

Many membrane trafficking steps have been reconstituted in cell-free and semi-intact cellular systems. These assays turned out to be powerful tools to study the molecular regulation of intracellular transport. To determine the molecular requirement for endocytic-recycling transport, this pathway has been reconstituted in semi-intact cells permeabilized with the pore-forming toxin streptolysin-O (SL-O). This toxin binds to cholesterol in the plasma membrane and, upon self-polymerisation, it creates openings (about 30 nm in diameter), through which endogenous cytosolic components can be washed out and /or exogenous molecules can be introduced into the cells. The goal of the experiments described below was to establish conditions that would make transferrin recycling in SL-O permeabilized cells dependent upon the addition of exogenously added cytosol. This experimental set-up offers the opportunity to manipulate the molecular compositions of the exogenous source of cytosol and thus to establish the molecular requirement for endocytic-recycling. In addressing this point I focused on the Rab machinery with the aim to test the hypothesis that the function of Rab5 and Rab4 in the endocytic-recycling pathway is molecularly co-ordinated.

2.2 *In vitro* reconstitution of the transferrin recycling pathway in SL-O-permeabilized cells

SL-O can be used to selectively permeabilize the plasma membrane without damaging intracellular organelles by first allowing it to bind to the plasma membrane at 4°C and then, after extensive washes, warming the cells to 37°C. At this temperature the toxin polymerizes and forms pores. Using this protocol, the toxin concentration allowing efficient permeabilization with minimal cellular toxicity was established by monitoring the release of a cytoslic enzyme such as the lactate dehydrogenase (LDH). Optimal toxin concentrations were defined as those required for releasing 60% of the total cellular content of LDH in 20 minutes (Ikonen et al., 1995). This criteria was followed to determine the SL-O concentration required to permeabilze A431 cells grown on glass coverslips (Figure7A). Under the established conditions no major morphological alterations of the early endosomal compartment were detected as shown by immunofluorescence staining with antibodies against transferrin receptor or EEA1 (Figure 7 B-E).

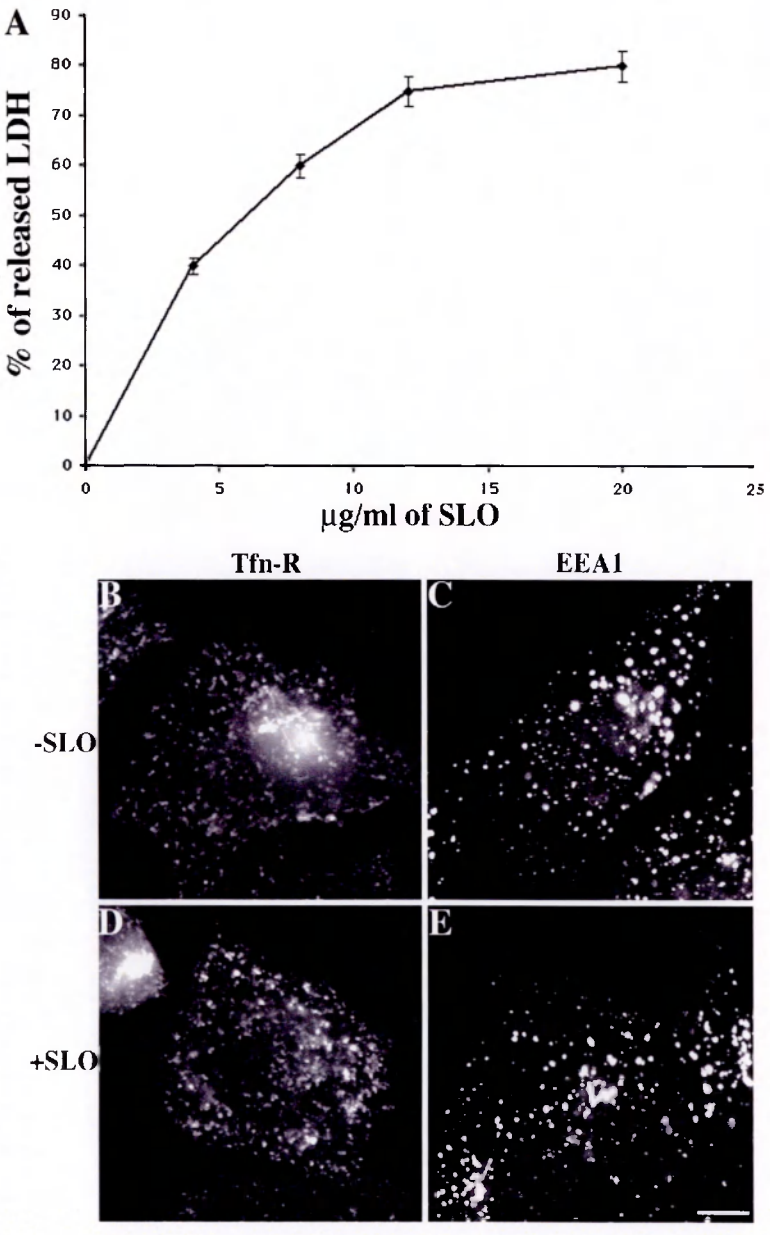

Figure 7: Release of cytosolic LDH with increasing concentration of SL-O (A) and immuno-fluorescence microscopy analysis of cell treated with SL-O (B-D)

(A) A431 cells grown on glass coverslips were treated in a final volume of 80 µl with increasing concentration of SL-O. After removing excess toxin, cells were incubated at 37 °C for 20 minutes and the amount of LDH released was measured and expressed as percent of the total cellular LDH. Data represent means ± SEM from three independent experiments performed in duplicate.

(B-E) A431 cells non-treated (B-C) or treated with 8µg/ml SL-O (D-E) were fixed and incubated with antibodies against transferrin receptor or EEA1, followed by FITC-labelled secondary antibodies. Samples were analyzed using fluorescence microscopy. To ensure that cells were efficiently permeabilized by SL-O, no detergent was used in the antibody labelling protocol (D-E). Scale bar represents 5 microns.

To follow transferrin recycling, rhodamine-transferrin was internalized for 30 minutes prior to SL- O permeabilization. Next, A431cells were allowed to bind SL-O for 10 minutes at 4° C, toxin excess was removed by ice-cold washes and cells were incubated for 3 minutes at 37° C to allow pore formation. Cells were then returned to ice and the endogenous cytosol was washed out by a further 20 minutes incubation at 4° C. This procedure allows cytosol diffusion while transferrin recycling is blocked because of the low temperature. Recycling was subsequently allowed to commence by raising the temperature once more to 37°C for 30 minutes with different reagents added to the incubation (see Figure 8).

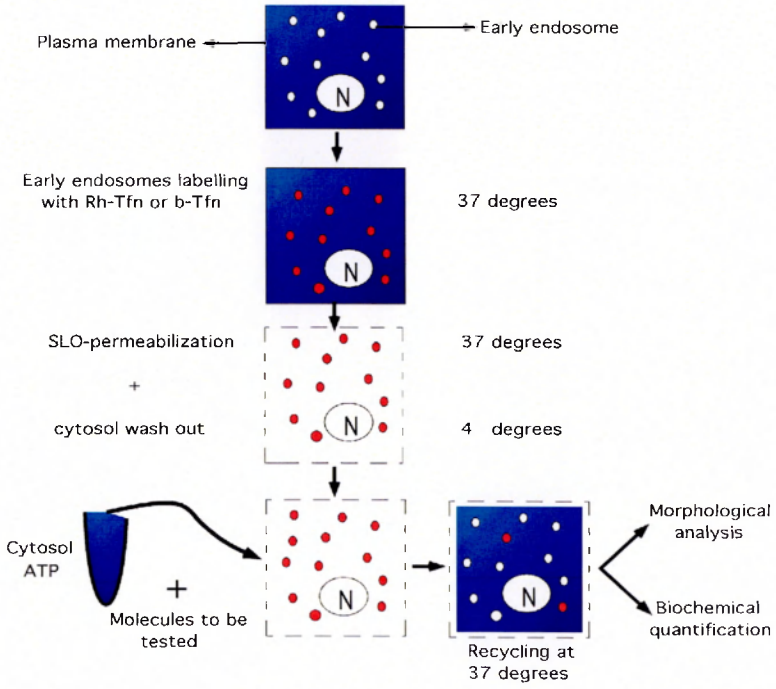

Figure 8: Schematic representation of the *in vitro* reconstituted transferrin recycling assay

As shown in Figure 9, only when cells were incubated with exogenous cytosol and an ATP regenerating system, recycling could be observed as demonstrated by the loss of intracellular rhodamine-transferrin signal.

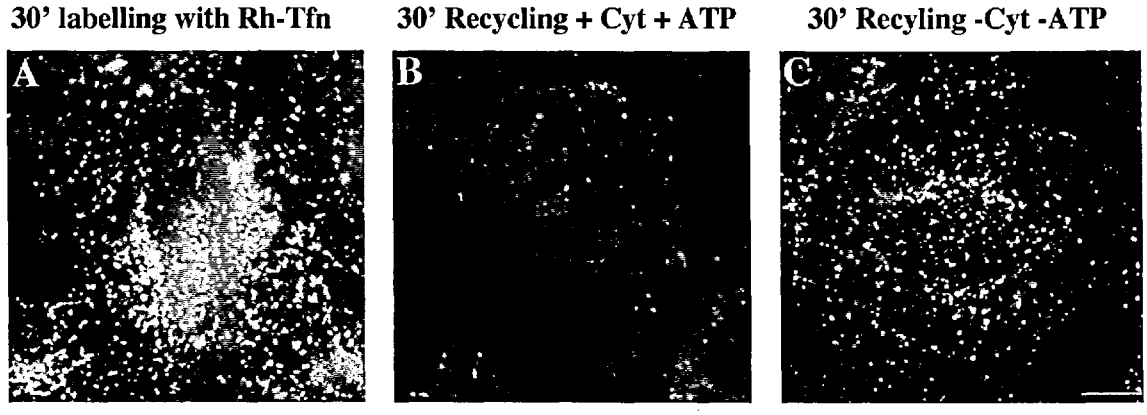

Figure 9: Fluorescent transferrin recycling assay in SL-O-permeabilized cells.
A431 cells grown on glass cover slips were loaded with rhodamine transferrin for 30 minutes, permeabilized with SL-O and either fixed (A) or incubated for a further 30 minutes at 37 °C with cytosol and ATP regenerating system (B) or buffer alone (C). Samples were fixed and analyzed using fluorescence microscopy. Scale bar represents 5 microns.

Recycling was specific for transferrin receptor since co-internalized EGF, a tracer for late endosomal transport, was retained intracellularly (Figure10). These results show that SL-O permeabilization does not significantly alter the sorting and recycling function of early endosomes and thus validate the use of this assay to study endocytic-recycling.

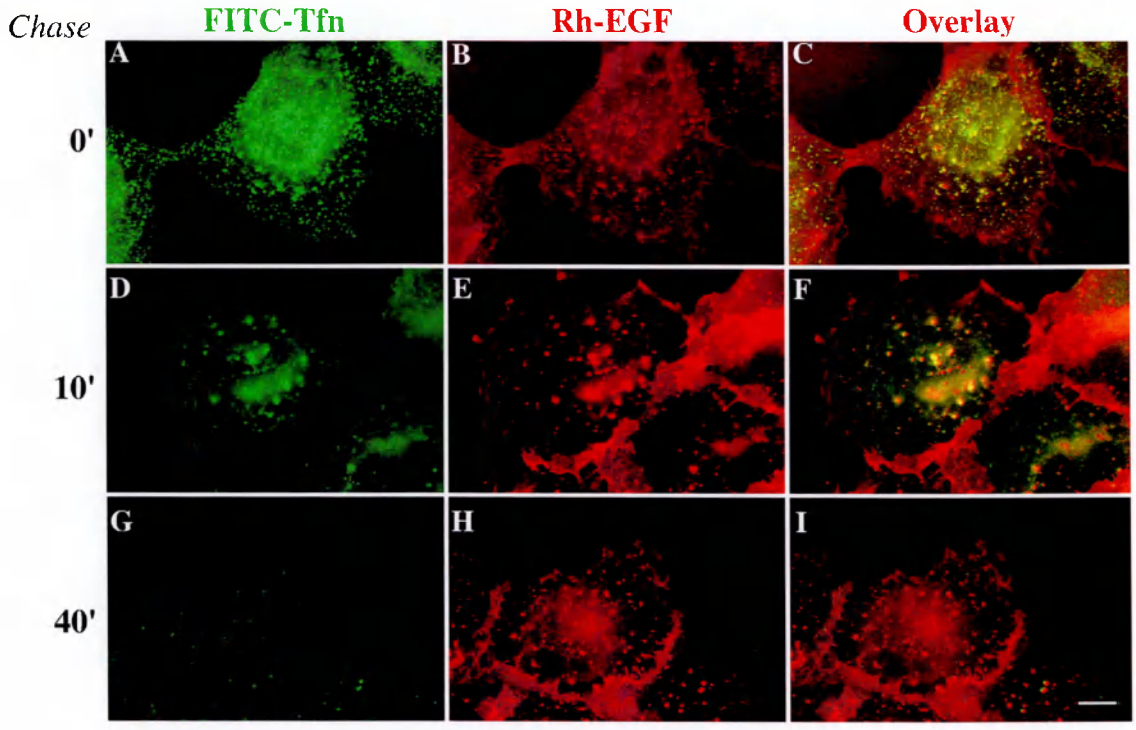

Figure 10: EGF is retained intracellularly in SL-O-permeabilized cells.
A431 cells grown on glass cover slips were loaded with FITC- transferrin for 30 minutes (A), or Rhodamine EGF (B), permeabilized with SL-O and either fixed (A-B) or incubated for a further 10 minutes (D-E) or 40 minutes (G-H) at 37 °C with cytosol and ATP regenerating system. Samples were fixed and analyzed using fluorescence microscopy. Scale bar represents 5 microns.

In order to biochemically quantify transferrin recycling in SL-O permeabilised cells, biotinylated-transferrin was internalized instead of rhodamine-transferrin and recycling was quantified as described in the methods (see section 4.7). Upon the addition of cytosol and energy, permeabilized cells could recycle as much as 60% of the total internalized transferrin whereas cells incubated with buffer alone, could only recycle 20%. Importantly, transferrin recycling was time- and temperature-dependent and its kinetics resemble those

observed in intact cells. Recycling was, however, never complete, even at higher cytosol concentrations or after longer incubation times (Figure 11, 12). This is not surprising, as in general all *in vitro* reconstituted transport assays are not as efficient as the corresponding reactions *in vivo*.

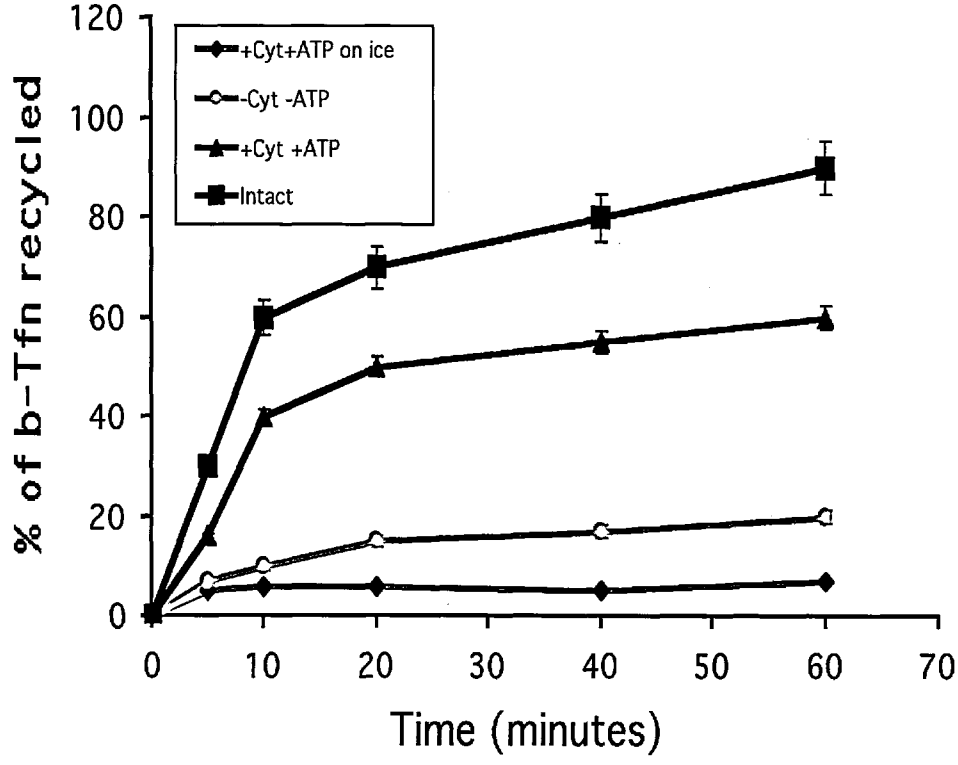

Figure 11: Biochemical quantification of transferrin recycling in SL-O-permeabilized cells.

A431 cells grown on glass cover slips were loaded with 10 µg/ml of biotinylated-transferrin for 30 minutes, permeabilized with SL-O and incubated for the indicated time points with the indicated reagents. Intact indicates cells non-permeabilized. Data represent means ± SEM from three independent experiments performed in duplicate.

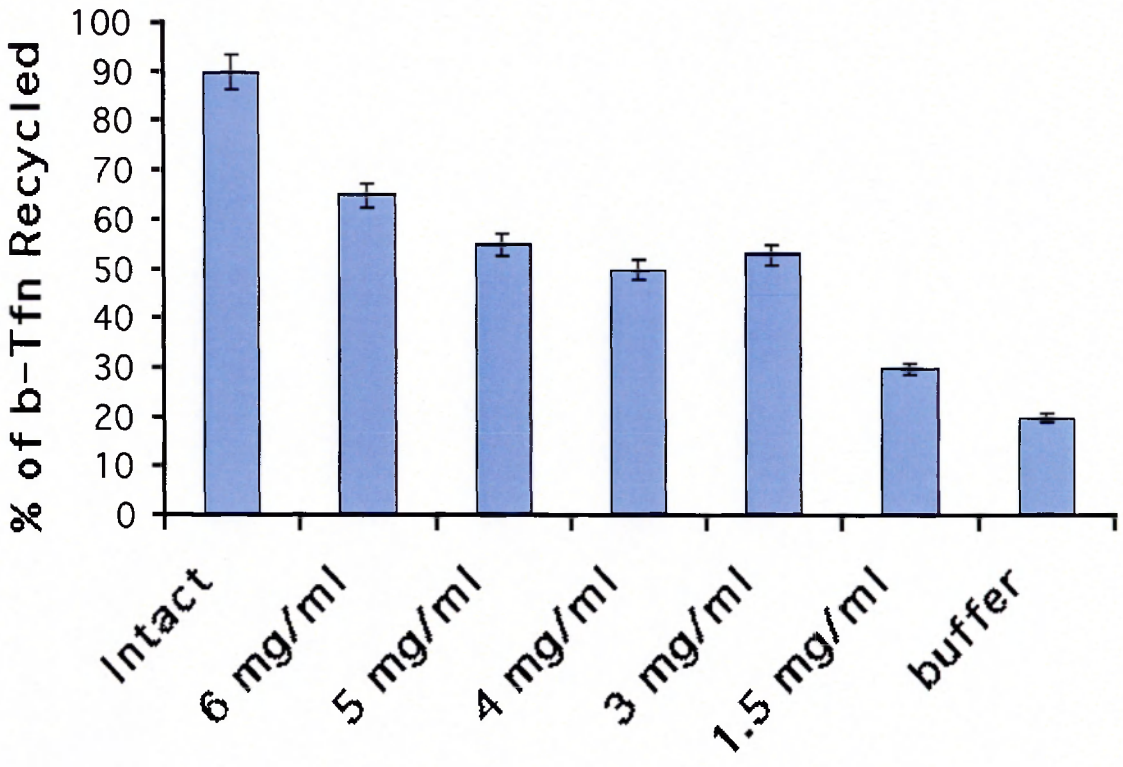

Figure 12: Reconstituted transferrin recycling is dependent on the concentration of exogenously added cytosol.

A431 cells grown on glass cover slips were loaded with 10 µg/ml of biotinylated-transferrin for 30 minutes, permeabilized with SL-O and incubated for 30 minutes with the indicated concentrations of cytosol. Intact cells are non-permeabilized cells. Buffer indicates cells incubated only with buffer and without cytosol. Data represent means ± SEM from three independent experiments performed in duplicate.

Next, to verify whether the *in vitro* reconstituted transferrin recycling was really due to fusion of transport intermediates with the plasma membrane and not due to leakage of small intracellular vesicles through the permeabilized plasma membrane, two complementary control experiments were performed. First, following the 30 minutes recycling time point, the medium was collected and was spun for 1h at 100 000 X g. As shown in Figure 13 A, 85% of the biotinylated-transferrin counts released from permeabilized cells were recovered in the

supernatant, indicating that the bulk of recycled transferrin was soluble and not membrane bound. Furthermore, as estimated by Western blotting the total amount of transferrin receptors remained constant throughout the time-course of recycling (Figure13 B), indicating that the loss of intracellular signal is not due to vesicle leakage.

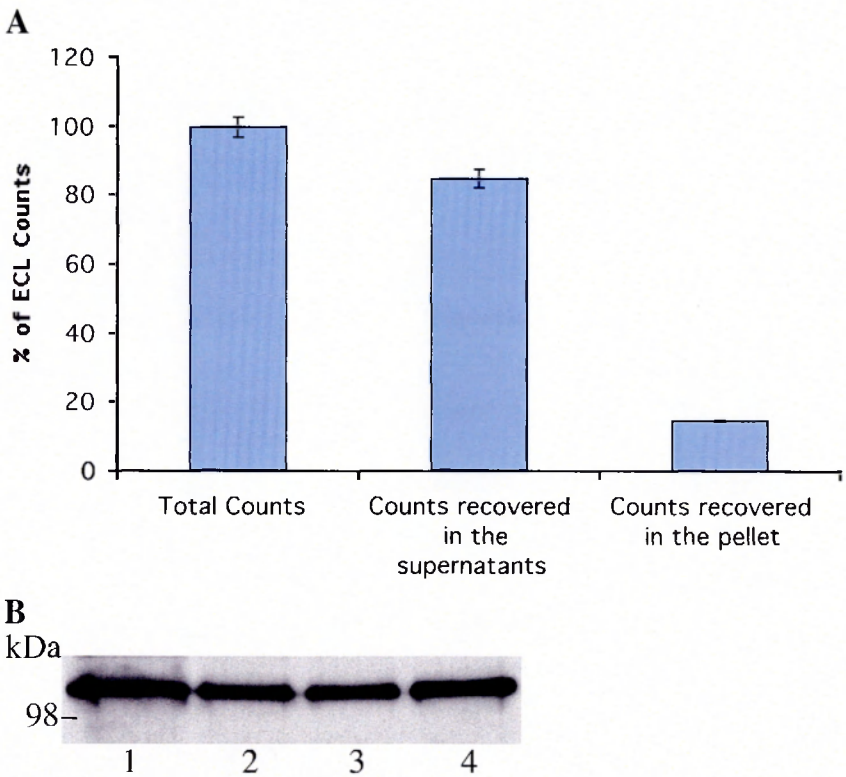

Figure 13: transferrin recycling in SL-O permeabilized cells is not due to vesicle leakage.

(A) A431 cells loaded with 10 µg/ml of biotinylated- transferrin were permeabilized with SL-O and incubated for 30 minutes with cytosol and ATP regenerating system in a final volume of 80 µl. Thereafter, the medium containing the recycled biotinylated transferrin was collected and either processed directly for quantification or spun for 1h at 100 000 X g before quantification.

(B) Western blot analysis of SL-O-permeabilized cells with anti-transferrin receptor antibodies. Cells were treated as in A and at the end of the 30 minutes recycling time point, the medium was discarded and cells were lysed into 200 µl of SDS-PAGE loading buffer and processed for Western blot analysis as described in the methods. 1= non permeabilized cells; 2= permeabilized cells at time 0 of recycling; 3= permeabilized cells after 10 minutes of recycling; 4= permeabilized cells after 30 minutes of recycling.

2.3 Rab GDI inhibits transferrin recycling in SL-O-permeabilized cells

Various Rab proteins have been implicated in the regulation of transferrin recycling. However, in no case has a direct functional requirement been demonstrated. To address this point, I tested whether transferrin recycling in SL-O permeabilized cells is sensitive to RabGDI. RabGDI has the dual function of both delivering and extracting Rab proteins to and from their resident membranes. These two functions depend on the concentration of free RabGDI versus RabGDI complexed to Rab proteins. If permeabilized cells or purified organelles are incubated with an excess of RabGDI, this molecule will extract endogenous Rab proteins from the organelle where they localize. However, if RabGDI is complexed in an equimolar ratio with a given Rab protein, it will deliver that specific Rab protein to the appropriate organelle. It has been previously demonstrated that bacterially expressed RabGDI is functional. I therefore expressed RabGDI as histidine tagged fusion protein using an *E.coli* expression system and purified it over a nickel-nitrilotriacetic acid column as described in the methods (see section 4.12.2) (Figure 14A). As shown in Figure 14B, treatment of permeabilized cells with increasing concentrations of purified RabGDI increasingly inhibited the cytosol-dependent stimulation of transferrin recycling. Maximal inhibition was observed at a concentration of 5μM.

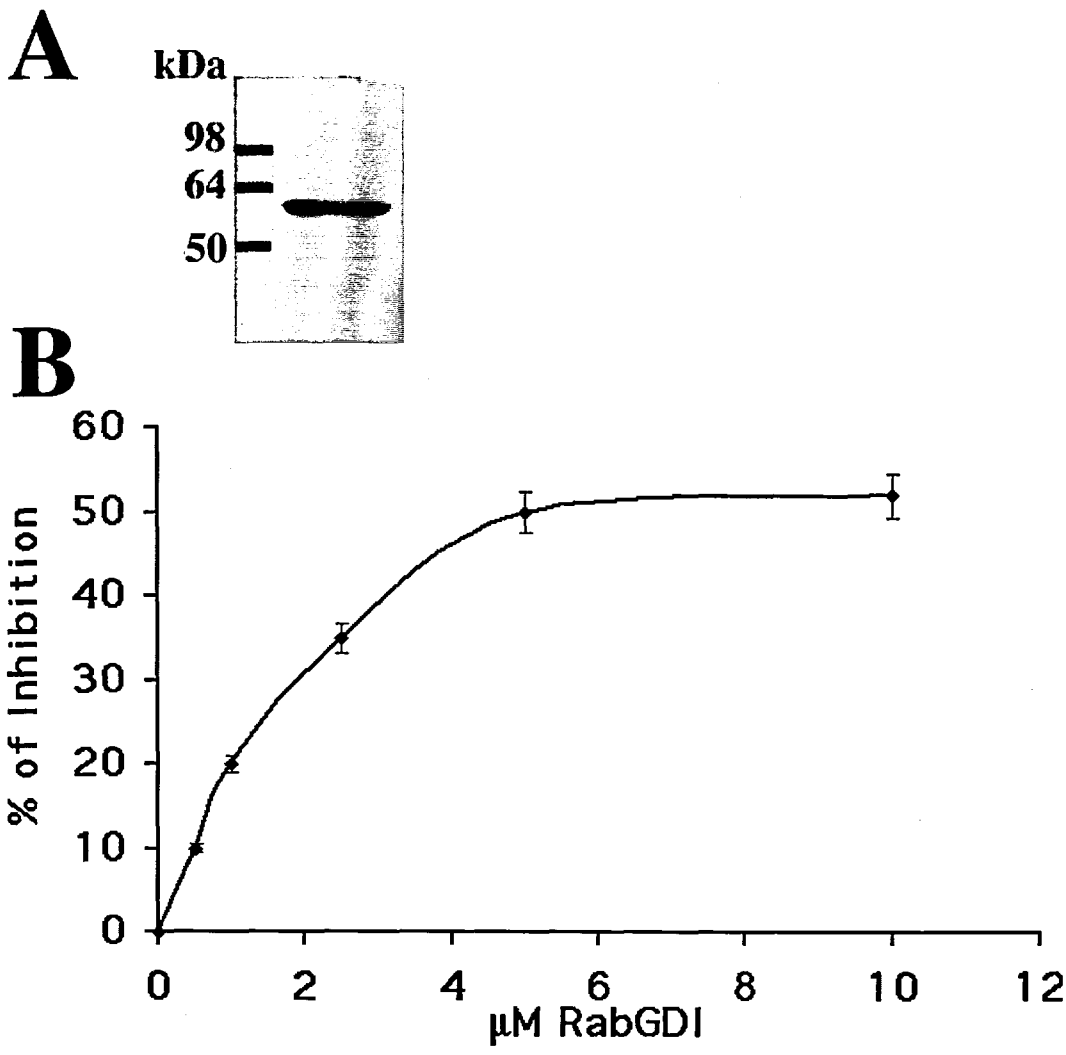

Figure 14: Recombinant RabGDI inhibits transferrin recycling in SL-O-permeabilized cells.

(A) Histidine-tagged RabGDI was purified as described in methods.

(B) A431 cells loaded with 10 µg/ml of biotinylated- transferrin were permeabilized with SL-O and incubated for 30 minutes with recombinant RabGDI at the indicated concentrations together with cytosol and an ATP regenerating system. Results are expressed as percent of inhibition of transferrin recycling after 30 minutes. 100% = transferrin recycling in the absence of RabGDI.

To verify whether under these conditions RabGDI effectively extracted Rab proteins from the membrane, SL-O permeabilized cells were incubated with RabGDI and the membrane association of two Rab proteins (Rab5 and Rab11)

was estimated by Western blot analysis -transferrin receptor served as control-. Figure 15 shows that at 5μM, the concentration of recombinant RabGDI required to inhibit transferrin recycling, both Rab5 and Rab11 were also quantitatively removed from the membrane.

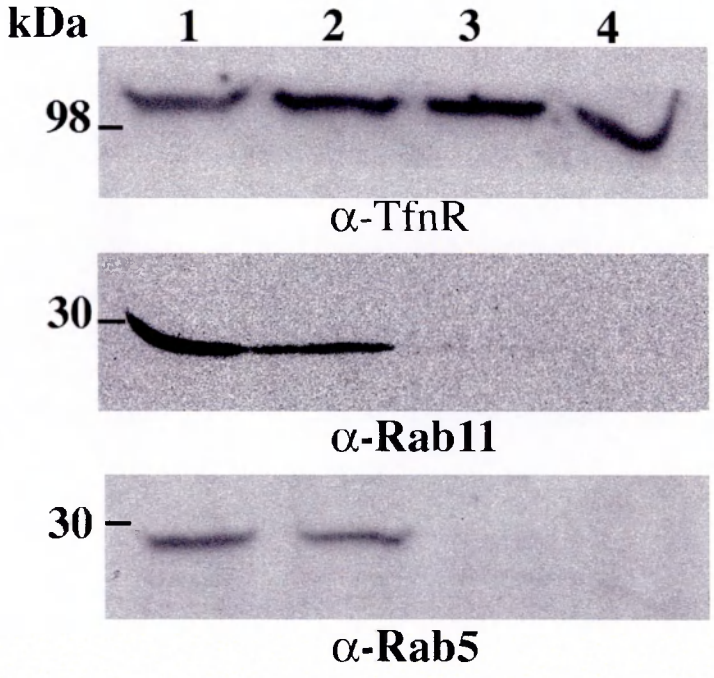

Figure 15: Recombinant RabGDI extracts Rab5 and Rab11 from the membranes in SL-O-permeabilized cells.

Recombinant RabGDI was incubated with SL-O-permeabilized cells for 30 minutes. Thereafter cells were extensively washed and solubilised in SDS-PAGE loading buffer. Samples were then processed for Western blot analysis using antibodies against transferrin receptor (TfnR) upper panel, Rab11 middle panel, Rab5 lower panel. Lane 1= Intact cells (-SL-O) + 10 μM RabGDI. Lane 2= SL-O-permeabilized cells –RabGDI. Lane 3= SL-O-permeabilized cells + 5μM RabGDI. Lane 4= SL-O-permeabilized cells + 10 μM RabGDI.

2.4 Rab 4 and Rab11 are required for transferrin recycling in SL-O permeabilized cells

The inhibitory effect of RabGDI, described in Figure 14 establishes that Rab proteins are required for transferrin recycling. As both Rab4 and Rab11 have been involved in the regulation of this pathway, I wished to test whether they were also functionally required. To perform this experiment, it was necessary to express these two GTPases in insect cells using the baculovirus expression system. This procedure ensures the appropriate post-translational modification (i.e. isoprenylation), necessary for Rab protein membrane association. Rab4 and Rab11 cDNAs were cloned in frame with a N-terminal histidine-tag sequence into an appropriate vector and recombinant baculoviruses were constructed (see methods section). Isoprenylated Rab4 and Rab11 were purified by solublising total cellular membranes of infected cells and by passing the supernatant of the so obtained membrane homogenate on a Ni- column. Bound proteins were eluted, separated by SDS-PAGE and stained with Coomassie blue. As shown in Figure 16, this procedure yielded recombinant Rab proteins with a purity close to 90%. To be delivered to their correct target membrane compartment, Rab proteins need to be complexed to RabGDI. To that aim, prenylated and purified Rab4 or Rab11 were incubated together with RabGDI and the dimeric complexes were further purified by gel filtration chromatography to remove any free RabGDI (Figure 17).

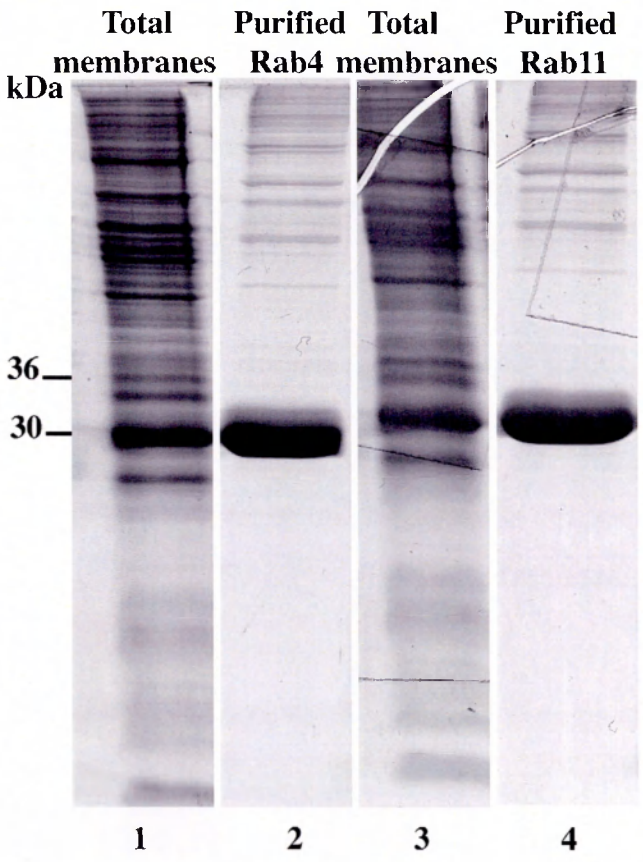

Figure 16: Histidine-tagged purified Rab4 and Rab11 expressed using the baculovirus expression system

Histidine-tagged Rab4 and Rab11 were expressed in insect cells and purified from total cellular membranes as described in the methods (see section 4.12.3).

Having generated these tools I could address the question whether Rab4 and Rab11 are required for transferrin recycling. To this aim, A431 cells labelled with biotinylated-transferrin were SL-O permeabilized and incubated with RabGDI for 20 minutes at 30° C to remove endogenous Rab proteins. Subsequently, cells were washed two times to remove RabGDI and incubated for a further 30 minutes at 37° C with different reagents. As shown in Figure 18, addition of both RabGDI:Rab4 and RabGDI:Rab11, but not RabGDI:Rab5

complexes, could rescue the inhibitory effect of RabGDI. The rescue, however, was not complete even though both Rab4 and Rab11 were added together, suggesting that either 1) the recombinant protein complexes were very partially active, or 2) that other(s) Rab protein(s) are also required. Possible candidates include Rab15, which has also been implicated in the regulation of transferrin recycling. As no other functional assay to measure the activity of these complexes (e. g. recruitment of effector proteins) was available, I could not address this point further. Nonetheless, these experiments suggest for the first time that Rab4 and Rab11 are indeed required for transferrin recycling. Furthermore, the *in vitro* assay I developed could be a suitable system to further investigate the molecular requirement for Rab effectors in the endocytic-recycling pathway.

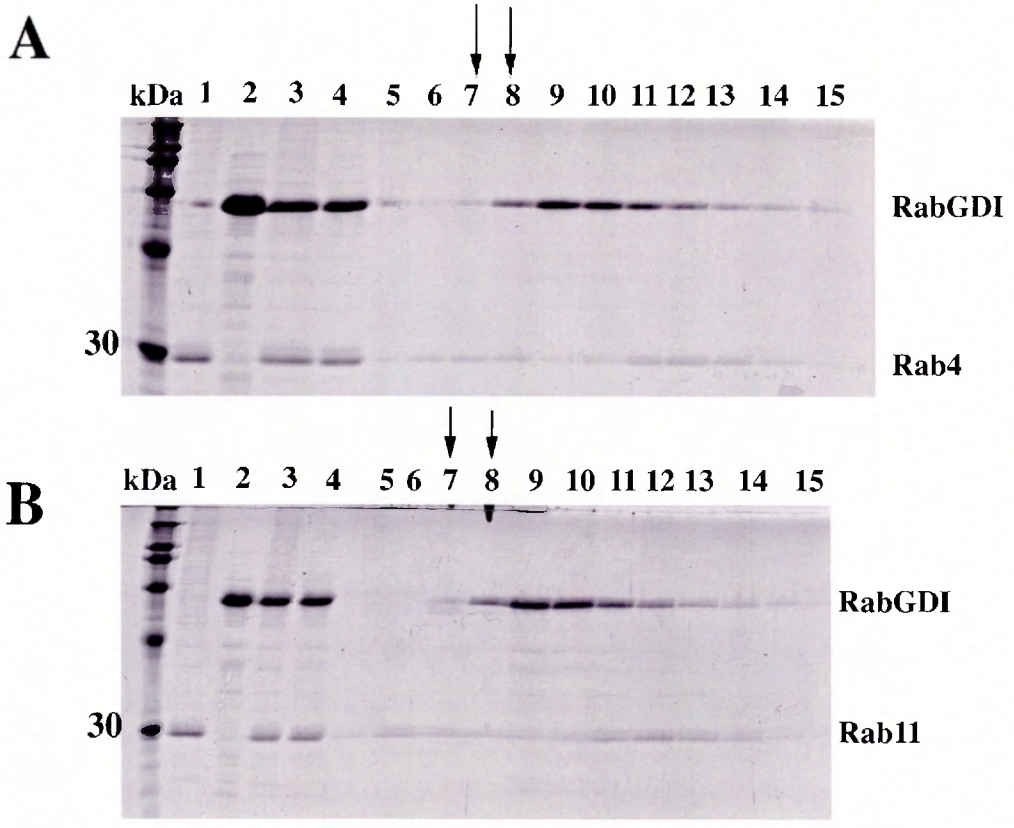

Figure 17: Purification of Rab4- and Rab11-RabGDI complexes by gel filtration chromatography.

Purified Rab4 (panel A) or Rab11 (panel B) were incubated together with RabGDI for 10 minutes at 30°C to allow Rab-RabGDI complex formation. The so-formed complexes were purified by gel filtration chromatography to remove any excess of RabGDI and unbound Rab4 or Rab11. Lane 1= Rab4 (A), Rab11 (B). Lane 2= RabGDI. Lane 3= Rab4 + RabGDI (A), or Rab11 + RabGDI (B) before gel filtration chromatography. Lane 4 = Rab4 + RabGDI (A), or Rab11 + RabGDI (B) before gel filtration chromatography and after spinning for 10 minutes at 14000 Xg to remove any precipitate. Lanes 5-15= collected fractions from gel filtration chromatography. The fractions indicated with an arrow containing the Rab-RabGDI complexes were pooled and used in the subsequent experiments.

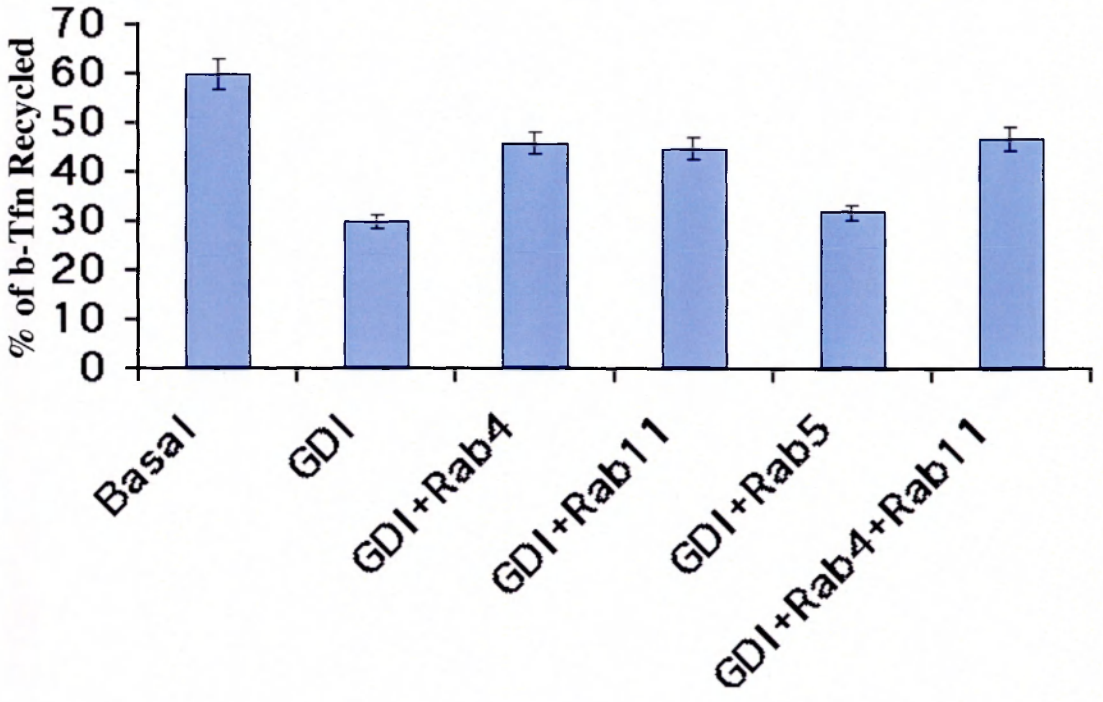

Figure 18: Purified Rab4- and Rab11-RabGDI complexes partially rescue the RabGDI inhibitory effect on transferrin recycling in SL-O-permeabilized cells.
A431 cells labelled with biotinylated transferrin and SLO-permeabilized were incubated with the indicated reagents in the presence of cytosol and an ATP-regenerating system for 30 minutes. Results are expressed as percentage of biotinylated transferrin recycled into the medium after 30 minutes. Data represent means ± SEM from three independent experiments performed in duplicate.

2.5 Studies on the function of Rabaptin-5 using the *in vitro* reconstituted transferrin recycling assay

Given the established function of Rab4 in regulating recycling, I further tested whether Rabaptin-5 is also required for endocytic-recycling. To address this point, cytosol immuno-depleted of this molecule was prepared and tested for its

competency to support transferrin recycling in SL-O permeabilized cells. As shown in Figure 19 cytosol immuno-depleted of Rabaptin -5 supports transferrin recycling to the same extent as non-treated cytosol or cytosol treated with pre-immune serum.

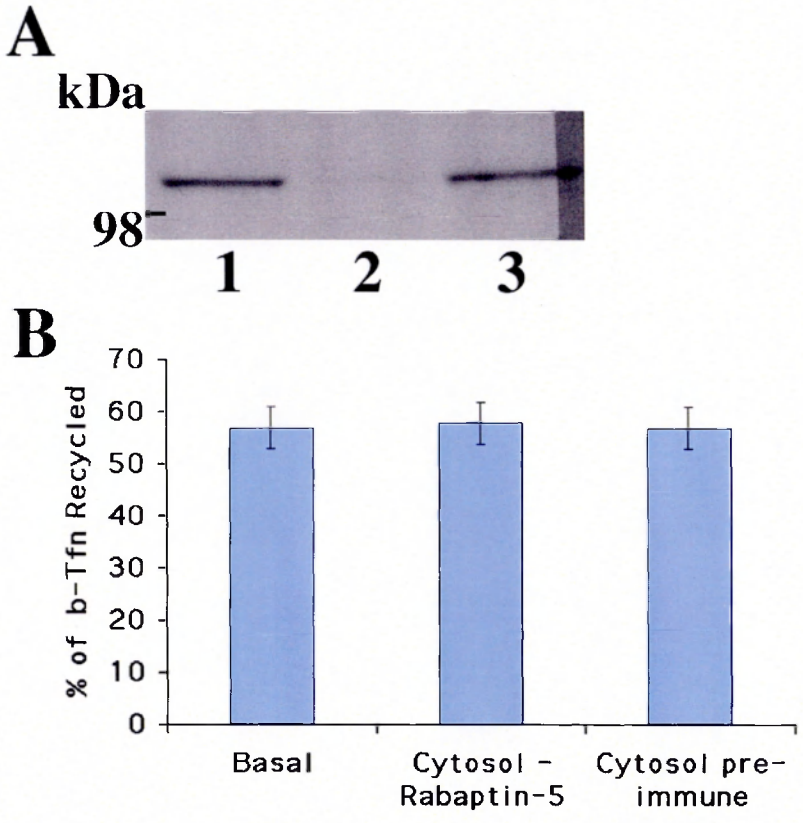

Figure 19: Rabaptin-5 immuno-depleted cytosol does not inhibit transferrin recycling in SL-O- permeabilized cells.

(A) Western blot analysis of HeLa cytosol immuno-depleted of Rabaptin-5. Lane 1=non treated cytosol; lane 2= Rabaptin-5 immunodepleted cytosol; lane 3= cytosol treated with pre-immune serum.

(B) Transferrin recycling assay in SL-O-permeabilized cells using Rabaptin-5 immuno-depleted cytosol. Basal indicates recycling in the presence of non treated (control) cytosol. Data represent means ± SEM from three independent experiments performed in duplicate.

These results do not necessarily exclude an involvement of Rabaptin-5 in endocytic-recycling. Indeed, a fraction of Rabaptin-5 remain associated with endosomes (Stenmark et al., 1995) and might be unaffected by cytosol-washout. As Rabaptin-5 membrane binding is Rab5- dependent, treatment of SL-O permeabilized cells with RabGDI should result in the release of the endosome-associated pool. This is indeed the case as shown in Figure 20 A. This strategy offers the possibility to test once more the effect of Rabaptin-5 immuno-depleted cytosol on transferrin recycling having removed any endogenous source of this protein. More precisely, this experiment was performed in the following way: cells were labelled and permeabilized as usual, then they were incubated for 20 minutes at 30° C with RabGDI and then recycling was started at 37° C by adding RabGDI:Rab4 complex and cytosol ± Rabaptin-5. However, with this approach as well no difference was measured between the different conditions (Figure 20B).

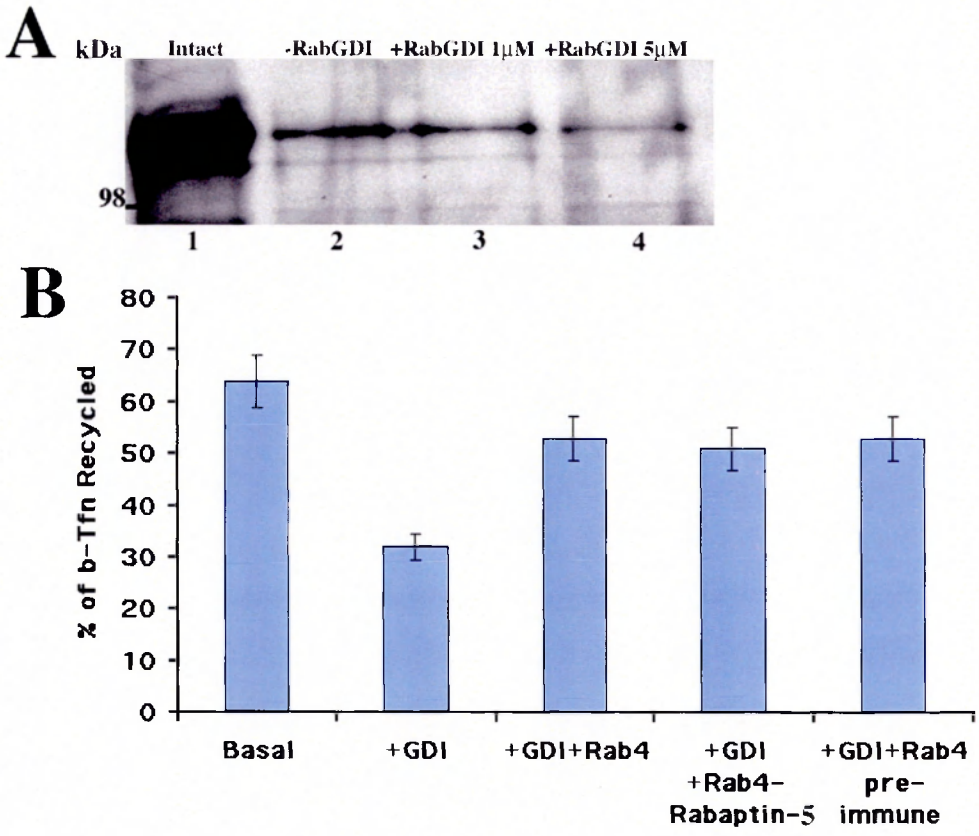

Figure 20: Rab GDI treatment of SLO-permeabilized cells increases the extraction of Rabaptin-5 from the membranes.

(A) Western blot analysis of SL-O-permeabilized cells treated with RabGDI using, anti-Rabaptin-5 antibodies.

(B) Transferrin recycling assay in SL-O-permeabilized cells treated with RabGDI. Basal= + cytosol +ATP regenerating system. +GDI= +cytosol +ATP regenerating system +RabGDI. +GDI+Rab4= +cytosol +ATP regenerating system + pre-treatment with RabGDI+Rab4:RabGDI complex. +GDI+Rab4-Rabaptin-5= as in +GDI+Rab4, but in the presence of cytosol immuno-depleted from Rabaptin-5. +GDI+Rab4 pre-immune= as in +GDI+Rab4 in the presence of pre-immune cytosol. Data represent means ± SEM from three independent experiments performed in duplicate.

Altogether, these results have several interpretations: 1) the experimental conditions established did not reconstitute but by-passed the transport steps which requires the co-ordination between Rab5 and Rab4 and thus the activity of Rabaptin-5. This is possible since the protocol of membrane permeabilization and

incubation times are such that transferrin may partially flow through peripheral recycling endosomes

2) Rabaptin-5 is not required for recycling and Rab4 regulates recycling through other effectors and independently from Rab5. 3) Rabaptin-5 is required for recycling but its immuno-depletion did not inhibit recycling because other proteins may perform a similar function.

On the basis of these considerations, I decided that the most important aspect to establish was the timing of action and compartmentalization of Rab5 and Rab4 in the endocytic-recycling pathway. Understanding this point may help in re-defining the experimental strategy required to address the co-ordination between the endocytic and recycling function of these two GTPases. In previous studies, Rab5 and Rab4 have been localized to early endosomes as indicated by their co-localization with the transferrin receptor (Bucci et al., 1992; Van Der Sluijs et al., 1991). However, not all the transferrin-receptor-containing structures harboured Rab5 or Rab4. Therefore, either these two GTPases are localized only to specific regions of the early endosomes or early endosomes are comprised of multiple populations. As these studies did not address directly the co-localization between Rab5 and Rab4, multiple scenarios could be envisaged: a) Rab5 and Rab4 localize to different endosomes; b) Rab5 and Rab4 localize to the same endosomes but in different membrane regions; c) Rab5 and Rab4 completely co-

localize to the same endosomes. The situations described in a) and b) were consistent with a series of surprising findings made in our laboratory which led to the proposal of a novel working model for the function of Rab proteins. As discussed in detail in the Introduction (see paragraph 1.7.5), this hypothesis is based on the mechanism of action of Rab5 and postulates that this GTPase, through the recruitment of effector proteins, organizes a membrane domain defining the site of entry into early endosomes. This model would predict that Rab proteins regulating membrane recycling (for example Rab4 and Rab11) should be localized to domains on early endosomes distinct from the ones occupied by Rab5. In the following section, I will describe the experiments conducted to address this hypothesis.

2.6 Introduction to results (part-2)

To get insight into the membrane compartmentalization of Rab proteins, I decided to perform a morphological analysis to visualize the trafficking of transferrin with respect to the endosomes where Rab4, Rab5 and Rab11 are localized. Although these three GTPases have already been localized to early (Rab4 and Rab5) and recycling (Rab11) endosomes, their co-localization with each other has never been investigated. Moreover, as the co-localization of each of these GTPases with the transferrin receptor was shown to be partial and the compartment boundaries between early and recycling endosomes are still poorly defined, the membrane compartmentalization of these three GTPases is still an open issue. Firstly, do Rab5, Rab4 and Rab11 localize to different endosomal populations? And secondly, do they occupy distinct domains on the same endosome or are they uniformly distributed within the plane of the membrane? To address these questions I decided to develop an *in vivo* system which would allow visualizing the membrane distribution of Rab5, Rab4 and Rab11 on cargo (transferrin) filled endosomes. To this aim stable cell lines expressing each of these three GTPases as GFP (green fluorescent protein) fusion protein were generated and their sub-cellular localization was studied using confocal microscopy. In combination with post imaging processing techniques, this system also offered the possibility to measure the transferrin kinetics of transport through

Rab5, Rab4 and Rab11-containing endosomes. This project was carried out in collaboration with two other members of the laboratory, Dr. Sonnichsen and Dr. Nielsen. In this thesis, I describe the experiments I have performed alone and I only summarize the conclusion of the experiments conducted by my colleagues. In the following paragraphs, I explain in more detail the experimental strategy of the *in vivo* –localization assay.

2.6.1 Why the GFP tag ?

Tagging Rab5, Rab4 and Rab11 for sub-cellular localization was required because: 1) As yet, despite extensive efforts, no antibodies against Rab4, sensitive enough to detect the endogenous protein, have been generated, and 2) antibodies against Rab5 and Rab11 are difficult to work with, since they require time-intensive affinity-purification and rapidly lose activity thereafter. GFP was chosen as a tag because its intrinsic fluorescent property allows studies of protein localization and dynamics in living cells. Moreover the fact that many GFP tagged proteins have been shown to behave indistinguishably from the WT-protein indicates that, in many cases, GFP interferes little with protein function *in vivo*. Indeed GFP chimeras have been successfully used to monitor cell migration, trafficking between organelles and many other cellular processes. Recently, GFP spectral variants (cyan fluorescent protein (CFP) and yellow fluorescent protein

(YFP)) differing in their fluorescent excitation and emission spectra have been created, thereby offering the option of double labelling with two different coloured GFP fusion proteins. Altogether, these considerations prompted me to use the GFP-tag to visualize Rab4, Rab5 and Rab11. To minimize possible interference with their functions, Rab5, Rab4 and Rab11 were tagged at their amino-terminal end as the Rab carboxy-terminal region (see Introduction) contains important determinants for Rab prenylation and localization. The cell line selected for these experiments was A431 for the reasons explained above (see section 1.11.2).

2.6.2 Why fluorescence microscopy ?

I used epi-fluorescence and confocal laser scanning microscopy to study the sub-cellular localization of the GFP-constructs. Confocal microscopy allows analysis of multiple focal planes of the same specimen, ensuring high resolution in the z-direction. Thus it is a more appropriate technique than non-confocal microscopy to analyze endocytic organelles, which can be relatively small (200-500 nm in diameter) and located in multiple focal planes (both underneath the plasma membrane as well as in the peri-nuclear region). The limit of resolution of light microscopy is ~ 200 nm, which is clearly a constraint in studying the sub-compartmentalization of organelles with diameters in the range of the resolution

limit. However, in comparison to higher resolution techniques such as electron microscopy, fluorescence microscopy allows a comparatively rapid analysis of a large number of samples and was therefore preferable in the initial phase of the project.

Moreover, fluorescence microscopy offers also other advantages. First, the fluorescent signal of GFP avoids all the problems connected with the use of antibodies (i.e. differences in density of labelling between different antibodies) required to visualize proteins by electron-microscopy. This point is particularly important for this project, given the lack of sensitive antibodies against Rab5, Rab4 and Rab11. Second, light microscopy allows the imaging of living cells. This firstly avoids possible artefacts of fixation and secondly, time-lapse sequences can be obtained, allowing dynamic processes to be followed.

2.7 The GFP-Rab4 A431 cell line.

In this paragraph, I describe the experiments I performed to generate the A431-GFP-Rab4 stable cell line. The protocol I followed comprised of four steps 1) Construction of an eukaryotic expression vector carrying the Rab4cDNA fused in frame to the GFP cDNA; 2) transfection of this vector into A431 cells; 3) selection of transfected cells and isolation of stable transfectant clones and 4) characterization of the isolated clones.

1) The human Rab4a cDNA was sub-cloned in frame with GFP cDNA into the pCEGFP eukaryotic expression vector (Clontech) using standard molecular biology techniques (see methods, section 4.17). pCEGFP contains the GFP cDNA under control of the Cyotomegalovirus (CMV) promoter. The CMV promoter is recognized by the transcription machinery of most mammalian cells and can be efficiently used to drive expression of exogenous genes when transfected into mammalian cells. The pEGFP vector also contains the neomycin-resistance gene. Thus cells transfected with this vector can be isolated from non-transfected cells on the basis of their resistance to this antibiotic. 2) The GFP-Rab4 expression vector was transfected into A431 cells using the lipofection technique (see methods, section 4.3) and cells were incubated for 48 hours to allow protein expressions. 3) Transfected-positive clones were selected by the following criteria: i) Capability to grow in the presence of the neomycin analogue G418 ii) GFP-Rab4 signal must be membrane associated with minor cytosolic background; iii) no major morphological alterations of endosomal compartments are tolerated and iv) each clone must exhibit a homogeneous cell population i.e. the majority (≥90) of the cells in the clone must exhibit these characteristics.

Figure 21 shows a representative cell expressing GFP-Rab4. Given the lack of sensitive antibodies against Rab4, I could not estimate the extent of over-expression relative to the endogenous Rab4 protein. However, Rab5 and Rab11

over-expression in GFP-Rab5 and GFP-Rab11 cell lines was estimated (by Western blot experiments) to be in the range of 5- to 10- fold over endogenous level. Given that GFP-Rab5 and GFP-Rab11 cell lines were generated with the same expression vectors and the same protocol used to generated the GFP-Rab4 cell line, the over-expression level of Rab4 is probably in the same range.

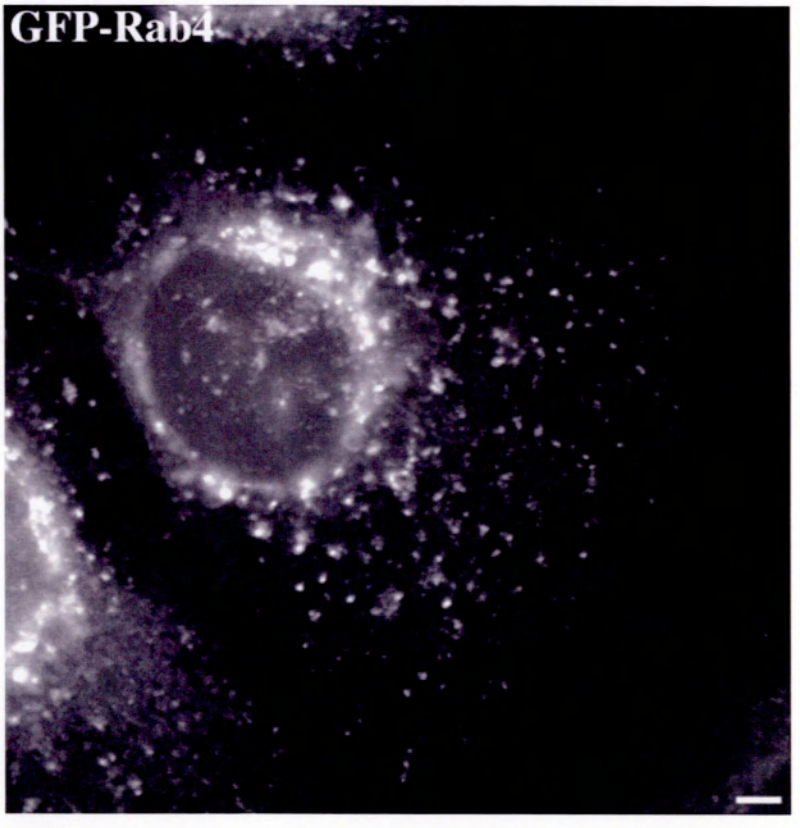

Figure 21: A431 cells expressing GFP-Rab4.
A431 cells transfected with GFP-Rab4 were fixed and analyzed by fluorescence microscopy. Scale bar represents 2 microns.

To verify whether GFP-Rab4 was correctly targeted to early endosomes, its co-localization with transferrin receptor was analyzed by immunofluorescence. As

shown in Figure 22 many structures containing GFP-Rab4 were also positive for transferrin receptor indicating that the GFP tag did not cause mistargeting of Rab4.

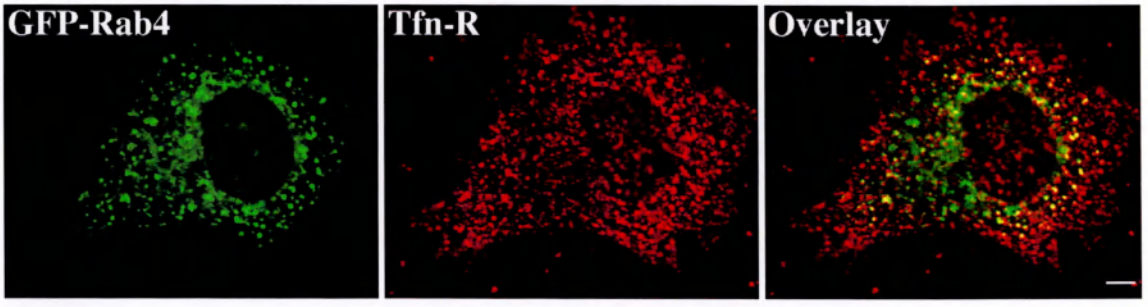

Figure 22: GFP-Rab4 is correctly localized to early endosomes.
A431 cells expressing GFP-Rab4 were fixed and stained with antibodies against transferrin receptor, followed by secondary antibodies coupled to rhodamine. This image represents an individual confocal section. Scale bar represents 2 microns.

Next, I tested whether the GFP-tag interfered with the proper shuttling of Rab4 between membrane and cytosol. To this aim, GFP-Rab4 cells were SL-O-permeabilised and incubated for 20 minutes at 37°C either with recombinant RabGDI or control buffer alone. After extensive washes, cells were fixed and analyzed by fluorescence microscopy. As shown in Figure 23, RabGDI efficiently extracted GFP-Rab4 from the endosomes, as judged by the decrease in GFP fluorescent signal. This result is further evidence that the GFP tag does not interfere with the localization and the membrane/cytosol cycle of Rab4. I next tested whether the over-expression of GFP-Rab4 interferes with the kinetics of transport along the endocytic-recycling pathway. To this end, the recycling of

transferrin was quantified. Biotinylated transferrin was internalized for 2 minutes at 37° C, surface-bound transferrin was removed by ice-cold acid washes and the amount of transferrin recycled to the medium over time was quantified (as described the methods). As shown in Figure 24 the kinetics of recycling in WT and GFP-Rab4 cells are almost identical (except a minor increase at early time points). Altogether, these results indicate that the GFP-Rab4 stable cell line represents a faithful system to analyze the membrane organization of the early endosomal compartment.

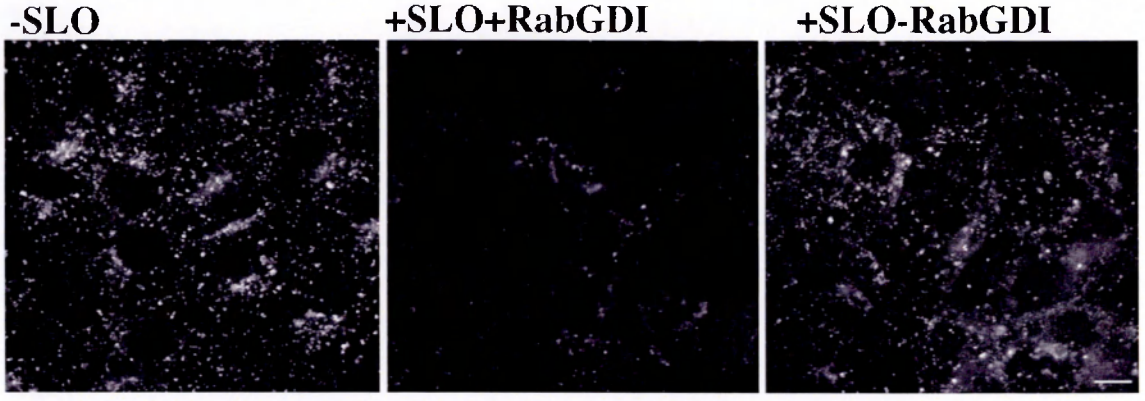

Figure 23: Fluorescence microscopy analysis of GFP-Rab4 expressing cell line treated with RabGDI.

GFP-Rab4 expressing cells were either directly fixed (-SL-O) or SL-O-permeabilised and treated either with 5 μM RabGDI (+SL-O+RabGDI) or with buffer alone (+SL-O-RabGDI) before fixation. Scale bar represents 10 microns.

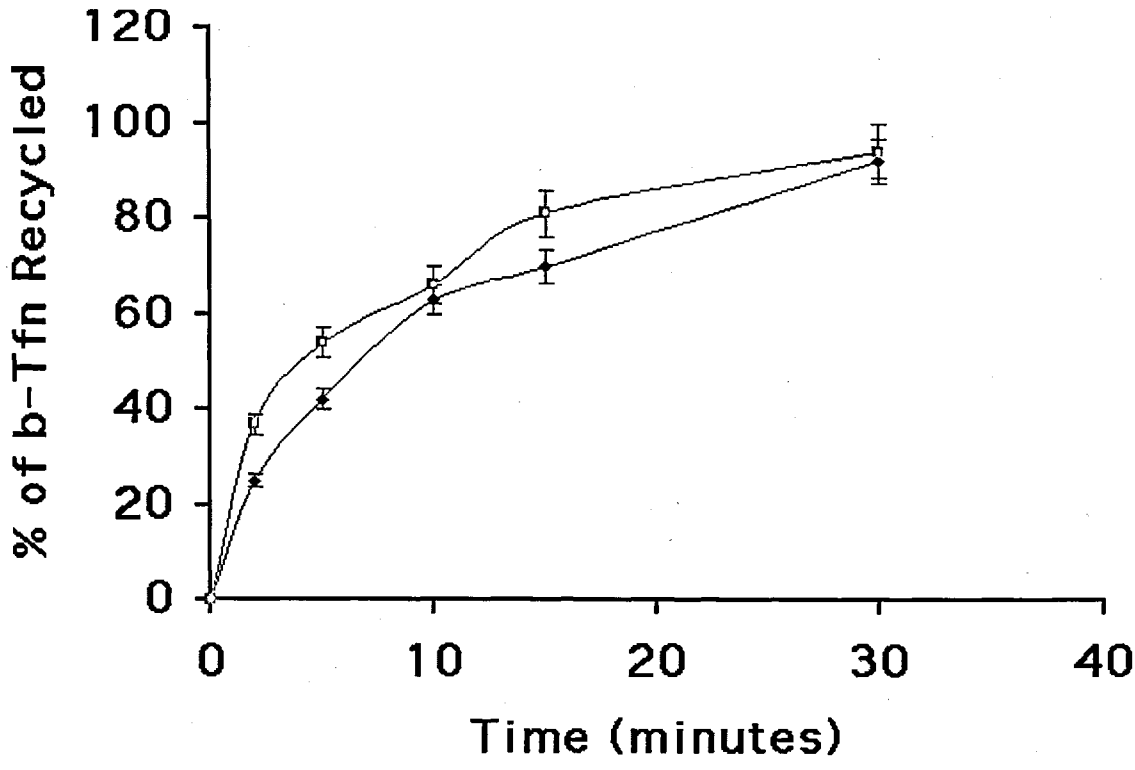

Figure 24: Biochemical measurement of transferrin recycling in A431 cells expressing GFP-Rab4.

A431 wild type cells (pink line) or A431 GFP-Rab4 expressing cells (blue line) were allowed to internalize 10 µg/ml of biotinylated transferrin for 2 minutes at 37 °C, followed by incubation in the presence of an excess of non-labelled transferrin. Medium was collected at the indicated time points and the amount of biotinylated tranferrin recycled quantified. Results are expressed as percentage of total (total=recycled+ intracellular). Data represent means ± SEM from three independent experiments performed in duplicate.

2.8 Transferrin moves sequentially through Rab5-Rab4 and Rab11 positive endosomes.

In agreement with previous studies, at steady state, the transferrin receptor only partially co-localizes with Rab4 (see Figure 22), suggesting that Rab4 is localized only to a sub-populations of early endosomes. To determine at which

stage of its trafficking cycle transferrin transit through Rab4 positive structures, GFP-Rab4 cells were allowed to internalize rhodamine transferrin for 2 minutes and then chased for various periods of times in medium without transferrin. After fixation, images were acquired and the overlap of fluorescence signal was quantified to assess co-localisation (see methods). As shown in Figure 25, after two minutes of internalization, 50% of transferrin positive endosomes also contained Rab4. This fraction rapidly increased up to 90% after the first five minutes of chase and then slowly decreased in the following 10 minutes to remain constant at about 70% as long as the rhodamine-transferrin signal was still detectable. These data indicate that Rab4 is localized only to a sub-population of early endosomes and that transferrin moves sequentially from Rab4-negative to Rab4-positive endosomes before recycling back to the plasma membrane.

Rab5 and Rab11 have been proposed to regulate endocytosis and recycling, respectively. It was therefore interesting to determine the kinetics of transport of transferrin through Rab5 and Rab11 positive endosomes. To this aim, GFP-Rab5 and GFP-Rab11 cell lines (which have been generated and characterized by Drs. Nielsen and Sonnichsen) were allowed to internalize rhodamine transferrin for 2 minutes and then chased in medium without transferrin for different time points. The extent of co-localisation between transferrin and either Rab5 or Rab11 at the different time points was calculated as

for Rab4. Consistent with the role of Rab5 in endocytosis, 2 minutes after internalization 70% of transferrin labelled endosomes contained also Rab5 (Figure 25). This association was transient and rapidly decreased after two minutes of chase, when transferrin started to fill Rab4 positive endosomes. In contrast to Rab5, only 20% of transferrin-labelled endosomes contained also Rab11 at the early time points. This number slowly increased up to 55% during the 30 minutes chase (Figure25), in agreement with the role of Rab11 in the slow recycling loop. Therefore, these results indicate that transferrin travels sequentially through Rab5, Rab4 and Rab11 structures and thus, are in agreement with the idea that these GTPases are not overlapping on the same endosomes, but are rather segregated either on different endosomes and /or on different sub-compartments of the same endosomes.

The sequential movement of transferrin from Rab5 to Rab4 positive structures could occur either in cis (i.e. if these two GTPases are compartmentalized within distinct membrane domains on the same endosomes) or in trans between two different endosomes, one carrying Rab5 and the other Rab4.

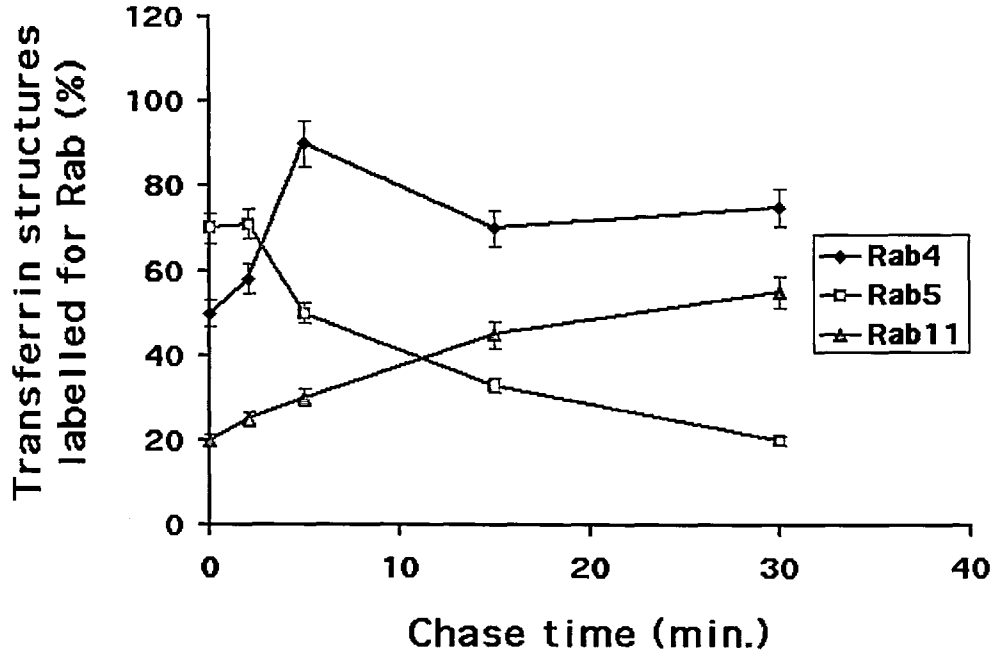

Figure 25: Morphological quantification of rhodamine transferrin trafficking in GFP-Rab4-, Rab5- and Rab11- cell lines.
A431 cells expressing Rab4 (blue) Rab5 (pink) and Rab11 (green) were allowed to internalize rhodamine transferrin for 2 minutes at 37 °C, followed by incubation in the presence of an excess of non-labelled transferrin for the indicated time points. Images of fixed cells were analyzed for fluorescent overlap as described in methods. Data represent means ± SEM from three independent experiments performed in duplicate.

To address this point it was necessary to visualize the trafficking of transferrin with respect to both Rab5 and Rab4 in the same cell. To this aim, eukaryotic expression vectors expressing CFP-Rab5 and YFP-Rab4 (CFP and YFP are colour-shifted variants of GFP that can be discriminated from each other as well as from fluorophores emitting in the red region of the spectrum) were microinjected directly into the nucleus of A431 cells. This technique of transfection allows precise control of over-expression level and it ensures co-

expression of two or more plasmids in the same cell. Six hours post-injection, Texas-red labelled transferrin was internalized for different lengths of time and, after fixation, confocal sections were obtained and processed with a deconvolution software before quantification of overlapping fluorescent signal (Figure 26).

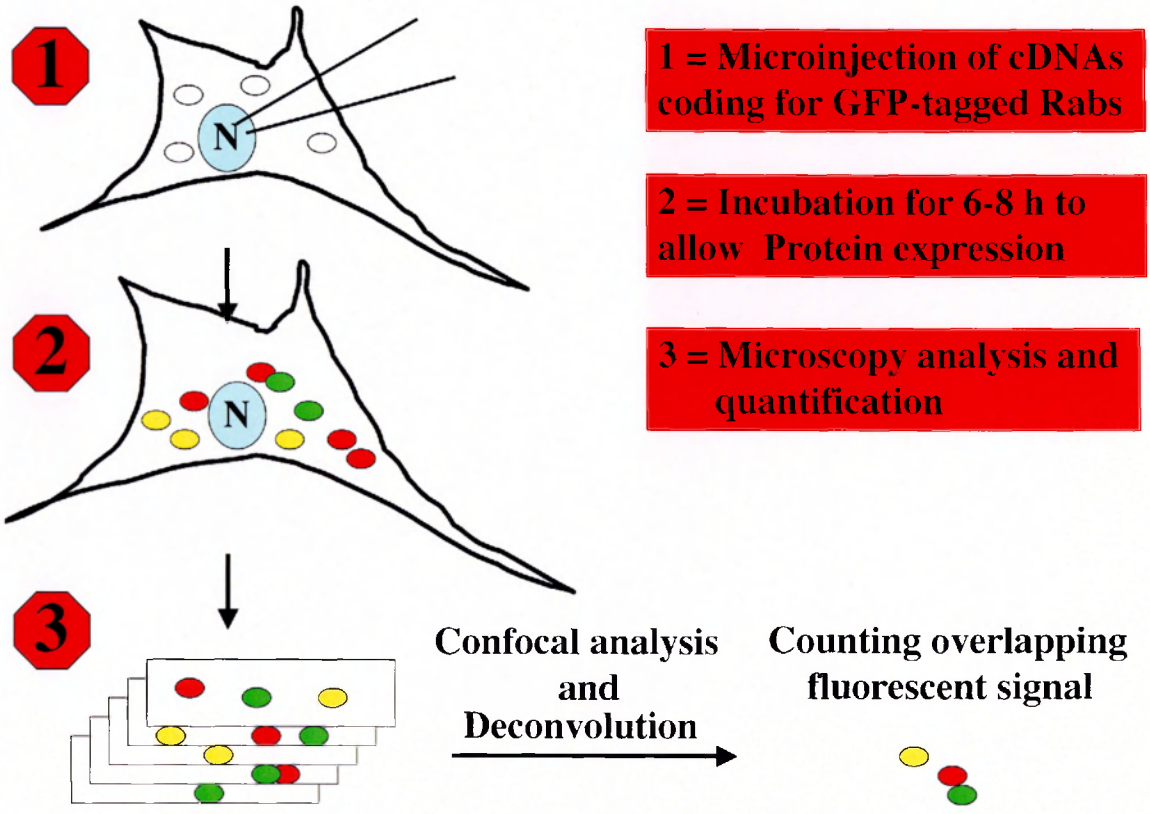

Figure 26: Schematic representation of the methods used to quantify the endosomal distribution of Rab4, Rab5 and Rab11

Empty circles represent unlabelled endosomes. Green circles represent endosomes labelled by YFP-Rab. Red circles represent endosomes labelled by CFP-Rab. Yellow circles represent endosomes labelled by both YFP- and CFP-Rab.

As shown in Figure 27 the Rab5 and Rab4 fluorescence signal was often seen to be segregated within the same continuous transferrin-filled endosomes.

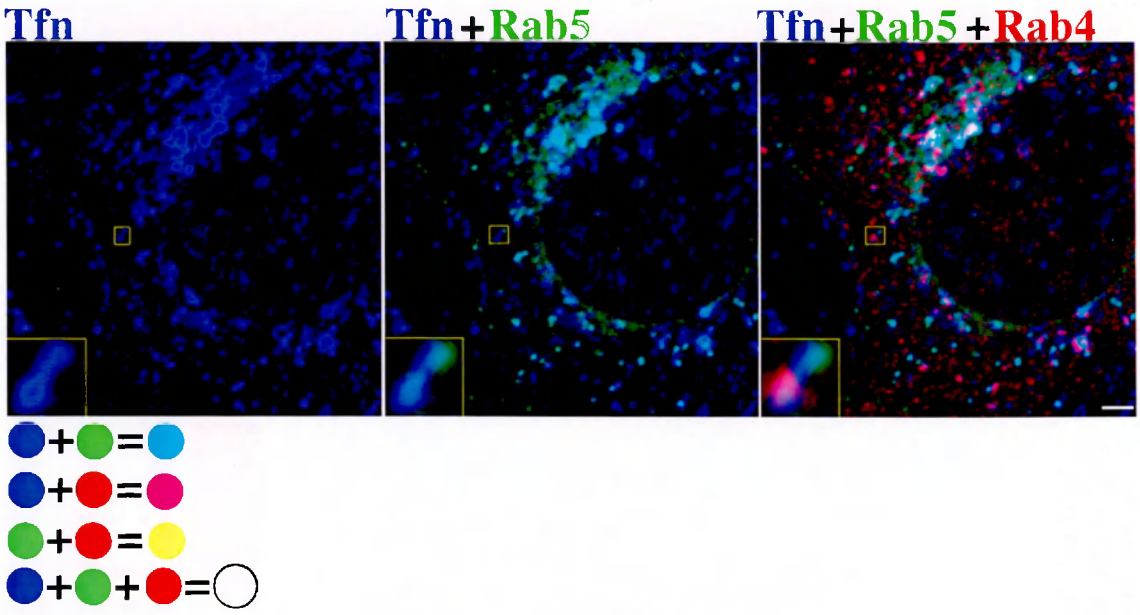

Figure 27: Confocal analysis of YFP-Rab4 and CFP-Rab5 on transferrin-filled endosomes.

A431 cells co-expressing YFP-Rab4 and CFP-Rab5 were allowed to internalize Texas-red transferrin for 30 minutes, fixed and analyzed by confocal microscopy. This image represents an individual confocal section. Tfn= transferrin. The scale bar represents 2 microns.

Recycling cargo is sorted from Rab5 to Rab4-positive structures early (within 5 minutes) after internalization. Within this time-frame, as much as 60% of transferrin-labelled endosomes contained both Rab5 and Rab4 (see Table 1), suggesting that transferrin is transported through distinct Rab5 and Rab4 membrane domains, residing on the same endosome. Transport through these endosomes is relatively fast compared to the overall length of the transferrin cycle. Indeed, at steady-state labelling, only ~25% of transferrin-positive endosomes harboured both Rab5 and Rab4 and transferrin was mainly found in Rab4 positive endosomes (Table 1). Cargo transport through Rab11 structures follows transit

through Rab4 endosomes. Consistently, experiments conducted in collaboration with Dr. Sonnichsen indicate that at steady state ~70% of transferrin-positive endosomes contained both Rab4 and Rab11, while only 20% contained Rab5 and Rab11 (Table1). Just like Rab5 and Rab4, Rab4 and Rab11 seemed to occupy distinct membrane domains on the same transferrin-filled endosome (Figure 28). It is therefore possible that also the sorting of cargo from Rab4 to Rab11-positive elements occurs within a continuous endosomal element.

Table 1. Quantification of Rab5, Rab4 and Rab11 on transferrin-labelled endosomes

	Rab5	**Rab4**	**Overlap**
Tfn endosomes, 2 min. internalization, 3 min. chase	66 ± 6	68 ± 1	51 ± 8
Tfn endosomes, 30 min. internalization (steady state)	51.5±8	79±4	23.5 ± 7
	Rab5	**Rab11**	**Overlap**
Tfn endosomes, 30 min. internalization (steady state)	54 ± 3	65 ± 1	19 ± 8
	Rab4	**Rab11**	**Overlap**
Tfn endosomes, 30 min. internalization (steady state)	84 ± 1	68 ± 4	63.5 ± 5

Fluorescence analysis: plasmids coding for two Rab proteins fused to YFP and CFP were expressed and Texas red–labelled transferrin was internalized for the indicated time. Numbers represent the percentage of endosomes labelled for the indicated combination of Rab proteins.

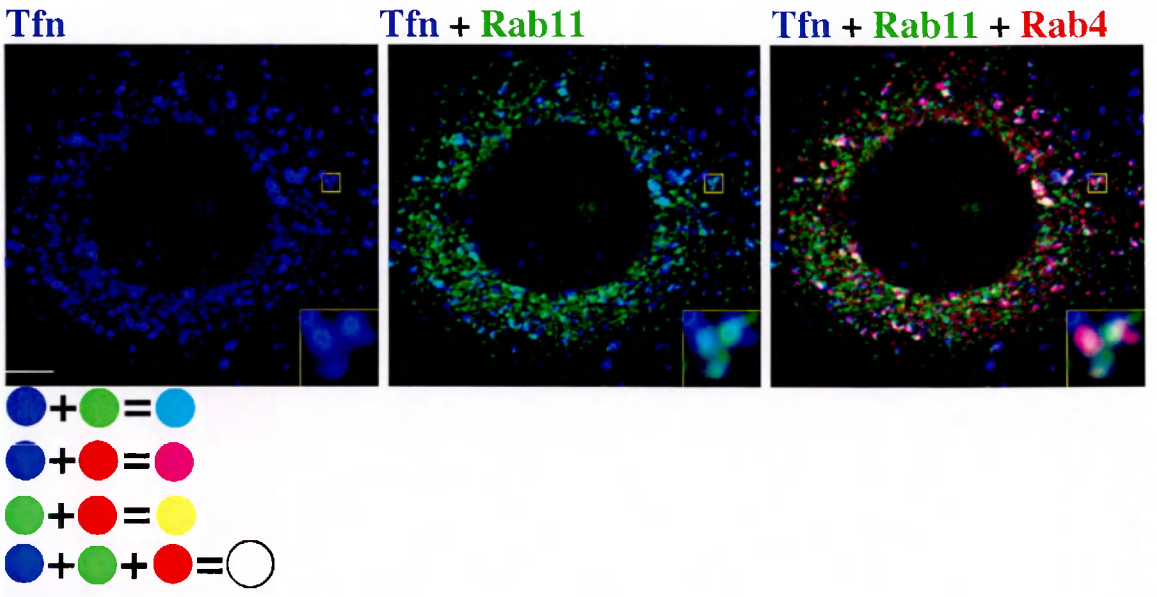

Figure 28: Confocal analysis of YFP-Rab4 and CFP-Rab11 on transferrin-filled endosomes.

A431 cells co-expressing YFP-Rab4 and CFP-Rab11 were allowed to internalize Texas-red transferrin for 30 minutes, fixed and analyzed by confocal microscopy. This image represents an individual confocal section. Tfn=transferrin. Scale bar represents 2 microns.

These data indicate that Rab4 is localized to two distinct endosomal populations: one carrying Rab5+Rab4 and another one Rab4+Rab11. To quantify this distribution, all the Rab4 endosomes were counted and the extent of co-localization with Rab5 and Rab11 was determined (Figure 29). About 50% of Rab4-positive endosomes contained also Rab5. Another pool similar in size contained Rab4 and Rab11 and about 20% of all the Rab4 endosomes contained all the three Rab proteins together. In contrast to the majority of Rab4-endosomes, which co-labelled with either Rab5 or Rab11, a significant portion of Rab5 endosomes (50%) did not co-label for Rab4 or Rab11.

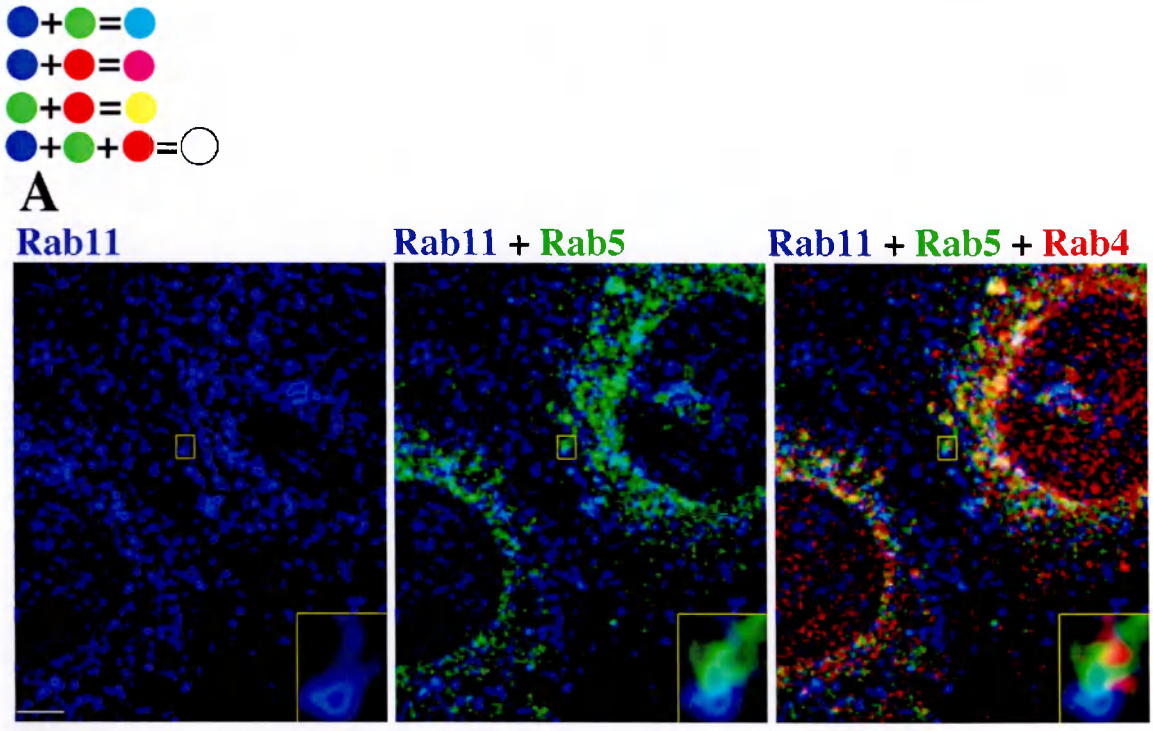

Figure 29: Confocal analysis of Rab4, Rab5 and Rab11 endosomes.
A431 cells co-expressing YFP-Rab4 and CFP-Rab5 were fixed and stained with antibodies against Rab11 followed by secondary antibodies conjugated to Texas-red. The image shown in A represents a single confocal section. Scale bar represents 2 microns. In B is shown the quantification of the overlapping fluorescence signal for Rab5, Rab4 and Rab11. Numbers represent the percentage of Rab5 endosomes alone or in combination with Rab4 and Rab11.

Therefore, with respect to the Rab5, Rab4 and Rab11 machinery, endosomes can be sub-divided in three major categories: one containing Rab5, another one harbouring both Rab5 and Rab4, and a third carrying Rab4 and Rab11. Upon internalization from the plasma membrane transferrin first enters

Rab5-positive endosomes, then it moves into endosomes harbouring both Rab5 and Rab4 and eventually accumulates in Rab4 and Rab11 positive endosomes, before recycling back to the plasma membrane. Altogether, these data suggest that cargo move sequentially through endosomes that are structured in distinct Rab domains.

2.9 The Rab5 effector EEA1 is specifically localized to Rab5 domains

The results so far obtained are consistent with the hypothesis that Rab5, Rab4 and Rab11 are compartmentalized within defined membrane domains. Given that Rab proteins function through membrane recruitment of specific sets of effector protein, one prediction is that also these effectors are compartmentalized within the corresponding Rab domain. For example, internalized cargo enters into early endosomes via the Rab5-domain presumably because the molecular machinery required for the fusion of incoming CCVs with early endosomes is localized in this membrane sub-compartment. A key component regulating the fusion between incoming vesicles and early endosomes is the Rab5 effector EEA1 (see Introduction). To test whether EEA1 is localized to the same membrane region as Rab5, the GFP-Rab5 cell line, or the GFP-Rab4 cell line as control, were stained with antibodies against EEA1. As shown in Figure 30, EEA1 completely co-localized with Rab5 and only partially with Rab4. Very interestingly, while the

EEA1 fluorescent signal always seemed to originate from round, dot-like structures, the Rab4 signal defines more tubular elongated structures. This difference was also evident in cases where Rab4 and EEA1 localized to the same endosome (see inset Figure 30 A-C).

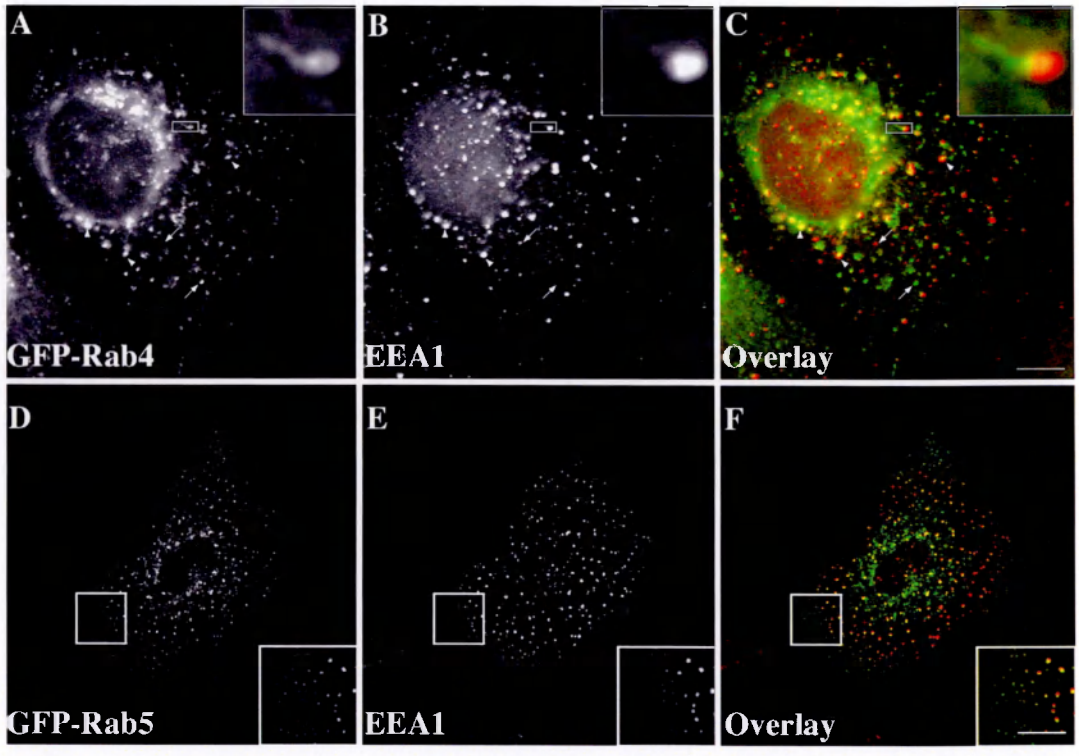

Figure 30: Localization of EEA1 in the GFP-Rab4 and GFP-Rab5 stable cell lines. A431 cells expressing GFP-Rab4 (A-C) or GFP-Rab5 (D-F) were fixed and stained with antibodies against EEA1, followed by secondary antibodies conjugated with Texas-red. Each image represents a single confocal section. Scale bar represents 2 microns (A-C) and 4 microns (D-F).

From ultra-structural investigations, early endosomes have been described to be composed of morphologically and functionally distinct vacuolar, cisternal and tubular sub-compartments (see Introduction). Endosome tubulation can be

enhanced by treating cells with Brefeldin A (BFA) (Lippincott-Schwartz et al., 1991). Treatment of GFP-Rab4 cells with BFA results in the formation of an extensive tubular network where Rab4 localized (Figure 31). Intriguingly, a fraction of membranes positive for Rab4, did not tubulate and remained in distinct globular structures, which were also positive for EEA1. Consistently, EEA1-positive endosomes were completely insensitive to BFA. I therefore tested whether Rab5 positive membranes were also BFA-insensitive. As shown in Figure 31, treatment of the GFP-Rab5 cell line with BFA did not cause tubulation of the Rab5 endosomes and, as in non-treated cells, EEA1 and Rab5 still co-localized on the same globular structures. However, Rab11-positive structures also responded to BFA and co-localized with Rab4 extensively in the tubular network. In contrast to Rab4, all the Rab11-positive membranes tubulate in response to BFA, whereas the non-tubulated Rab4 structures did not contain Rab11 (Figure 32). In summary, endosomes comprised of Rab5 and Rab4 domains are insensitive to BFA, while the opposite is true for those endosomes composed of Rab4 and Rab11 domains. The different pharmacological sensitivity supports the idea that Rab5, Rab4 and Rab11 domains represents biochemical and presumably functionally distinct environments.

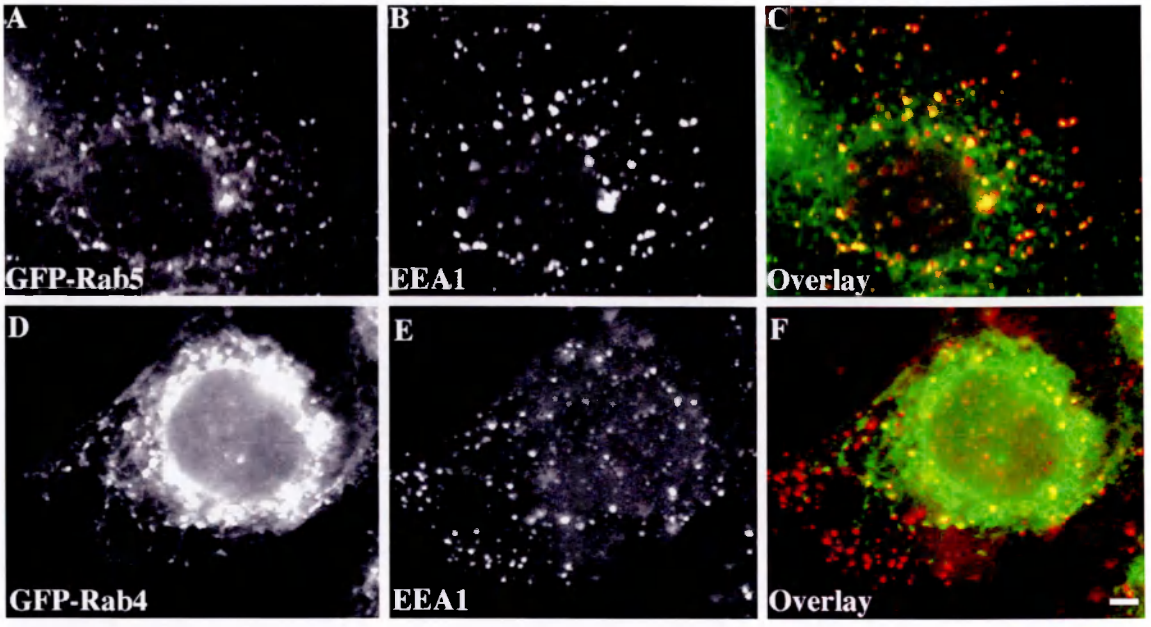

Figure 31: Differential response of Rab5 and Rab4-positive endosomes to BFA.
A431 cells expressing GFP-Rab5 (A-C) or GFP-Rab4 (D-F) were treated for 10 minutes with BFA (5 µg/ml), fixed and stained with antibodies against EEA1, followed by secondary antibodies conjugated to Texas-red. This image represents an individual confocal section. Scale bar represents 2 microns.

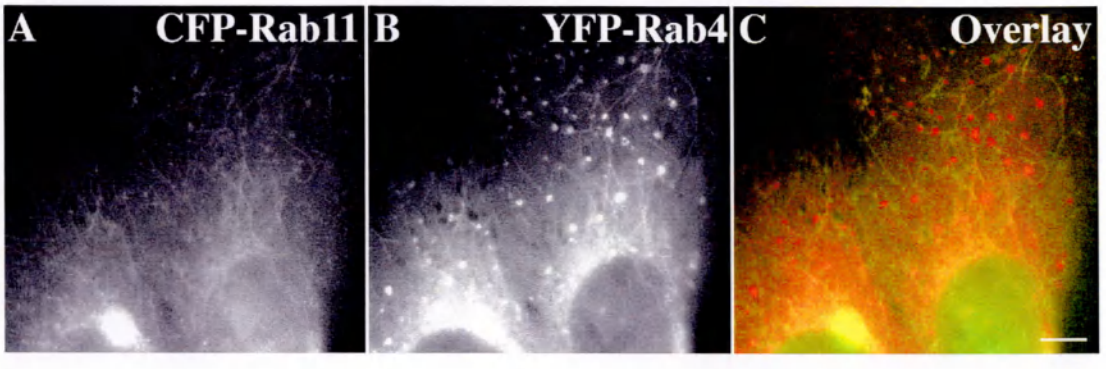

Figure 32: Differential response of Rab4 and Rab11 positive endosomes to BFA.
A431 cells co-expressing CFP-Rab11 and YFP-Rab4 were treated for 10 minutes with BFA (5 µg/ml), fixed and processed for fluorescence microscopy analysis. Scale bar represents 1 micron.

2.10 Introduction to results (part-3)

The morphological analysis performed in the previous section support the hypothesis that Rab5, Rab4 and Rab11 are compartmentalized within defined membrane domains. Multiple combinations of these domains define three major endosomal populations: one containing only Rab5, a second Rab5 and Rab4, and a third Rab4 and Rab11. The steady-state association between these domains is not random and recycling cargo moves sequentially from Rab5 to Rab4 and from Rab4 to Rab11 domains. Therefore, regulatory mechanisms must exist to control the association and to ensure co-ordination between neighbouring domains. For example Rab5 and Rab4 domains must be joined together to allow fast recycling. The Rab11 domain should then be connected to the Rab4 domain, as these two sub-compartments are located in the peri-nuclear recycling endosomes.

Since Rab proteins regulate membrane tethering and Rab effectors have been demonstrated to be tethering molecules, one possible point of regulation for combining Rab domains would be at the level of Rab effectors. In particular, the finding that Rabaptin-5 interacts with both Rab5 and Rab4 supports this hypothesis. How can this model be experimentally tested? Once, a recycling receptor (like the transferrin receptor) is internalized, it first enters the Rab5 domain in early endosomes, and then progresses through Rab5/Rab4 and

Rab4/Rab11 endosomes before recycling back to the surface. According to the experiments depicted in Figure 25, the sorting of recycling cargo from Rab5 to Rab4 domains occurs within the first five minutes after internalization and thus the function of the common Rab5 and Rab4 effectors might be limited to this time frame. Therefore, it is likely that the *in vitro* recycling assay, which I have developed, is not a suitable system to study this transport step. As shown in Figure 25, after 30 minutes of internalization (the time of internalization used in this assay), transferrin has already exited from Rab5 structures and is mainly found in Rab4 and Rab11 positive-endosomes. These observations may also explain why immunodepletion of Rabaptin-5 did not inhibit recycling despite the demonstration of a Rab4-requirement for recycling. Due to technical limitations the time of internalization and the time required to achieve permeabilisation can not be reduced to less than eight minutes. Thus, the only possibility to reconstitute the transition of cargo from Rab5 to Rab4 positive structures in this *in vitro* assay, would be to reconstitute both endocytosis and recycling in permeabilised cells by internalizing transferrin after permeabilisation. However, the results of such experiments would always be difficult to interpret because any putative effect on recycling may always be an indirect consequence of an inhibition of endocytosis. Given the difficulties with the biochemical assay, I turned to the *in vivo* Rab localization assay to examine the possibility of Rab5-Rab4 co-ordination. This

system allows high resolution mapping of endosomal morphology and might therefore be useful in assessing possible functions of Rab effectors in controlling domains association. Furthermore, the assay can simultaneously detect kinetic effects on transferrin trafficking, possibly resulting from altered domain architecture. In particular, I have used this assay to test the hypothesis whether molecules, which have the ability to bind both Rab5 and Rab4, can regulate the association between Rab5 and Rab4 domains and thus affect the transport of cargo along the endocytic-recycling pathway. In the following paragraphs, I will describe the experiments I have performed to this aim.

2.11 Identification of proteins interacting with both active Rab5 and Rab4.

By developing an affinity chromatography approach, Christoforidis and co-workers in our laboratories could show that active (GTP-Bound) Rab5 specifically interacts with over twenty-two proteins (Christoforidis et al., 1999). This finding raises the question whether Rab4 would also interact with a similar multitude of effectors and if so, whether Rabaptin-5 is the only common Rab5 and Rab4 effector. To approach this problem, I developed an experimental strategy based on two sequential steps of affinity chromatography. The first step served to purify the Rab5 interacting proteins and the second step consisted of the absorption of these

proteins on GST (glutathione S-transferase)-Rab4 bound to glutathione beads (see Figure 33 for a schematic representation of the methods).

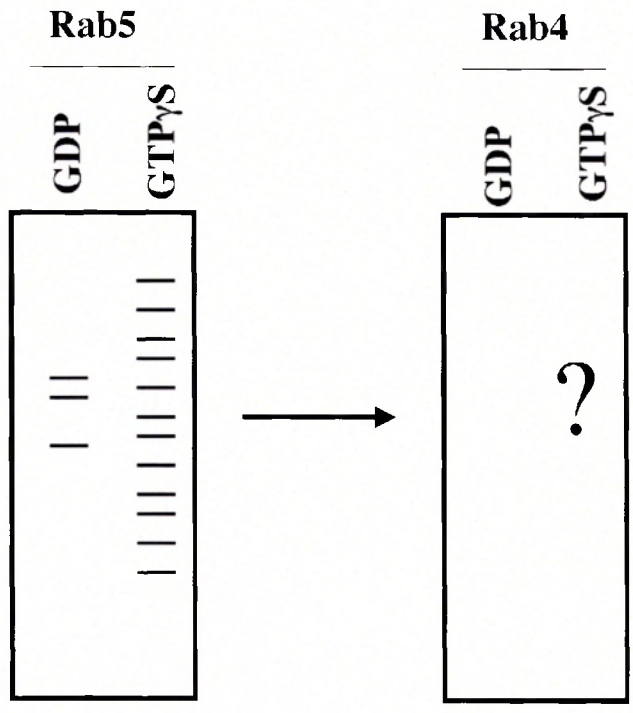

Figure 33: Schematic representation of sequential affinity chromatography strategy.

The purification of Rab5 effectors was conducted according to the protocol established by Christoforidis and co-workers. This method is based on the ability of bacterially expressed GST-Rab5 (immobilized on glutathione beads) to interact with its effectors in a nucleotide-dependent manner. Rab5 can be efficiently stabilized in its active GTP-bound conformation in the presence of the slowly hydrolysable GTP analogue GTPγS. Thus, when glutathione beads containing GST-Rab5 loaded with GTPγS are incubated with a source of cellular proteins

(such as bovine brain cytosol), Rab5 effectors will be specifically retained on the beads. As the interaction of Rab proteins with their effectors is GTP dependent, Rab5 effectors can be specifically eluted from the beads by changing the nucleotide-bound state of Rab5 via removal of the nucleotide from the binding pocket.

To perform the sequential affinity chromatography experiment, glutathione beads coated with GST-Rab5 loaded with GTPγS, were incubated with bovine brain cytosol. The bound proteins were eluted, dialyzed against nucleotide-free buffer and applied to a column containing GST-Rab4 in the presence of GTPγS, or as control, GDP. Bound proteins were eluted from the beads, separated on SDS-PAGE and stained with silver nitrate. Figure 34 shows the results of this experiment. Rabaptin-5 has already been shown to interact with both Rab5 and Rab4. Therefore, I was expecting to find at least three proteins on the Rab4 column: Rabaptin-5, its binding partner Rabex-5 and Rabaptin5-β. However, four bands instead of three were found in the eluate from Rab4-GTPγs (lane 2) but not Rab4-GDP column (lane 3). By using a combination of mass spectrometry and Western blot experiments, these bands were found to correspond to Rabaptin-5, Rabaptin-5β, Rabex-5 and, the fourth one to Rabenosyn-5 (see Figure 34B lane 2). The specificity of these interactions is validated by the observation that, under the same experimental conditions, two of the most abundant Rab5 effectors, EEA1

and p110β did not interact with Rab4 (Figure 34B lane1-2). Rabenosyn-5 was previously identified as a Rab5 effector regulating membrane tethering/fusion at the stage of entry into early endosomes. Similar to the Rab5 effector EEA1, it binds PI(3)P through a FYVE finger domain and it is recruited to early endosomes in a Rab5 and PI-3-kinase-dependent fashion. Consistently, both Rabenosyn5 and EEA1 co-localise within the Rab5-positive endosomal domain (Nielsen et al., 2000). The finding that this protein can also interact with Rab4 suggests an additional role for Rabenosyn-5 in early endosome function. I therefore decided to further characterize the interaction between Rab4 and Rabenosyn-5.

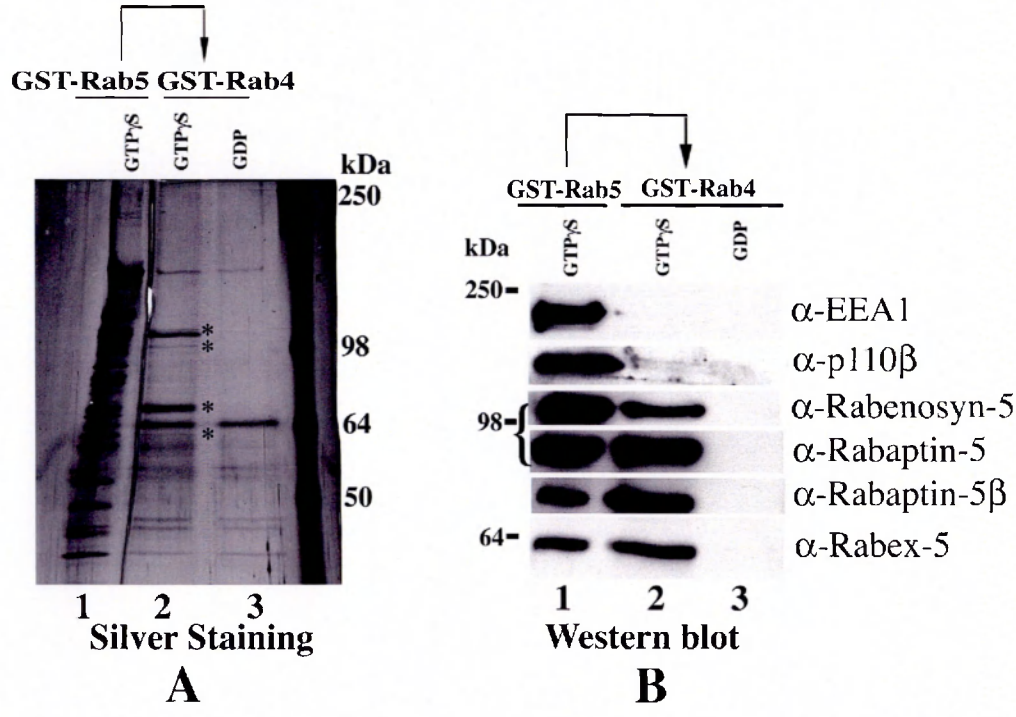

Figure 34: Purification and identification of Rab5 and Rab4 common effectors using sequential affinity chromatography

(A) GST-Rab5:GTPγS affinity columns were incubated with bovine brain cytosol. Bound proteins were eluted (lane 1), and subsequently incubated with GST-Rab4:GTPγS (lane 2) or GST-Rab4:GDP (lane 3). Bound proteins were eluted and analyzed by gradient SDS- (PAGE) and silver staining.

(B) Western blot analysis of proteins interacting with both active Rab5 and Rab4 (lane1-2) purified as in (A). The four bands indicated with an asterisk in (A) were detected by anti-Rabaptin-5, -Rabaptin-5β, -Rabex-5 and -Rabenosyn-5 antibodies (lane 2).

2.12 Biochemical characterization of the interaction between Rabenosyn-5 and Rab4.

To confirm that the interaction of Rabenosyn-5 with Rab4 was not peculiar to the experimental condition used, I tested whether Rab4 and Rabenosyn-5 were also able to interact independently of the pre-Rab5 purification on the Rab5 affinity chromatography. GST-Rab4 was incubated directly with bovine brain cytosol, bound proteins were eluted and analyzed by Western blot with an anti-Rabenosyn-5 antibody. Figure 35 shows that also under these conditions, Rabenosyn-5 specifically interacted with Rab4:GTPγS (lane3) but not with Rab4:GDP (lane2).

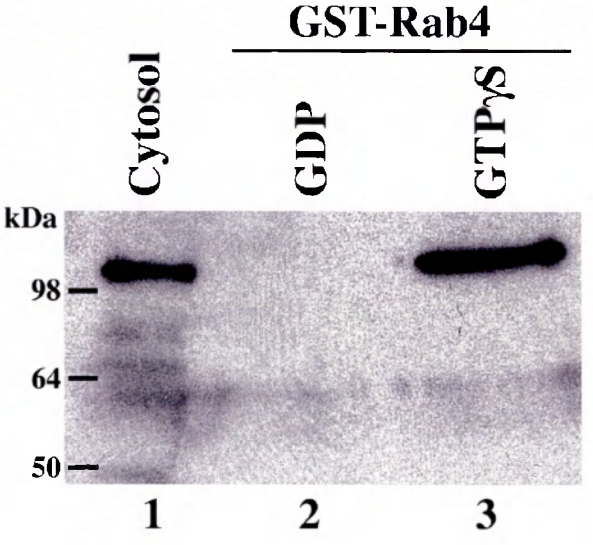

Figure 35: Cytosolic Rabenosyn-5 interacts with Rab4.
Bovine brain cytosol (lane 1) was incubated with GST-Rab4:GDP (lane 2) or GST-Rab4:GTPγS (lane 3). Bound proteins were eluted, separated by SDS-PAGE and analyzed by immunoblotting with antibodies against Rabenosyn-5.

Next, I tested whether the interaction between Rabenosyn-5 and Rab4 is direct or is mediated by a third cytosolic component. In cytosol, Rabenosyn-5 is complexed with hVPS45, a Sec-1 related protein regulating the assembly between endosomal v- and t-SNAREs. The interaction between Rab5 and Rabenosyn-5 is direct, whereas hVPS45 interacts with Rab5 only through Rabenosyn-5 (Nielsen et al., 2000). To test if similar molecular principles control the interaction between Rab4, Rabenosyn-5 and hVPS45 I performed affinity chromatography experiments using *in vitro* translated proteins. Rabenosyn-5 and hVPS45 were either translated separately or co-translated and incubated with glutathione beads containing GST-Rab4. Rabenosyn-5 interacted directly with Rab4 in a nucleotide-specific manner (Figure 36 lanes 1-2). No interaction was detected between hVPS45 and Rab4, unless it was co-translated with Rabenosyn-5 (Figure 36, compare lanes 3-4 with lanes 4-5). These results showed that Rabenosyn-5 binds directly to Rab4 and, by analogy to Rab5, this interaction might serve as a link between Rab4 and hVPS45.

The binding of Rabenosyn-5 to both Rab5 and Rab4 raises the question whether Rabenosyn-5 would interact also with other Rab proteins localized to early and recycling endosomes. In particular, due to the double association of Rab4 domains with both Rab5 and Rab11 domains, I investigated whether Rab11 and Rabenosyn-5 also interact. To this aim, GST-Rab11 or, as control GST-Rab4,

were incubated with *in vitro* translated Rabenosyn-5 in the presence of GDP or GTPγS. Figure 37 (lanes 2-3) shows that Rabenosyn-5 does not interact with Rab11.

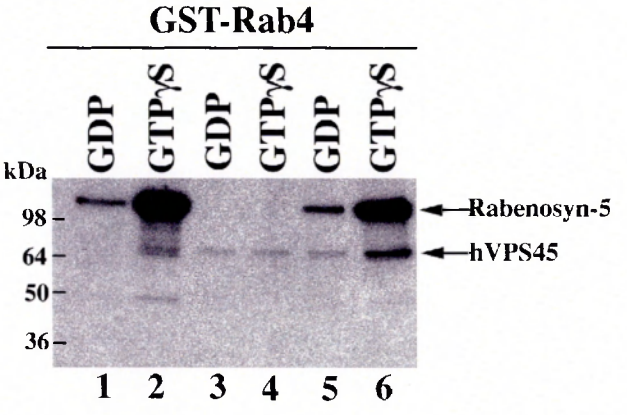

Figure 36: Rabenosyn-5 interacts directly with Rab4 and recruits hVPS45 to Rab4
GST-Rab4:GDP (lanes 1-3-5) or GST-Rab4:GTPγS (lanes 2-4-6) were incubated with ^{35}S methionine-labelled *in vitro* translated Rabenosyn-5 alone (lanes 1-2), hVPS45 alone (lanes 3-4) or co-translated Rabenosyn-5 and hVPS45 (lanes 5-6). Bound proteins were eluted and analyzed by SDS-PAGE followed by autoradiography.

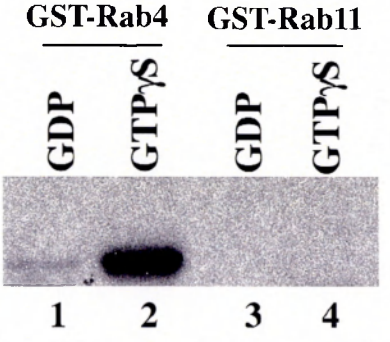

Figure 37: Rabenosyn-5 does not interact with Rab11.
GST-Rab4:GDP (lane 1), GST-Rab4:GTPγS (lane 2), GST-Rab11:GDP (lane 3), GST-Rab4:GTPγS (lane 4), were incubated with ^{35}S methionine-labelled *in vitro*-translated Rabenosyn-5. Bound proteins were eluted and analyzed by SDS-PAGE followed by autoradiography.

2.13 Rabenosyn-5 labels the endosomes where Rab5 and Rab4 co-localise.

In addition to its established role in Rab5-dependent endocytic membrane fusion, Rabenosyn-5 may play a role in the functional connection between Rab5 and Rab4 domains. In this case, one would expect this protein to localize to those endosomes that contain both Rab proteins. Alternatively, if the interaction with Rab4 is functionally independent of that with Rab5, Rabenosyn-5 may be localized to membranes harbouring only Rab4 or Rab5. To distinguish between these two possibilities, I used the same approach as described in the previous sections used to visualize and quantify the distribution of Rab5, Rab4 and Rab11 to distinct domains of early and recycling endosomes.

A431 cells co-expressing CFP-Rab5 and YFP-Rab4 were fixed and stained with affinity-purified anti-Rabenosyn-5 antibodies. Confocal serial sections were obtained and processed with a deconvolution software before quantification of overlapping fluorescence signal. The result of this triple labelling experiment is shown in Figure 38. Ninety-five percent of the endosomes harbouring Rabenosyn-5 contained also Rab5 (Figure 38D) and, of those, 55% were positive for Rab4 (Figure 38E). Importantly, the latter pool corresponds to those endosomes containing both Rab5 and Rab4 (Figure 38F) as well as all three together (Figure 38G). Therefore, whenever endosomes contained both Rab5 and Rab4, they were also positive for Rabenosyn-5 (arrows in Figure 38 D, E, F, G and for

quantification, panel H). Interestingly, as shown in the inset of Figure 38, while Rab5 and Rabenosyn-5 localized always to the same endosomal domain, Rab4 was often seen to segregate into elongated structures. These morphological data support the hypothesis that Rabenosyn-5 may regulate the functional link between Rab5 and Rab4 domains.

The particular localization of Rabenosyn-5 might reflect a higher affinity for Rab5 over Rab4 or being the consequence of both Rab5 and PI(3)P binding sites as co-operative targeting determinants. To discriminate between these two different possibilities I sought to measure the affinity constant of the interaction between Rab5 and Rab4 with Rabenosyn-5. To this aim, *in vitro*-translated Rabenosyn-5 was incubated for 1 hour at room temperature with serial dilutions of glutathione–sepharose beads containing GST-Rab4 or -Rab5 (with the total concentration of Rabenosyn-5 being always well below that of GST-Rab to ensure maximal binding). Beads were spun through a 1 ml 40 % sucrose cushion to separate bound from unbound Rabenosyn-5. Proportional aliquots of bound, unbound and total fractions were separated by SDS-PAGE, and analyzed with a phosphoimager reader for quantification.

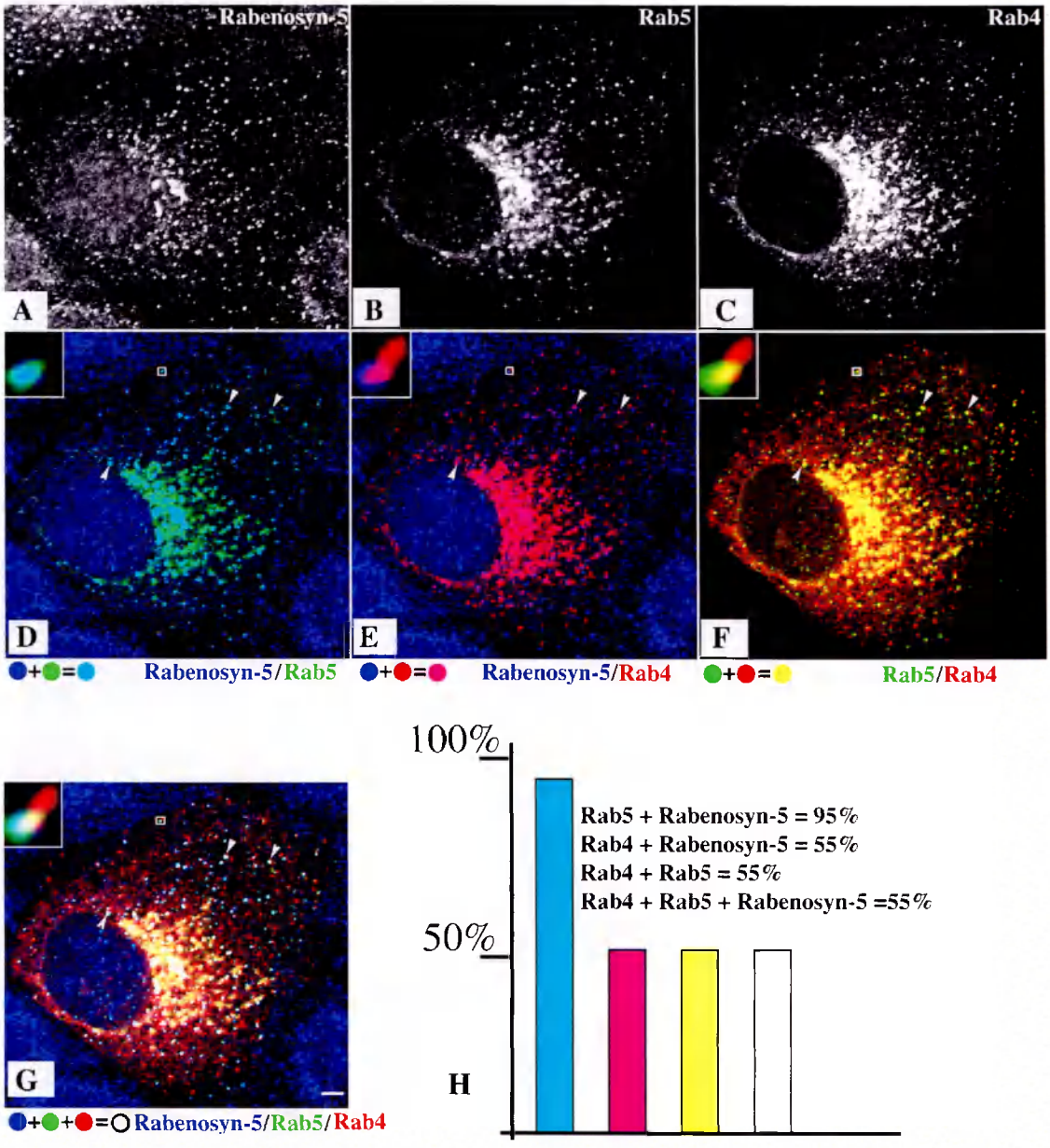

Figure 38: Confocal immunofluorescence analysis of Rab5, Rab4 and Rabenosyn-5 labelled endosomes

(A-G) A431 cells expressing CFP-Rab5 and YFP-Rab4 were fixed and stained with antibodies against Rabenosyn-5 followed by secondary antibodies conjugated to Texas-red. Individual confocal sections are shown. Bar = 3 microns.

(H) The extent of co-localization between Rab5, Rab4 and Rabenosyn-5 was quantified as described in the methods section. Colours in the histogram correspond to the colours used in the merge of double or triple fluorescent signals in the overlay panels.

Binding of Rabenosyn-5 to empty GST beads was considered as background and therefore subtracted from each binding value before calculating percentage of binding. The result of this experiment showed that Rab5 and Rab4 interact with Rabenosyn-5 with similar affinity (Kd ~400nM, Figure 39). Therefore, I favour the possibility that targeting of this protein to Rab5 domain is the consequence of both Rab5 and PI(3)P binding. In agreement with this proposal is the observation that the FYVE finger domain of Rabenosyn-5 is necessary for its endosomal localization (Nielsen et al., 2000). In addition, as in the case of Rab4 endosomes, a substantial fraction of Rab5 positive structures (ca. 40%) do not co-localize with Rabenosyn-5, indicating that Rab binding alone is not sufficient for Rabenosyn-5 localization.

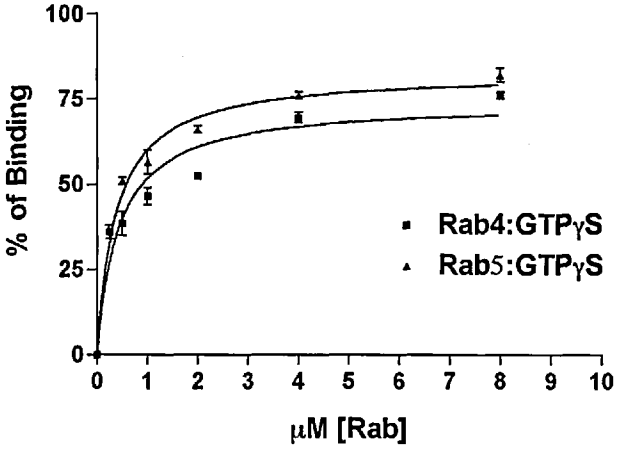

Figure 39: Rabenosyn-5 interacts with similar affinity with Rab5 and Rab4.
Rabenosyn-5 was in vitro transcribed-translated in the presence of 35S-methionine and the percentage of binding to Rab5 and Rab4 was calculated as described in the methods (see section 4.11). Data represent means (SEM from two independent experiments performed in duplicate.

2.14 Rabenosyn-5 interacts simultaneously with both active Rab5 and Rab4

I next sought to determine whether Rab5 and Rab4 bind simultaneously or if their binding is mutually exclusive. To this aim, Rabenosyn-5/hVPS45 were co-expressed in insect cells using the baculovirus expression system, as bacterially expressed Rabenosyn-5 alone was found to be insoluble. Forty-eight hours post infection, cytosol from either mock- or Rabenosyn-5/hVPS45 infected cells was prepared and analyzed by Western-blotting to assay Rabenosyn-5 over-expression. As shown in Figure 40 Rabenosyn-5 was expressed only in the Rabenosyn-5/hVPS45 infected lysate, and when cytosol was separated from total membranes by ultracentrifugation, Rabenosyn-5 was quantitatively recovered in the cytosolic fraction.

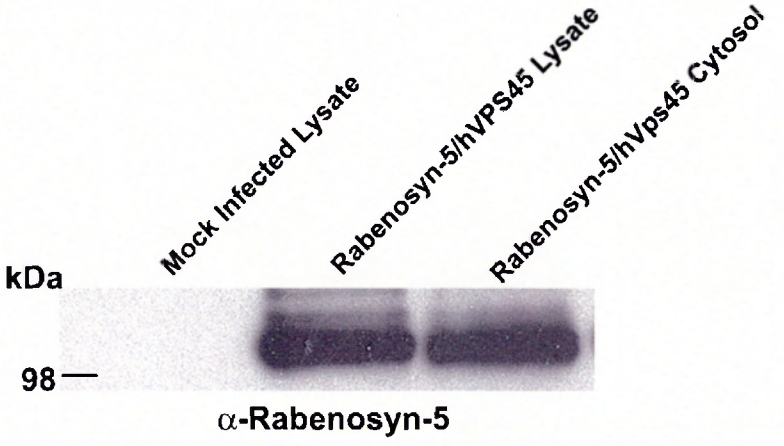

Figure 40: Western blot analysis of Rabenosyn-5 over-expression in insect cells.
Insect cells over-expressing Rabenosyn-5 and hVPS45 were harvested, lysed and lysate samples were either directly processed for Western blot analysis or first spun for 1 hour at 40000 Xg to separate total membranes from cytosolic extract.

GST-Rab4 immobilized on sepharose beads and loaded with GTPγS was incubated with Rabenosyn-5/hVPS45 over-expressing cytosol for two hours. Unbound Rabenosyn-5/hVPS45 complex was removed by three washes and the GST-Rab4 column was further incubated with purified Rab5, or as control Rab11, loaded with GTPγS. After extensive washes, bound proteins were eluted and analyzed by Ponceau staining and Western blotting (Figure 41 A and B). Rab5 specifically interacted with GST-Rab4 only if GST-Rab4 was pre-incubated with Rabenosyn-5/hVPS45 over-expressing cytosol but not if the pre-incubation was performed with either mock cytosol or BSA (Figure 41 A and B). Besides Rab5, four other proteins were eluted from the column. Two were common to all the lanes and corresponded to BSA (used to block non-specific binding) and to GST-Rab4 leaked during the elution step, respectively. The second and the third one, corresponded to Rabenosyn-5 and hVPS45. This result indicates that *in vitro* Rab5 and Rab4 can bind to Rabenosyn-5 at the same time.

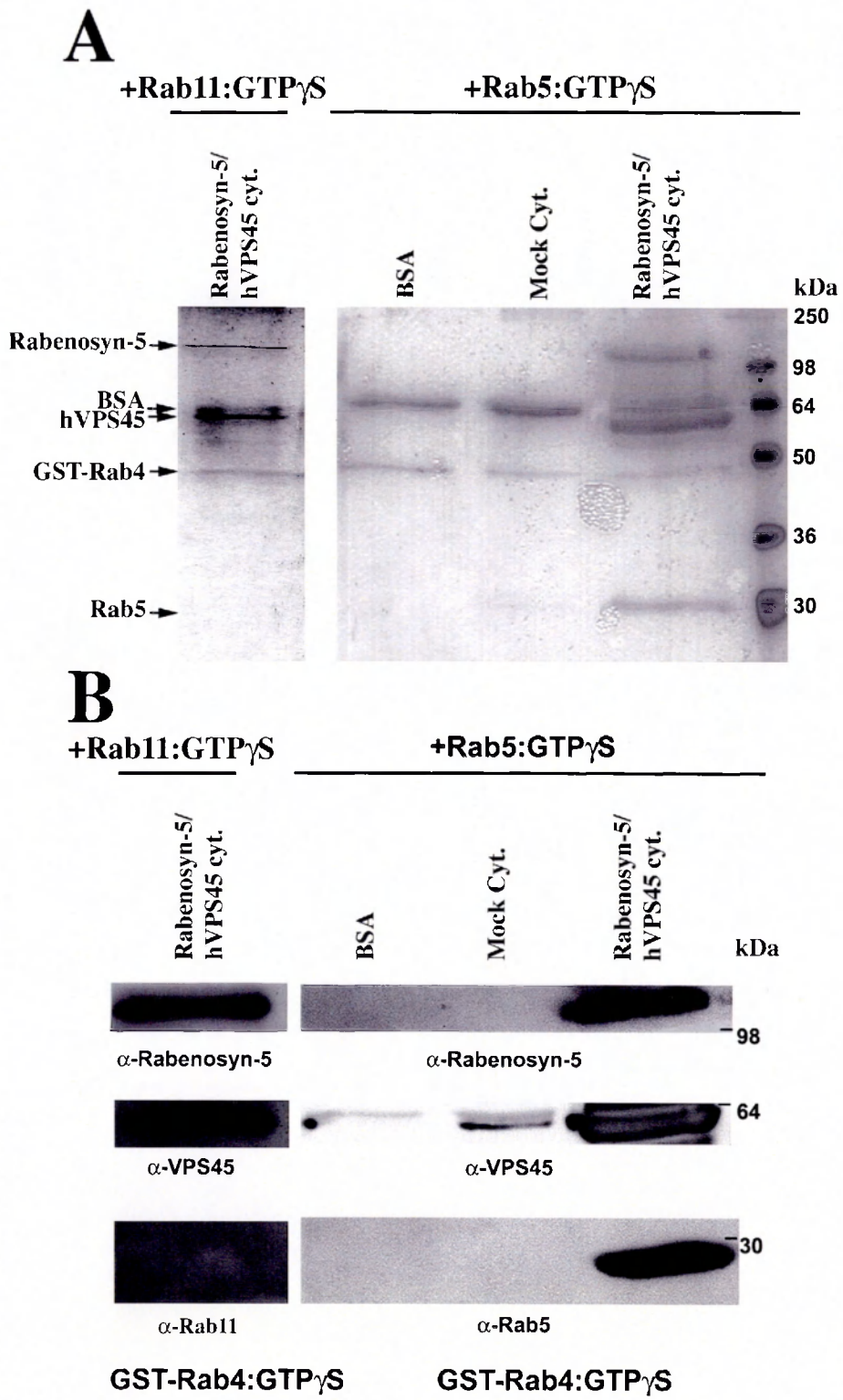

Figure 41: Rabenosyn-5 can bind simultaneously to Rab5 and Rab4.

(A) Ponceau staining of GST-Rab4 bound proteins. GST-Rab4 was incubated either with Rabenosyn-5/hVPS45 over-expressing cytosol either with mock infected cytosol or BSA. After extensive washes a second incubation was performed with purified Rab5 and BSA. Bound proteins were eluted, separated by SDS-PAGE and transferred to nitrocellulose for Ponceau staining or for Western blot analysis **(B)**.

2.15 Over-expression of Rabenosyn-5 increases the overlap between Rab5 and Rab4, but not between Rab5 and Rab11 endosomal domains.

Under basal conditions, ~50% of early endosomes contain both Rab5 and Rab4 domains, the rest being segregated. To examine if the amount of Rabenosyn-5 influences the co-distribution of Rab5 and Rab4 on endosomes I tested whether its over-expression could result in an increase in the population of endosomes containing both Rab5 and Rab4. A431 cells were microinjected with plasmids encoding CFP-Rab5, YFP-Rab4 and Rabenosyn-5 and the number of endosomes containing both Rab5 and Rab4 was quantified as before (Figure 38). As illustrated in Figure 42 (panels A, B, C) over-expression of Rabenosyn-5 had two effects. First, it induced the appearance of large endosomal structures. Second, it drastically altered the segregation between Rab4 and Rab5 endosomes. Rab4 now almost completely co-localized with Rab5 and Rabenosyn-5 on the same endosomal structures (~90% vs.~55% control; see also Table 2).

Since Rabenosyn-5 is complexed with hVPS45 in cytosol and this complex interacts with Rab4, the possibility existed that the phenotype observed could be due to a titration of endogenous hVPS45. However, co-expression of hVPS45 and Rabenosyn-5 did not revert the phenotype observed upon over-expression of Rabenosyn-5 (Table 2). Over-expression of hVPS45 alone had also no effect on

the segregation between Rab5 and Rab4 domains, indicating that the phenotype observed is caused by Rabenosyn-5. I therefore tested whether overexpression of Rabaptin-5, that also interacts with both Rab5 and Rab4, can induce a redistribution of Rab5- and Rab4-positive structures. Indeed, a similar phenotype was observed upon over-expression of Rabaptin-5 (80% of Rab4 endosomes containing Rab5 versus 52% control; Figure 42 D, E, F and Table 2). In contrast, over-expression of EEA1, which binds to PI(3)P and Rab5 but not to Rab4, caused a significant enlargement of the Rab5-positive compartment but did not significantly alter the distribution of Rab5 and Rab4 domains (Figure 42 G, H, I and Table 2). Therefore, the ability to cluster and/or fuse Rab5 and Rab4 domains together seems to be restricted to proteins that bind directly to both Rab5 and Rab4.

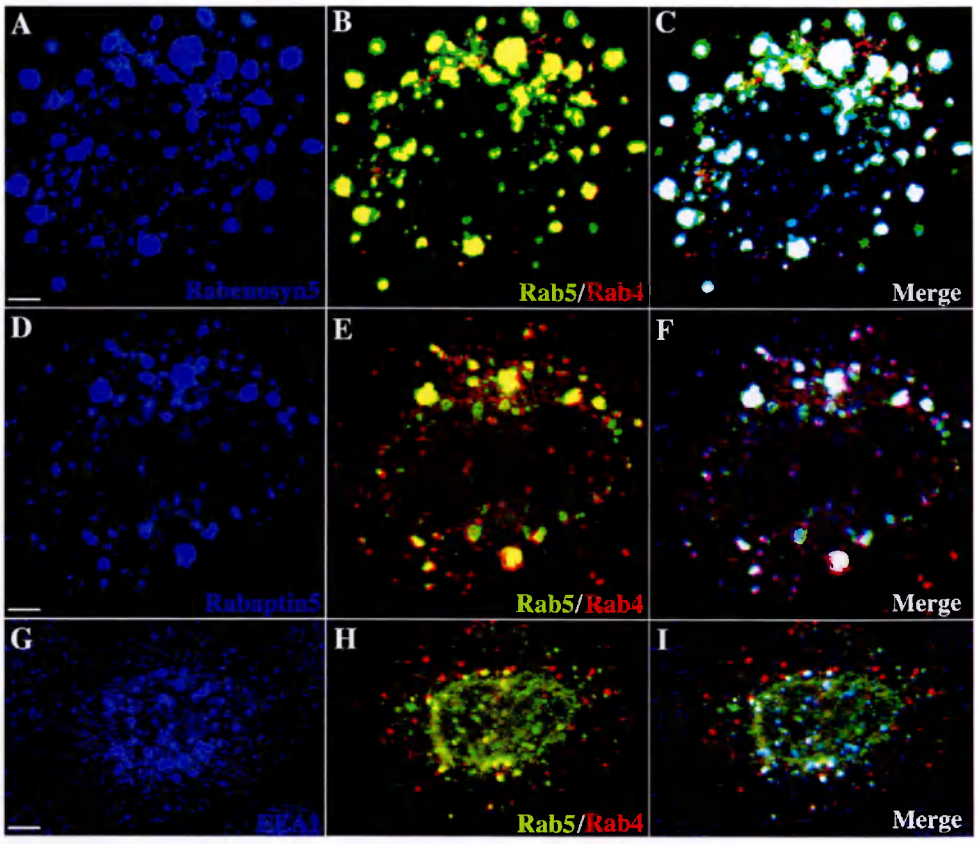

Figure 42: Over-expression of Rabenosyn-5 and Rabaptin-5, but not of EEA1, increases the co-localization between Rab5 and Rab4

(A-I) Rabenosyn-5 (A-C), Rabaptin-5 (D-F), or EEA1 (G-I) were co-expressed together with CFP-Rab5 and YFP-Rab4 in A431 cells. Cells were fixed and stained with antibodies against Rabenosyn-5 (A-C), Rabaptin-5 (D-F), and EEA1 (G-I). Individual confocal sections are shown. Bar = 4μm (A-D) and 5μm (G).

At the light microscopy level, over-expression of Rabenosyn-5 caused an apparent enlargement of endosomes. To examine if this phenotype is analogous to the vacuolation induced by uncontrolled homotypic early endosome fusion upon expression of the active mutant of Rab5 (Rab5Q79L) (Bucci et al., 1992), I inspected the morphology of the enlarged structures at the ultra-structural level. To this end, I performed immunoelectron microscopy experiments (in collaboration with Gareth Griffith) on cells over-expressing Rabenosyn-5. Affinity-purified anti-

Rabenosyn-5 antibodies followed by protein A coupled to 10nm gold, were used to identify the endosomes where this protein localized. Rather than single big vacuoles, Rabenosyn-5-positive endosomes appeared as clustered tubulo-vesicular membranes (Figure 43). These results suggest that the phenotypic alterations induced by Rabenosyn-5 are not due to massive homotypic endosome fusion but primarily to clustering of endosomal elements. Whether this reflects *de novo* formation of tubular extensions, or tethering/docking of pre-existing endosomes, remains to be determined.

To determine whether Rabenosyn-5/Rab4 interaction is necessary to redistribute Rab4 endosomes, a Rabenosyn-5 mutant missing the Rab4 binding sites was designed and the effect of its over-expression was analyzed. To this end, a series of Rabenosyn-5 truncation mutants were constructed and tested for their ability to interact with Rab5 and Rab4 using affinity chromatography (see Figure 44). The Rab4 binding site was mapped between amino-acids 264-500, immediately downstream of the FYVE finger domain.

Figure 43: Electron microscopy analysis of cells over-expressing Rabenosyn-5.
A431 cells over-expressing Rabenosyn-5 were fixed and stained with an affinity purified anti-Rabenosyn-5 antibody followed by protein A coupled to 10 nm gold. Bar =250nm

This region shared no homology with Rabaptin-5 or Rabip4 another FYVE finger containing protein recently identified as a novel Rab4 effector (Cormont et al., 2001). The Rab5 binding site was mapped to the very c-terminal end of the protein from amino acid 627 to 784. A second low affinity Rab5 binding site (~15-20% of total binding) is also located in the region containing the Rab4 binding site. Based on these mapping studies, I therefore succeeded in generating a Rabenosyn-5 mutant (δ 264-500) devoid of the Rab4 binding site, but still capable of interacting with Rab5 and PI(3)P.

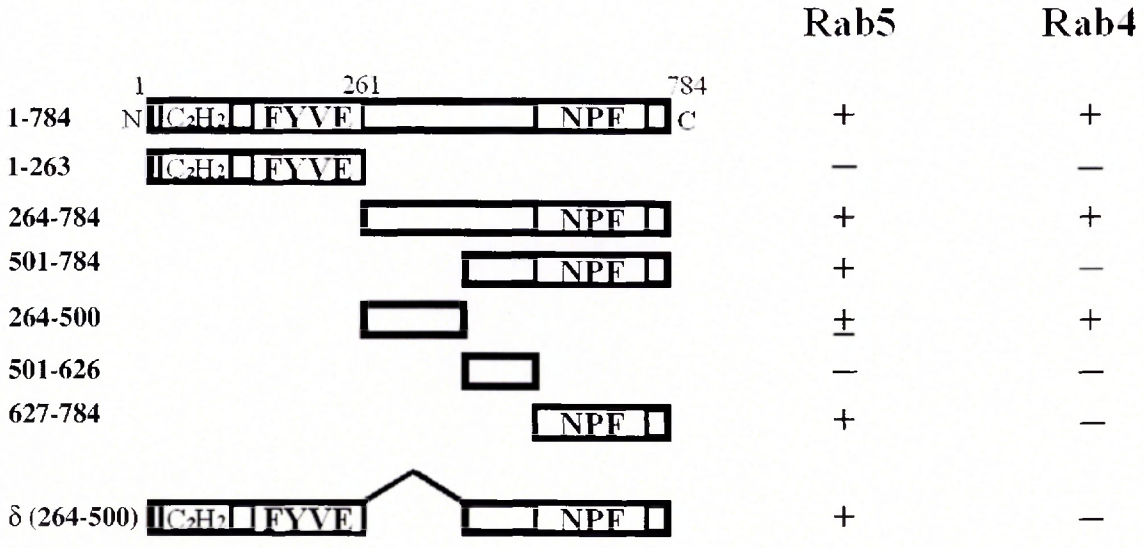

Figure 44: Summary of the in vitro binding assay results to determine Rab4 and Rab5 binding sites of Rabenosyn-5.

Rabenosyn-5 full length or truncation mutants were *in vitro*-translated in the presence of ^{35}S-methionine and incubated with glutathione beads containing GST-Rab4 or GST-Rab5. Bound proteins were eluted and analyzed by SDS-PAGE, followed by autoradiography.

Over-expression of this mutant failed to re-distribute Rab4 endosomes (Figure 45 and table 2), although completely co-localized to Rab5-positive endosomes and caused morphological alteration (clustering-enlargement) of these structures. This result demonstrates that Rabenosyn-5 over-expression re-distributes Rab4 endosomes because of its interaction with Rab4.

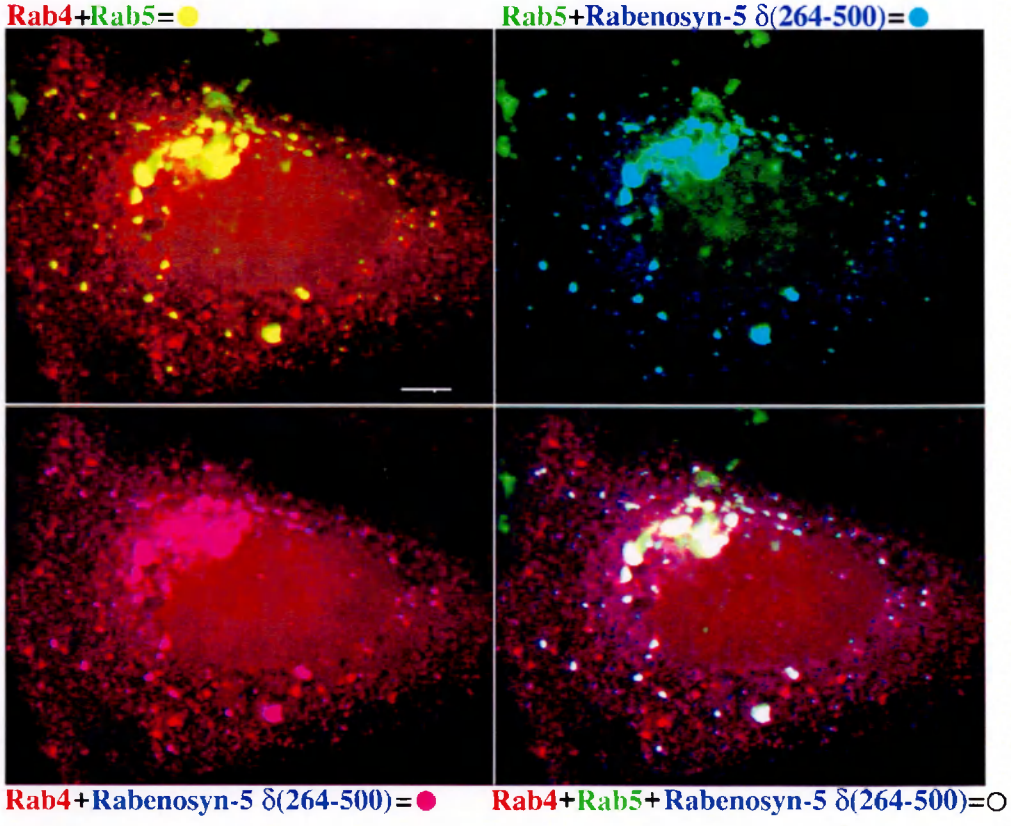

Figure 45: Rabenosyn-5/Rab4 interaction is necessary to redistribute Rab4 endosomes.

Myc-tagged Rabenosyn-5 δ264-500 was co-expressed together with CFP-Rab5 and YFP-Rab4 in A431 cells. Cells were fixed and stained with antibodies against Myc. Individual confocal sections are shown. Scale bar represents 4 microns.

Rabenosyn-5 does not interact with Rab11. If the effect of Rabenosyn-5 on the distribution of Rab5 and Rab4 domains is specific, the fraction of endosomes harbouring both Rab5 and Rab11 domains should remain unaffected upon Rabenosyn-5 over-expression. Consistent with this assumption, I found that the typical peri-nuclear localization of Rab11-positive membranes was not changed upon Rabenosyn-5 over-expression (Figure 46). Moreover, concomitant with the increase in endosomes harbouring both Rab5 and Rab4, over-expression of Rabenosyn-5 reduced the proportion of endosomes labelled for both Rab4 and Rab11 (Table 2). In summary, over-expression of Rabenosyn-5 selectively shifted the distribution of Rab4 domains from the Rab4-Rab11 to the Rab5-Rab4 endosomal population. Therefore, the selective re-distribution of Rab5, Rab4 and Rab11 endosomes observed morphologically, is consistent with the selective pattern of biochemical interactions between Rabenosyn-5 and these Rab proteins.

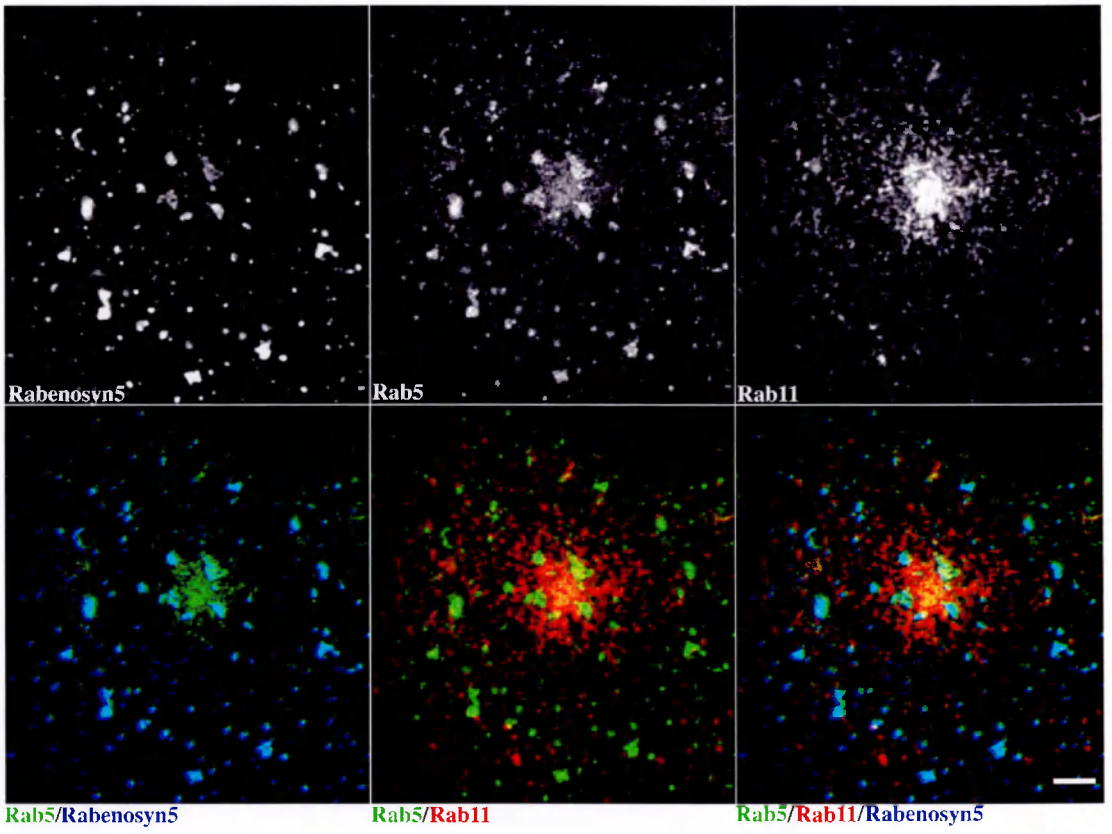

Figure 46: Rabenosyn-5 over-expression does not change the peri-nuclear localization of Rab11-postive membranes

A431 cells expressing CFP-Rab5, YFP-Rab11 and Rabenosyn-5 were fixed and stained with anti-Rabenosyn-5 affinity-purified antibodies followed by secondary antibodies conjugated to Texas red. Individual confocal sections are shown. Scale bar represents 5 microns.

Table 2. Quantification of Rab5, Rab4 and Rab11 overlap on the same endosomes

	Rab5+Rab4	Rab4+Rab11	Rab5+Rab4+Rab11
Control	52 ± 4	50 ± 1	23 ± 2
+Rabenosyn-5	90 ± 6	17 ± 3	ND
+Rabenosyn-5 (δ 264-500)	58 ± 5	ND	ND
+hVPS45	50 ± 3	ND	ND
+Rabenosyn-5+hVPS45	92 ± 4	ND	ND
+Rabaptin-5	80 ± 3	ND	ND
+EEA1	60 ± 5	ND	ND

Fluorescence analysis: plasmids coding for the proteins indicated in the first column were microinjected into the nucleus of A431 cells. Numbers represent the percentage of endosomes labelled for the indicated combination of Rab proteins.

2.16 Over-expression of Rabenosyn-5 stimulates transferrin recycling and diverts it from peri-nuclear recycling endosomes.

Endocytosed transferrin moves sequentially through Rab5, Rab4 and Rab11 endosomal domains before recycling back to the plasma membrane. Since over-expression of Rabenosyn-5 increases the association between Rab5 and Rab4 at the expense of the connection with Rab11, I tested whether these changes imply qualitative or quantitative differences in the sorting activity of endosomes and in recycling of endocytic markers. I therefore analyzed the transport of transferrin receptor through the endocytic and recycling pathway in cells over-expressing Rabenosyn-5. In control cells, after 15 minutes of continuous internalization, transferrin localized both in peripheral small structures corresponding to early endosomes as well as in peri-nuclear recyling endosomes (Figure 47 A). In contrast, in cells over-expressing Rabenosyn-5, transferrin accumulated in peripheral enlarged structures, but peri-nuclear recycling endosomes were poorly labelled (Figure 47 C, D, E). Quantification of these data is shown in Figure 47 B. It is unlikely that this effect is due to a general block of exit from early endosomes, as transferrin was efficiently internalized, implying that its receptor can cycle between endosomes and the plasma membrane. It is possible instead that transferrin is less efficiently transported to perinuclear recycling endosomes. To test this, I performed the following experiment. Cells were allowed to internalize

two consecutive pulses of transferrin, the first (rhodamine-labelled transferrin) for 1 hour and the second (Alexa-488-labelled transferrin) for 15 minutes. In control cells (Fig.7 F, G, and H), both rhodamine and Alexa-488 transferrin co-localized in peri-nuclear recycling endosomes. Single peripheral structures labelled either by Alexa-488- transferrin or by rhodamine-transferrin were also observed. In contrast, in cells over-expressing Rabenosyn-5, recycling endosomes were not labelled by transferrin after 15 minutes of internalization (Figure 47 I). Only after 1 h of internalization, could labelling of peri-nuclear recycling endosomes be observed (Figure 47 L). Whereas in control cells, the two consecutively internalized transferrin pulses co-localized in peri-nuclear recycling endosomes (Figure 47 H), in Rabenosyn-5 over-expressing cells co-localization between the two markers was restricted to the peripheral enlarged structures (Figure 47 M). These results therefore indicate that Rabenosyn-5 over-expression favours the recycling of transferrin directly from early endosomes and diminishes transport to peri-nuclear recycling endosomes.

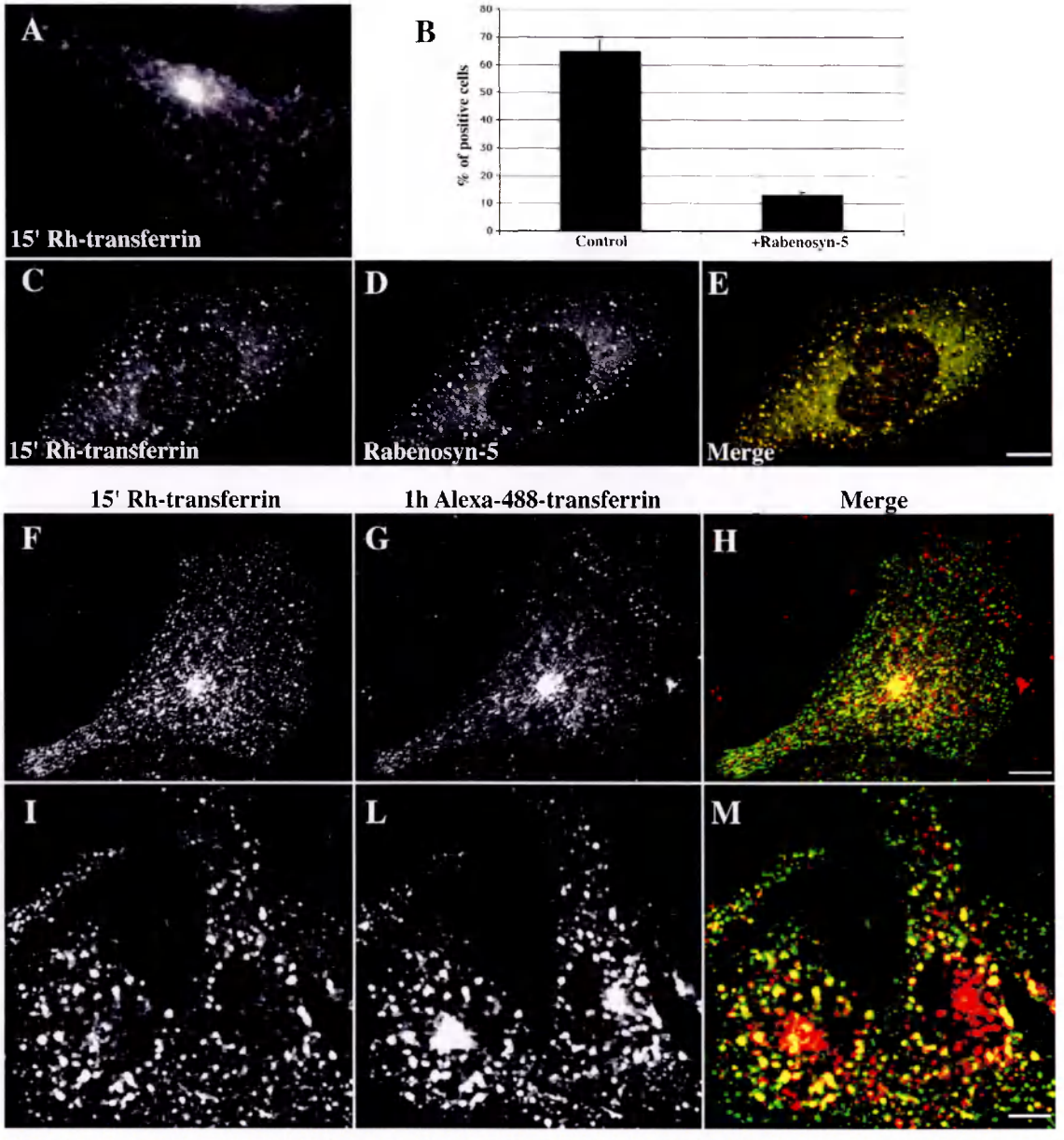

Figure 47: Morphological analysis of transferrin trafficking

(A and C-E) CHO cells (A) and CHO cells over-expressing Rabenosyn-5 (C-E) were allowed to internalize 30μg/ml of rhodamine-transferrin for 15 minutes at 37° C. After extensive washes, cells were fixed and stained with anti-Rabenosyn-5 antibodies followed by secondary antibodies conjugated to Alexa-488. Individual confocal sections are shown. Scale bar represents 4μm.

(B) Percentage of cells showing labelling of peri-nuclear recycling endosomes after 15 minutes of rhodamine-transferrin internalization (n=200).

(F-M) CHO (F-H) or CHO cells over-expressing Rabenosyn-5 (I-M) were allowed to internalize two consecutive pulses of transferrin. Rhodamine- transferrin was internalized for 1 hour and Alexa-488-transferrin for 15 minutes. Individual confocal sections are shown. Scale bar represents 4μm.

To substantiate this conclusion, I measured the kinetics of transferrin recycling in cells over-expressing Rabenosyn-5. To quickly obtain homogenous level of strong over-expression, cells were transfected with plasmids carrying the desired cDNAs under the control of T7 promoter. Over-expression was then achieved by infecting cells with recombinant vaccinia virus encoding the T7 polymerase and by a subsequent four hours incubation. Transfection efficiency was verified by immuno-fluorescence on duplicate samples and only if more than 80% of cells were transfected, biochemical measurements were performed. First, Rabenosyn-5 over-expression induced a moderate, but significant increase in the steady-state distribution of transferrin receptor on the plasma membrane (35% on the surface versus 25% control). Second, to test whether the overall efficiency of the recycling pathway was perturbed, cells were labelled to steady state by internalizing biotinylated-transferrin for 1 hour at 37°C. Surface bound ligand was removed by ice-cold acid washes and recycling was restored by switching the temperature back to 37°C. The amount of transferrin recycled into the medium was quantified as described in methods. As shown in Figure 48, over-expression of Rabenosyn-5 did not alter the total amount of recycled cargo but rather accelerated the initial rate of recycling.

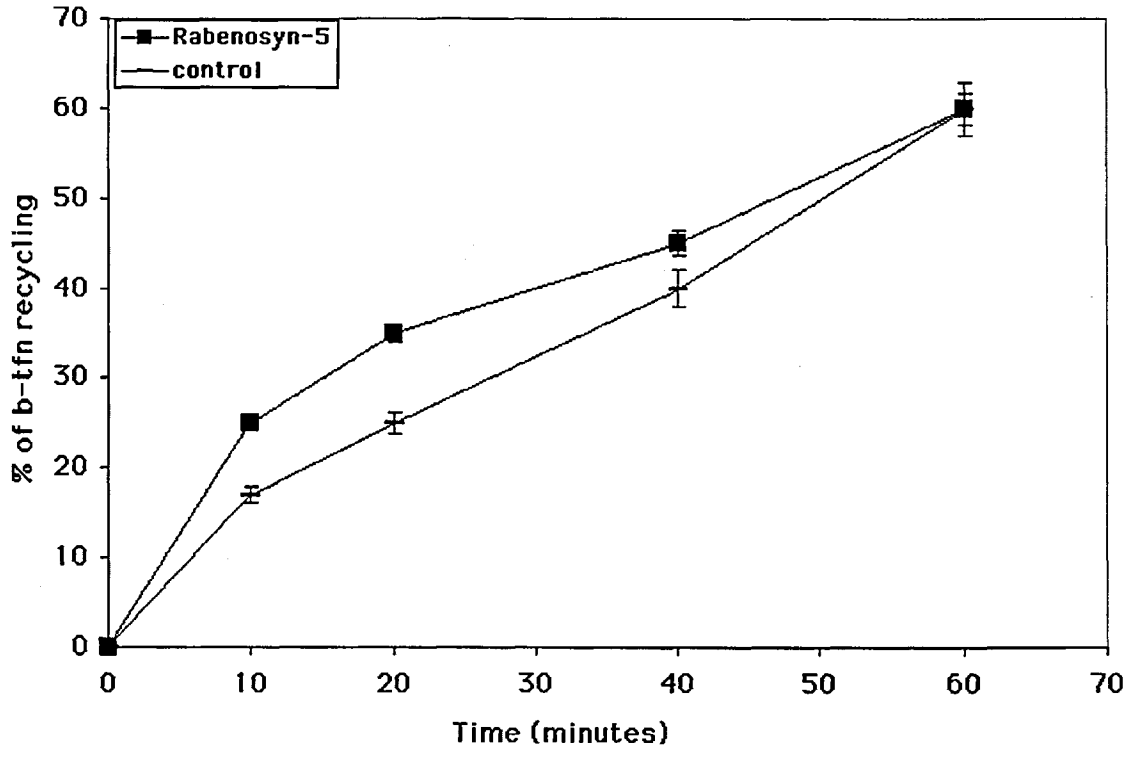

Figure 48: Effects of Rabenosyn-5 over-expression on transferrin recycling.
HeLa cells were transfected with the indicated plasmids and infected with recombinant T7 RNA polymerase vaccinia virus. Cells were allowed to internalize 10 μg/ml of biotinylated transferrin for 1 hour at 37° C. Cells were washed, stripped of surface bound transferrin, and incubated at 37° C in medium containing an excess of transferrin. The extent of release of biotinylated transferrin into the medium was monitored at various times. Results are expressed as percentage of recycled biotinylated transferrin (ratio between marker in the medium/ total= medium+intracellular). Data represent means ± SEM from three independent experiments performed in duplicate.

The stimulation of recycling was even more evident after a short pulse (two minutes) of transferrin internalization at 37°C. Under these conditions, I observed that over-expression of Rabenosyn-5 but not of Rabenosyn-5 δ (264-500), the Rab4 binding mutants, induced a ~3-to 4-fold stimulation of transferrin recycling (Figure 49). The stimulation was particularly evident in the first 4 minutes of the cycle, which corresponds to a $T_{1/2}$ of transferrin recycling ≤ 3 minutes.

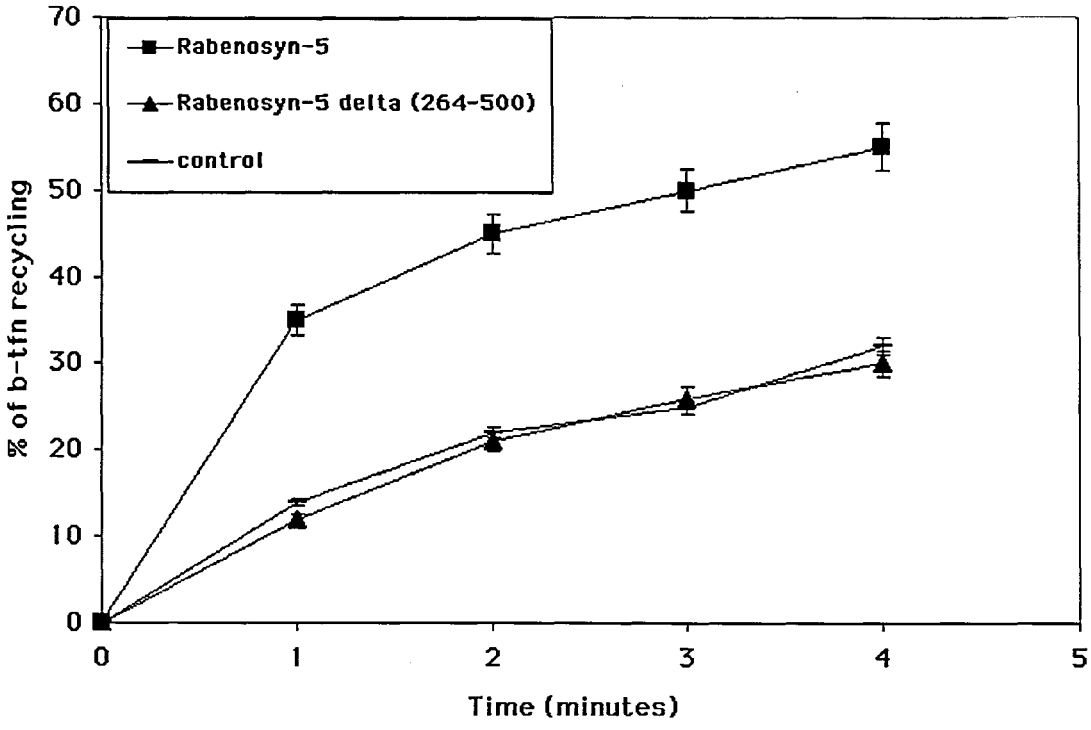

Figure 49: Effects of Rabenosyn-5 over-expression on transferrin recycling.
HeLa cells were transfected with the indicated plasmids and infected with recombinant T7 RNA polymerase vaccinia virus. Cells were allowed to internalize 10 μg/ml of biotinylated transferrin for 2 minutes at 37° C. Cells were washed, stripped of surface bound transferrin, and incubated at 37° C in medium containing unlabeled transferrin. The extent of release of biotinylated transferrin into the medium was monitored at various time points. Results are expressed as percentage of recycled biotinylated transferrin (ratio between marker in the medium/ total= medium+intracellular). Data represent means ± SEM from three independent experiments performed in duplicate.

Third, to synchronize recycling from early endosomes, transfected cells were allowed to internalize biotinylated-transferrin for 1 hour at 16°C. At this temperature, transferrin receptor is still efficiently internalized into early endosomes but subsequent exit either to recycling endosome or to the cell surface is impeded (Sipe et al., 1991). Consistent with the results of Figure 49, Rabenosyn-5 over-expression significantly stimulated transferrin recycling during the first five minutes (Figure 50), without inhibiting the total amount of recycling

at later time points. Importantly, this increase was dependent on the Rabenosyn-5/Rab4 interaction as 1) over-expression of the Rabenosyn-5 δ-264-500 mutant failed to stimulate recycling and 2) co-expression of the Rab4 dominant negative mutant (Rab4S22N, GDP-bound) neutralized this stimulation.

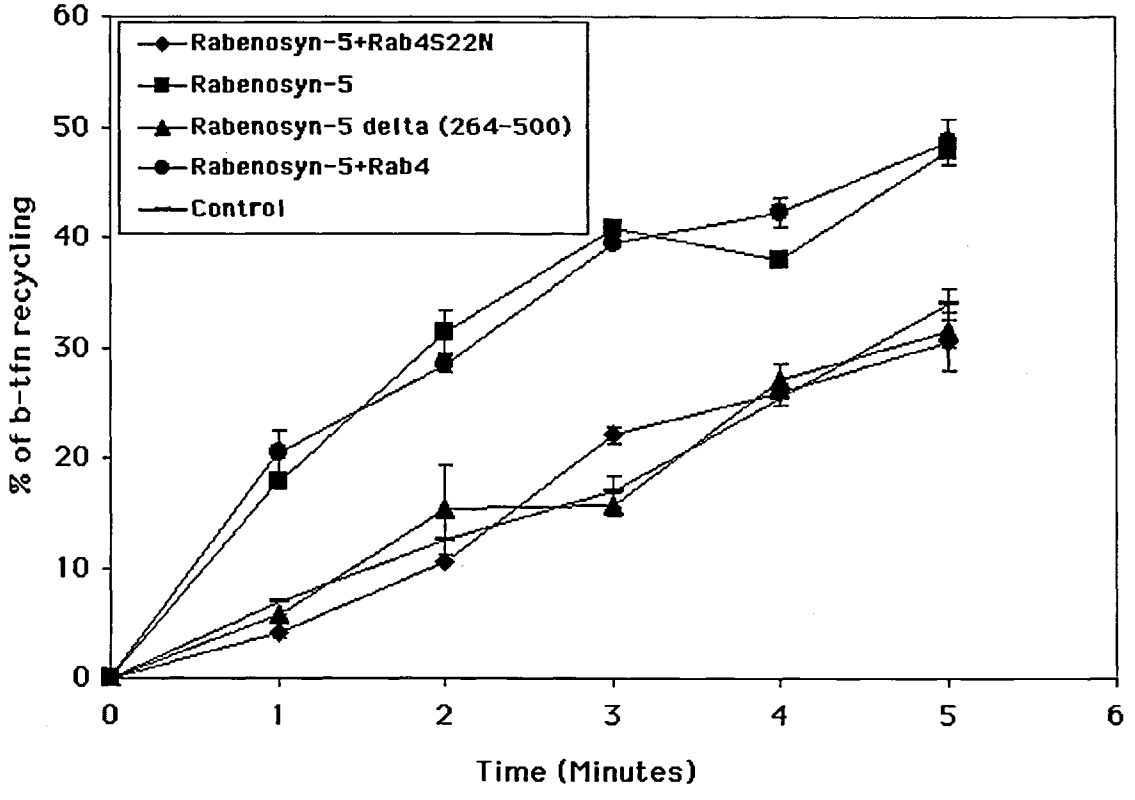

Figure 50: Effects of Rabenosyn-5 over-expression on transferrin recycling.
HeLa cells were transfected with the indicated plasmids and infected with recombinant T7 RNA polymerase vaccinia virus. Cells were allowed to internalize 10 μg/ml of biotinylated transferrin for 1 hour at 16° C. Cells were washed, stripped of surface-bound transferrin, and incubated at 37° C in medium containing unlabeled transferrin. The extent of release of biotinylated transferrin into the medium was monitored at various time points. Results are expressed as percentage of recycled biotinylated transferrin (ratio between marker in the medium/ total= medium+intracellular). Data represent means ± SEM from three independent experiments performed in duplicate.

Finally, I tested whether Rabenosyn-5 over-expression affects also another stage of endocytic transport, i.e. from early to late endosomes/lysosomes. To this aim, I measured the effect of its over-expression on EGF degradation and found only a moderate kinetic delay (30% inhibition during the first 20 min.) (Figure 51). As for transferrin receptor, also the EGF receptor may be more efficiently recycled to the cell surface. Nevertheless, these results indicate that Rabenosyn-5 over-expression does not block transport to late endosomes and lysosomes.

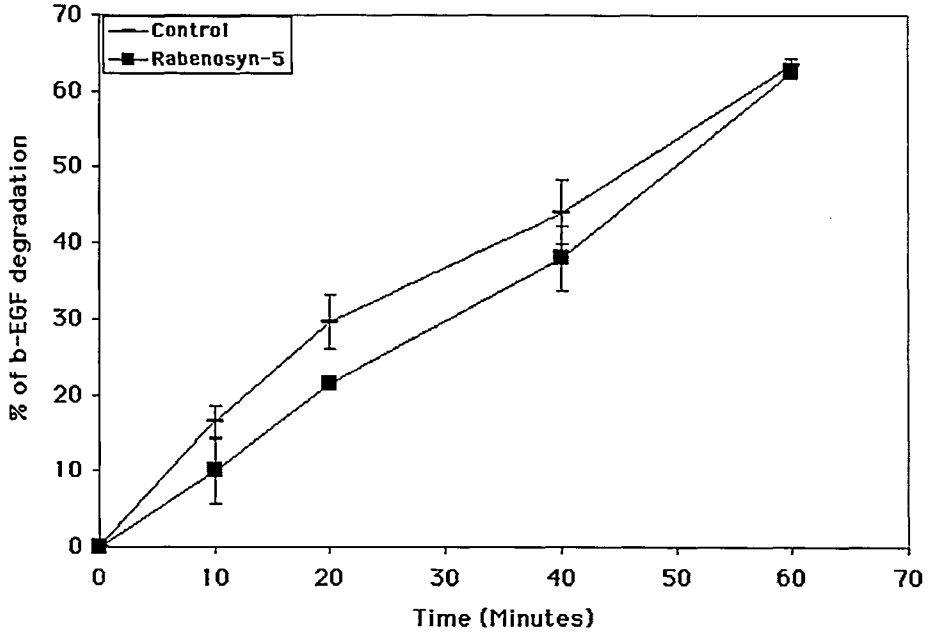

Figure 51: Effects of Rabenosyn-5 over-expression on EGF degradation.
HeLa cells were transfected with the indicated plasmids and infected with recombinant T7 RNA polymerase vaccinia virus. Cells were allowed to internalize 1nM of biotinylated-EGF for five minutes at 37°C and chased at the same temperature for the indicated time after extensive washes. EGF degradation was estimated by quantifying the amount of biotinylated-EGF accessible to anti-EGF antibody, by using the same electrochemiluminescence detection system utilized to quantify biotinylated-transferrin recycling. Data represent means ± SEMfrom three independent experiments performed in duplicate.

3. DISCUSSION

In this thesis I have investigated the role of Rab5, Rab4 and Rab11 in the structural and functional organization of the early endosomal compartment. The results of the experiments I performed provide molecular support to the Rab domain hypothesis and to the idea that the function of these three GTPases along the endocytic-recycling pathway is molecularly co-ordinated through the binding of common effector proteins.

Visualization of Rab5, Rab4 and Rab11 showed that these three GTPases are localized in distinct membrane domains, which can reside on the same cargo-filled endosome. The different combinations of Rab5, Rab4 and Rab11 domains define multiple early endosomal populations: one containing only Rab5, a second Rab5 and Rab4 and a third Rab4 and Rab11. These different endosomal populations display different kinetics of transport and specific pharmacological proprieties, reflecting their biochemical and functional diversity. Recycling cargo en route to the plasma membrane moves sequentially from Rab5 to Rab4 and from Rab4 to Rab11 domains with the overall domain composition of the endosomes being constant during the cycle.

These observations are therefore in agreement with the idea that Rab5, Rab4 and Rab11 belong to the intrinsic structural and functional machinery of endosomes. These results led to the next point addressed in this thesis, that can be

formulated in the two following and related questions: i) what are the molecular principles regulating the association between distinct Rab domains? ii) How is membrane transport between adjacent domains co-ordinated? The answers to these questions would provide an important step forward towards an understanding of the mechanisms responsible for the sequential transport of endocytosed cargo through early endosomes. Given that Rab effectors have been recognized to be membrane-tethering molecules (Allan et al., 2000; Cao et al., 1998; Christoforidis et al., 1999; Guo et al., 1999; Price et al., 2000), one possible point of regulation for joining Rab domains would be at the level of these proteins. The findings that the Rab5 effector Rabaptin-5 binds also to Rab4 (Vitale et al., 1998) and that a significant fraction of Rab5 containing endosomes harboured also Rab4 domains provides support for this idea. On this basis, I have hypothesized that bridging molecules, which have the property to bind or to regulate the activity of two distinct Rab proteins, may regulate the association between the corresponding Rab domains. To test this model I focused on the link between Rab5 and Rab4 domains by searching for, and investigating the function of, divalent Rab5 and Rab4 effectors. Consistent with the hypothesis formulated above, I could demonstrate that over-expression of the bi-functional Rab5/Rab4 effectors changes the compositions of early endosomes by specifically increasing the link between Rab5 and Rab4 domains. Importantly, this effect is dependent on

the capacity of these proteins to bind both Rab5 and Rab4. Moreover, these changes are accompanied by corresponding changes in the sorting and recycling capacity of early endosomes. Altogether these results are significant because they contribute to the understanding in molecular terms of the membrane organization and function of early endosomes and provide novel insights into the regulation of the endocytic-recycling pathway.

3.1 Visualization of Rab4, Rab5 and Rab11 domains on early endosomes

The correct localization of the GFP-tagged-Rab proteins, their accessibility to RabGDI and the kinetic of transferrin recycling indicate that the experimental strategy I have followed allows the faithful visualization of early endosomal organelles. The morphological quantification I have performed to determine the distribution of Rab5, Rab4 and Rab11 on the different endosomal populations is in good agreement with two other independent studies. Using a gradient fractionation method, Sheff could isolate endosome populations with a remarkably similar Rab protein composition to the one shown in Table 1 (Sheff et al., 1999). Trischler obtained almost identical results by using an immuno-isolation approach, (Trischler et al., 1999). However, these biochemical studies did not provide any information concerning the topological distribution of Rab proteins.

The observed segregation of Rab proteins on cargo-filled endosomes is a good indication that these regulatory components occupy distinct domains onto continuous membrane structures. However, it has to be noted that, theoretically, the segregation I have observed could also represent physically distinct elements at a distance ≤ of 200nm and therefore below the resolution power of light microscopy. This seems not to be the case, as immuno-electron microscopy analysis of purified early endosomes also showed segregation of Rab proteins and their effectors within discrete regions of the same organelle (Sonnichsen et al., 2000). Nevertheless, assuming that the structures harbouring different Rab proteins are indeed separate vesicles rather than contiguous subcompartments of the same endosomes, these data would demonstrate an unexpected diversification of early endosomal species (i. e. Rab5 endosomes, Rab4 endosomes, etc.).

The compartmentalization of Rab proteins within restricted membrane domains establishes an important point for the functional understanding and the molecular definition of early endosomes. Most importantly, this concept implies that the membrane surface of these organelles is functionally polarised. This model is also in agreement with the structure of the early endosomes. Indeed, the membrane of these organelles is partitioned in morphologically and functionally distinct sub-compartments, vesicles, cisternae and tubules (Marsh et al., 1986). The molecular principles that lead to partitioning of the endosome membrane into

different areas would ensure that little or no intermixing between domains occur, despite the extensive flow of membrane through the early endosomes. Moreover, the arrangement of the machineries controlling membrane targeting, protein sorting and membrane-cytoskeleton interactions into domains may have the advantage to increase efficiency and co-ordination between these processes. For example, in the case of Rab5, this mechanism may guarantee functional co-ordination and correct timing between endosome fusion and motility events. At the same time the segregation of functional distinct machineries may allow multiple reactions to occur simultaneously while avoiding mixing between its regulatory elements. In addition, the polarised distribution of Rab proteins determines directionality of membrane transport through endocytic organelles. Recycling cargo enters into early endosomes through the Rab5 domain and exits it through Rab4 and Rab11 domains. The role of Rab5 in regulating the inward leg of the endocytic pathway is well established and is therefore consistent with this order of events. It is in the membrane region specified by this GTPase that the membrane tethering and fusion machinery is concentrated and localized (Zerial and McBride, 2001). Rab4 and Rab11 are involved in the endocytic-recycling pathway presumably by regulating the formation and/or targeting of recycling vesicles (Ullrich et al., 1996; van der Sluijs et al., 1992). Consistently, these two

GTPases occupy distinct membrane domains from Rab5 and cargo transit through these structures after leaving Rab5 domains.

According to this model, early endosomes can be considered to be organized as a mosaic of different Rab domains (see model in Figure 52). These domains would be organized by Rab proteins themselves (as suggested by the mechanism of action of Rab5) through the recruitment of specific effector proteins. It is therefore the *ensemble* of these effectors that specifies the function(s) of each domain. As Rab proteins belong to the intrinsic-resident machinery, which specify organelle functionality, their specific distribution has important consequences for the definition of organelles of the early endosomal system. The distinction between peripheral early endosomes and peri-nuclear recycling endosomes as two separate compartments interconnected by vesicular traffic has to be revisited. With respect to the distribution of Rab proteins both sorting and recycling endosomes are structured into Rab5, Rab4 and Rab11 domains (see model in Figure 52). Only the relative amount of these domains is different. According to the kinetics of cargo transport I have measured, early endosomes are composed of Rab5 and Rab4 domains and fewer Rab11 domains. Whereas, recycling endosomes contain mainly Rab4 and Rab11 domains and fewer Rab5. Also the geographical segregation between these different endosomal populations is not as stringent as previously proposed. Rab4-Rab11-containing

endosomes are localized both in the peri-nuclear region as well as in the cell periphery. The same is true for Rab5 and Rab4 domains.

The model that Rab proteins define functionally distinct membrane domains is in agreement with the most recent advances in the organization of biological membranes (see Introduction). Recent developments in light microscopy techniques have allowed the visualization of membrane fusion

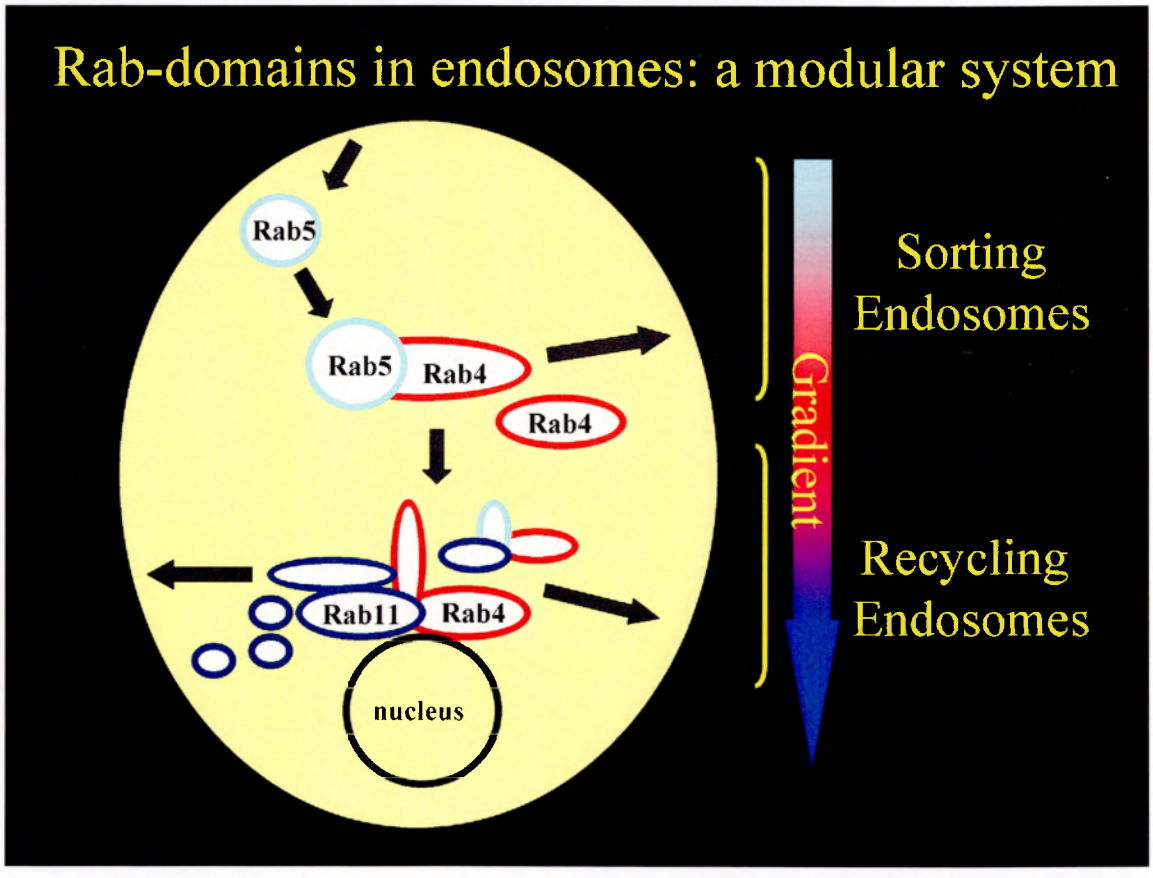

Figure 52: Model proposing the sub-compartment organization of the early endosomal system in different Rab domains.
Rab5, Rab4 and Rab11 domains are depicted as mint, red and blue ovals. Arrows trace the endocytic-recycling trafficking of transferrin receptor. Sorting-early endosomes are mainly composed of Rab5 and Rab4 and fewer Rab11 domains while Rab4 and Rab11 domains mainly define recycling endosomes.

events at the plasma membrane. Using total internal reflection fluorescence microscopy (TIRF) it was possible to follow fusion of post-Golgi derived vesicles with the plasma membrane. One striking observation of these studies was that fusion seemed to occur preferentially at specific sites (hot spots) of the plasma membrane (Toomre et al., 2000). These results are consistent with the idea that the membrane docking and fusion machinery controlling this transport step is not randomly distributed on the plane of the plasma membrane but rather concentrated in defined regions. Using a similar approach it was possible to visualize also the assembly of the AP-2 machinery on the plasma membrane. Again, this process occurred preferentially in specific regions, suggesting that the budding machinery is also preferentially assembled in specific regions (Gaidarov et al., 1999). By analogy, Rab domains on the endosomes define hot spot for membrane fusion or fission reaction events. Consistent with this model is the different pharmacological sensitivity of Rab5, Rab4 and Rab11 domains. The tubulation of the Rab4-Rab11 domains induced by Brefeldin A is most likely due to the inhibition of Arf dependent processes and implies that these two domains act as a platform for the assembly of components required for vesicle budding. Indeed coated buds have been observed on tubular extension on the early endosomes (Stoorvogel et al., 1996). The AP-1 sub-unit γ-adaptin has been localized to these structures and, at least in polarised cells, seems to play a role in transferrin recycling (Futter et al.,

1998). Interesting in this respect is the observation that Rabaptin-5 interacts with γ-adaptin (Page et al., 1999). The functional meaning of this interaction has not yet been investigated. One possibility is that Rab4 through Rabaptin-5 participates in the formation of γ-adaptin-containing vesicles. This possibility may reflect the finding that over-expression of dominant negative mutant of Rab4 inhibits coated bud assembly on endosomes (de Wit et al., 2001). Conversely to Rab4 and Rab11, Rab5 domains do not tubulate in response to BFA but they are sensitive to the PI-3 kinases inhibitor, wortmannin (Sonnichsen et al., 2000). The function of Rab5 is indeed centred on the formation of a PI(3)P enriched membrane domain on its site of action. Local clustering of active Rab5 and PI(3)P is essential for the recruitment of a group of regulatory molecules that have in common the capability to bind both Rab5 and PI(3)P. It is via these effectors that Rab5 functions (Miaczynska and Zerial, 2002). PI(3)P is specifically localized to sub-domains on sorting endosomes (Gaullier et al., 2000) and pharmaceutical inhibition of its production alters both the morphology as well as the functionality of these domains . Upon inhibition of PI(3)P synthesis, all Rab5-dependent functions are impeded. In a few minutes the Rab5 domain disorganizes and its effectors redistribute to cytosol: fusion events are reduced by more than 80% (as measured in an *in vitro* endosomes fusion assay) (Simonsen et al., 1998), binding of endosomes to cytoskeleton elements is mis-regulated and minus end directed

motility of endosomes along microtubules is inhibited (Nielsen et al., 1999). These functional alterations correspond also to morphological changes: the spherical cisternal shape of the Rab5 domain is converted into a tubular one (Sonnichsen et al., 2000).

It has been long appreciated that the kinetics of transferrin recycling are biphasic being composed of a fast and a slow component (Hopkins, 1983). By mathematical modelling, Sheff and co-workers proposed that the kinetics of transferrin recycling pathway are best described by two recycling stations. The first is filled within the first five minutes after internalization and subsequently transferrin accumulates in the second one, which displays slower recycling kinetics (Sheff et al., 1999). According to the data presented in Figure 25, fast recycling coincides with transferrin transit from Rab5 to Rab4 domains. At a later stage of the cycle, transferrin accumulates in Rab4-Rab11-containing endosomes which presumably exert slower kinetics of recycling and sorting proprieties. Thus, Rab4 may be involved in both fast and slow recycling, while Rab11 would mainly regulate slow recycling. The obvious question raised by this model is why are there two recycling stations with different kinetic properties? What is the advantage of this system? To understand these problems it is necessary to consider the role of the early endosomal system in polarised cells. In these cells endocytic-recycling must be polarised in order to maintain distinct basolateral and apical

plasma membrane composition. Moreover, transport of trans-cytotic cargo across the epithelia requires an additional sorting step. Studies conducted in polarised MDCK cells showed that recycling from sorting endosomes is rapid being completed within the first ten minutes after internalization. These organelles seem, however, not to be able to sort trans-cytotic cargo. This function appears to be a prerogative of the recycling compartment. According to this order of events, at each endocytic cycle a fraction of receptors are transported from sorting to recycling endosomes. It is in this latest compartment that polarised sorting occurs and trans-cytotic receptors are sorted away from the rest of recycling components, which return to the plasma membrane (Sheff et al., 1999). The simplest interpretation for the different kinetics of recycling is that the fast recycling implies a single transport route, whereas slower recycling reflects passage through recycling endosomes. By this view the recycling pathway consists of two compartments which function in tandem to ensure efficient recycling and accurate sorting.

3.2 Molecular regulation of transport through Rab domains

The sequential transport of cargo through membrane domains selectively occupied by Rab proteins implies the existence of mechanisms co-ordinating

neighbouring domains, and dictating the timing and the specificity of each coupling event.

In the second part of my thesis I address the molecular link between Rab5 and Rab4 domains. I tested the hypothesis that bi-functional Rab effectors could regulate the communication between two consecutive Rab-domains on the endosome membrane. First, I designed a strategy of sequential affinity chromatography to search for Rab5 effectors that could also interact with Rab4. Besides the Rabaptin-5 proteins, I identified Rabenosyn-5, as a novel Rab4-interacting protein. I also provide experimental evidence for a role of Rabenosyn-5 and Rabaptin-5 in the functional link between Rab5 and Rab4 domains supporting a role for these Rab effectors in the recycling pathway. First, Rabenosyn-5 was localized to endosomal structures harbouring both Rab5 and Rab4. Second, over-expression of Rabenosyn-5 and Rabaptin-5 increased the fraction of endosomal structures that were positive for both Rab5 and Rab4 at the expense of Rab4 and Rab11-containing structures. Importantly, neither the Rab5 effector EEA1 nor the SNARE regulator hVPS45 had a similar effect. Third, over-expression of Rabenosyn-5 increased the rate of transferrin recycling from early endosomes to the plasma membrane. Since this phenotype was accompanied by a reduced passage of transferrin from peripheral early endosomes to perinuclear recycling endosomes, these results suggest that transferrin has been deviated from

recycling endosomes and preferentially recycled via the fast route. Rabenosyn-5 is therefore a Rab effector that plays a dual role in entry of cargo into the early endosome and sorting in the recycling pathway.

Based on these data, I propose the following order of events in the endocytic/recycling pathway. Cargo molecules incorporated into CCVs budding from the plasma membrane are delivered to early endosomes. This process is regulated by Rab5 and requires its downstream effectors Rabaptin-5 (Stenmark et al., 1995), the PI3-K hVPS34/p150 (Christoforidis et al., 1999), EEA1 (Christoforidis et al., 1999) and Rabenosyn-5 (Nielsen et al., 2000). The functional link between Rab5 and PI3-K is important for the membrane recruitment of EEA1 and Rabenosyn-5, which are clustered in a specific region of the early endosome. Following entry into the Rab5- PI3(P)-positive domain, recycling molecules are sorted away from the degradative pathway and transported back to the surface. Rab4 and Rab11 have been implicated in this regulation. Over-expression of Rab4 alters the transferrin receptor cycle by redistributing the receptor to the surface, with the internal pool accumulating in vesicles and tubules (van der Sluijs et al., 1992). This phenotype suggests a sorting function for Rab4 in the "fast" recycling loop at the level of the early endosome, regulating the access of cargo to recycling structures. Rab11 regulates the "slow" branch of the recycling route through perinuclear recycling endosomes (Ullrich et al., 1996). Indeed, endocytosed

transferrin sequentially travels through Rab5, Rab4 and Rab11-positive domains on endosomes. My data indicate that Rabenosyn-5, in conjunction with Rabaptin-5, regulates the transition of cargo from the Rab5- and PI(3)P-positive domain to the subsequent Rab4-domain. This transport step must be regulated since at steady state, only about half of the membranes labelled for Rab5 also harbour Rab4. In line with the membrane tethering function of Rab effectors (Allan et al., 2000; Cao et al., 1998; Christoforidis et al., 1999; Guo et al., 1999; Price et al., 2000), Rabenosyn-5 may tether Rab5-with Rab4-containing membranes. Rabenosyn-5 is complexed to the Sec-1-related protein hVPS45 and this protein interacts with various syntaxins (syntaxin4, 6 and 13) of the early endocytic pathway (Nielsen et al., 2000). It is easy to imagine that the Rabenosyn-5/hVPS45 complex could provide a regulatory function to the pairing of SNAREs following Rab5-Rab4 membrane tethering and/or during recycling from early endosomes to the plasma membrane. Another possibility is that Rabenosyn-5 stimulates the homotypic fusion between domains of the same type, i.e. Rab5-Rab5 and Rab4-Rab4. However, while this is possible for Rab5, it seems unlikely in the case of the Rab4 domain which, when uncoupled from Rab5, harbours no detectable Rabenosyn-5. Furthermore, instead of the expected equal increase in Rab5-Rab4 and Rab4-Rab11 positive structures, Rabenosyn-5 overexpression led Rab4 to shift from Rab11 to Rab5 (Table II). A third possibility considers that, if Rab5 and Rab4

domains are in dynamic equilibrium between fusion and fission events, Rabenosyn-5 and Rabaptin-5 may stabilize the connection between the two domains and counteract fission. They may also confer a specific structural configuration to the junction between endosomal sub-compartments (e.g. connect vacuoles and tubules) (see model in Figure 53).

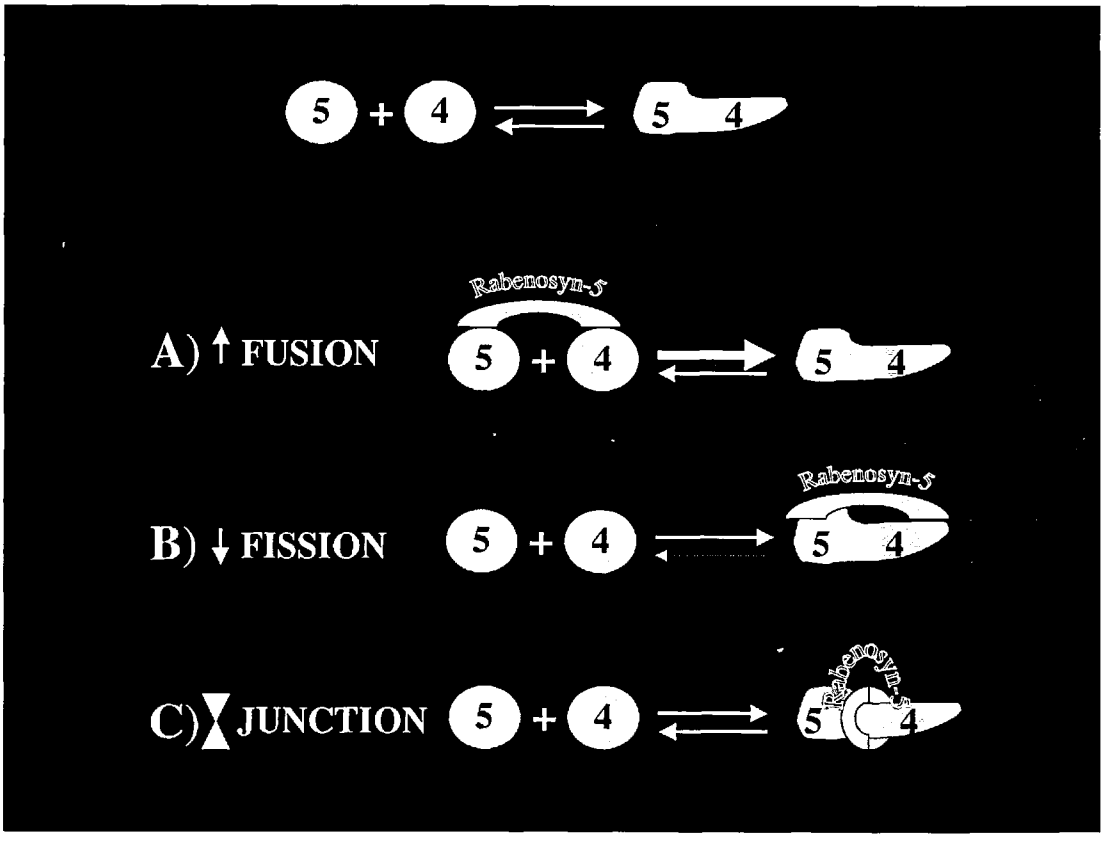

Figure 53: Model proposing the function of Rabenosyn-5 in coupling Rab5 and Rab4 domains.

Rab5 and Rab4 labelled endosomes are depicted as red and green ovals, respectively. At steady state, Rab5 and Rab4 domains are in equilibrium between fusion and fission reactions. Three possibilities, not necessary mutually exclusive, may explain why over-expression of Rabenosyn-5 increases the association between Rab5 and Rab4 domains. Possibility A), Rabenosyn-5 facilitates the fusion between Rab5 and Rab4 domains. Possibility B), Rabenosyn-5 inhibits fission between Rab5 and Rab4 domains. Possibility C), Rabenosyn-5 confers structural integrity to the junction between Rab5 (vacuolar) and Rab4 (tubular) domains.

Several molecular requirements may be needed for a physical connection between Rab5 and Rab4 domains. I have determined that a key regulatory step of this process lies in the ability of Rabenosyn-5 to directly interact with Rab4. First, Rabenosyn-5 contains separate Rab5- and Rab4-binding sites displaying similar binding affinities. Furthermore, binding to these two GTPases is not mutually exclusive. Second, a mutant of Rabenosyn-5 lacking the Rab4-binding activity failed to enhance the association between Rab5 and Rab4 domains. The distribution of Rab5 and Rab4 domains together with the localization of Rabenosyn-5 implies that only a fraction of Rabenosyn-5 is bound to Rab4 at steady state. This interaction depends on several factors. Firstly, the ability of Rabenosyn-5 and Rabaptin-5 to interact with Rab4 depends on the GTP-bound state of this GTPase (Figure 34 A and B). Rabaptin-5 is complexed to Rabex-5 and the exchange activity of the latter may ensure the activation of Rab5 at the Rab5-Rab4 junction for the recruitment of Rabenosyn-5. An open question is which guanine nucleotide exchange factor (GEF) activates Rab4? An interesting possibility is that Rabex-5 itself may catalyze GDP/GTP exchange also on Rab4. In this case, the activation of Rab4 would be dependent on the prior activation of Rab5 and recruitment of the Rabaptin-Rabex-5 complex. Secondly, Rabenosyn-5, as well as Rabaptin-5, appear to be rate-limiting components for the coupling between Rab5 and Rab4 domains. A single Rabenosyn-5 molecule is probably not

sufficient and multiple Rabenosyn-5-Rab4 complexes may be required to bridge the Rab5 and Rab4 domains. This implies that an important regulatory factor is the density of free and active Rab4 in the Rab4 domain. However, Rab4 is presumably engaged in interactions with other Rab4 effectors such as Rabip4 (Cormont et al., 2001). An exciting possibility raised by my findings is that some of these molecules may regulate the specific association between Rab4 and Rab11 domains. Thirdly, other Rabenosyn-5-interacting factors may participate in the Rab5-Rab4 coupling. Rabenosyn-5 shows structural and functional similarity to Vac1p (Nielsen et al., 2000), which mediates transport from the Golgi complex to a pre-vacuolar endosome in yeast (Weisman and Wickner, 1992). However, Rabenosyn-5 appears to have additional structural features that are absent in the yeast protein. Most notably, it contains a much longer carboxyl-terminal region downstream of the FYVE finger that includes 5 NPF motifs. The presence of these protein-protein interaction motifs suggests that Rabenosyn-5 can functionally associate with other proteins of early endosomes in addition to Rab5 and Rab4. In particular, NPF motifs have been shown to interact with proteins containing EH-domains, such as those involved in clathrin-coated vesicles formation (Salcini et al., 1997), suggesting a possible link between Rabenosyn-5 and clathrin coat assembly on endosomes. These structural features suggest that Rabenosyn-5 has acquired additional functional properties throughout evolution that are peculiar to

animal cells. Interestingly, Rabaptin-5 is not found in yeast. It could be that the activity of these two Rab effectors has evolved to support the Rab4-dependent role in protein sorting and transport from endosomes to the surface.

The reasons why Rabenosyn-5 stimulates transferrin recycling are presumably two-fold. First, assuming that the transition from the Rab5 to the Rab4 domain is necessary for recycling, Rabenosyn-5 over-expression would facilitate this process as most Rab5 domains are joined to Rab4 (see Table I). Second, by favouring the link between Rab5 and Rab4 against Rab4/Rab11 domains, an excess of Rabenosyn-5 would increase the probability of transferrin receptor to recycle via the fast route. One might envisage a similar coupling between Rab4 and Rab11 domains via distinct Rab effectors. Over-expression of Rabenosyn-5 would sequester the fraction of Rab4 available for such interactions reducing the pool of Rab4 normally coupled to Rab11. This explanation is consistent with the reduction in structures positive for both Rab4 and Rab11. Upon entry in the Rab4 and Rab11 domains, cargo would then be incorporated in tubular structures that bud from endosomes and fuse with the plasma membrane. In this process, recycling receptors may be selectively and efficiently captured by coat proteins, since coated buds were observed on the tubules (Stoorvogel et al., 1996). Interestingly, conditions that inhibit coat assembly on the endosomes also perturb the structural organization of Rab4 and Rab11 domains. Coated vesicles may also

serve to recycle components back to the plasma membrane although this mechanism does not appear to be essential.

In conclusion, the function of divalent Rab effectors such as Rabenosyn-5 may define a novel mechanism regulating the structure, sorting and transport activities of the early endosomal compartment. This mechanism is based on the functional link between distinct Rab domains and could in principle operate also in biosynthetic transport. The activity of divalent Rab effectors should help in understanding how recycling from early endosomes is regulated and, hopefully, clarify the yet elusive function of recycling endosomes. In relation to this, particularly informative will be the studies of polarised cells, where recycling endosomes have been implicated in the trafficking of molecules along the trans-cytotic route.

3.3 Open questions and future directions

The conclusions drawn from this study opens a series of questions whose answers may have an important impact on the understanding of the biogenesis and function of endocytic organelles. Firstly, to what extent do Rab proteins organize a membrane domain? The molecular characterization of the Rab5 effectors would argue that this GTPase plays an active role in the biogenesis of a membrane domain, although formal proof for this proposal has not yet been provided.

However, to generalize this concept it will be necessary to provide experimental evidence also that other Rab proteins function in a similar way. In this context, it will be important to characterize the Rab4 and Rab11 effectors. This approach will not only address this point, but will also help to define more precisely the function of these two GTPases and thus will contribute to the molecular understanding of the endocytic-recycling pathway. In collaboration with other colleagues in the laboratory of Dr. Zerial, I have already started this project and obtained preliminary results. As Rab5, Rab4 and Rab11 also interact with a multiplicity of effectors. This finding *per se* does not yet add much information, but provides the necessary condition to support, at least theoretically, the idea that these three GTPases may function in a similar way. Most importantly, the discovery that some of the Rab4 effectors interact also with Rab11 suggests that, by analogy to the common Rab5 and Rab4 effectors, these molecules may regulate the association between Rab4 and Rab11 domains. Given that recycling cargo (transferrin) transits from Rab4 to Rab11 domains at a later stage of its cycle, the *in vitro* recycling assay which I developed during the first part of my Ph.D. thesis work, may represent a valid assay to study the function of the common Rab4 and Rab11 effectors. Indeed as already discussed in paragraphs 2.5 and 2.3, the experimental conditions established in this assay are presumably reconstituting late rather than early stage of recycling.

Recently it has been reported that one of the Rab5 effector, the lipid kinase VPS34, also interacts with Rab7 (Stein et al. (2001) MBC Abstracts-1367- volume 12, pg. 149), implying that these two GTPases are also functionally linked. Thus, it appears that divalent Rab effectors are a common theme in the mechanism of action of these GTPases. It will be interesting to investigate whether Rab7, which functions downstream of Rab5 in regulating trafficking from early to late endosomes, would also be localized to defined membrane domains. And if so, would these domains be linked to Rab5 domains as suggested by the finding of the common Rab5 and Rab7 effector? If this will prove to be the case, it means that the model I have proposed to explain how Rab5 and Rab4 domains are linked can be applied also to explain the link between other Rab domains. This mechanism therefore may represent a general principle regulating the function and the sub-compartmentalization of early endosomes (see model in Figure 54). Even more, it is attractive to speculate that this model, based on functionally distinct Rab domains linked by common effectors, could be applied also to other organelles. Secondly, it will be necessary to incorporate the function of other regulatory components of the transport machinery, such as members of the Rho and ARF GTPases family and their effectors. Cross-talk between these machineries could possibly link vesicle formation with vesicle targeting and with the role of cytoskeleton in organelle structure and motility.

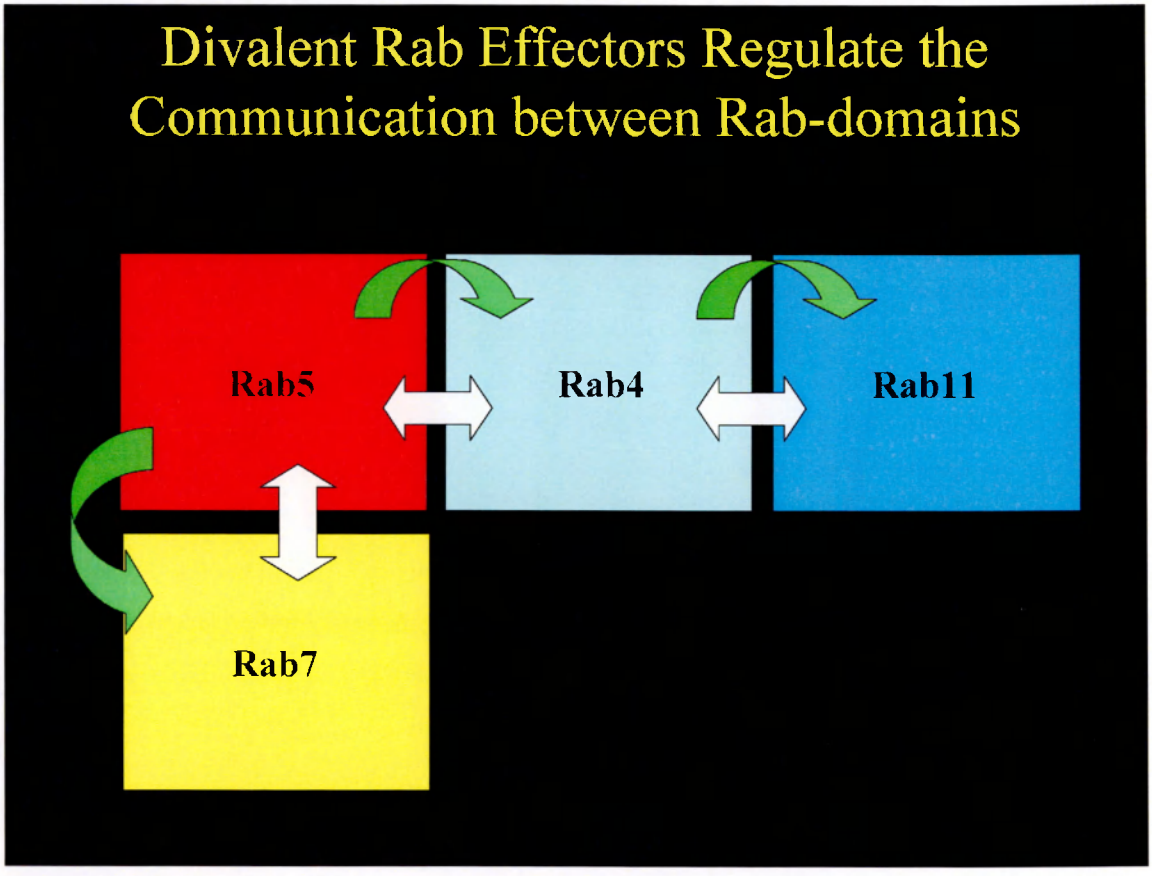

Figure 54: Model proposing the function of divalent Rab effectors in regulating the communication between Rab domains along the endocytic pathway.
Rab5, Rab4, Rab11 and Rab7 labelled endosomes are depicted as coloured rectangles. White arrows represent divalent Rab effectors linking two adjacent domains. Green arrows indicate the directionality of trafficking along the recycling route (Rab5→Rab4→Rab11) or the degradative route (Rab5→Rab7). See text for more details.

Another open question concerns the localization and the size of a Rab domain. For example does a single Rab5 domain occupy the entire membrane surface of the vacuolar portion of the early endosome, or do many Rab5 micro-domains concentrate in this region? To approach these problems it will be necessary to perform ultrastructural studies on both purified endosomes as well as in intact cells. Such experiments are now in progress in the laboratory in

collaboration with A. Mironov, P. Verkade and R. Parton. Important insights may come also from the analysis of endocytic organelles using atomic force microscopy. This technique may indeed allow a description of the surface of these organelles at atomic level. In addition, to better define the mechanisms responsible for the compartmentalization of biological membranes, it will be also necessary to reconstitute *in vitro* (for example using proteoliposome membranes) the clustering and the organization of the regulatory components of the membrane transport machinery.

4. Materials and Methods

4.1 Cell culture

A431 and HeLa cells (American Type Culture Collection (ATCC) Manassas, VA USA) were grown in D-MEM (Dulbecco's Modified Eagle's Medium) supplemented with 10% (v/v) heat-inactivated fetal calf serum, 100U/ml penicillin, 100μg/ml streptomycin and 2mM L-glutamine. Stable A431 cell line over-expressing GFP-Rab4, GFP-Rab5 and GFP-Rab11 were grown in the same medium as A431 cells plus 0.4 mg/ml Neomicyin G418. CHO-K1 (American Type Culture Collection (ATCC) Manassas, VA USA) were cultured in Ham's F-12 medium supplemented with 10% (v/v) heat-inactivated fetal calf serum,100U/ml penicillin, and 100μg/ml streptomycin. 1 l stocks of D-MEM (Dulbecco's Modified Eagle's Medium) and Ham's F-12 were prepared by the Cell Biology department media kitchen EMBL (Heidelberg). Fetal Calf Serum (FCS) was purchased from Gibco. To inactivate the serum complement, the FCS was heated 30 min at 56°C, aliquoted and stored frozen at -20°C. Frozen stocks of 200 mM L-glutamine and antibiotics (10 mg/ml streptomycin - 10^4 U/ml penicillin) were from Gibco-Brl. The solutions were distributed into 10-ml aliquots and stored frozen at -20°C. Media were prepared by adding antibiotics, L-glutamine, FCS and, if required, other components to the media stocks and stored

at 4°C. Cells were routinely cultured in a H_2O-saturated atmosphere containing 5% CO_2 on 10 cm diam. plastic petri dishes (Nunc) with 10 ml of medium. For passaging, the cells were washed 1-2 times with Ca^{2+}/Mg^{2+} free PBS (PBS^-) and detached from the dish using a 0.25% trypsin/EDTA solution (Gibco). After detachment of the cells, medium was added to 10 ml and the cells gently resuspended.

4.2 Transient expression systems in eukaryotic cells

4.2.1 Infection of HeLa cells with vaccinia virus T7

HeLa cells, grown on plastic dishes, were trypsinized 24 h prior to transfection, and seeded onto 11 mm round coverslips. Infections with the purified virus were done on 80% confluent BHK-21 cells. Trypsinized stock vaccinia virus prepared as described in Bucci C. et al (1992), was thawed and diluted in D-MEM, containing 20 mM HEPES, pH 7.2, 20 μg/ml soybean trypsin inhibitor (Sigma), to a concentration of approximately 3.4 p.f.u/ml. Cells on coverslips were rinsed once with D-MEM and infected with 200 μl of the virus mixture. The cells were then incubated at room temperature for 30 min, with occasional rocking of the dishes. Transfection were done by lipofection using the cationic lipid N-[1-(2.3Dioleoyloxy)propyl]-N,N,N-trimethylammoniumsulfate (DOTAP) (Boehringer Mannheim). The plasmid DNAs were first diluted to 20 μl in

transfection buffer (TB; 20 mM HEPES, 150 mM NaCl, pH 7.4) in a polystyrene tube. In a second polystyrene tube, 10 μl of DOTAP were diluted with 10 μl of TB. The plasmid solution was added dropwise to the DOTAP solution, mixed and left at room temperature for 10 min. From the infected cells, the medium was removed and the transfection mix added. 200 μl of medium containing 10 mM hydroxyurea were also added in order to block the viral DNA replication. The cells were then incubated at 37°C in medium devoid of serum for 4 h. Thereafter, samples were processed for immuno-fluorescence experiments to assess transfection efficiency and protein over-expression level or processed for biochemical measurement of transferrin recycling and EGF degradation.

4.2.2 Microinjection of plasmid DNAs into A431 and CHO cell nucleus.

In order to study the effects of Rabenosyn-5 over-expression on the endosomal localisation of Rab proteins, appropriate plasmids were injected into the cell nucleus of A431 cells using a micromanipulator and transjector (Eppendorf). Expression of the CFP constructs was generally lower compared to the YFP fusion proteins. A mixture of 7ng/μl YFP, 20ng/μl CFP and 50ng/μl Rabenosyn-5 or Rabaptin-5 or EEA1 plasmid DNAs were chosen as standard concentration in all microinjection experiments. CHO cells were grown on glass coverslips

(MatTek Corp., Ashland, MA) and microinjected with 50ng/μl of the appropriate plasmids as described above.

4.3 Generation of A431 cells stably expressing GFP-Rab4

Rab4 cDNAs cloned in frame into pEGFP expression vector (Clontech) were cotransfected into A431 cells using lipofection technique. 20 μg of plasmid DNAs were diluted to 250 μl of DOTAP buffer (20 mM Hepes, 150 mM NaCl, pH 7.4) in a polystyrene tube. In a second tube a 1:1 mixture of DOTAP:buffer was prepared. The plasmid solution was then added dropwise, gently mixed, and left 10 min at room temperature. This suspension was added dropwise to a 10 cm dish of A431 cells, which had been split, 1 : 5 from a confluent dish the previous day. After 20 min, 10 ml of fresh medium was added and the dish incubated for 6 h at 37°C. The cells were cultured in 10 ml of fresh medium for 20 h. The following day, the transfected cells were split at different densities (1%, 2%, 5%, 10%, and 82%) onto 10 cm dishes in medium containing 0.5 mg/ml G418 (Gibco). The selection media was changed every 4 days and after 12 - 15 days colonies were isolated using cloning rings (6 mm internal diam). The colonies were encircled at the bottom of the dish using a felt pen. The plates were washed once with PBS-. The cloning rings were put on the colonies using Glisseal™ (Borer Chemie A.G.) and ~50 μl of trypsin solution applied. The cells were resuspended

and transferred into 24 well plates in 1 ml of medium containing 0.5 mg/ml G418 and expanded.

Expressing colonies were screened by immunofluorescence microscopy. Positive clones were expanded, and lines were finally subcloned to obtain a high number of expression cells.

4.4 Permeabilization of A431 cells with Streptolysin O.

A431 cells were grown for 48 hours into 24-multiwell plates to 80-90 % confluence. Cells were washed twice with 1 ml of ice-cold buffer 1 (115 mM K-acetate, 25mM HEPES pH 7.4, 2.5 mM $MgCl_2$) and placed on ice. Streptolysin O was obtained from Dr. Bhakdi S. (University of Mainz, Mainz, Germany). SL-O was activated in buffer 1 containing 10 mM DDT at 37° C for 30 minutes and incubated for further 10 minutes on ice before use. Cells were then incubated with 200 µl of ice-cold buffer 1 containing different concentration of SL-O for 10 minutes on ice, washed 2 times with 1 ml of ice cold buffer1, and incubated in 200 µl of buffer 2 (115 mM K-acetate, 25mM HEPES pH 7.4, 2.5 mM $MgCl_2$, 5 mM EGTA and 2.5 mM $CaC0_3$, 1 mM DTT) at 37 ° C for 2 minutes to allow pore formation. Cells were then returned to ice and incubated with 500 µl of buffer 2 for an additional 30 minutes to wash out the endogenous cytosol. The efficiency of permeabilisation was estimated by measuring the amount of cytosolic lactate

dehydrogenase (LDH) released into the medium. LDH enzymatic activity measurements are based on the decrease in the absorbance at 340 nm of the NADH in the presence of pyruvate and LDH. This decrease within a defined period of time (OD/min.) is proportional to the concentration of LDH.

To quantify the amount of LDH released from SL-O-permeabilized cells, 200 µl of samples containing the washed out cytosol were mixed with 800 µl of buffer 1, mixed and incubated with 5µl of 20 mg/ml NADH (Sigma) and 10 µl of 60 mM Na-pyruvate. The absorbance at 340 nm was followed during the first 2 minutes of the reaction, using the ultraspec 2100 spectrophotometer, according to manufacturer's instructions (Pharmacia).

4.5 *In vitro* recycling assay in SL-O-permeabilized A431 cells.

For each assay cells were grown and permeabilised as described above with the only exception that they were loaded with 10 µg/ml of biotinylated transferrin before permeabilisation. Following the incubation on ice to allow cytosol diffusion, cells were incubated in ice-cold buffer 2 for 10-30 min. The buffer 2 was removed, and 300 µl of the regeneration solutions were added to the respective wells: donor cytosol and ATP regeneration solution (1 mM ATP, 8 mM creatine phosphate, and 40 units/ml creatine phosphokinase) in buffer 2, an ATP regeneration solution buffer 2, or buffer 2 alone. All regeneration solutions

contained approximately 1mg/ml of unlabelled transferrin. For most experiments, HeLa cytosol at 3 mg/ml was used. Cells were incubated in the regenerating solutions for 5 min at 4 °C, and the plate was then transferred to a 37 °C water bath. The medium (effluxed Tf) was removed and collected at various time points and the cells were washed once in phosphate-buffered saline. This wash was pooled with the efflux medium. The cells were solubilized in 2% Triton X-100. The efflux and cell-associated biotinylated transferrin were determined as described in paragraph 4.7.

4.6 Cytosol Preparation of Spinner Hela cells

Five confluent medium sized flasks (175 cm^2) of Hela in S-MEM (containing L-Glutamine, non-essential amino acids Fetal Calf Serum (5%), Penicillin/Streptomycin) were trypsinized and added to 600 ml of S-MEM media in a 1 litre spinner flask (Wheaton), placed on a stirrer and incubated at 37°C for 2 days. After this time, the 600 ml were split into two 3-litres spinner flasks, each scaled up to 2 litres, placed on a stirrer and incubated at 37°C for 4 days. At a confluency of about 0.8 $x10^6$ cells/ml, cells were harvested by sedimenting at 3000 rpm, 10 min, at 4°C and washed 2 times in 1X PBS. The obtained pellet of about 7.5 ml was resuspended in 7.5 ml buffer (containing 50 mM HEPES, pH 7.4, 50 mM KCl, 2 mM $MgCl_2$, 1 mM DTT, 10µg/ml Aprotinin, 10µg/ml Leupetin,

10μg/ml Pepstatin, 10μg/ml Antipain and 0.4 mM Pheenylmethylsulfonyl Fluoride (PMSF)). Cells were cracked in a cell cracker (EMBL) using ball bearing size 8.004 and two 10-ml syringes by passing through the cracker 8-10 times. Efficient breakage was checked under the microscope. Homogenate was spun in TLA 100.4 Beckman ultracentifuge, at 80K rpm for 30 min, at 4°C resulting in about 6.5 ml supernatant (cytosol).

4.7 Kinetic Analysis of Transferrin recycling and EGF degradation

For T7 promoter driven over-expression experiments, HeLa cells were grown to 60% confluence, transfected with the appropriate plasmids and infected with T7 polymerase recombinant vaccinia virus as described in paragraph 4.2.1. Four hours post-infection cells were washed 2 times with PBS and biotinylated transferrin was internalised at a concentration of 10μg/ml for the indicated time. Unbound and surface bound transferrin was removed by washing the cells with ice cold PBS containing 1mg/ml cold transferrin followed by cold low pH buffer (150 mM Nacl, 10mM acetic acid pH 3.5, 1mg/ml cold transferrin) washes. This procedure was repeated 2 times resulting in the removal of 95-98% of surface-bound ligand (from cells that had been incubated with biotinylated transferrin for 1h on ice). To measure recycling, cells were returned to 37°C, and incubated with 1ml of medium containing 1mg/ml of unlabelled transferrin. At each time point an

aliquot of the medium was collected. At the end of the time course cells were washed 2 times with ice cold PBS and homogenised in 1ml of lysis buffer (PBS containing 2% TRITON X-100, 0.4% Sodium dodecyl sulfate). 30µl of the collected medium containing the recycled biotinylated-transferrin, or 30 µl of the lysate, containing the cell-associated biotinylated-transferrin, were quantified as described below. For each time point, results were expressed as percent of the total signal.

EGF trafficking was followed by internalising 1nM of biotinylated-EGF for 5 minutes at 37°C and chased at the same temperature for the indicated time after extensive washes. EGF degradation was estimated by quantifying the amount of biotinylated-EGF accessible to anti-EGF antibody, by using the same electrochemiluminescence detection system utilised to quantify biotinylated-transferrin recycling (see below)

4.7.1 Detection systems – Electrochemiluminescence (ECL) Detection System

An electrochemiluminescence-based technology was used to quantify transferrin recycling and EGF degradation. The ECL-Analyser System was purchased from IGEN (Igen, Rockville, MD, USA).The ECL reaction is illustrated in Figure 53.

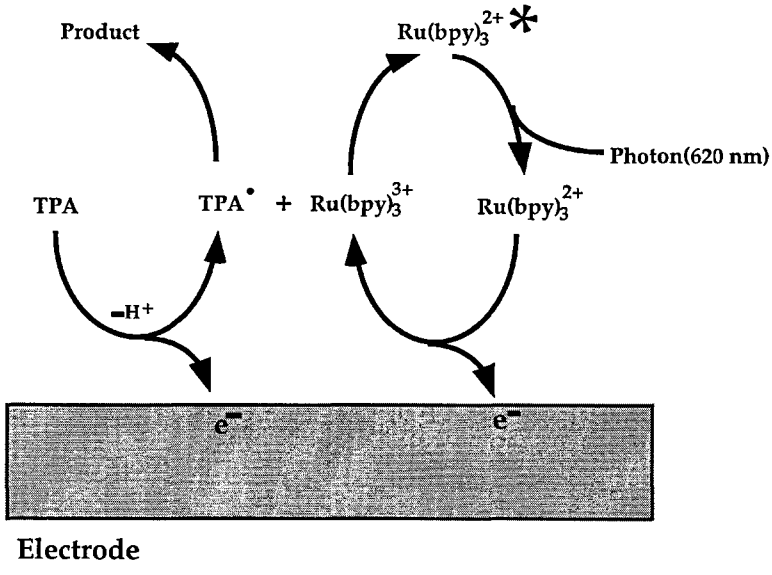

Figure 55. The electrochemiluminescence reaction

The ruthenium TAG coupled with the secondary antibodies and the tripopilamine (TPA) supplied by the Assay Buffer (Igen) were activated by oxidation at the electrode which serves as a sink or source of electrons and whose potential controls the amplitude of the electrochemical reaction. The oxidised, active TAG then reacts with the oxidised TPA to create the electronically excited state of TAG. The excited state luminesces at 620 nm wavelength, and the light produced is directly proportional to the amount of TAG activated in the reaction. Streptavidin-coated paramagnetic beads were used in order to capture the following immune-complexes: biotinylated transferrin/anti-tf sheep serum/ruthenium labelled anti-sheep IgG; or biotinylated EGF/anti-EGF rabbit

IgG/ruthenium labelled goat anti-rat IgG. Within the Analyser electrochemical flow cell, the beads present in the sample are drawn to the electrode with a magnet. Subsequently a "cleaning cycle" is performed with the Cell Cleaner Buffer (Igen), the magnet is then dropped, a voltage waveform is applied to the cell, and the light generated is measured. After flushing the cell with Cell Cleaner Buffer, the electrochemical flow cell is reconditioned with Assay Buffer and the cycle is repeated for the next sample.

For transferrin recycling, samples containing biotinylated transferrin were incubated first with 1 μl of M-280 Streptavidine Dynabeads, then with 1.25 μl of sheep anti-human transferrin serum (SAPU, Law Hospital Carluke, Scotland) diluted in 400 μl of Wash Buffer (50 mM Tris-HCl, pH 7.4, 100 mM NaCl, 2% Triton X-100, 0.2% BSA) and finally with 2 μg/ml ruthenium-labelled rabbit anti-sheep IgG. All the incubation steps were performed at RT for 1 h. Between the different incubation steps M-280 Streptavidine Dynabeads were washed 3 times with Wash Buffer using a Dynal MPC-E Magnetic Particle Concentrator (Dynal, Oslo, Norway). After the last washing step the Dynabeads were resuspended in 100 μl of Wash Buffer and 100 μl of Assay Buffer and subsequently quantified by the ECL-Analyser. For EGF degradation assays, samples containing biotinylated EGF (500 μl, final volume) were incubated first with 2 μl (5nM final) of rabbit anti-human EGF IgG (Dianova) for 30 minutes and then 1 μl of M-280

Streptavidin Dynabeads was added to the mixture and incubated for 1 hour. Thereafter, M-280 Streptavidin Dynabeads were washed 3 times with Wash Buffer diluted in 400 µl of Wash Buffer (50 mM Tris-HCl, pH 7.4, 100 mM NaCl, 2% Triton X-100, 0.2% BSA) containing 2 µg/ml (1:400) of ruthenium-labelled goat anti-rabbit IgG.

4.7.2 Ruthenium labelling of secondary antibodies

The N-hydroxysuccinimide ester of the ruthenium chelate (ORIGEN TAG-NHS ester, IGEN) was utilised to label the following secondary antibodies: affinity pure anti-rat IgG $F(ab')_2$ fragment specific antibody and rabbit anti-sheep IgG (Dianova). All secondary antibodies were obtained from Dianova (Hamburg, Germany). The ruthenium chelate was dissolved immediately before use in the appropriate volume of DMSO in order to obtain a stock solution of 1.5 µg/µl. To achieve a 10:1 labelling molar ratio, 24 µl of Origen Tag-NHS ester stock were added to 278 µl of the affinity pure secondary antibodies (1.8 mg/ml). The volume of the reaction was adjusted to 500 µl by adding 198 µl of Phosphate Buffer (0.01 M Na_2HPO_4/NaH_2PO_4, pH 8.0, 0.25 M NaCl). The tube content was gently vortexed and incubated at room temperature for 60 min in the dark. The labelling reaction was stopped by adding 20 µl of 2 M glycine, pH 2.8, and incubating at room temperature for 10 min in the dark. To remove the uncoupled Origen Tag

label, the mixture was subsequently loaded onto a PD-10 column (Pharmacia) equilibrated with PBS-2 (0.15 M K_2HPO_4/KH_2PO_4 buffer, pH 7.2, 0.15 M NaCl) The labelled antibodies were eluted with PBS-2 and the protein concentration of the collected and pooled fractions was determined using the Biorad protein assay and the gamma globulin standard. In order to calculate the conjugation ratio obtained, the absorbance of the Origen Tag-IgG was measured at 455 nm using a 1 cm path cuvette. The conjugation ratio typically ranged between 4 to 8 molecules of Tag: molecule of antibody. The antibody conjugates were stabilized by adding BSA at the final concentration of 3%, aliquoted and stored at -20°C.

4.8 Confocal Microscopy, Image Processing and Quantitation of Signal Overlap on Fixed Cells

Confocal microscopy was performed on a Compact Confocal Camera (CCC). For multi-channel imaging, fluorescent dyes were imaged sequentially in either frame-interlace or line-interlace modes to eliminate cross talk between the channels. CFP was excited with a 430-nm laser line (Directly Doubled Diode/D3, Coherent) and imaged through a combination of 440–505nm bandpass and 525nm longpass emission filters. YFP was exited with the 514-nm Argon laser line and imaged through a 525-nm longpass emission filter. Texas-red was excited with the

594-nm Helium Neon laser line and imaged through a 610-nm longpass emission filter.

Serial sections of images were acquired satisfying the Nyquist criteria for sampling and processed on a multiprocessor SGI Unix computer using the Huygens System 2.2 (Scientific Volume Imaging BV). A Maximum Likelihood Estimation (MLE) based algorithm was used for image reconstruction. Z-stacks of images were exported as TIFF files, and individual sections were analyzed for fluorescent signal overlap by visual inspection. Using Adobe Photoshop 5, a grid of 5 by 5cm was projected onto the image of the reference channel (for example Texas-red transferrin), and in every second grid square all fluorescent structures were marked on a separate, superimposed layer. Signals were referred to as individual structures if they comprised of a continuous patch of intensity values above 50 (in a range of 0 to 255). This layer was then projected onto the corresponding images for the other two channels (for example YFP-Rab4 and CFP-Rab5), and the underlying image was analyzed for fluorescent signal at the marked position. At least two sections per cell were counted, ensuring that peripheral and perinuclear structures were equally taken into account. Immunofluorescence labelling was performed according to standard procedures. Cells were mounted in ProLong™ Antifade (Molecular Probes).

4.9 Electron Microscopy

A431 cells grown to 70% confluence in 10cm dishes were transfected with 10μg of pCDNA3-Rabenosyn-5 by using SuperFect (Qiagen). 24 hours post transfection cells were fixed by adding to 8 ml of growth medium an equal volume of 2X fixative consisting of 0.4% EM Grade glutaraldehyde (Merck) and 4% paraformaldehyde in 0.4M potassium phosphate, pH7.4. After 10 minutes the mixture was replaced by fresh 1X fixative and incubated for 3 hours at room temperature. Cells were washed with PBS and free aldehyde groups blocked by incubation for 10 minutes with 50mM ammonium chloride in PBS. Cells were washed with PBS, scraped and the pellet embedded in 2% low melting point agarose in PBS. After the agarose was hardened by chilling, small blocks were cut, infiltrated overnight in 2.1M sucrose and frozen in liquid nitrogen. Ultrathin cryosection were cut at –100° with a Leica FCS cryomicrotome using a Drukker Knife. Sections were collected and transferred to grids coated with formva and carbon, and freshly glow-discharged. Unspecific binding sites were blocked with 0.5 % (v/v) fish skin gelatine, 20mM glycine in PBS for 10min. Antibodies against Rabenosyn-5 were diluted in blocking solution at 1/30. Protein A conjugated to 10nm gold was diluted according to the manufacturer's instructions (Slot and Geuze, University of Utrecht). Labelled grids were embedded in aqueous 2% methylcellulose, 3% uranyl acetate to add contrast and prevent

shrinking upon drying. Grids were observed with a Zeiss EM-10 microscope at 80 KV.

4.10 Sequential Affinity Chromatography

To purify Rab5 effectors, bacterial DH5α cells (30 l) were grown to express GST-Rab5 and the protein was purified using 5ml of glutathione beads according to the manufacturer's instructions (Pharmacia). This material was then incubated with nucleotide-exchange buffer (buffer A) containing 20 mM HEPES, 100 mM NaCl, 10 mM EDTA, 5 mM MgCl2, 1mM DTT, 1 mM GTPγS, pH 7.5, for 90 min at room temperature under rotation. Afterwards, buffer A was removed and the GTPγS form of GST–Rab5 was stabilized with buffer (buffer B) containing 20 mM HEPES, 100 mM NaCl, 5 mM MgCl2, 1mM DTT, pH 7.5, in the presence of 1 mM GTPγS for 20 min at room temperature under rotation. Beads were then incubated for 120 min at 4 °C with bovine brain cytosol. Thereafter, beads were washed with 10 column volumes of buffer B containing 10 μM GTP-S, 10 column volumes of buffer B containing 250 mM NaCl final concentration and 10 μM GTPγS, and 1 column volume of 20 mM HEPES, 250 mM NaCl, 1 mM DTT, pH 7.5. Bound proteins were eluted with 1.5 column volumes of buffer C containing 20 mM HEPES, 1.5 M NaCl, 20 mM EDTA, 1mM DTT, 5 mM GDP, pH 7.5, incubated with the beads for 20 min at room

temperature under rotation. Eluted proteins were first treated twice for 1 h at 4 °C with 0.2 ml glutathione-Sepharose beads to remove GST–Rab5 which leaked from the affinity column during the elution step. The sample was then desalted using PD10 columns (Pharmacia) in a nucleotide free buffer containing 20 mM HEPES, 150 mM NaCl, 1mM DTT, pH 7.5. The Rab5 interacting proteins obtained were then incubated with 1ml of glutathione beads containing GST-Rab4 loaded with either GTPγS or as control GDP. GST–Rab4 was prepared as described above for GST-Rab5. For the GDP form of GST–Rab4 the following changes were made: all buffers contained GDP instead of GTPγS, except for the elution buffer which contained GTPγS (1 mM) instead of GDP. Bound proteins were eluted with buffer C, separated by SDS-PAGE and analysed by Western blot or mass spectroscopy.

4.11 *In Vitro* Binding Assay and affinity measurement

Rabenosyn5 and hVPS45 DNAs were *in vitro* transcribed and translated in the presence of ^{35}S-methionine using a TnT coupled transcription-translation kit (Promega). Binding assays were performed by incubating 50µl of the translated proteins with 30 µl of GST-Rab5, Rab4 or Rab11 loaded with either GDP or GTPγS. Bound proteins were eluted, separated by SDS-PAGE and analysed by autoradiography. For the binding experiments using insect cells over-expressed proteins, recombinant baculovirus carrying Rabenosyn-5 and hVPS45 cDNAs was

generated according to manufacturer's instructions (Life Technologies). To achieve optimal protein expression levels, 500 ml of suspension grown ExpresSf+ (Protein Science) insect cells (1 X 10^6 cells/ml) were infected at M.O.I of 2 and incubated for a further 52 hours. Cells were harvested by centrifugation and cytosol prepared as described below. Approximately 8 mg of total proteins were incubated for 2 hours at 4° C with 100 µl beads containing ~400 µg GST-Rab4 loaded with GTPγS. After extensive washes with buffer B, beads were further incubated for 1 hour with ~200 µg of purified Rab5:GTPγS and 10mg/ml BSA diluted in buffer B. Beads were washed with 10 ml of buffer B and bound proteins were eluted as described above.

The dissociation constants (Kd) of the interaction between Rab5-Rabenosyn-5 and Rab4- Rabenosyn-5 were determined following the method of Butner et al. to measure the affinity between tau proteins and tubulin Butner et al. (1991). Briefly, Rabenosyn-5 was *in vitro* translated in the presence of ^{35}S-methionine using a TnT coupled transcription-translation kit (Promega). 20 microliters of translated protein were incubated for 1 hour at room temperature with serial dilution of glutathione–Sepharose beads containing GST-Rab4 or Rab5 in 200 µl of buffer B (with the total amount of Rabenosyn-5 being always well below the concentration of GST-Rab to ensure maximal binding). Beads were spun through a 1 ml 40 % sucrose cushion to separate bound from the unbound

Rabenosyn-5. Proportional aliquots of bound, unbound and total loaded fractions were separated by SDS-PAGE, and analysed with a phosphoimager for quantification. Binding of Rabenosyn-5 to empty GST beads was considered as background and therefore subtracted from each binding value before calculating percentage of binding. The Kd was calculated by fitting the obtained saturation binding curve data to a model with a non-linear regression method using the Graph Prism program (http://www.graphpad.com)

4.12 Expression and purification of recombinant proteins

4.12.1 Production of GST fusion proteins in bacteria

1-litre stationary cultures of bacterial cells BL21 strain of *E. Coli* (transformed with the corresponding construct designed to express GST fusion proteins) were diluted to 12 litres of LB medium in the presence of Ampicillin (100 μg/ml) and grown at 37° C with shaking (200 rpm) until an OD of 0.6 at 600 nm. Induction of GST-fusion protein expression was achieved by adding 0.1 mM isopropyl-β-D-thiogalactopyranoside (IPTG) to the culture and incubating for 3 additional hours. The cells were sedimented by centrifugation at 4000 rpm for 20 minutes in a Sorvall HG4L rotor at 4° C and then resuspended in 200 ml of PBS, containing 200 μl proteases inhibitor mixtures (Sigma). Cells were broken by pressure using a french press (SLM AMINCO) and the lysates were centrifuged at 10000 rpm for

20 minutes in a SS34 rotor at 4° C. The supernatant was incubated with 1 ml of packed glutathione agarose beads for 2 hours at 4° C with shaking. Beads were sedimented by centrifugation at 1000 rpm for 5 minutes on a table-top centrifuge at 4° C and washed 3 times with 10 beads volume ice-cold PBS. Bound proteins were eluted from the beads with 1 ml elution buffer (15 mM glutathione, 50 mM Tris-HCL pH 8).

4.12.2 Production of Histidine-tagged proteins in bacteria

E. coli strain BL21 (DE3) were transformed with plasmid pRSET A containing Rab-GDI cDNA cloned into the BamHI site. A preculture of 10 ml was grown from a single colony in Terrific broth (TB) containing 50μg/ml ampicillin at 37°C for 6 hr. The preculture was used to inoculate a 10-litres overnight culture in TB containing 50μg/ml ampicillin that was shaken vigorously at 37°C without induction by IPTG. The bacteria were harvested by centrifugation in a Sorvall centrifuge (Norwalk, CT) with GS-3 rotor at 5000 rpm for 10 min at 4°C, and the pellet (70 g bacteria/10 liter) was washed once with BPS (resuspended and pelletted again). After freezing (-80°C) and thawing of the pellet, bacteria were resuspended in 140 ml (2 vol of wet weight) of lysis buffer (50 mM Na_2HPO_4, pH 8.0/0.3 M NaCl/10 mM 2-mercaptoethanol) containing 1 mg/ml lysozyme, 0.1 mM phenylmethylsulfonyl fluoride, and 5μg/ml DnaseI and were incubated for 30

min on ice. Cells were sonicated (Sonifier B-12, Branson, Danburry, CT) on ice in 10 15-sec intervals with cooling on ice for 1 min between each sonication and the lysate was centrifuged at 25,000 rpm for 1hr at 4°C in a Beckman (Palo Alto, CA) SW 27 rotor. The supernatant was incubated on a rotating wheel for 1 h at 4°C with 10 ml Ni^{2+}-NTA-agarose (Qiagen, Chatsworth, CA) equilibrated in lysis buffer. The beads were spun down at 1000 g for 2 min and washed (resuspended and pelleted again) in batches 3 times with 40 ml lysis buffer, pH 8.0; 3 times with 40 ml of lysis buffer, pH 6.0, containing 0.3% Triton X-100; and 2 times in 40 ml lysis buffer, pH 8.0. Beads were loaded onto a 10-ml Poly-Prep chromatography column (Bio-Rad, Richmond, CA), washed with 10 cold volumes lysis buffer, pH 8.0, and eluted with 20 ml of 200 mM imidazole in lysis buffer. Fractions of 1.5 ml were collected, and the purity and protein concentration were analysed by SDS -PAGE followed by Coomassie blue staining. Fractions containing His_6-Rab-GDI (fractions 5-10) were pooled, dialysed overnight against 20 mM HEPES/KOH, pH 7.2/10 mM 2- mercaptoethanol, and stored at -80°C.

4.12.3 Expression and purification of Rab4 and Rab11 using the Baculovirus expression System.

Hi-5 insect cells adapted to serum free medium were cultured in suspension and infected at a concentration of $0.5x10^6$ cells/ml with 6.0 ml of P3 amplified

baculovirus containg Histidine-tagged Rab4 or Rab11 in 250 ml. Cells were cultured in 1.8 liter Fernbach shaking flasks and incubated at 27°C, 60 rpm for 72 hours. The cells were harvested by sedimenting at 1600 rpm, 15 min, at 4°C, and washed one time in 1X PBS. For purification of prenylated Rab4 and Rab11 membrane fraction were prepared by resuspending the cell pellet in 8.0 ml Lysis buffer (containing 20 mM HEPES, pH 7.4, 50 mM KCl, 10 mM $MgCl_2$ and 1 mM DTT). Cells were cracked in the cell cracker (EMBL) using a ball bearing size 8.004 and two 10 ml syringes by passing through the cracker about 10 times. Efficient breakage was checked under the microscope. Post-nuclear supernatant (PNS) was obtained by centrifugation of the homogenate at 1000 g for 5 minutes at 4 °C. PNS was then centrifuged at 160,000 g (Beckman SW40 rotor 30,000 rpm) for 30 minutes at 4 °C. The pellet (membrane fraction) was then resuspended in 4 ml of ice cold buffer containing 0.6% CHAPS (Sigma), 20 mM HEPES, pH 7.4, 50 mM KCl, 10 mM $MgCl_2$ and 1 mM DTT, sonicated for 10 seconds on ice and incubated for 1 hour at 4 °C on a rotating wheel. The suspension was centrifuged at 160,000 g for 30 minutes at 4 °C, and the supernatant (4 ml) containing Histidine-tagged Rab4 or Rab11 was incubated on a rotating wheel for 1 hour with 200 µl Ni-NTA-agarose beads and Histidine-tagged Rab4 or Rab11 purified according to manufacturer's instructions (Qiagen, Chatsworth, CA).

4.12.4 Purification of Rab4 and Rab11- RabGDI complex by Gel –filtration column chromatography.

In order to allow complex formation between Rab5 or Rab11 and RabGDI, 1 nmole of prenylated and purified Rab4 or Rab11 was incubated with 1 nmole of purified RabGDI in 500 µl buffer containing 20 mM HEPES pH7.4, 100 mM K-acetate 2.5mM MgCl2, 1 µM GDP, and 0.005% Triton-x100. The samples were incubated for 10 minutes at 30 °C and then loaded onto a Superose 12 HR 10/30 gel-filtration column (Pharmacia, NJ). Fractions of 0.4 µl were collected and 30 ml aliquots analysed by SDS-PAGE and Coomassie blue staining.

4.12.5 Expression of Rabenosyn-5/hvps45 ExpresSf+ using the baculovirus expression system

Expression of the recombinant protein in insect cells was achieved with the use of baculovirus expression system (Life Technologies). The recombinant plasmid pfastBac-Dual-Rabenosyn-5/hvps45 was transformed into DH10Bac competent cells, which contain the bacmid with a mini-attTn7 target site and the helper plasmid. Colonies containing recombinant bacmids were identified by disruption of the lacZá gene. High molecular mini-prep DNA was prepared from selected *E. coli* clones containing the recombinant bacmid. This DNA was then transfected in Sf-9 insect cells After 3 rounds of virus amplification the protein

was expressed by infection with the Rabenosyn-5/hvps45 baculovirus in ExpresSf+ (Protein Science) insect cells according to the manufacturer's instructions.

4.13 Rabenosyn-5/hvps45 ExpresSf+ Cytosol Preparation.

ExpresSf+ serum free insect cells were cultured in suspension and infected at a concentration of $1.0x10^6$ cells/ml with 3.6ml of P3 amplified baculovirus containing Rabenosyn-5 and hvps45 at a MOI of 4 in 500 ml. Cells were cultured in 1.8 liter Fernbach shaking flasks and incubated at 27°C, 60 rpm for 64 hours. Cells were harvested and sedimented at 1600 rpm, 15 min, at 4°C and the pellet was washed one time in 1X PBS. The obtained pellet of about 8.0 ml was resuspended in 8.0 ml Lysis buffer (containing 50 mM HEPES, pH 7.4, 50 mM KCl, 5 mM $MgCl_2$ and 1 mM DTT). Cells were cracked in the cell cracker (EMBL) using ball bearing size 8.004 and two 10 ml syringes by passing through the cracker about 20 times. Efficient breakage was checked under the microscope. Homogenate was spun in a S100-AT6 Sorvall, at 100 K rpm for 30 min, at 4°C resulting in about 8 ml supernatant (cytosol).

4.14 Western Blot analysis

Immunoblot was carried out at room temperature on a rocking platform. Unspecific binding sites were blocked by incubating the membrane with blocking

solution (PBS containing 0.1% Tween- 20; 5% non-fat milk powder) for 30 minutes. Subsequently, the membrane was incubated with the primary antibody diluted 1: 1,000 in blocking solution for 1 h. The membrane was washed 3 times before incubation for 1 h with the second antibody goat anti-rabbit IgG coupled to peroxidase (Dianova) diluted 1: 5,000 in blocking solution. The membrane was developed with the ECL system (Amersham) following the instructions of the manufacturer.

4.15 Silver staining of protein

The SDS-PAGE gel was fixed with Fixer buffer 2X times for 15-20 minutes. Reducer buffer was added and incubated for 30 minutes. The gel was washed 3X times for 10 minutes with distilled water and incubated for 30 minutes in the silver nitrate buffer. The gel was then rinsed briefly with H_2O, and with a small amount of Developer buffer. Developer buffer was added in excess and the developing reaction was stopped by addition of Quenching buffer.

4.16 Protein sequencing

Protein sequence information was obtained by nano-electrospray mass spectrometry (Wilm et al., 1996) in collaboration with the M. Wilm group at EMBL

4.17 Antibodies and Plasmids

Polyclonal rabbit antibodies against Rabenosyn-5 and hVPS45 were available in the laboratory and have been described (Nielsen, E. *et al.* (2000)). Antibodies were affinity-purified as described below and used at (1:1000). Polyclonal rabbit antibodies against Rabaptin-5, Rabaptin-5β, p110β, and Rabex-5 were used as crude serum at 1:1000 (Western blotting) or 1:200 (immunofluorescence). Human anti-EEA1 serum (1:1000) was a gift from Ban Hok Toh (Monash Medical School, Adelaide, Australia). Monoclonal mouse anti-transferrin receptor antibodies (B3/25) were purchased from Roche (Mannheim). Secondary antibodies conjugates (HRP and fluorescently labelled) were purchased from Dianova.

Plasmids

Cloning was performed according to standard procedures (Sambrook et al. 1989). PCR amplified sequences were checked by sequencing.

pEGFP-Rab4 and pEYFP-Rab4 construct

Human Rab4 cDNA was amplified by PCR from pGEM-Rab4 vector available in the laboratory with the insertion of (5',) *XhoI* and (3,) *Hind III*; using the following primers: forward 5' AAAACTCGAG ATG TCC GAAACCTACGATTT; reverse 5' AAAAAAGCTT

CTAACAACCACACTCCTGA and cloned in frame into the pEGFP-C3 vector (Clontech) cut *XhoI* and (3,) *Hind III*. For cloning into the pEYFP vector, human Rab4 cDNA was amplified with the insertion of (5',) *KpnI* and (3,) *BamHI*.

pFastBac Hta-Rab4 construct

To express Rab4 using the baculovirus expression the Rab4 cDNA was amplified by PCR from pGEM-Rab4 with the insertion of (5,) *Xho I* and (3,) *Hind* III and cloned in frame into the Histidine-tagged vector pFastBacHta (Gibco) cut *Xho I* and (3,) *Hind* III.

Rabenosyn-5; Rabaptin-5; EEA1 and hVPS45 constructs

Rabenosyn-5 was amplified by PCR from pGEM-myc-Rabenosyn-5 with the insertion of (5') *Hind III* and (3') *EcoRI* and cloned into pDNA3 cut HindIII and *EcoRI*. To generate Rabenosyn-5 truncation mutant constructs (amino acid) 1-263; 264-784; 501-784; 264-500; 501-626; 627-784; the Rabenosyn-5 cDNA was amplified by PCR from pGEM-Rabenosyn-5 with the appropriate primers with the insertion of (5') *Hind III* and (3') *EcoRI* and cloned into pGEM-Myc4 cut with EcoRI, HindIII or into pCDNA3.1 Myc (frame3) vector cut EcoRI/ EcorV, (in this last case the HindIII site was filled in). To generate recombinant Rabenosyn-5 / hvps45 complex baculovirus, Rabenosyn-5 was amplified by PCR from pGEM-myc-Rabenosyn-5 with the insertion of (5') *EcoR I* and (3') *Hind III*; hvps45 was amplified from pGEX-hvps45 with insertion of (5') *Sma I* and (3')

Kpn I. These PCR products were then digested with *EcoR I* and *Hind III* (Rabenosyn-5), *Sma I* and *Kpn I* (hvps45) into pFastBac-Dual expression vector (Life Technologies) to yield in the untagged pFastBac-Dual-110Fyve-hvps45 construct. The construct was confirmed by sequencing to avoid PCR-induced mutations. Rabaptin-5, EEA1, hVPS45 were subcloned into the mammalian expression vector pcDNA3 (Clontech).

4.18 Preparation of competent *E. coli* for electroporation.

A single colony of a strain of *E. coli* XL1Blue, SURE was used to inoculate 10 ml of LB medium which was grown overnight at 37°C with shaking. 2 ml of saturated culture were then transferred to 1000 ml of the same medium and the culture was grown until it reached an OD of 0.6 at 600 nm. Cells were then collected by centrifugation at 4000 rpm for 20 min at 4°C in 1 liter bottles using a Sorvall HG4L rotor. The resulting pellet was gently resuspended in 500 ml ice-cold water. Cells were then sedimented again by centrifugation and resuspended in 300 ml cold water. Cells were centrifuged at 4000 rpm for 10 minutes at 4°C in a GSA rotor and pellets were then resuspended in 100 ml 10% glycerol. The pellets were sedimented again under the same conditions and resuspended in 20 ml of 10% glycerol. 100-µl aliquots were rapidly frozen in liquid N_2 and stored at –80°C.

4.19 Plasmid preparation in large scale (Maxi-prep) and small scale Mini-prep

Plasmid Maxi-preps were done according to QIAGEN plasmid® purification protocols. The DNA concentration was estimated by comparison to serial dilutions of a DNA standard separated by electrophoresis on an agarose gel stained with ethidium bromide. The stained gel was photographed with HEROLAB UVT-20 M/W Gel Documentation System. Plasmid Mini-preps were done according to QIAGEN plasmid® purification protocols

4.20 Electroporation of *E. coli*

Electroporation of DNA into *E. coli* cells was performed with a BioRad Gene pulser with a pulse controller. 40 µl of a suspension of bacterial electrocompetent cells was mixed on ice with 5 µl of DNA dissolved in H_2O and placed into the bottom of an ice cold electroporation cuvette (BioRad 0.2cm separation). The cuvette was then placed into a holder of the electroporator and the cells were subjected to an electric pulse of 2.5 kV (capacitance setting 25 µF and resistance setting 200 Ω). 1 ml of LB medium was then added immediately to the cell suspension, which was incubated at 37°C for 60 min. Cells were then sedimented at 6000 rpm for 3 min in a bench top microcentrifuge and resuspended

in 100 µl LB medium. Cells were plated on LB plates (containing 100µg/ml ampicillin if selection was required) and incubated overnight at 37°C.

4.21 Restriction enzyme digestion of DNA

Restriction enzyme digestions of DNA were performed by incubation of DNA with 5 units of enzyme per µg of DNA for a minimum of 2 hr at 37°C, under the conditions recommended by the manufacturer's (Roche). The digested DNA sample was then extracted with phenol/chloroform and chloroform, and precipitated with 100% ethanol. The pellet was washed with 80% ethanol and resuspended in 1 µl of H_2O per µg of DNA. Cleavage was monitored by electrophoresis in an agarose gel stained with ethidium bromide.

4.22 Ligation of DNA

Standard ligation reactions were done in 10µl final volume (with 3:1 insert:vector ratio) in the presence of 1µl of 10X Ligase buffer and 10 units of Ligase (NEB). The reactions were incubated from 4 to 12 h at 16°C.

ACKNOWLEDGMENTS

First of all, I am extremely grateful to my advisor, Marino Zerial, for constant support, scientific advice and patience that have characterised these years of intense interaction. I would also like to thank all current and former lab members for their help and for the nice work environment that they have contributed to create. I am particularly grateful to Jochen Rink, Anja Runge and Judith Nicholls for having proof read various versions of this thesis and for their helpful comments. I am very greatful to the EMBL PhD program and to all my friends at EMBL (Italians and non-Italians) for having made my experience at EMBL unforgettable. Many thanks also to my new friends-colleagues at the MPI-CBG in Dresden for continuing to make my life and scientific experience in Germany happy and stimulating. I would also like to thank my thesis supervisors Dr. Kai Simons and Dr. Mark Marsh. Last, but not least, I thank my future wife Anja Runge. Words are too limited to explain why.

5. References

Aalto, M. K., Ronne, H., and Keranen, S. (1993). Yeast syntaxins Sso1p and Sso2p belong to a family of related membrane proteins that function in vesicular transport. Embo J *12*, 4095-104.

Adams, R. J., and Pollard, T. D. (1989). Binding of myosin I to membrane lipids. Nature *340*, 565-8.

Ahle, S., and Ungewickell, E. (1990). Auxilin, a newly identified clathrin-associated protein in coated vesicles from bovine brain. J Cell Biol *111*, 19-29.

Alexandrov, K., Horiuchi, H., Steele-Mortimer, O., Seabra, M. C., and Zerial, M. (1994). Rab escort protein-1 is a multifunctional protein that accompanies newly prenylated rab proteins to their target membranes. Embo J *13*, 5262-73.

Allan, B. B., Moyer, B. D., and Balch, W. E. (2000). Rab1 recruitment of p115 into a cis-SNARE complex: programming budding COPII vesicles for fusion. Science *289*, 444-8.

Allan, V. (1995). Membrane traffic motors. FEBS Lett *369*, 101-6.

Aniento, F., Emans, N., Griffiths, G., and Gruenberg, J. (1993). Cytoplasmic dynein-dependent vesicular transport from early to late endosomes. J Cell Biol *123*, 1373-87.

Apodaca, G., Katz, L. A., and Mostov, K. E. (1994). Receptor-mediated transcytosis of IgA in MDCK cells is via apical recycling endosomes. J Cell Biol *125*, 67-86.

Armstrong, S. A., Seabra, M. C., Sudhof, T. C., Goldstein, J. L., and Brown, M. S. (1993). cDNA cloning and expression of the alpha and beta subunits of rat Rab geranylgeranyl transferase. J Biol Chem *268*, 12221-9.

Axline, S. G., and Reaven, E. P. (1974). Inhibition of phagocytosis and plasma membrane mobility of the cultivated macrophage by cytochalasin B. Role of subplasmalemmal microfilaments. J Cell Biol *62*, 647-59.

Bahadoran, P., Aberdam, E., Mantoux, F., Busca, R., Bille, K., Yalman, N., de Saint-Basile, G., Casaroli-Marano, R., Ortonne, J. P., and Ballotti, R. (2001). Rab27a: A key to melanosome transport in human melanocytes. J Cell Biol *152*, 843-50.

Barlowe, C., Orci, L., Yeung, T., Hosobuchi, M., Hamamoto, S., Salama, N., Rexach, M. F., Ravazzola, M., Amherdt, M., and Schekman, R. (1994). COPII: a membrane coat formed by Sec proteins that drive vesicle budding from the endoplasmic reticulum. Cell *77*, 895-907.

Barlowe, C., and Schekman, R. (1993). SEC12 encodes a guanine-nucleotide-exchange factor essential for transport vesicle budding from the ER. Nature *365*, 347-9.

Barroso, M., and Sztul, E. S. (1994). Basolateral to apical transcytosis in polarized cells is indirect and involves BFA and trimeric G protein sensitive passage through the apical endosome. J Cell Biol *124*, 83-100.

Becherer, K. A., Rieder, S. E., Emr, S. D., and Jones, E. W. (1996). Novel syntaxin homologue, Pep12p, required for the sorting of lumenal hydrolases to the lysosome-like vacuole in yeast. Mol Biol Cell *7*, 579-94.

Beck, T., Schmidt, A., and Hall, M. N. (1999). Starvation induces vacuolar targeting and degradation of the tryptophan permease in yeast. J Cell Biol *146*, 1227-38.

Benli, M., Doring, F., Robinson, D. G., Yang, X., and Gallwitz, D. (1996). Two GTPase isoforms, Ypt31p and Ypt32p, are essential for Golgi function in yeast. Embo J *15*, 6460-75.

Bennett, M. K., and Scheller, R. H. (1994). Molecular correlates of synaptic vesicle docking and fusion. Curr Opin Neurobiol *4*, 324-9.

Black, M. W., and Pelham, H. R. (2001). Membrane traffic: How do GGAs fit in with the adaptors? Curr Biol *11*, R460-2.

Black, M. W., and Pelham, H. R. (2000). A selective transport route from Golgi to late endosomes that requires the yeast GGA proteins. J Cell Biol *151*, 587-600.

Bloom, G. S. (1992). Motor proteins for cytoplasmic microtubules. Curr Opin Cell Biol *4*, 66-73.

Boguski, M. S., and McCormick, F. (1993). Proteins regulating Ras and its relatives. Nature *366*, 643-54.

Boman, A. L., Zhang, C., Zhu, X., and Kahn, R. A. (2000). A family of ADP-ribosylation factor effectors that can alter membrane transport through the trans-Golgi. Mol Biol Cell *11*, 1241-55.

Bomsel, M., Parton, R., Kuznetsov, S. A., Schroer, T. A., and Gruenberg, J. (1990). Microtubule- and motor-dependent fusion in vitro between apical and basolateral endocytic vesicles from MDCK cells. Cell *62*, 719-31.

Bonifacino, J. S., and Weissman, A. M. (1998). Ubiquitin and the control of protein fate in the secretory and endocytic pathways. Annu Rev Cell Dev Biol *14*, 19-57.

Bourne, H. R. (1988). Do GTPases direct membrane traffic in secretion? Cell *53*, 669-71.

Brown, D. A., and London, E. (1998). Functions of lipid rafts in biological membranes. Annu Rev Cell Dev Biol *14*, 111-36.

Brown, H. A., Gutowski, S., Moomaw, C. R., Slaughter, C., and Sternweis, P. C. (1993). ADP-ribosylation factor, a small GTP-dependent regulatory protein, stimulates phospholipase D activity. Cell *75*, 1137-44.

Bucci, C., Parton, R. G., Mather, I. H., Stunnenberg, H., Simons, K., Hoflack, B., and Zerial, M. (1992). The small GTPase rab5 functions as a regulatory factor in the early endocytic pathway. Cell *70*, 715-28.

Buss, F., Arden, S. D., Lindsay, M., Luzio, J. P., and Kendrick-Jones, J. (2001). Myosin VI isoform localized to clathrin-coated vesicles with a role in clathrin-mediated endocytosis. Embo J *20*, 3676-84.

Cao, X., Ballew, N., and Barlowe, C. (1998). Initial docking of ER-derived vesicles requires Uso1p and Ypt1p but is independent of SNARE proteins. Embo J *17*, 2156-65.

Carroll, K. S., Hanna, J., Simon, I., Krise, J., Barbero, P., and Pfeffer, S. R. (2001). Role of Rab9 GTPase in facilitating receptor recruitment by TIP47. Science *292*, 1373-6.

Chatterjee, S., Smith, E. R., Hanada, K., Stevens, V. L., and Mayor, S. (2001). GPI anchoring leads to sphingolipid-dependent retention of endocytosed proteins in the recycling endosomal compartment. Embo J *20*, 1583-92.

Chavrier, P., Parton, R. G., Hauri, H. P., Simons, K., and Zerial, M. (1990). Localization of low molecular weight GTP binding proteins to exocytic and endocytic compartments. Cell *62*, 317-29.

Chen, M. S., Obar, R. A., Schroeder, C. C., Austin, T. W., Poodry, C. A., Wadsworth, S. C., and Vallee, R. B. (1991). Multiple forms of dynamin are encoded by shibire, a Drosophila gene involved in endocytosis. Nature *351*, 583-6.

Chen, Y. A., and Scheller, R. H. (2001). SNARE-mediated membrane fusion. Nat Rev Mol Cell Biol *2*, 98-106.

Christoforidis, S., McBride, H. M., Burgoyne, R. D., and Zerial, M. (1999). The Rab5 effector EEA1 is a core component of endosome docking. Nature *397*, 621-5.

Christoforidis, S., Miaczynska, M., Ashman, K., Wilm, M., Zhao, L., Yip, S. C., Waterfield, M. D., Backer, J. M., and Zerial, M. (1999). Phosphatidylinositol-3-OH kinases are Rab5 effectors. Nat Cell Biol *1*, 249-52.

Clague, M. J., Urbe, S., Aniento, F., and Gruenberg, J. (1994). Vacuolar ATPase activity is required for endosomal carrier vesicle formation. J Biol Chem *269*, 21-4.

Cohn, Z. A. (1966). The regulation of pinocytosis in mouse macrophages. I. Metabolic requirements as defined by the use of inhibitors. J Exp Med *124*, 557-71.

Cole, N. B., and Lippincott-Schwartz, J. (1995). Organization of organelles and membrane traffic by microtubules. Curr Opin Cell Biol *7*, 55-64.

Conradt, B., Haas, A., and Wickner, W. (1994). Determination of four biochemically distinct, sequential stages during vacuole inheritance in vitro. J Cell Biol *126*, 99-110.

Cormont, M., Mari, M., Galmiche, A., Hofman, P., and Le Marchand-Brustel, Y. (2001). A FYVE-finger-containing protein, Rabip4, is a Rab4 effector involved in early endosomal traffic. Proc Natl Acad Sci U S A *98*, 1637-42.

Corvera, S., D'Arrigo, A., and Stenmark, H. (1999). Phosphoinositides in membrane traffic. Curr Opin Cell Biol *11*, 460-5.

Cremona, O., Di Paolo, G., Wenk, M. R., Luthi, A., Kim, W. T., Takei, K., Daniell, L., Nemoto, Y., Shears, S. B., Flavell, R. A., McCormick, D. A., and De Camilli, P. (1999). Essential role of phosphoinositide metabolism in synaptic vesicle recycling. Cell *99*, 179-88.

D'Hondt, K., Heese-Peck, A., and Riezman, H. (2000). Protein and lipid requirements for endocytosis. Annu Rev Genet *34*, 255-295.

D'Souza-Schorey, C., Li, G., Colombo, M. I., and Stahl, P. D. (1995). A regulatory role for ARF6 in receptor-mediated endocytosis. Science *267*, 1175-8.

Damke, H. (1996). Dynamin and receptor-mediated endocytosis. FEBS Lett *389*, 48-51.

Damke, H., Baba, T., Warnock, D. E., and Schmid, S. L. (1994). Induction of mutant dynamin specifically blocks endocytic coated vesicle formation. J Cell Biol *127*, 915-34.

Daro, E., Sheff, D., Gomez, M., Kreis, T., and Mellman, I. (1997). Inhibition of endosome function in CHO cells bearing a temperature-sensitive defect in the coatomer (COPI) component epsilon-COP. J Cell Biol *139*, 1747-59.

Daro, E., van der Sluijs, P., Galli, T., and Mellman, I. (1996). Rab4 and cellubrevin define different early endosome populations on the pathway of transferrin receptor recycling. Proc Natl Acad Sci U S A *93*, 9559-64.

Dascher, C., Matteson, J., and Balch, W. E. (1994). Syntaxin 5 regulates endoplasmic reticulum to Golgi transport. J Biol Chem *269*, 29363-6.

de Vos, A. M., Tong, L., Milburn, M. V., Matias, P. M., Jancarik, J., Noguchi, S., Nishimura, S., Miura, K., Ohtsuka, E., and Kim, S. H. (1988). Three-dimensional structure of an oncogene protein: catalytic domain of human c-H-ras p21. Science *239*, 888-93.

de Wit, H., Lichtenstein, Y., Kelly, R. B., Geuze, H. J., Klumperman, J., and van Der Sluijs, P. (2001). Rab4 Regulates Formation of Synaptic-like Microvesicles from Early Endosomes in PC12 Cells. Mol Biol Cell *12*, 3703-15.

Dell'Angelica, E. C., Klumperman, J., Stoorvogel, W., and Bonifacino, J. S. (1998). Association of the AP-3 adaptor complex with clathrin. Science *280*, 431-4.

Dell'Angelica, E. C., Mullins, C., and Bonifacino, J. S. (1999). AP-4, a novel protein complex related to clathrin adaptors. J Biol Chem *274*, 7278-85.

Dell'Angelica, E. C., Puertollano, R., Mullins, C., Aguilar, R. C., Vargas, J. D., Hartnell, L. M., and Bonifacino, J. S. (2000). GGAs: a family of ADP ribosylation factor-binding proteins related to adaptors and associated with the Golgi complex. J Cell Biol *149*, 81-94.

Deretic, D., Puleo-Scheppke, B., and Trippe, C. (1996). Cytoplasmic domain of rhodopsin is essential for post-Golgi vesicle formation in a retinal cell-free system. J Biol Chem *271*, 2279-86.

Dirac-Svejstrup, A. B., Sumizawa, T., and Pfeffer, S. R. (1997). Identification of a GDI displacement factor that releases endosomal Rab GTPases from Rab-GDI. Embo J *16*, 465-72.

Doms, R. W., Russ, G., and Yewdell, J. W. (1989). Brefeldin A redistributes resident and itinerant Golgi proteins to the endoplasmic reticulum. J Cell Biol *109*, 61-72.

Dunn, K. W., McGraw, T. E., and Maxfield, F. R. (1989). Iterative fractionation of recycling receptors from lysosomally destined ligands in an early sorting endosome. J Cell Biol *109*, 3303-14.

Durrbach, A., Louvard, D., and Coudrier, E. (1996). Actin filaments facilitate two steps of endocytosis. J Cell Sci *109*, 457-65.

Echard, A., Jollivet, F., Martinez, O., Lacapere, J. J., Rousselet, A., Janoueix-Lerosey, I., and Goud, B. (1998). Interaction of a Golgi-associated kinesin-like protein with Rab6. Science *279*, 580-5.

Entchev, E. V., Schwabedissen, A., and Gonzalez-Gaitan, M. (2000). Gradient formation of the TGF-beta homolog Dpp. Cell *103*, 981-91.

Felder, S., Miller, K., Moehren, G., Ullrich, A., Schlessinger, J., and Hopkins, C. R. (1990). Kinase activity controls the sorting of the epidermal growth factor receptor within the multivesicular body. Cell *61*, 623-34.

Feng, Y., Press, B., and Wandinger-Ness, A. (1995). Rab 7: an important regulator of late endocytic membrane traffic. J Cell Biol *131*, 1435-52.

Fernandez-Borja, M., Wubbolts, R., Calafat, J., Janssen, H., Divecha, N., Dusseljee, S., and Neefjes, J. (1999). Multivesicular body morphogenesis requires phosphatidyl-inositol 3-kinase activity. Curr Biol *9*, 55-8.

Ferro-Novick, S., and Jahn, R. (1994). Vesicle fusion from yeast to man. Nature *370*, 191-3.

Finger, F. P., Hughes, T. E., and Novick, P. (1998). Sec3p is a spatial landmark for polarized secretion in budding yeast. Cell *92*, 559-71.

Frischknecht, F., Moreau, V., Rottger, S., Gonfloni, S., Reckmann, I., Superti-Furga, G., and Way, M. (1999). Actin-based motility of vaccinia virus mimics receptor tyrosine kinase signalling. Nature *401*, 926-9.

Fujimoto, L. M., Roth, R., Heuser, J. E., and Schmid, S. L. (2000). Actin assembly plays a variable, but not obligatory role in receptor-mediated endocytosis in mammalian cells. Traffic *1*, 161-71.

Futter, C. E., Gibson, A., Allchin, E. H., Maxwell, S., Ruddock, L. J., Odorizzi, G., Domingo, D., Trowbridge, I. S., and Hopkins, C. R. (1998). In polarized MDCK cells basolateral vesicles arise from clathrin-gamma-adaptin-coated domains on endosomal tubules. J Cell Biol *141*, 611-23.

Gagescu, R., Demaurex N, Parton RG, Hunziker W, Huber LA, Gruenberg J. (2000) The recycling endosome of Madin-Darby canine kidney cells is a mildly acidic compartment rich in raft components. Mol Biol Cell *11*, 2775-91

Gaidarov, I., Santini, F., Warren, R. A., and Keen, J. H. (1999). Spatial control of coated-pit dynamics in living cells. Nat Cell Biol *1*, 1-7.

Galli, T., Chilcote, T., Mundigl, O., Binz, T., Niemann, H., and De Camilli, P. (1994). Tetanus toxin-mediated cleavage of cellubrevin impairs exocytosis of transferrin receptor-containing vesicles in CHO cells. J Cell Biol *125*, 1015-24.

Gallwitz, D., Donath, C., and Sander, C. (1983). A yeast gene encoding a protein homologous to the human c-has/bas proto-oncogene product. Nature *306*, 704-7.

Garcia, E. P., Gatti, E., Butler, M., Burton, J., and De Camilli, P. (1994). A rat brain Sec1 homologue related to Rop and UNC18 interacts with syntaxin. Proc Natl Acad Sci U S A *91*, 2003-7.

Garcia, E. P., McPherson, P. S., Chilcote, T. J., Takei, K., and De Camilli, P. (1995). rbSec1A and B colocalize with syntaxin 1 and SNAP-25 throughout the axon, but are not in a stable complex with syntaxin. J Cell Biol *129*, 105-20.

Gaullier, J. M., Ronning, E., Gillooly, D. J., and Stenmark, H. (2000). Interaction of the EEA1 FYVE finger with phosphatidylinositol 3-phosphate and early endosomes. Role of conserved residues. J Biol Chem *275*, 24595-600.

Geuze, H. J., Slot, J. W., Strous, G. J., Lodish, H. F., and Schwartz, A. L. (1983). Intracellular site of asialoglycoprotein receptor-ligand uncoupling: double-label immunoelectron microscopy during receptor-mediated endocytosis. Cell *32*, 277-87.

Geuze, H. J., Stoorvogel, W., Strous, G. J., Slot, J. W., Bleekemolen, J. E., and Mellman, I. (1988). Sorting of mannose 6-phosphate receptors and lysosomal membrane proteins in endocytic vesicles. J Cell Biol *107*, 2491-501.

Gorvel, J. P., Chavrier, P., Zerial, M., and Gruenberg, J. (1991). rab5 controls early endosome fusion in vitro. Cell *64*, 915-25.

Goud, B., Salminen, A., Walworth, N. C., and Novick, P. J. (1988). A GTP-binding protein required for secretion rapidly associates with secretory vesicles and the plasma membrane in yeast. Cell *53*, 753-68.

Greenberg, S., Burridge, K., and Silverstein, S. C. (1990). Colocalization of F-actin and talin during Fc receptor-mediated phagocytosis in mouse macrophages. J Exp Med *172*, 1853-6.

Greenberg, S., el Khoury, J., di Virgilio, F., Kaplan, E. M., and Silverstein, S. C. (1991). Ca(2+)-independent F-actin assembly and disassembly during Fc receptor-mediated phagocytosis in mouse macrophages. J Cell Biol *113*, 757-67.

Griffiths, G., Back, R., and Marsh, M. (1989). A quantitative analysis of the endocytic pathway in baby hamster kidney cells. J Cell Biol *109*, 2703-20.

Griffiths, G., Hoflack, B., Simons, K., Mellman, I., and Kornfeld, S. (1988). The mannose 6-phosphate receptor and the biogenesis of lysosomes. Cell *52*, 329-41.

Gruenberg, J. (2001). The endocytic pathway: a mosaic of domains. Nat Rev Mol Cell Biol *2*, 721-30.

Gruenberg, J., Griffiths, G., and Howell, K. E. (1989). Characterization of the early endosome and putative endocytic carrier vesicles in vivo and with an assay of vesicle fusion in vitro. J Cell Biol *108*, 1301-16.

Gruenberg, J., and Maxfield, F. R. (1995). Membrane transport in the endocytic pathway. Curr Opin Cell Biol *7*, 552-63.

Gu, F., and Gruenberg, J. (2000). ARF1 regulates pH-dependent COP functions in the early endocytic pathway. J Biol Chem *275*, 8154-60.

Guo, W., Roth, D., Walch-Solimena, C., and Novick, P. (1999). The exocyst is an effector for Sec4p, targeting secretory vesicles to sites of exocytosis. Embo J *18*, 1071-80.

Haas, A., Scheglmann, D., Lazar, T., Gallwitz, D., and Wickner, W. (1995). The GTPase Ypt7p of *Saccharomyces ceerevisiae* is required on both partner vacuoles for the homotypic fusion step of vacuole inheritance. EMBO J. *14*, 5258-5270.

Haigler, H. T., McKanna, J. A., and Cohen, S. (1979). Direct visualization of the binding and internalization of a ferritin conjugate of epidermal growth factor in human carcinoma cells A-431. J Cell Biol *81*, 382-95.

Hanson, P. I., Roth, R., Morisaki, H., Jahn, R., and Heuser, J. E. (1997). Structure and conformational changes in NSF and its membrane receptor complexes visualized by quick-freeze/deep-etch electron microscopy. Cell *90*, 523-35.

Harder, T., Kellner, R., Parton, R. G., and Gruenberg, J. (1997). Specific release of membrane-bound annexin II and cortical cytoskeletal elements by sequestration of membrane cholesterol. Mol Biol Cell *8*, 533-45.

Harder, T., and Simons, K. (1997). Caveolae, DIGs, and the dynamics of sphingolipid-cholesterol microdomains. Curr Opin Cell Biol *9*, 534-42.

Hardwick, K. G., and Pelham, H. R. (1992). SED5 encodes a 39-kD integral membrane protein required for vesicular transport between the ER and the Golgi complex. J Cell Biol *119*, 513-21.

Hata, Y., Slaughter, C. A., and Sudhof, T. C. (1993). Synaptic vesicle fusion complex contains unc-18 homologue bound to syntaxin. Nature *366*, 347-51.

Helliwell, S. B., Losko, S., and Kaiser, C. A. (2001). Components of a ubiquitin ligase complex specify polyubiquitination and intracellular trafficking of the general amino acid permease. J Cell Biol *153*, 649-62.

Herman, G. A., Bonzelius, F., Cieutat, A. M., and Kelly, R. B. (1994). A distinct class of intracellular storage vesicles, identified by expression of the glucose transporter GLUT4. Proc Natl Acad Sci U S A *91*, 12750-4.

Hill, E., van Der Kaay, J., Downes, C. P., and Smythe, E. (2001). The role of dynamin and its binding partners in coated pit invagination and scission. J Cell Biol *152*, 309-23.

Hinshaw, J. E., and Schmid, S. L. (1995). Dynamin self-assembles into rings suggesting a mechanism for coated vesicle budding. Nature *374*, 190-2.

Hirst, J., Lui, W. W., Bright, N. A., Totty, N., Seaman, M. N., and Robinson, M. S. (2000). A family of proteins with gamma-adaptin and VHS domains that

facilitate trafficking between the trans-Golgi network and the vacuole/lysosome. J Cell Biol *149*, 67-80.

Hofmann, K., and Falquet, L. (2001). A ubiquitin-interacting motif conserved in components of the proteasomal and lysosomal protein degradation systems. Trends Biochem Sci *26*, 347-50.

Hopkins, C. R. (1983). Intracellular routing of transferrin and transferrin receptors in epidermoid carcinoma A431 cells. Cell *35*, 321-30.

Hopkins, C. R., Gibson, A., Shipman, M., and Miller, K. (1990). Movement of internalized ligand-receptor complexes along a continuous endosomal reticulum. Nature *346*, 335-9.

Hopkins, C. R., Gibson, A., Shipman, M., Strickland, D. K., and Trowbridge, I. S. (1994). In migrating fibroblasts, recycling receptors are concentrated in narrow tubules in the pericentriolar area, and then routed to the plasma membrane of the leading lamella. J Cell Biol *125*, 1265-74.

Horiuchi, H., Giner, A., Hoflack, B., and Zerial, M. (1995). A GDP/GTP exchange-stimulatory activity for the Rab5-RabGDI complex on clathrin-coated vesicles from bovine brain. J Biol Chem *270*, 11257-62.

Horiuchi, H., Lippe, R., McBride, H. M., Rubino, M., Woodman, P., Stenmark, H., Rybin, V., Wilm, M., Ashman, K., Mann, M., and Zerial, M. (1997). A novel Rab5 GDP/GTP exchange factor complexed to Rabaptin-5 links nucleotide exchange to effector recruitment and function. Cell *90*, 1149-59.

Hunt, J. M., Bommert, K., Charlton, M. P., Kistner, A., Habermann, E., Augustine, G. J., and Betz, H. (1994). A post-docking role for synaptobrevin in synaptic vesicle fusion. Neuron *12*, 1269-79.

Ikonen, E., Tagaya, M., Ullrich, O., Montecucco, C., and Simons, K. (1995). Different requirements for NSF, SNAP, and Rab proteins in apical and basolateral transport in MDCK cells. Cell *81*, 571-80.

Jackman, M. R., Shurety, W., Ellis, J. A., and Luzio, J. P. (1994). Inhibition of apical but not basolateral endocytosis of ricin and folate in Caco-2 cells by cytochalasin D. J Cell Sci *107*, 2547-56.

Jahn, R. (2000). Sec1/Munc18 proteins: mediators of membrane fusion moving to center stage. Neuron *27*, 201-4.

Jedd, G., Mulholland, J., and Segev, N. (1997). Two new Ypt GTPases are required for exit from the yeast trans-Golgi compartment. J Cell Biol *137*, 563-80.

Jedd, G., Richardson, C., Litt, R., and Segev, N. (1995). The Ypt1 GTPase is essential for the first two steps of the yeast secretory pathway. J Cell Biol *131*, 583-90.

Johnson, K. F., and Kornfeld, S. (1992). The cytoplasmic tail of the mannose 6-phosphate/insulin-like growth factor-II receptor has two signals for lysosomal enzyme sorting in the Golgi. J Cell Biol *119*, 249-57.

Johnson, K. F., and Kornfeld, S. (1992). A His-Leu-Leu sequence near the carboxyl terminus of the cytoplasmic domain of the cation-dependent mannose 6-phosphate receptor is necessary for the lysosomal enzyme sorting function. J Biol Chem *267*, 17110-5.

Jones, D. H., Morris, J. B., Morgan, C. P., Kondo, H., Irvine, R. F., and Cockcroft, S. (2000). Type I phosphatidylinositol 4-phosphate 5-kinase directly interacts with ADP-ribosylation factor 1 and is responsible for phosphatidylinositol 4,5-bisphosphate synthesis in the golgi compartment. J Biol Chem *275*, 13962-6.

Jones, S. M., Crosby, J. R., Salamero, J., and Howell, K. E. (1993). A cytosolic complex of p62 and rab6 associates with TGN38/41 and is involved in budding of exocytic vesicles from the trans-Golgi network. J Cell Biol *122*, 775-88.

Jost, M., Simpson, F., Kavran, J. M., Lemmon, M. A., and Schmid, S. L. (1998). Phosphatidylinositol-4,5-bisphosphate is required for endocytic coated vesicle formation. Curr Biol *8*, 1399-402.

Katzmann, D. J., Babst, M., and Emr, S. D. (2001). Ubiquitin-dependent sorting into the multivesicular body pathway requires the function of a conserved endosomal protein sorting complex, ESCRT-I. Cell *106*, 145-55.

Kelly, R. B. (1990). Microtubules, membrane traffic, and cell organization. Cell *61*, 5-7.

Kelly, R. B. (1999). New twists for dynamin. Nat Cell Biol *1*, E8-9.

Kirchhausen, T. (2000). Clathrin. Annu Rev Biochem *69*, 699-727.

Kobayashi, T., Gu, F., and Gruenberg, J. (1998). Lipids, lipid domains and lipid-protein interactions in endocytic membrane traffic. Semin Cell Dev Biol *9*, 517-26.

Kobayashi, T., Stang, E., Fang, K. S., de Moerloose, P., Parton, R. G., and Gruenberg, J. (1998). A lipid associated with the antiphospholipid syndrome regulates endosome structure and function. Nature *392*, 193-7.

Kobayashi, T., Yamaji-Hasegawa, A., and Kiyokawa, E. (2001). Lipid domains in the endocytic pathway. Semin Cell Dev Biol *12*, 173-82.

Kornfeld, S., and Mellman, I. (1989). The biogenesis of lysosomes. Annu Rev Cell Biol *5*, 483-525.

Krengel, U., Schlichting, L., Scherer, A., Schumann, R., Frech, M., John, J., Kabsch, W., Pai, E. F., and Wittinghofer, A. (1990). Three-dimensional structures of H-ras p21 mutants: molecular basis for their inability to function as signal switch molecules. Cell *62*, 539-48.

Ktistakis, N. T., Brown, H. A., Waters, M. G., Sternweis, P. C., and Roth, M. G. (1996). Evidence that phospholipase D mediates ADP ribosylation factor-dependent formation of Golgi coated vesicles. J Cell Biol *134*, 295-306.

Kubler, E., and Riezman, H. (1993). Actin and fimbrin are required for the internalization step of endocytosis in yeast. Embo J *12*, 2855-62.

Lapierre, L. A., Kumar, R., Hales, C. M., Navarre, J., Bhartur, S. G., Burnette, J. O., Provance, D. W., Jr., Mercer, J. A., Bahler, M., and Goldenring, J. R. (2001). Myosin vb is associated with plasma membrane recycling systems. Mol Biol Cell *12*, 1843-57.

Lawe, D. C., Patki, V., Heller-Harrison, R., Lambright, D., and Corvera, S. (2000). The FYVE domain of early endosome antigen 1 is required for both

phosphatidylinositol 3-phosphate and Rab5 binding. Critical role of this dual interaction for endosomal localization. J Biol Chem *275*, 3699-705.

Le Borgne, R., Griffiths, G., and Hoflack, B. (1996). Mannose 6-phosphate receptors and ADP-ribosylation factors cooperate for high affinity interaction of the AP-1 Golgi assembly proteins with membranes. J Biol Chem *271*, 2162-70.

Le Borgne, R., Schmidt, A., Mauxion, F., Griffiths, G., and Hoflack, B. (1993). Binding of AP-1 Golgi adaptors to membranes requires phosphorylated cytoplasmic domains of the mannose 6-phosphate/insulin-like growth factor II receptor. J Biol Chem *268*, 22552-22556.

Levkowitz, G., Waterman, H., Zamir, E., Kam, Z., Oved, S., Langdon, W. Y., Beguinot, L., Geiger, B., and Yarden, Y. (1998). c-Cbl/Sli-1 regulates endocytic sorting and ubiquitination of the epidermal growth factor receptor. Genes Dev *12*, 3663-74.

Lin, R. C., and Scheller, R. H. (1997). Structural organization of the synaptic exocytosis core complex. Neuron *19*, 1087-94.

Linderman, J. J., and Lauffenburger, D. A. (1988). Analysis of intracellular receptor/ligand sorting in endosomes. J Theor Biol *132*, 203-45.

Lippe, R., Miaczynska, M., Rybin, V., Runge, A., and Zerial, M. (2001). Functional Synergy between Rab5 Effector Rabaptin-5 and Exchange Factor Rabex-5 When Physically Associated in a Complex. Mol Biol Cell *12*, 2219-28.

Lippincott-Schwartz, J., Yuan, L., Tipper, C., Amherdt, M., Orci, L., and Klausner, R. D. (1991). Brefeldin A's effects on endosomes, lysosomes, and the TGN suggest a general mechanism for regulating organelle structure and membrane traffic. Cell *67*, 601-16.

Lombardi, D., Soldati, T., Riederer, M. A., Goda, Y., Zerial, M., and Pfeffer, S. R. (1993). Rab9 functions in transport between late endosomes and the trans Golgi network. Embo J *12*, 677-82.

Lutcke, A., Jansson, S., Parton, R. G., Chavrier, P., Valencia, A., Huber, L. A., Lehtonen, E., and Zerial, M. (1993). Rab17, a novel small GTPase, is specific for epithelial cells and is induced during cell polarization. J Cell Biol *121*, 553-64.

Mammoto, A., Sasaki, T., Kim, Y., and Takai, Y. (2000). Physical and functional interaction of rabphilin-11 with mammalian Sec13 protein. Implication in vesicle trafficking. J Biol Chem *275*, 13167-70.

Marsh, M., Griffiths, G., Dean, G. E., Mellman, I., and Helenius, A. (1986). Three-dimensional structure of endosomes in BHK-21 cells. Proc Natl Acad Sci U S A *83*, 2899-903.

Mayer, A., and Wickner, W. (1997). Docking of yeast vacuoles is catalyzed by the Ras-like GTPase Ypt7p after symmetric priming by Sec18p (NSF). J Cell Biol *136*, 307-17.

Mayer, A., Wickner, W., and Haas, A. (1996). Sec18p (NSF)-driven release of Sec17p (alpha-SNAP) can precede docking and fusion of yeast vacuoles. Cell *85*, 83-94.

Mayor, S., Presley, J. F., and Maxfield, F. R. (1993). Sorting of membrane components from endosomes and subsequent recycling to the cell surface occurs by a bulk flow process. J Cell Biol *121*, 1257-69.

Mayor, S., Sabharanjak, S., and Maxfield, F. R. (1998). Cholesterol-dependent retention of GPI-anchored proteins in endosomes. Embo J *17*, 4626-38.

McBride, H. M., Rybin, V., Murphy, C., Giner, A., Teasdale, R., and Zerial, M. (1999). Oligomeric complexes link Rab5 effectors with NSF and drive membrane fusion via interactions between EEA1 and syntaxin 13. Cell *98*, 377-86.

McKanna, J. A., Haigler, H. T., and Cohen, S. (1979). Hormone receptor topology and dynamics: morphological analysis using ferritin-labeled epidermal growth factor. Proc Natl Acad Sci U S A *76*, 5689-93.

McLauchlan, H., Newell, J., Morrice, N., Osborne, A., West, M., and Smythe, E. (1998). A novel role for Rab5-GDI in ligand sequestration into clathrin-coated pits. Curr Biol *8*, 34-45.

McMurtrie, E. B., Barbosa, M. D., Zerial, M., and Kingsmore, S. F. (1997). Rab17 and rab18, small GTPases with specificity for polarized epithelial cells: genetic mapping in the mouse. Genomics *45*, 623-5.

McNew, J. A., Parlati, F., Fukuda, R., Johnston, R. J., Paz, K., Paumet, F., Sollner, T. H., and Rothman, J. E. (2000). Compartmental specificity of cellular membrane fusion encoded in SNARE proteins. Nature *407*, 153-9.

Mellman, I. (1996). Endocytosis and molecular sorting. Annu Rev Cell Dev Biol *12*, 575-625.

Menasche, G., Pastural, E., Feldmann, J., Certain, S., Ersoy, F., Dupuis, S., Wulffraat, N., Bianchi, D., Fischer, A., Le Deist, F., and de Saint Basile, G. (2000). Mutations in RAB27A cause Griscelli syndrome associated with haemophagocytic syndrome. Nat Genet *25*, 173-6.

Meyer, C., Zizioli, D., Lausmann, S., Eskelinen, E. L., Hamann, J., Saftig, P., von Figura, K., and Schu, P. (2000). mu1A-adaptin-deficient mice: lethality, loss of AP-1 binding and rerouting of mannose 6-phosphate receptors. Embo J *19*, 2193-203.

Miaczynska, M., and Zerial, M. (2002). Mosaic Organization of the Endocytic Pathway. Exp Cell Res *272*, 8-14.

Micheva, K. D., Kay, B. K., and McPherson, P. S. (1997). Synaptojanin forms two separate complexes in the nerve terminal. Interactions with endophilin and amphiphysin. J Biol Chem *272*, 27239-45.

Mukherjee, S., Soe, T. T., and Maxfield, F. R. (1999). Endocytic sorting of lipid analogues differing solely in the chemistry of their hydrophobic tails. J Cell Biol *144*, 1271-84.

Mulholland, J., Preuss, D., Moon, A., Wong, A., Drubin, D., and Botstein, D. (1994). Ultrastructure of the yeast actin cytoskeleton and its association with the plasma membrane. J Cell Biol *125*, 381-91.

Mundigl, O., and De Camilli, P. (1994). Formation of synaptic vesicles. Curr Opin Cell Biol *6*, 561-7.

Nagahama, M., Orci, L., Ravazzola, M., Amherdt, M., Lacomis, L., Tempst, P., Rothman, J. E., and Sollner, T. H. (1996). A v-SNARE implicated in intra-Golgi transport. J Cell Biol *133*, 507-16.

Nielsen, E., Christoforidis, S., Uttenweiler-Joseph, S., Miaczynska, M., Dewitte, F., Wilm, M., Hoflack, B., and Zerial, M. (2000). Rabenosyn-5, a novel rab5 effector, is complexed with hVPS45 and recruited to endosomes through a FYVE finger domain. J Cell Biol *151*, 601-12.

Nielsen, E., Severin, F., Backer, J. M., Hyman, A. A., and Zerial, M. (1999). Rab5 regulates motility of early endosomes on microtubules. Nat Cell Biol *1*, 376-82.

Novick, P., and Brennwald, P. (1993). Friends and family: the role of the Rab GTPases in vesicular traffic. Cell *75*, 597-601.

Novick, P., and Zerial, M. (1997). The diversity of Rab proteins in vesicle transport. Curr Opin Cell Biol *9*, 496-504.

Orci, L., Palmer, D. J., Ravazzola, M., Perrelet, A., Amherdt, M., and Rothman, J. E. (1993). Budding from Golgi membranes requires the coatomer complex of non-clathrin coat proteins. Nature *362*, 648-52.

Owen, D. J., and Luzio, J. P. (2000). Structural insights into clathrin-mediated endocytosis. Curr Opin Cell Biol *12*, 467-74.

Paek, I., Orci, L., Ravazzola, M., Erdjument-Bromage, H., Amherdt, M., Tempst, P., Sollner, T. H., and Rothman, J. E. (1997). ERS-24, a mammalian v-SNARE implicated in vesicle traffic between the ER and the Golgi. J Cell Biol *137*, 1017-28.

Page, L. J., Sowerby, P. J., Lui, W. W., and Robinson, M. S. (1999). Gamma-synergin: an EH domain-containing protein that interacts with gamma-adaptin. J Cell Biol *146*, 993-1004.

Palade, G. (1975). Intracellular aspects of the process of protein synthesis. Science *189*, 347-58.

Pelham, H. R. (1991). Multiple targets for brefeldin A. Cell *67*, 449-51.

Pelham, H. R. (2001). SNAREs and the specificity of membrane fusion. Trends Cell Biol *11*, 99-101.

Peter, F., Nuoffer, C., Pind, S. N., and Balch, W. E. (1994). Guanine nucleotide dissociation inhibitor is essential for Rab1 function in budding from the endoplasmic reticulum and transport through the Golgi stack. J Cell Biol *126*, 1393-406.

Pevsner, J., Hsu, S. C., and Scheller, R. H. (1994). n-Sec1: a neural-specific syntaxin-binding protein. Proc Natl Acad Sci U S A *91*, 1445-9.

Pfeffer, S. R. (1994). Rab GTPases: master regulators of membrane trafficking. Curr Opin Cell Biol *6*, 522-6.

Pfeffer, S. R. (2001). Rab GTPases: specifying and deciphering organelle identity and function. Trends Cell Biol *11*, 487-91.

Pfeffer, S. R., Soldati, T., Geissler, H., Rancano, C., and Dirac-Svejstrup, B. (1995). Selective membrane recruitment of Rab GTPases. Cold Spring Harb Symp Quant Biol *60*, 221-7.

Piguet, V., Gu, F., Foti, M., Demaurex, N., Gruenberg, J., Carpentier, J. L., and Trono, D. (1999). Nef-induced CD4 degradation: a diacidic-based motif in Nef functions as a lysosomal targeting signal through the binding of beta-COP in endosomes. Cell *97*, 63-73.

Poirier, M. A., Xiao, W., Macosko, J. C., Chan, C., Shin, Y. K., and Bennett, M. K. (1998). The synaptic SNARE complex is a parallel four-stranded helical bundle. Nat Struct Biol *5*, 765-9.

Poodry, C. A., and Edgar, L. (1979). Reversible alteration in the neuromuscular junctions of Drosophila melanogaster bearing a temperature-sensitive mutation, shibire. J Cell Biol *81*, 520-7.

Prekeris, R., Klumperman, J., Chen, Y. A., and Scheller, R. H. (1998). Syntaxin 13 mediates cycling of plasma membrane proteins via tubulovesicular recycling endosomes. J Cell Biol *143*, 957-71.

Price, A., Seals, D., Wickner, W., and Ungermann, C. (2000). The docking stage of yeast vacuole fusion requires the transfer of proteins from a cis-SNARE complex to a Rab/Ypt protein. J Cell Biol *148*, 1231-8.

Pruyne, D. W., Schott, D. H., and Bretscher, A. (1998). Tropomyosin-containing actin cables direct the Myo2p-dependent polarized delivery of secretory vesicles in budding yeast. J Cell Biol *143*, 1931-45.

Pryer, N. K., Wuestehube, L. J., and Schekman, R. (1992). Vesicle-mediated protein sorting. Annu Rev Biochem *61*, 471-516.

Puertollano, R., Aguilar, R. C., Gorshkova, I., Crouch, R. J., and Bonifacino, J. S. (2001). Sorting of mannose 6-phosphate receptors mediated by the GGAs. Science *292*, 1712-6.

Qualmann, B., Kessels, M. M., and Kelly, R. B. (2000). Molecular links between endocytosis and the actin cytoskeleton. J Cell Biol *150*, F111-6.

Reggiori, F., and Pelham, H. R. (2001). Sorting of proteins into multivesicular bodies: ubiquitin-dependent and -independent targeting. Embo J *20*, 5176-86.

Riezman, H., Woodman, P. G., van Meer, G., and Marsh, M. (1997). Molecular mechanisms of endocytosis. Cell *91*, 731-8.

Robinson, M. S. (1994). The role of clathrin, adaptors and dynamin in endocytosis. Curr Opin Cell Biol *6*, 538-44.

Robinson, M. S., and Bonifacino, J. S. (2001). Adaptor-related proteins. Curr Opin Cell Biol *13*, 444-53.

Robinson, M. S., and Kreis, T. E. (1992). Recruitment of coat proteins onto Golgi membranes in intact and permeabilized cells: effects of brefeldin A and G protein activators. Cell *69*, 129-38.

Robinson, M. S., and Pearse, B. M. (1986). Immunofluorescent localization of 100K coated vesicle proteins. J Cell Biol *102*, 48-54.

Robinson, M. S., Watts, C., and Zerial, M. (1996). Membrane dynamics in endocytosis. Cell *84*, 13-21.

Rohn, W. M., Rouille, Y., Waguri, S., and Hoflack, B. (2000). Bi-directional trafficking between the trans-Golgi network and the endosomal/lysosomal system. J Cell Sci *113*, 2093-101.

Roos, J., and Kelly, R. B. (1999). The endocytic machinery in nerve terminals surrounds sites of exocytosis. Curr Biol *9*, 1411-4.

Rothman, J. E., and Warren, G. (1994). Implications of the SNARE hypothesis for intracellular membrane topology and dynamics. Curr Biol *4*, 220-33.

Rothman, J. E., and Wieland, F. T. (1996). Protein sorting by transport vesicles. Science *272*, 227-34.

Rozelle, A. L., Machesky, L. M., Yamamoto, M., Driessens, M. H., Insall, R. H., Roth, M. G., Luby-Phelps, K., Marriott, G., Hall, A., and Yin, H. L. (2000). Phosphatidylinositol 4,5-bisphosphate induces actin-based movement of raft-enriched vesicles through WASP-Arp2/3. Curr Biol *10*, 311-20.

Rubino, M., Miaczynska, M., Lippe, R., and Zerial, M. (2000). Selective membrane recruitment of EEA1 suggests a role in directional transport of clathrin-coated vesicles to early endosomes. J Biol Chem *275*, 3745-8.

Rybin, V., Ullrich, O., Rubino, M., Alexandrov, K., Simon, I., Seabra, M. C., Goody, R., and Zerial, M. (1996). GTPase activity of Rab5 acts as a timer for endocytic membrane fusion. Nature *383*, 266-9.

Sacher, M., Jiang, Y., Barrowman, J., Scarpa, A., Burston, J., Zhang, L., Schieltz, D., Yates, J. R., 3rd, Abeliovich, H., and Ferro-Novick, S. (1998). TRAPP, a highly conserved novel complex on the cis-Golgi that mediates vesicle docking and fusion. Embo J *17*, 2494-503.

Salcini, A. E., Confalonieri, S., Doria, M., Santolini, E., Tassi, E., Minenkova, O., Cesareni, G., Pelicci, P. G., and Di Fiore, P. P. (1997). Binding specificity and in vivo targets of the EH domain, a novel protein-protein interaction module. Genes Dev *11*, 2239-49.

Sallusto, F., Cella, M., Danieli, C., and Lanzavecchia, A. (1995). Dendritic cells use macropinocytosis and the mannose receptor to concentrate macromolecules in the major histocompatibility complex class II compartment: downregulation by cytokines and bacterial products. J Exp Med *182*, 389-400.

Salminen, A., and Novick, P. J. (1987). A ras-like protein is required for a post-Golgi event in yeast secretion. Cell *49*, 527-38.

Sato, K., and Wickner, W. (1998). Functional reconstitution of ypt7p GTPase and a purified vacuole SNARE complex. Science *281*, 700-2.

Schmid, S. L., Fuchs, R., Male, P., and Mellman, I. (1988). Two distinct subpopulations of endosomes involved in membrane recycling and transport to lysosomes. Cell *52*, 73-83.

Schmidt, A., Wolde, M., Thiele, C., Fest, W., Kratzin, H., Podtelejnikov, A. V., Witke, W., Huttner, W. B., and Soling, H. D. (1999). Endophilin I mediates synaptic vesicle formation by transfer of arachidonate to lysophosphatidic acid. Nature *401*, 133-41.

Schott, D., Ho, J., Pruyne, D., and Bretscher, A. (1999). The COOH-terminal domain of Myo2p, a yeast myosin V, has a direct role in secretory vesicle targeting. J Cell Biol *147*, 791-808.

Schroer, T. A., Schnapp, B. J., Reese, T. S., and Sheetz, M. P. (1988). The role of kinesin and other soluble factors in organelle movement along microtubules. J Cell Biol *107*, 1785-92.

Schroer, T. A., Steuer, E. R., and Sheetz, M. P. (1989). Cytoplasmic dynein is a minus end-directed motor for membranous organelles. Cell *56*, 937-46.

Schulze, K. L., Broadie, K., Perin, M. S., and Bellen, H. J. (1995). Genetic and electrophysiological studies of Drosophila syntaxin-1A demonstrate its role in nonneuronal secretion and neurotransmission. Cell *80*, 311-20.

Seabra, M. C. (1996). Nucleotide dependence of Rab geranylgeranylation. Rab escort protein interacts preferentially with GDP-bound Rab. J Biol Chem *271*, 14398-404.

Seabra, M. C., Brown, M. S., Slaughter, C. A., Sudhof, T. C., and Goldstein, J. L. (1992). Purification of component A of Rab geranylgeranyl transferase: possible identity with the choroideremia gene product. Cell *70*, 1049-57.

Seabra, M. C., Goldstein, J. L., Sudhof, T. C., and Brown, M. S. (1992). Rab geranylgeranyl transferase. A multisubunit enzyme that prenylates GTP-binding proteins terminating in Cys-X-Cys or Cys-Cys. J Biol Chem *267*, 14497-503.

Segev, N. (2001). Ypt and Rab GTPases: insight into functions through novel interactions. Curr Opin Cell Biol *13*, 500-11.

Segev, N., Mulholland, J., and Botstein, D. (1988). The yeast GTP-binding YPT1 protein and a mammalian counterpart are associated with the secretion machinery. Cell *52*, 915-24.

Sever, S., Muhlberg, A. B., and Schmid, S. L. (1999). Impairment of dynamin's GAP domain stimulates receptor-mediated endocytosis. Nature *398*, 481-6.

Sheff, D. R., Daro, E. A., Hull, M., and Mellman, I. (1999). The receptor recycling pathway contains two distinct populations of early endosomes with different sorting functions. J Cell Biol *145*, 123-39.

Shen, F., and Seabra, M. C. (1996). Mechanism of digeranylgeranylation of Rab proteins. Formation of a complex between monogeranylgeranyl-Rab and Rab escort protein. J Biol Chem *271*, 3692-8.

Silverstein, S. C., Steinman, R. M., and Cohn, Z. A. (1977). Endocytosis. Annu Rev Biochem *46*, 669-722.

Simons, K., and Ikonen, E. (1997). Functional rafts in cell membranes. Nature *387*, 569-72.

Simons, K., and Toomre, D. (2000). Lipid rafts and signal transduction. Nat Rev Mol Cell Biol *1*, 31-9.

Simons, K., and van Meer, G. (1988). Lipid sorting in epithelial cells. Biochemistry *27*, 6197-202.

Simons, K., and Zerial, M. (1993). Rab proteins and the road maps for intracellular transport. Neuron *11*, 789-99.

Simonsen, A., Gaullier, J. M., D'Arrigo, A., and Stenmark, H. (1999). The Rab5 effector EEA1 interacts directly with syntaxin-6. J Biol Chem *274*, 28857-60.

Simonsen, A., Lippe, R., Christoforidis, S., Gaullier, J. M., Brech, A., Callaghan, J., Toh, B. H., Murphy, C., Zerial, M., and Stenmark, H. (1998). EEA1 links PI(3)K function to Rab5 regulation of endosome fusion. Nature *394*, 494-8.

Simpson, F., Bright, N. A., West, M. A., Newman, L. S., Darnell, R. B., and Robinson, M. S. (1996). A novel adaptor-related protein complex. J Cell Biol *133*, 749-60.

Simpson, F., Hussain, N. K., Qualmann, B., Kelly, R. B., Kay, B. K., McPherson, P. S., and Schmid, S. L. (1999). SH3-domain-containing proteins function at distinct steps in clathrin-coated vesicle formation. Nat Cell Biol *1*, 119-24.

Sipe, D. M., Jesurum, A., and Murphy, R. F. (1991). Absence of Na+,K(+)-ATPase regulation of endosomal acidification in K562 erythroleukemia cells. Analysis via inhibition of transferrin recycling by low temperatures. J Biol Chem *266*, 3469-74.

Sogaard, M., Tani, K., Ye, R. R., Geromanos, S., Tempst, P., Kirchhausen, T., Rothman, J. E., and Sollner, T. (1994). A rab protein is required for the assembly of SNARE complexes in the docking of transport vesicles. Cell *78*, 937-48.

Soldati, T., Riederer, M. A., and Pfeffer, S. R. (1993). Rab GDI: a solubilizing and recycling factor for rab9 protein. Mol Biol Cell *4*, 425-34.

Soldati, T., Shapiro, A. D., Svejstrup, A. B., and Pfeffer, S. R. (1994). Membrane targeting of the small GTPase Rab9 is accompanied by nucleotide exchange. Nature *369*, 76-8.

Sollner, T., Bennett, M. K., Whiteheart, S. W., Scheller, R. H., and Rothman, J. E. (1993). A protein assembly-disassembly pathway in vitro that may correspond to sequential steps of synaptic vesicle docking, activation, and fusion. Cell *75*, 409-18.

Sollner, T., Whiteheart, S. W., Brunner, M., Erdjument-Bromage, H., Geromanos, S., Tempst, P., and Rothman, J. E. (1993). SNAP receptors implicated in vesicle targeting and fusion. Nature *362*, 318-24.

Sonnichsen, B., De Renzis, S., Nielsen, E., Rietdorf, J., and Zerial, M. (2000). Distinct membrane domains on endosomes in the recycling pathway visualized by multicolor imaging of Rab4, Rab5, and Rab11. J Cell Biol *149*, 901-14.

Spiro, D. J., Boll, W., Kirchhausen, T., and Wessling-Resnick, M. (1996). Wortmannin alters the transferrin receptor endocytic pathway in vivo and in vitro. Mol Biol Cell *7*, 355-67.

Sprong, H., van der Sluijs, P., and van Meer, G. (2001). How proteins move lipids and lipids move proteins. Nat Rev Mol Cell Biol *2*, 504-13.

Stamnes, M. A., and Rothman, J. E. (1993). The binding of AP-1 clathrin adaptor particles to Golgi membranes requires ADP-ribosylation factor, a small GTP-binding protein. Cell *73*, 999-1005.

Steinman, R. M., and Swanson, J. (1995). The endocytic activity of dendritic cells. J Exp Med *182*, 283-8.

Stenmark, H., and Aasland, R. (1999). FYVE-finger proteins--effectors of an inositol lipid. J Cell Sci *112*, 4175-83.

Stenmark, H., Aasland, R., Toh, B. H., and D'Arrigo, A. (1996). Endosomal localization of the autoantigen EEA1 is mediated by a zinc-binding FYVE finger. J Biol Chem *271*, 24048-54.

Stenmark, H., Vitale, G., Ullrich, O., and Zerial, M. (1995). Rabaptin-5 is a direct effector of the small GTPase Rab5 in endocytic membrane fusion. Cell *83*, 423-32.

Stoorvogel, W., Oorschot, V., and Geuze, H. J. (1996). A novel class of clathrin-coated vesicles budding from endosomes. J Cell Biol *132*, 21-33.

Sudhof, T. C. (1995). The synaptic vesicle cycle: a cascade of protein-protein interactions. Nature *375*, 645-53.

Sweitzer, S. M., and Hinshaw, J. E. (1998). Dynamin undergoes a GTP-dependent conformational change causing vesiculation. Cell *93*, 1021-9.

Tall, G. G., Hama, H., DeWald, D. B., and Horazdovsky, B. F. (1999). The phosphatidylinositol 3-phosphate binding protein Vac1p interacts with a Rab GTPase and a Sec1p homologue to facilitate vesicle-mediated vacuolar protein sorting. Mol Biol Cell *10*, 1873-89.

Tanigawa, G., Orci, L., Amherdt, M., Ravazzola, M., Helms, J. B., and Rothman, J. E. (1993). Hydrolysis of bound GTP by ARF protein triggers uncoating of Golgi-derived COP-coated vesicles. J Cell Biol *123*, 1365-71.

Taunton, J., Rowning, B. A., Coughlin, M. L., Wu, M., Moon, R. T., Mitchison, T. J., and Larabell, C. A. (2000). Actin-dependent propulsion of endosomes and lysosomes by recruitment of N-WASP. J Cell Biol *148*, 519-30.

Toomre, D., Steyer, J. A., Keller, P., Almers, W., and Simons, K. (2000). Fusion of constitutive membrane traffic with the cell surface observed by evanescent wave microscopy. J Cell Biol *149*, 33-40.

Traub, L. M., Ostrom, J. A., and Kornfeld, S. (1993). Biochemical dissection of AP-1 recruitment onto Golgi membranes. J Cell Biol *123*, 561-73.

Trimble, W. S., Cowan, D. M., and Scheller, R. H. (1988). VAMP-1: a synaptic vesicle-associated integral membrane protein. Proc Natl Acad Sci U S A *85*, 4538-42.

Trischler, M., Stoorvogel, W., and Ullrich, O. (1999). Biochemical analysis of distinct Rab5- and Rab11-positive endosomes along the transferrin pathway. J Cell Sci *112*, 4773-83.

Tulp, A., Verwoerd, D., Dobberstein, B., Ploegh, H. L., and Pieters, J. (1994). Isolation and characterization of the intracellular MHC class II compartment. Nature *369*, 120-6.

Ullrich, O., Horiuchi, H., Bucci, C., and Zerial, M. (1994). Membrane association of Rab5 mediated by GDP-dissociation inhibitor and accompanied by GDP/GTP exchange. Nature *368*, 157-60.

Ullrich, O., Reinsch, S., Urbe, S., Zerial, M., and Parton, R. G. (1996). Rab11 regulates recycling through the pericentriolar recycling endosome. J Cell Biol *135*, 913-24.

Ungermann, C., Sato, K., and Wickner, W. (1998). Defining the functions of trans-SNARE pairs. Nature *396*, 543-8.

Ungewickell, E., Ungewickell, H., Holstein, S. E., Lindner, R., Prasad, K., Barouch, W., Martin, B., Greene, L. E., and Eisenberg, E. (1995). Role of auxilin in uncoating clathrin-coated vesicles. Nature *378*, 632-5.

Vale, R. D., Schnapp, B. J., Reese, T. S., and Sheetz, M. P. (1985). Movement of organelles along filaments dissociated from the axoplasm of the squid giant axon. Cell *40*, 449-54.

van der Bliek, A. M., and Meyerowitz, E. M. (1991). Dynamin-like protein encoded by the Drosophila shibire gene associated with vesicular traffic. Nature *351*, 411-4.

van der Bliek, A. M., Redelmeier, T. E., Damke, H., Tisdale, E. J., Meyerowitz, E. M., and Schmid, S. L. (1993). Mutations in human dynamin block an intermediate stage in coated vesicle formation. J Cell Biol *122*, 553-63.

van der Sluijs, P., Hull, M., Webster, P., Male, P., Goud, B., and Mellman, I. (1992). The small GTP-binding protein rab4 controls an early sorting event on the endocytic pathway. Cell *70*, 729-40.

Van Der Sluijs, P., Hull, M., Zahraoui, A., Tavitian, A., Goud, B., and Mellman, I. (1991). The small GTP-binding protein rab4 is associated with early endosomes. Proc Natl Acad Sci U S A *88*, 6313-7.

Vitale, G., Rybin, V., Christoforidis, S., Thornqvist, P., McCaffrey, M., Stenmark, H., and Zerial, M. (1998). Distinct Rab-binding domains mediate the interaction of Rabaptin-5 with GTP-bound Rab4 and Rab5. Embo J *17*, 1941-51.

Waters, M. G., Serafini, T., and Rothman, J. E. (1991). 'Coatomer': a cytosolic protein complex containing subunits of non-clathrin-coated Golgi transport vesicles. Nature *349*, 248-51.

Weisman, L. S., and Wickner, W. (1992). Molecular characterization of VAC1, a gene required for vacuole inheritance and vacuole protein sorting. J Biol Chem *267*, 618-23.

Wendland, B., Emr, S. D., and Riezman, H. (1998). Protein traffic in the yeast endocytic and vacuolar protein sorting pathways. Curr Opin Cell Biol *10*, 513-22.

Wickner, W., and Haas, A. (2000). Yeast homotypic vacuole fusion: a window on organelle trafficking mechanisms. Annu Rev Biochem *69*, 247-75.

Wilcke, M., Johannes, L., Galli, T., Mayau, V., Goud, B., and Salamero, J. (2000). Rab11 Regulates the Compartmentalization of Early Endosomes Required for Efficient Transport from Early Endosomes to the trans-Golgi Network. J Cell Biol *151*, 1207-1220.

Wood, S. A., and Brown, W. J. (1992). The morphology but not the function of endosomes and lysosomes is altered by brefeldin A. J Cell Biol *119*, 273-85.

Yamashiro, D. J., Tycko, B., Fluss, S. R., and Maxfield, F. R. (1984). Segregation of transferrin to a mildly acidic (pH 6.5) para-Golgi compartment in the recycling pathway. Cell *37*, 789-800.

Yang, B., Steegmaier, M., Gonzalez, L. C., Jr., and Scheller, R. H. (2000). nSec1 binds a closed conformation of syntaxin1A. J Cell Biol *148*, 247-52.

Zacchi, P., Stenmark, H., Parton, R. G., Orioli, D., Lim, F., Giner, A., Mellman, I., Zerial, M., and Murphy, C. (1998). Rab17 regulates membrane trafficking through apical recycling endosomes in polarized epithelial cells. J Cell Biol *140*, 1039-53.

Zerial, M., and McBride, H. (2001). Rab proteins as membrane organizers. Nat Rev Mol Cell Biol *2*, 107-17.

Zhao, L., Helms, J. B., Brugger, B., Harter, C., Martoglio, B., Graf, R., Brunner, J., and Wieland, F. T. (1997). Direct and GTP-dependent interaction of ADP ribosylation factor 1 with coatomer subunit beta. Proc Natl Acad Sci U S A *94*, 4418-23.

Zhu, Y., Doray, B., Poussu, A., Lehto, V. P., and Kornfeld, S. (2001). Binding of GGA2 to the lysosomal enzyme sorting motif of the mannose 6-phosphate receptor. Science *292*, 1716-8.

Zot, H. G. (1995). Phospholipid membrane-associated brush border myosin-I activity. Cell Motil Cytoskeleton *30*, 26-37.

Zuk, P. A., and Elferink, L. A. (1999). Rab15 mediates an early endocytic event in Chinese hamster ovary cells. J Biol Chem *274*, 22303-12.

PhD PUBLICATIONS

Some of the results presented in this thesis appear in the following publications:

1) Sonnichsen B, **De Renzis S**, Nielsen E, Rietdorf J, Zerial M. Distinct membrane domains on endosomes in the recycling pathway visualized by multicolor imaging of Rab4, Rab5, and Rab11. J Cell Biol (2000) 15 149:901-14

2) **De Renzis S**, Sonnichsen B, Zerial M. Divalent Rab effectors regulate the sub-compartmental organization and sorting of early endosomes. Nat Cell Biol 2002 Jan 14